



Faces and extreme points of convex sets for the resolution of inverse problems

Vincent Duval

► To cite this version:

Vincent Duval. Faces and extreme points of convex sets for the resolution of inverse problems. Signal and Image processing. Ecole doctorale SDOSE, 2022. tel-03718371

HAL Id: tel-03718371

<https://theses.hal.science/tel-03718371>

Submitted on 8 Jul 2022

HAL is a multi-disciplinary open access archive for the deposit and dissemination of scientific research documents, whether they are published or not. The documents may come from teaching and research institutions in France or abroad, or from public or private research centers.

L'archive ouverte pluridisciplinaire **HAL**, est destinée au dépôt et à la diffusion de documents scientifiques de niveau recherche, publiés ou non, émanant des établissements d'enseignement et de recherche français ou étrangers, des laboratoires publics ou privés.

MÉMOIRE D'HABILITATION À DIRIGER DES RECHERCHES

Université de recherche Paris Sciences et Lettres
PSL Research University

Préparé à l'Université Paris Dauphine - PSL

Faces et points extrémaux des ensembles convexes pour la résolution des problèmes inverses

École doctorale SDOSE

SCIENCES DE LA DÉCISION, DES ORGANISATIONS, DE LA SOCIÉTÉ
ET DE L'ÉCHANGE

Spécialité MATHÉMATIQUES

COMPOSITION DU JURY :

Mme Laure Blanc-Féraud
CNRS et Université Côte d'Azur, Rapporteure

M. Kristian Bredies
Universität Graz, Rapporteur

M. Martin Burger
Friedrich Alexander Universität, Rapporteur

Mme Julie Delon
Université Paris Cité, Membre du jury

M. Rémi Gribonval
Inria Lyon, Membre du jury

M. Guillaume Carlier
Université Paris Dauphine-PSL, Coordinateur

Soutenu par **Vincent Duval**
le 23 juin 2022

Coordonné par **Guillaume Carlier**

Remerciements

Mes premiers remerciements vont aux rapporteurs Kristian Bredies, Martin Burger et Laure Blanc-Féraud, qui ont contribué par leur temps et leur expertise à l'examen de ce long mémoire. Tous trois sont des spécialistes mondialement reconnus des problèmes inverses, et leurs travaux ont eu une grande influence sur les miens. Leurs commentaires sont d'autant plus appréciés. Julie Delon et Rémi Gribonval, membres éminents de la communauté des mathématiques appliquées, m'ont également fait l'honneur d'accepter d'être membre du jury et je les en remercie. Enfin, Guillaume Carlier, analyste de renom et estimé collègue, m'a fait la joie d'accepter d'être coordinateur de ce mémoire. Tous sont de remarquables scientifiques et j'ai beaucoup de chance d'avoir un aussi beau jury.

L'habilitation à diriger des recherches est l'occasion de se retourner et de mesurer le chemin parcouru depuis la thèse. Tout ce chemin n'aurait pas été parcouru sans l'intervention bienveillante de Gabriel Peyré, qui a permis mon retour à la recherche après deux années hors du monde académique. Ma dette envers lui est immense, et je mesure la chance que j'ai d'avoir pu travailler avec lui. Son dynamisme, sa générosité et son insatiable curiosité mathématique sont des modèles pour moi et pour notre communauté.

Je souhaite remercier également Jean-David Benamou et Guillaume Carlier (à nouveau !) qui m'ont accueilli chaleureusement à MOKAPLAN, ainsi que tous les membres et anciens membres de l'équipe : Thomas Gallouët (mon conseiller vélo), Irène Waldspurger, Paul Pegon (mon conseiller informatique), Flavien Léger, François-Xavier Vialard, Luca Nenna... des gens si talentueux qu'ils seraient intimidants s'ils n'étaient pas aussi sympathiques. Merci également à Derya Gök pour sa bonne humeur et le soutien sans faille qu'elle apporte à l'équipe.

La recherche est une activité tantôt solitaire tantôt collaborative, mais pour moi les plus belles étincelles se sont produites grâce aux discussions avec des collègues remarquables, voire exceptionnels : Antonin Chambolle (bienvenue à MOKAPLAN ☺), Claire Boyer et Yohann De Castro (on finira bien par la faire démarrer cette 4L), Frédéric de Gournay et Pierre Weiss (dont le talent est tel qu'ils arrivent à placer "platypus" dans un exposé de mathématiques sans que cela ne choque personne !), Charles Dossal, Bernhard Schmitzer (qui m'a initié à la devise de Hilbert "*Wir müssen wissen. Wir werden wissen.*"), Jean-Marie Mirebeau, et Jérémy Bleyer.

J'ai eu la chance pour mes débuts d'encadrant de travailler avec des doctorants ou des postdoctorants très doués, et dont j'ai pu voir le talent éclore ou se confirmer : Quentin Denoyelle, Paul Catala, Clarice Poon, Jean-Baptiste Courbot, Romain Petit, Robert Tovey et João-Miguel Machado... je suis convaincu qu'ils sont destinés à une très belle carrière dans la recherche. Ce mémoire découle en partie de leurs travaux (et de leurs relectures !) et je les en remercie. J'essaie de leur apporter ce que mes directeurs de thèse Yann Gousseau et Jean-François Aujol m'ont apporté lorsque j'étais à leur place. Je n'oublie pas non plus les anciens collègues de l'ANSSI, auxquels je pense très souvent. J'ai beaucoup appris auprès d'eux, en particulier de nombreux "trucs" d'informatique qui me servent au quotidien.

Par ailleurs, je serai bien ingrat si je ne remerciais pas Inria pour les excellentes conditions de travail dont je bénéficie, et le CEREMADE pour les moyens mis à notre disposition. Merci à César Faivre et Isabelle Bellier pour leur aide, en particulier pour l'organisation de la soutenance!

Mais par dessus tout, c'est à ma famille et à ma belle famille que j'exprime ma plus profonde gratitude, pour avoir toujours répondu "présent". En particulier, les mathématiques seraient bien ternes sans la présence lumineuse, dans ma vie, de Diane et de nos deux enfants Grégoire et Éléonore.

Introduction et résumé en français

Les *problèmes inverses*, qui consistent à tenter d'identifier l'état d'un système physique à partir de quelques mesures indirectes, sont omniprésents en sciences appliquées : supprimer le flou dans les images biologiques (microscopie optique), estimer la disposition des organes ou des os à partir d'images à rayons X obtenues sous différents angles (tomographie axiale calculée) ou à partir de leur réponse à un fort champ magnétique (IRM, Imagerie à Résonance Magnétique), décrire la composition du sous-sol à partir de mesures du champ gravitationnel (prospection gravimétrique)... ne sont que quelques exemples de problèmes inverses rencontrés quotidiennement par les scientifiques.

En termes plus mathématiques, soient V , \mathcal{H} deux ensembles, et une application $\Phi : V \rightarrow \mathcal{H}$ appelée opérateur d'observation (qui décrit le *problème direct*). Le problème inverse associé consiste à essayer de retrouver une inconnue $u \in V$ à partir de l'observation de $\Phi(u)$. Le point délicat est qu'en général Φ n'est pas injective : il y a une perte d'information, l'observation est partielle ; ou alors Φ est très mal conditionnée. De plus il est très courant que l'observation soit entachée de bruit, de sorte que nous n'avons pas accès à $\Phi(u)$ mais à une version corrompue $y \approx \Phi(u)$. Un tel problème est mal posé et requiert une régularisation. La littérature concernant les problèmes inverses est vaste [Tik43, Mor84, CK94, EHBN00, HKPS07, SKHK12, Ker16] et aborde de nombreuses questions telles que l'identifiabilité de l'inconnue u (peut-on la retrouver en l'absence de bruit ?) ou la stabilité de sa reconstruction (peut-on borner l'erreur entre la reconstruction et l'inconnue ? à quel vitesse de convergence lorsque le bruit diminue ?).

Tandis que la plupart des résultats sont formulés en termes de norme (par exemple la norme euclidienne) ou de divergence de Bregman, le présent mémoire se concentre sur les propriétés structurelles des solutions. Au cours des vingt dernières années, les chercheurs ont conçu des termes de régularisation pour les méthodes variationnelles promouvant certaines structures (parcimonie, faible rang, constance par morceaux...) que l'inconnue est supposée posséder. Notre objectif est de comprendre si les (ou des) solutions obtenues ont bien la même structure que l'inconnue, et de déterminer si cette structure est robuste au bruit ou à la régularisation. De plus, nous montrons que l'on peut exploiter cette structure dans des méthodes numériques pour obtenir des algorithmes efficaces.

Dans tout le présent document, nous nous concentrons sur les problèmes inverses *linéaires*, c'est-à-dire que nous supposons que V et \mathcal{H} sont des espaces vectoriels et que Φ est linéaire. Bien que cela paraisse restrictif, ce cadre de travail couvre déjà de nombreux exemples intéressants tels que ceux mentionnés ci-dessus. De plus, nous nous intéressons essentiellement aux méthodes variationnelles *convexes* pour la résolution des problèmes inverses. Comme nous le démontrons dans les chapitres suivants, la plupart des réponses à nos questions résident dans l'étude des faces et des points extrémaux de quelques ensembles convexes bien choisis.

Résumé détaillé

Chapter 1: A representer theorem for variational problems. Une formulation variationnelle typique pour la résolution des problèmes inverses est le programme de minimisation

$$\min_{u \in V} R(u) + f(\Phi u, \tau), \quad (1)$$

où $R : V \rightarrow \mathbb{R} \cup \{+\infty\}$ est une fonction convexe appelée *terme de régularisation* et $f(\cdot, \tau)$ est une fonction convexe arbitraire appelée *terme de fidélité aux données*. La variable τ est un paramètre, typiquement $\tau = (\lambda, y)$, où λ encode le compromis entre la fidélité aux données et la régularisation, et y est une observation. En supposant que des solutions de (1) existent, nous cherchons à *les représenter*, à l’aide d’une somme de briques élémentaires que nous nommons “atomes”. Ces atomes sont les points extrémaux (ou points des rayons extrémaux) des ensembles de niveau de R , et dans les grandes lignes, le résultat principal établit qu’il existe une solution qui est une combinaison convexe d’au plus M tels atomes, où M est le nombre d’observations linéaires (en supposant que $\mathcal{H} = \mathbb{R}^M$ avec $M < +\infty$). Ce principe de représentation est déjà apparu dans la littérature pour des cas particuliers de (1), notamment pour la reconstruction de mesures de Radon ou de splines [Zuh48, FJ75]. Il a été récemment remis en lumière par M. Unser et ses collaborateurs, qui ont souligné son intérêt pour l’étude des splines généralisées ou les réseaux de neurones profonds [UFW17, GFU18, Uns19] (voir aussi [FW19]). Nous donnons ici une formulation générale abstraite de ce principe qui met en évidence sa nature géométrique. Nous nous appuyons sur une formulation épigraphique pour prendre en compte l’interaction entre la régularisation et le terme de fidélité. Les limites de ce principe sont également discutées.

Chapter 2: The faces of the total gradient variation unit ball. Nous illustrons le principe mentionné ci-dessus avec la variation totale (du gradient),

$$R^{(\text{BV})}(u) = \int_{\mathbb{R}^d} |Du|, \quad (2)$$

où $u \in L^{d/(d-1)}(\mathbb{R}^d)$ est à variation bornée, et Du désigne le gradient de u au sens des distributions, vu comme une mesure de Radon. Des expériences numériques suggèrent que considérer uniquement les points extrémaux des ensembles de niveau de $R^{(\text{BV})}$ fournit une représentation trop pauvre et qu’il est nécessaire de comprendre finement leurs faces de dimension finie. En conséquence de la formule de la coaire, ces faces sont déterminées par une famille d’ensembles de périmètre fini qui a une structure (il s’agit d’un anneau d’ensembles). Nous décrivons cette famille et nous démontrons que les faces de dimension finie de la boule unité de la variation totale ont un nombre fini de points extrémaux, ce sont des polytopes. nous en déduisons également une représentation en structure d’arbre des fonctions qui rappelle l’arbre des formes [MG00, BCM03] utilisé en analyse d’images [Mon99, DK00, LAG09]. Ce chapitre relate essentiellement des travaux non publiés.

Chapter 3: Sensitivity analysis in inverse problems. Comprendre la stabilité des représentations fournies dans Chapter 1 quand le paramètre $\tau = (\lambda, y)$ varie nécessite des outils plus élaborés. Nous expliquons comment la théorie classique de la dualité [ET76, Roc89] est intéressante pour cela. Les solutions du problème dual donnent accès à une normale à l’épigraphe de R , ce qui fournit des informations sur une face (mais pas forcément la face minimale) qui contient les solutions de (1). Nous décrivons comment la

normale correspondante évolue lorsque τ varie. En particulier, quand $\lambda \rightarrow 0$ (c'est-à-dire que l'on peut se permettre de régulariser un tout petit peu, par exemple quand le bruit est petit), cette normale est déterminée par un objet que nous appelons *certificat de norme minimale*.

Chapter 4: Finding the minimal-norm certificate. Comme nous le montrons dans les chapitres suivants, le certificat de norme minimale est crucial pour identifier la face des solutions (et donc leur représentation) à faible bruit. Il fournit aussi une condition suffisante pour assurer l'identifiabilité du signal recherché. Nous discutons ici des moyens de le déterminer. S'agissant de la solution d'un problème convexe sous contraintes, il n'a en général pas d'expression analytique. Toutefois, nous montrons que si l'on est capable de deviner la face minimale (dans l'ensemble des points admissibles du problème dual) qui le contient, on peut alors le calculer en utilisant la pseudoinverse d'une restriction de Φ . Au fond, cela revient à généraliser la construction de J.-J. Fuchs dans [Fuc04] pour les problèmes régularisés par la norme ℓ^1 . Nous illustrons ce principe dans le cas de la norme ℓ^1 (LASSO) lorsque le support n'est pas stable, et sur des problèmes régularisés par la variation totale des mesures (BLASSO). Dans le cas de la variation totale du gradient des fonctions, cette technique ne fonctionne plus, et nous discutons du cas plus simple du débruitage, où des exemples de certificats de norme minimale sont donnés par les fonctions indicatrices des ensembles calibrables (au sens de [BCN02, ACC05a]).

Chapter 5: Support stability. Nous étudions la stabilité des représentations dans les problèmes régularisés par la norme ℓ^1 , la variation totale de mesures et la variation totale du gradient des fonctions. Dans ces cas l'objet d'intérêt est le support du signal (ou de son gradient). La convergence du support au sens de Kuratowski est obtenue sous des hypothèses assez générales, et nous nous demandons si de plus il a la même structure que la limite. Pour la régularisation ℓ^1 cela est vrai si le certificat dual limite est dit *strict*, mais nous montrons que cette condition n'est pas suffisante dans le cadre continu (BLASSO). Nous introduisons une hypothèse de non-dégénérescence (avec une condition sur les dérivées secondes qui apparaît également dans [CFG14, AdCG15] pour des raisons différentes) qui assure la stabilité désirée, au sens de solutions qui ont le même nombre de masses de Dirac, avec des amplitudes et des positions qui convergent vers celles de la solution limite.

Chapter 6: Below the “Rayleigh limit”. Une des limitations du BLASSO est son incapacité à distinguer des impulsions de signes opposés qui sont trop proches. Cependant, nous montrons que lorsque toutes les impulsions ont le même signe, le BLASSO est capable de les distinguer, sous des hypothèses raisonnables, en dimension $d = 1$. L'hypothèse principale est essentiellement une condition de non-dégénérescence spéciale d'un objet que nous introduisons, le précertificat aux $(2s - 1)$ -dérivées nulles, la limite des certificats de norme minimale lorsque les points de support se concentrent. Nous donnons des conditions suffisantes pour cette non-dégénérescence dans le cas où la famille d'autocorrélation de la réponse impulsionnelle forme un *système totalement positif étendu*, une propriété qui est liée à la propriété de T -système.

Chapter 7: Exploiting the structure of the solutions. L'intérêt du principe de représentation n'est pas seulement théorique, il sert également dans la conception de méthodes numériques. Nous décrivons l'algorithme Frank-Wolfe (ou gradient conditionnel) classique dans un cadre abstrait et nous expliquons comment il construit des itérées qui ont une structure similaire à nos solutions “décomposables”, étant une combinaison

convexe d'un nombre fini de points extrémaux. En nous inspirant d'une idée de K. Bredies and H. Pikkarainen [BP13] d'améliorer la convergence en effectuant une descente non-convexe sur le choix des points extrémaux de la combinaison, nous déduisons deux algorithmes de minimisation pour le BLASSO. Le premier, appelé *Sliding Frank-Wolfe*, travaille dans l'espace des mesures et ajoute itérativement des masses de Dirac aux itérées, avec une descente non convexe sur les amplitudes et les positions. Si la solution recherchée a une structure parcimonieuse non-dégénérée la méthode converge après un nombre fini d'itérations principales. Le second, appelé *Fourier Frank-Wolfe*, travaille dans l'espace des matrices de moments (trigonométriques) et ajoute itérativement des matrices de rang un aux itérées, avec une descente non convexe également. Les matrices de moments sont grandes et difficiles à manipuler, mais en exploitant leur structure Toeplitz et le fait que les itérées sont de faible rang, notre algorithme bénéficie de calculs rapides (s'appuyant notamment sur la transformée de Fourier rapide) et d'une faible empreinte mémoire.

Les deux méthodes fournissent des algorithmes de résolution efficaces pour le BLASSO dans un cadre complètement continu. Nous montrons qu'ils sont parfaitement adaptés aux applications en les confrontant à des jeux de données de microscopie à super-résolution par localisation de molécule unique (SMLM).

Foreword

This thesis summarizes the research I have conducted from 2013 to early 2021, first as a postdoctoral fellow at Paris-Dauphine University (CEREMADE), for one year and a half, and then as a researcher at Inria in the MOKAPLAN team. Rather than summarizing my published papers with a bird’s eye view, I have tried to “tell the story” that seems to emerge from most of my works.

Step by step, trying to present things in a unified way, I realized that I had to state some results quite differently from their originally published version, and therefore had to provide their proofs. It results in a (perhaps) unusually detailed document for a habilitation thesis, and I apologize to the reviewers for that. A second consequence of that choice is that some papers could not “fit” into this story, and even though they do matter to me, I have decided not to present them. Such is the case for my papers related to mechanics [2] and optimal transport [4, 1].

It must be said that the research presented here stems not only from my own effort, but also from interactions and collaborations with valuable and talented colleagues. I have tried to acknowledge their contributions at the beginning of each chapter. More specifically, I have made my first steps towards “*diriger des recherches*” by co-supervising with Gabriel Peyré the PhD theses of Quentin Denoyelle and Paul Catala. The present document owes a lot to them.

Introduction

Trying to identify the state of a physical system from the knowledge of a few indirect measurements is an ubiquitous problem in applied sciences known as *inverse problem*: removing the blur in biological images (optical microscopy), estimating the disposition of organs or bones from X-radiations from different angles (computed tomography) or from their response to a strong magnetic field (MRI), describing the composition of the ground by measuring the gravity field on the surface (gravimetric prospection)... are a few examples of inverse problems that scientists routinely face.

In more mathematical terms, let V , \mathcal{H} be two sets, and a map $\Phi : V \rightarrow \mathcal{H}$, called a forward operator. The inverse problem consists in trying to recover some unknown $u \in V$ from the observation of $\Phi(u)$. The issue is that Φ is in general not injective: there is a loss of information, the observation is partial. Moreover, it is very common that the observation is contaminated with noise, so that we do not have access to $\Phi(u)$, but to some corrupted version $y \approx \Phi(u)$. Solving such a problem is severely ill-posed and requires some regularization. The literature on inverse problems is large [Tik43, Mor84, CK94, EHBN00, HKPS07, SKHK12, Ker16], and addresses many questions such as the identifiability of an unknown u (can one recover it if there is no noise?) or the stability of its reconstruction (can one bound the error between the reconstruction and the unknown? at what convergence rate when the noise decays?).

While most results are formulated in terms of norms (*e.g.* Euclidean) or Bregman divergence, the present thesis focuses on structural properties. In the last two decades, researchers have carefully designed regularizers in variational approaches so as to promote solutions with a specific structure (sparsity, low rank, piecewise constancy...) that the unknown supposedly has. Our goal is to understand if some solutions have indeed the same structure as the unknown, and to understand whether it is stable to noise or regularization. Moreover, we show that exploiting that structure in numerical methods can help designing efficient solvers.

Throughout the document, we focus on *linear* inverse problems, *i.e.* we assume that V and \mathcal{H} are vector spaces and Φ is linear. Though that may seem restrictive, that framework already covers many interesting examples such as those mentioned above. Moreover, we are mainly interested in convex variational methods for the resolution of inverse problems. As we prove in the next chapters, most answers to our questions rely in the study of the faces and extreme points of some well chosen convex sets.

Detailed summary

Chapter 1: A representer theorem for variational problems. A typical variational formulation for the resolution of inverse problems is the minimization program

$$\min_{u \in V} R(u) + f(\Phi u, \tau), \tag{3}$$

where $R : V \rightarrow \mathbb{R} \cup \{+\infty\}$ is a convex function called a *regularizer* and $f(\cdot, \tau)$ is an arbitrary convex function called a *data fitting term*. The variable τ is a parameter, typically $\tau = (\lambda, y)$, where λ encodes the balance between the fidelity and regularization terms, and y is an observation. Granted that solutions to (3) exist, we focus on *representing them*, with a sum of building blocks that we call “atoms”. Those atoms are the extreme points (or points in the extreme rays) of the level sets of R , and roughly speaking, the main result states that there is a solution which is a convex combination of at most M such atoms, where M is the number of linear measurements (assuming $\mathcal{H} = \mathbb{R}^M$ with $M < +\infty$). That principle has already appeared in the literature for specific instances of (3), especially for the recovery of Radon measures or splines [Zuh48, FJ75]. It was recently revived by M. Unser and collaborators who pointed out its interest for the study of generalized splines or deep neural networks [UFW17, GFU18, Uns19] (see also [FW19]). We provide here a general abstract formulation which emphasizes the geometric essence of that principle. We rely on an epigraphical formulation to take into account the interactions between the regularizer and the fidelity term. The limitations of that principle are also discussed.

Chapter 2: The faces of the total gradient variation unit ball. We illustrate the above-mentioned principle on the total (gradient) variation of functions,

$$R^{(\text{BV})}(u) = \int_{\mathbb{R}^d} |Du|, \quad (4)$$

where $u \in L^{d/(d-1)}(\mathbb{R}^d)$ has bounded variation, and Du denotes the distributional gradient of u , seen as a Radon measure. Numerical experiments suggest that considering only the extreme points of the level sets of $R^{(\text{BV})}$ yields a representation which is too poor, and that it is necessary to finely understand the finite-dimensional faces instead. As a consequence of the coarea formula, those faces are determined by a family of sets of finite perimeters which has some structure (it is a ring of sets). We describe those families and we prove that the finite-dimensional faces of the total variation unit ball have a finite number of extreme points, they are polytopes. We also deduce a tree representation of functions which is reminiscent of the tree of shapes of images [MG00, BCM03] used in image analysis [Mon99, DK00, LAG09]. This chapter covers mostly unpublished work.

Chapter 3: Sensitivity analysis in inverse problems. As we aim at understanding the stability of the representation provided in Chapter 1 when the parameter $\tau = (\lambda, y)$ varies, we need to use more sophisticated tools. We explain how the classical duality theory [ET76, Roc89] is relevant for that. The solutions to the dual problem give access to a normal to the epigraph of R , providing information on a face (but not necessarily the minimal one) which contains the solutions to (3). We describe how the corresponding normal evolves as τ varies. In particular, when $\lambda \rightarrow 0$ (*i.e.*, when one may regularize only a little, for instance if the noise is small), that normal is determined by an object that we call the *minimal-norm certificate*.

Chapter 4: Finding the minimal-norm certificate. As we show in subsequent chapters, the minimal-norm certificate is crucial when trying to identify the face of the solutions (hence their representation) at low noise. It also provides a sufficient way to ensure identifiability of the signal to reconstruct. We discuss here how to find it. Being the solution of a constrained convex problem, it does not have any closed-form expression in general. However, we show that if one is able to guess its minimal face beforehand (in the set of feasible points of the dual problem), it can be computed

using the pseudoinverse of a restriction of Φ . In essence, this is a generalization of the construction of J.-J. Fuchs in [Fuc04] for ℓ^1 -regularized problems. We illustrate that principle in the case of ℓ^1 -regularized problems (LASSO) where the support is not stable, and on problems regularized with the total variation of measures (BLASSO). In the case of the total (gradient) variation of functions, that trick does not hold, and we discuss the simpler case of denoising, where examples of minimal norm certificates are provided by the indicator functions of calibrable sets (in the sense of [BCN02, ACC05a]).

Chapter 5: Support stability. We examine the stability of the representation in problems regularized by the ℓ^1 -norm, the total variation of measures and the total gradient variation of functions. In those cases the support of the signal (or its gradient) is the object of interest. The convergence of the support in the sense of Kuratowski is obtained under fairly general assumptions, and we ask if furthermore it has the same structure as the support of the limit. In ℓ^1 -regularization this is true, a sufficient condition is the *tightness* of the limit dual certificate, while we show that tightness is not sufficient in the continuous setting (BLASSO). We introduce a non-degeneracy assumption (with a condition on second derivatives which also appears in [CFG14, AdCG15] for different reasons) which ensures the desired stability providing measures with the same number of Dirac masses, with amplitudes and locations which converge towards those of the limit solution.

Chapter 6: Below the “Rayleigh limit”. One limitation of the BLASSO is its inability to resolve spikes with opposite signs which are too close. However, we show that when the spikes all have the same sign, the BLASSO is able to resolve them, under mild assumptions, in dimension $d = 1$. The assumption is essentially a special non-degeneracy condition on an object that we introduce, the $(2s - 1)$ -vanishing dual precertificate, the limit of the minimal-norm certificates as the points cluster. We provide sufficient conditions for that non-degeneracy condition in the case where the family of autocorrelations form an *extended totally positive system*, a property which is related to the T -system property.

Chapter 7: Exploiting the structure of the solutions. The representation principle is not only of theoretical interest, it can also be exploited in numerical methods. We describe the classical Frank-Wolfe (or conditional gradient) algorithm in an abstract setting and we explain how it builds iterate which have a similar structure as our “decomposable” solutions, being a convex combination of finitely many extreme points. Relying on an idea of K. Bredies and H. Pikkariainen [BP13], that is, to improve the convergence by performing a non-convex descent on the choice of extreme points in the combination, we derive two minimization algorithms for the BLASSO. The first one, the Sliding Frank-Wolfe, works in the space of measures and iteratively adds Dirac masses to the iterate, with a non-convex descent on the amplitudes and locations. If the sought-after solution has a sparse non-degenerate structure, the method converges after finitely many outer iterations. The second one, the Fourier Frank-Wolfe, works in the space of (trigonometric) moment matrices and iteratively adds rank-one matrices to the iterate, with a non-convex descent as well. Moment matrices are large and cumbersome, but taking advantage of their Toeplitz structure and the fact that the iterates have low rank, our algorithm benefits from fast computations (with the use of the Fast Fourier Transform) and a low memory footprint.

Both methods provide efficient solvers for the BLASSO in a fully continuous setting. We show that they are perfectly suitable for applications by testing them on single-

molecule localization microscopy (SMLM) datasets.

Publications of the author since the PhD

- [1] Jean-David Benamou and Vincent Duval. Minimal convex extensions and finite difference discretisation of the quadratic Monge–Kantorovich problem. *European Journal of Applied Mathematics*, 30(6):1041–1078, 2019. Publisher: Cambridge University Press.
- [2] J. Bleyer, G. Carlier, V. Duval, J.-M. Mirebeau, and G. Peyré. A Γ -Convergence Result for the Upper Bound Limit Analysis of Plates. *ESAIM: Mathematical Modelling and Numerical Analysis*, 2016.
- [3] Claire. Boyer, Antonin. Chambolle, Yann De. Castro, Vincent. Duval, Frédéric. de Gournay, and Pierre. Weiss. On Representer Theorems and Convex Regularization. *SIAM Journal on Optimization*, 29(2):1260–1281, 2019.
- [4] Guillaume Carlier, Vincent Duval, Gabriel Peyré, and Bernhard Schmitzer. Convergence of entropic schemes for optimal transport and gradient flows. *SIAM Journal on Mathematical Analysis*, 49(2):1385–1418, 2017.
- [5] Paul Catala, Vincent Duval, and Gabriel Peyré. A Low-Rank Approach to Off-the-Grid Sparse Superresolution. *SIAM Journal on Imaging Sciences*, 12(3):1464–1500, 2019. Publisher: Society for Industrial and Applied Mathematics.
- [6] Antonin Chambolle, Vincent Duval, Gabriel Peyré, and Clarice Poon. Geometric properties of solutions to the total variation denoising problem. *Inverse Problems*, 33(1):015002, 2016.
- [7] Jean-Baptiste Courbot, Vincent Duval, and Bernard Legras. Sparse analysis for mesoscale convective systems tracking. *Signal Processing: Image Communication*, 85:115854, 2020.
- [8] Quentin Denoyelle, Vincent Duval, and Gabriel Peyré. Support recovery for sparse super-resolution of positive measures. *Journal of Fourier Analysis and Applications*, 2016.
- [9] Quentin Denoyelle, Vincent Duval, Gabriel Peyré, and Emmanuel Soubies. The sliding Frank–Wolfe algorithm and its application to super-resolution microscopy. *Inverse Problems*, 36(1):014001, 2019.
- [10] Charles Dossal, Vincent Duval, and Clarice Poon. Sampling the fourier transform along radial lines. *SIAM Journal on Numerical Analysis (SINUM)*, 55(6):2540–2564, 2017.

- [11] Vincent Duval. A characterization of the Non-Degenerate Source Condition in super-resolution. *Information and Inference: A Journal of the IMA*, 9(1):235–269, 2020.
- [12] Vincent Duval. An Epigraphical Approach to the Representer Theorem. *Journal of Convex Analysis*, 28(3), 2021.
- [13] Vincent Duval and Gabriel Peyré. Exact support recovery for sparse spikes deconvolution. *Foundations of Computational Mathematics*, 15(5):1315–1355, 2015.
- [14] Vincent Duval and Gabriel Peyré. Sparse spikes super-resolution on thin grids II: the continuous basis pursuit. *Inverse Problems*, 33(9):095008, 2017.
- [15] Vincent Duval and Gabriel Peyré. Sparse regularization on thin grids I: the Lasso. *Inverse Problems*, 33(5):055008, 2017.

Contents

1	A representer theorem for variational problems	19
1.1	Representer theorems for inverse problems	20
1.1.1	Representer theorems for measures.	20
1.1.2	“Representer theorems” for convex sets	21
1.1.3	Statement of the main theorem	22
1.2	Convex sets, faces and extreme points	24
1.2.1	Convex sets and their faces	24
1.2.2	Linearly bounded and linearly closed sets	26
1.3	An epigraphical approach to the representer theorem	27
1.3.1	A relation between the faces of the epigraphs	28
1.3.2	From the faces in the epigraphs to the faces in the level sets. . . .	29
1.3.3	Proof of the main theorem	29
1.3.4	The case of level sets containing lines	30
1.4	Examples	31
1.4.1	Point source reconstruction	31
1.4.2	Semi-definite programs	33
1.4.3	Interactions between the regularizer and the sensing operator . . .	34
1.5	Conclusion	35
1.5.1	Summary	35
1.5.2	Discussion with respect to prior works and extensions	35
2	The faces of the total gradient variation unit ball	39
2.1	A representation using only the extreme points	40
2.1.1	Functional setting	40
2.1.2	Fleming’s result	41
2.1.3	Numerical experiments	41
2.2	Structural properties of the faces of C_{BV}	42
2.2.1	Set “algebra”	43
2.2.2	Decomposability	45
2.3	The finite-dimensional faces of C_{BV} are polytopes	46
2.3.1	Chains in \mathcal{E}	46
2.3.2	Maximal chains	48
2.3.3	Extreme points of finite-dimensional faces	49
2.4	The tree of shapes of a function	50
2.4.1	A decomposition of u using simple sets	50
2.4.2	The tree structure of the decomposition	51
2.5	Examples of finite dimensional faces	53
2.6	Conclusion	56
2.6.1	Summary	56
2.6.2	Discussion with respect to prior works and extensions	56

3	Sensitivity analysis in inverse problems	59
3.1	General results	60
3.1.1	Regularized inverse problems	60
3.1.2	Duality for face identification	60
3.1.3	The positively homogeneous case	61
3.2	Examples	62
3.2.1	Inverse problems in the space of measures	62
3.2.2	Finite-dimensional ℓ^1 -regularized inverse problems	64
3.2.3	Inverse problems involving the total gradient variation	64
3.3	Strong duality and existence of dual solutions	66
3.3.1	The case $\lambda > 0$	66
3.3.2	The case $\lambda = 0$	67
3.4	Identifiability, source condition and low noise regimes	69
3.4.1	The source condition to ensure identifiability	69
3.4.2	Convergence for $\lambda \rightarrow 0^+$ and minimal norm certificate	71
3.5	Conclusion	73
4	Finding the minimal-norm certificate	75
4.1	General principle	76
4.1.1	Projecting onto the span of the minimal face	76
4.1.2	The polyhedral case	76
4.1.3	The semi-infinite programming case	77
4.2	The case of ℓ^1 -synthesis recovery	79
4.2.1	The tight case and the Fuchs precertificate	79
4.2.2	The non-tight case: finding the extended support	80
4.3	Sparse-spike recovery in the space of measures	80
4.3.1	Non-degenerate certificates	81
4.3.2	The vanishing-derivatives precertificate	82
4.3.3	Connection with interpolation problems	83
4.3.4	Examples	84
4.3.5	How to ensure non-degeneracy?	87
4.4	Total (gradient) variation denoising	88
4.4.1	Calibrable sets	88
4.4.2	Convex sets	93
4.5	Conclusion	96
4.5.1	Summary	96
4.5.2	Discussion with respect to prior works and comments	96
5	Support stability	99
5.1	Set convergence for supports and level lines	100
5.1.1	Definition	100
5.1.2	Convergence of the support for the BLASSO	101
5.1.3	Convergence of level lines in total gradient variation regularization	104
5.2	Support stability on a continuous domain	108
5.2.1	A counterexample to support stability	108
5.2.2	Non-degenerate certificates for support stability	110
5.3	Support stability for the LASSO problem on discrete grids	112
5.3.1	The existence of a tight dual certificate implies support recovery	112
5.3.2	The LASSO on thin grids	113
5.3.3	Support (in)stability on thin grids	116
5.4	Conclusion	119

5.4.1	Summary	119
5.4.2	Discussion with respect to prior works and comments	119
6	Below the “Rayleigh limit”	123
6.1	Close opposite spikes are not recoverable	124
6.1.1	The separation requirement is fundamental	124
6.1.2	The case of the ideal low-pass filter	125
6.2	Clustering spikes and the $(2s - 1)$ -vanishing derivatives precertificate . . .	126
6.2.1	An approximate factorization	127
6.2.2	The $(2s - 1)$ -vanishing dual precertificate	128
6.2.3	Support recovery for clustered spikes	131
6.3	Extended totally positive kernels	132
6.3.1	A characterization of the Non-degenerate Source Condition (NDSC) . . .	132
6.3.2	Extended-totally positive kernels and non-degeneracy	134
6.4	Conclusion and comments	137
6.4.1	Summary	137
6.4.2	Comments	137
7	Exploiting the structure of the solutions	139
7.1	The Frank-Wolfe algorithm	140
7.1.1	Description of the algorithm	140
7.1.2	Convergence results	141
7.1.3	Discussion	142
7.2	The Sliding Frank-Wolfe in the space of measures	142
7.2.1	Description of the algorithm	143
7.2.2	Illustration of the finite-time convergence	146
7.2.3	Application to fluorescence microscopy	147
7.3	The Fourier-Frank-Wolfe algorithm in the space of Moment matrices . . .	154
7.3.1	Spectral approximation	154
7.3.2	Atomic norm reformulation	155
7.3.3	The Fourier-Frank-Wolfe Algorithm	158
7.3.4	Extracting the support from the moment matrices	160
7.3.5	Numerical examples	161
7.4	Conclusion	162
7.4.1	Summary	162
7.4.2	Comments	164
8	Conclusion and perspectives	167
A	Reminder on the properties of BV functions	171
B	Duality and subdifferentials	173
B.1	Duality pairing	173
B.1.1	Definition	173
B.1.2	Choice of a topology	173
B.1.3	Legendre-Fenchel conjugation	174
B.2	Normals and subdifferentials	174
B.2.1	Normal cones and exposed faces	175
B.3	Subdifferentials	176
B.4	Dual problems	177
B.4.1	Perturbed problems.	177

B.4.2	Duality in our inverse problem.	178
B.4.3	Uniqueness in the dual problem for almost every data	179
C	Reminder on Γ-convergence	181

Chapter 1

A representer theorem for variational problems

Contents

1.1	Representer theorems for inverse problems	20
1.1.1	Representer theorems for measures.	20
1.1.2	“Representer theorems” for convex sets	21
1.1.3	Statement of the main theorem	22
1.2	Convex sets, faces and extreme points	24
1.2.1	Convex sets and their faces	24
1.2.2	Linearly bounded and linearly closed sets	26
1.3	An epigraphical approach to the representer theorem	27
1.3.1	A relation between the faces of the epigraphs	28
1.3.2	From the faces in the epigraphs to the faces in the level sets.	29
1.3.3	Proof of the main theorem	29
1.3.4	The case of level sets containing lines	30
1.4	Examples	31
1.4.1	Point source reconstruction	31
1.4.2	Semi-definite programs	33
1.4.3	Interactions between the regularizer and the sensing operator	34
1.5	Conclusion	35
1.5.1	Summary	35
1.5.2	Discussion with respect to prior works and extensions	35

Our study of variational methods for inverse problems begins with a basic theorem which describes the structure of the solution set. Let V denote a real vector space (which models, *e.g.* a space of signals), and $\Phi : V \rightarrow \mathbb{R}^M$ be a linear map. Typically, Φ is called a *sensing operator*, as it provides M measurements on some unknown signal u_0 that we wish to recover. In most of the present dissertation, we focus on problems of the form

$$\inf_{u \in V} R(u) + f(\Phi u, \tau), \quad (1.1)$$

where $R : V \rightarrow \mathbb{R} \cup \{+\infty\}$ is a convex function called a *regularizer* and $f(\cdot, \tau)$ is an arbitrary convex function called a *data fitting term*. The variable τ is a parameter, typically $\tau = (\lambda, y)$, where λ encodes the balance between the fidelity and regularization

terms, and y is a reference observation. As in the present chapter we consider τ fixed, we drop the dependency in τ for the rest of the chapter.

Problems of the form (1.1) have been considered in the field of inverse problems since (at least) the work of A. N. Tikhonov [Tik43, Tik63]. The choice of R (and f) may be guided by Bayesian arguments or by structural properties which are characteristic of the unknown signal u_0 (e.g. sparsity or low rank) and that one wishes to promote when solving (1.1). We adopt the latter point of view, and the goal of this chapter is to emphasize the connection between the faces of the level sets of R and the structure of the solutions to (1.1).

While most of the early works focus on R (and f) being the square of the Euclidean norm, more modern approaches employ convex regularizers having non-trivial faces in their level sets, such as the indicator of the nonnegative orthant [DT05], the ℓ^1 -norm [Tib96] or its composition with a linear operator [ROF92], or the nuclear norm [CR09]. That change of paradigm has yielded dramatic improvement, stimulating the emergence of the compressed sensing theory [Don06] and contributing to major progress in tasks such as matrix completion [CR09] or point-source deconvolution [TBSR13, CFG14] - to name a few. The success of such regularizations in promoting structured signals is interpreted in [CRPW12] as follows: when R is positively homogeneous, R is the convex gauge of some collection of points, the extreme points of $\{u \in V \mid R(u) \leq 1\}$, and any solution u to (1.1) which lies on a low dimensional face of that level set is a convex combination of such extreme points. The theorems of this chapter advocate for the same philosophy, but they make the statement more precise.

Collaboration. This chapter revisits the results of [3], a joint work with Claire Boyer, Antonin Chambolle, Yohann De Castro, Frédéric de Gournay, and Pierre Weiss. While our original proof was built upon the argument of [Kle63], we have developed for this manuscript an alternative approach which is closer to the original paper [Dub62] and which involves the epigraphs of the functions. It has been published in [12]. The main advantage of this epigraphical approach is to handle natively convex fidelity terms $u \mapsto f(\Phi u)$ instead of the hard constraint $\Phi u = y$. It also paves the way for the discussion on the stability of such representations in Chapter 3.

As the writing of the present thesis took longer than expected, and since the alternative approach has an independent interest, we published that approach in [12], where the most technical details of the proof have been moved to.

1.1 Representer theorems for inverse problems

We call a *representer theorem* a theorem which describes the (or some) solutions to (1.1) as a convex (or linear) combination of some “atoms”.

1.1.1 Representer theorems for measures.

Although inverse problems in the space of measures have drawn a lot of attention in recent years, that topic dates at least from the 1940’s, and it provides one of the oldest examples of a representer theorem. Consider for instance the problem

$$\min_{m \in \mathcal{M}(X)} |m|(X) \quad \text{s.t.} \quad \Phi m = y \quad (1.2)$$

where $X \subseteq \mathbb{R}^d$, $\mathcal{M}(X)$ denotes the space of bounded Radon measures, $|m|(X)$ is the total variation of the measure m (see Section 1.4.1) and Φm is a vector of *generalized moments*,

i.e. $\Phi m = \left(\int_X \varphi_i(x) dm(x)\right)_{1 \leq i \leq M}$ where $\{\varphi_i\}_{1 \leq i \leq M}$ is a family of continuous functions (which “vanish at infinity” if Ω is not compact). Problems of the form (1.2) have received considerable attention since the pioneering works of A. Beurling [Beu38] and M. Krein [Kre38], sometimes under the name *L-moment problem* (see the monograph [KN77]). To the best of our knowledge, the first “representer theorem” for problems of the form (1.1) is given for (1.2) by S. Zuhovickii [Zuh48] (see [Zuh62, Th. 3] for an English version). It essentially states that

$$\text{There exists a solution to (1.2) of the form } \sum_{i=1}^r a_i \delta_{x_i}, \text{ with } r \leq M. \quad (1.3)$$

A more precise result was given by Fisher and Jerome in [FJ75]. When considering the problem (1.2), and for a bounded domain Ω , the result reads as follows:

$$\begin{aligned} &\text{The extreme points of the solution set to (1.2) are of the form} \\ &\sum_{i=1}^r a_i \delta_{x_i}, \text{ with } r \leq M. \end{aligned} \quad (1.4)$$

Incidentally, the Fisher-Jerome theorem considers more general problems of the form:

$$\min_{u \in V} |Lu|(X) \quad \text{s.t.} \quad Lu \in \mathcal{M}(\Omega) \quad \text{and} \quad \Phi u = y, \quad (1.5)$$

where $V \subseteq \mathcal{D}'(\Omega)$ is a suitably defined Banach space of distributions, $L : \mathcal{D}'(\Omega) \rightarrow \mathcal{D}'(\Omega)$ maps V onto $\mathcal{M}(\Omega)$ and $\Phi : V \rightarrow \mathbb{R}^M$ is a continuous linear operator. We refer to [FJ75, UFW17] for precise assumptions. Let us mention that the initial results by Fisher-Jerome were extended to a significantly more general setting in [UFW17].

It is important to note that the Fisher-Jerome theorem [FJ75] provides a much finer description of the solution set than Zuhovickii’s result [Zuh48]. Indeed, the Krein-Milman theorem states that, if V is endowed with the topology of a locally convex Hausdorff vector space and $C \subset V$ is compact convex, then C is the closed convex hull of its extreme points,

$$\text{cl conv}(\text{extr}(C)) = C. \quad (1.6)$$

In other words, the solutions described by the Fisher-Jerome theorem are sufficient to recover *the whole set of solutions*. Let us mention that the Krein-Milman theorem was extended by V. Klee [Kle57] to unbounded sets: if C is locally compact, closed, convex, and contains no line, then

$$\text{cl conv}(\text{extr}(C) \cup \text{rext}(C)) = C, \quad (1.7)$$

where $\text{rext}(C)$ denotes the union of the extreme rays of C (see Section 1.2 below).

1.1.2 “Representer theorems” for convex sets

As the Dirac masses are the extreme points of the total variation unit ball, each of the above-mentioned “representer theorems” for inverse problems actually reflects some phenomenon in the geometry of convex sets. In that regard, the celebrated Minkowski-Carathéodory theorem (see for instance [HUL93, Th. III.2.3.4]) is fundamental: any point of a compact convex set in an M -dimensional space is a convex combination of (at most) $M+1$ of its extreme points. In [Kle63, Th. (3)], V. Klee removed the boundedness assumption and obtained the following extension: any point of a closed convex set which contains no line and which lies in an M -dimensional space is a convex combination of

(at most) $M + 1$ extreme points, or M points, each an extreme point or a point in an extreme ray.

The present chapter discusses the connection between the Fisher-Jerome theorem and a lesser known theorem by L. Dubins [Dub62]:

The extreme points of the intersection of C with an affine space of codimension M are convex combination of (at most)¹ $M + 1$ extreme points of C ,

provided C is linearly bounded and linearly closed (see Section 1.2). That theorem was extended by V. Klee [Kle63] to deal with the unbounded case and to describe the higher-dimensional faces of the intersection.

Although the connection with the Fisher-Jerome theorem is striking, Dubins' theorem actually provides one extreme point too many. In the case of (1.2), it would yield two Dirac masses for one linear measurement. We provide in this chapter a refined analysis of the case of variational problems, which ensures at most M extreme points.

1.1.3 Statement of the main theorem

Let $R : V \rightarrow \mathbb{R} \cup \{+\infty\}$, $f : \mathbb{R}^M \rightarrow \mathbb{R} \cup \{+\infty\}$ be two convex functions, and $\Phi : V \rightarrow \mathbb{R}^M$ be linear. Possibly redefining f and reducing M , it is not restrictive to assume that Φ is surjective. The main result of this chapter describes the faces² of the solution set \mathcal{S} to the problem

$$\min_{u \in V} R(u) + f(\Phi u). \quad (\mathcal{P})$$

Under some assumptions detailed below, it describes the points $p \in \mathcal{S}$ as a convex combinations of “atoms”, *i.e.* extreme points (or points in extreme rays), of the level set

$$\{R \leq R(p)\} \stackrel{\text{def.}}{=} \{u \in V \mid R(u) \leq R(p)\}. \quad (1.8)$$

To state the theorem, we also need to introduce the level set of the fidelity term,

$$\{f \leq f(\Phi p)\} \stackrel{\text{def.}}{=} \{w \in \mathbb{R}^M \mid f(w) \leq f(\Phi p)\}. \quad (1.9)$$

The main result of this chapter is the following theorem; its proof is sketched in Section 1.3 below.

Theorem 1.1 ([12, Thm. 1]). *Let $R : V \rightarrow \mathbb{R} \cup \{+\infty\}$, $f : \mathbb{R}^M \rightarrow \mathbb{R} \cup \{+\infty\}$ be two convex functions, and let $\Phi : V \rightarrow \mathbb{R}^M$ be linear. Assume that $R(p) + f(\Phi p) = \min(\mathcal{P}) < +\infty$, and that p belongs to a face of \mathcal{S} with dimension $j < +\infty$.*

Let k (resp. ℓ) denote the dimension of the minimal face of p in $\{R \leq R(p)\}$ (resp. Φp in $\{f \leq f(\Phi p)\}$). Then $k + \ell \leq s$, where

$$s \stackrel{\text{def.}}{=} \begin{cases} M + j - 2 & \text{if } p \text{ satisfies the double obliqueness condition described in Definition 1.1,} \\ M + j - 1 & \text{if } (R(p) > \inf R) \text{ or } (f(\Phi p) > \inf f), \\ M + j & \text{otherwise.} \end{cases} \quad (1.10)$$

¹In the rest of the chapter, we omit the mention “at most”, with the convention that some points may be chosen identical.

²Though the reader may be familiar with them, the notions from convex analysis such as face, extreme point, linear closure... are recalled in Section 1.2 below.

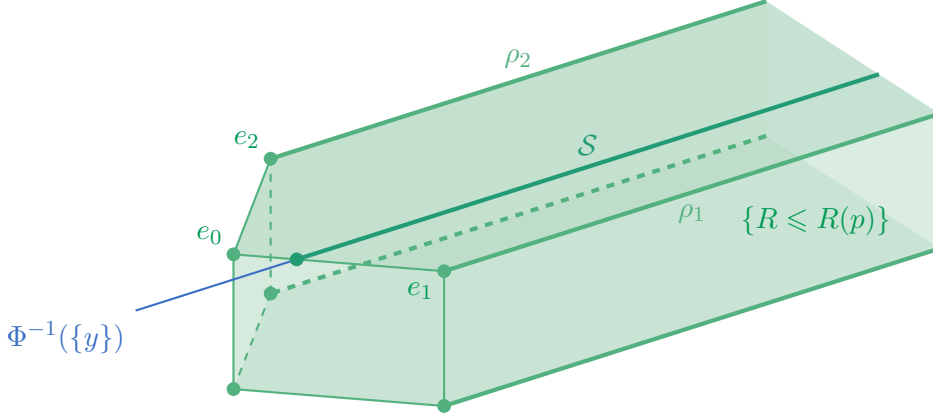


Figure 1.1: An illustration of [Corollary 1.1](#), for $M = 2$, $f(w) = \chi_{\{y\}}(w)$ and $R(p) > \inf R$. The solution set $\mathcal{S} = \{R \leq R(p)\} \cap \Phi^{-1}(\{y\})$ is made of an extreme point and an extreme ray. The extreme point is a convex combination of $\{e_0, e_1\}$. Depending on their position, the points in the ray are a convex combination of $\{e_0, e_1, e_2\}$ or a pair of points, one in ρ_1 and the other in ρ_2 .

The double obliqueness condition relates the faces in the level sets of R and f respectively, and those of the corresponding points in their epigraphs. We postpone its description to [Definition 1.1](#) below.

Combining [Theorem 1.1](#) with Klee's extension of the Minkowski-Carathéodory theorem, one obtains

Corollary 1.1 ([12, Cor. 1]). *Under the assumptions of [Theorem 1.1](#), if, moreover, $\{R \leq R(p)\}$ is linearly closed and contains no line, then p can be written as a convex combination of (at most) $k+1$ extreme points of $\{R \leq R(p)\}$, or k points of $\{R \leq R(p)\}$, each an extreme point or a point in an extreme ray, with the inequality $k \leq s - \ell$.*

A variant where $\{R \leq R(p)\}$ contains a line is discussed in [Section 1.3.4](#).

Example of the equality constraint problem. Let us fix some $y \in \mathbb{R}^M$ and set $f(w) = \chi_{\{y\}}(w)$, i.e. $f(w) = 0$ if $w = y$ and $+\infty$ otherwise. In that case $\ell = 0$ and the double obliqueness condition never holds, yielding the upper-bound $k \leq M + j - 1$ or $k \leq M + j$, depending on whether $R(p) > \inf R$ or not.

That choice encompasses the problems considered in [Section 1.1.1](#). If R is the total variation of measures, $R(p) = \inf R$ implies $p = 0$, so the conclusion of [Corollary 1.1](#) is trivial. For $R(p) > \inf R = 0$ and $j = 0$, the theorem describes *each extreme point* of \mathcal{S} as a convex combination of M extreme points of $\{R \leq R(p)\}$, i.e. rescaled signed Dirac masses. We recover the M atoms of the Fisher-Jerome theorem.

For more general regularizers, the level set $\{R \leq R(p)\}$ might be unbounded and the description might involve a convex combination of $M - 1$ points, each an extreme point or a point in an extreme ray. Points where $j = 1$ are also worth examining: *each point p on an extreme ray* of \mathcal{S} is a convex combination of $M + 1$ extreme points of $\{R \leq R(p)\}$, or a convex combination of M points of $\{R \leq R(p)\}$, each an extreme point or in an extreme ray. Hence, provided the assumptions of Klee's theorem (see (1.7)) hold, [Theorem 1.1](#) completely characterizes the solution set. An illustration is provided in [Figure 1.1](#).

Example of strictly convex fidelity terms f . More generally, if f is strictly convex, then $\ell = 0$ and we obtain the same conclusions as in the case of the equality constraint.

Positive values of ℓ . Whereas the cases of the equality constraint and the strictly convex fidelity term are the most common, one might be interested in polyhedral fidelity terms such as the ℓ^1 or the ℓ^∞ norms. In that case, it is worth considering that Φp might lie on a face with dimension $\ell > 0$.

Comparison with the Dubins-Klee theorem. Our theorem is directly inspired by the Dubins theorem (see Section 1.1.2 for its statement) and its extension to unbounded sets by V. Klee [Kle63]. In the case of equality constraints, observing that the solution set is $\mathcal{S} = \{R \leq R(p)\} \cap \Phi^{-1}\{y\}$, it is tempting to apply the Dubins-Klee theorem to deduce Theorem 1.1. However, it only yields the more pessimistic part of the theorem (*i.e.* $R(p) = \inf R$ and $f(\Phi p) = \inf f$), where $\{R \leq R(p)\}$ and $\Phi^{-1}(\{y\})$ can be in arbitrary positions. Compared to (1.3) and (1.4), it describes a solution with (at most) $M+1$ “atoms” instead of M (*e.g.* one measurement would be explained by a signal with two spikes, which is too much).

As we have shown in [3], that situation is not representative of most convex optimization problems, where $R(p) > \inf R$. That property imposes constraints on the relative positions of $\{R \leq R(p)\}$ and $\Phi^{-1}(\{y\})$, thus reducing the dimension of the face and the number of atoms.

1.2 Convex sets, faces and extreme points

This section is a reminder of some basic facts and definitions about convex sets in a real vector space. Convexity and the properties of convex sets play a crucial part in the present dissertation. While most of them are well-known and can be found in Rockafellar’s monograph [Roc97], the exposition in [Roc97] focuses on a finite-dimensional setting, which is too restrictive for our purpose. Hence, we refer here to the papers [Dub62, Kle57] and the treatise [Bou07b]. Once the appropriate definitions and their immediate consequences have been introduced, the proof of the main theorem is relatively straightforward.

1.2.1 Convex sets and their faces

Let V denote a (finite or infinite-dimensional) real vector space. Given two points x and y in V , we define the closed interval (or line segment) joining x to y as $[x, y] \stackrel{\text{def.}}{=} \{tx + (1-t)y \mid 0 \leq t \leq 1\}$, and the open interval joining x to y as $]x, y[\stackrel{\text{def.}}{=} [x, y] \setminus \{x, y\}$. A line (resp. an open half line) is a set of the form $a + \mathbb{R}v$ (resp. $\{a + tv \mid t > 0\}$) where $a, v \in V$ and $v \neq 0$. In the following, $C \subseteq V$ denotes a *convex set*, *i.e.* for any $x, y \in C$, the segment $[x, y]$ lies in C .

Internal points. Let $W \subseteq V$ be an affine space containing C . A point $u \in C$ is called an *internal point to C with respect to W* if, for any line L of W which contains u , there is an open interval in $L \cap C$ which contains u . In other words,

$$\forall v \in W, \quad \exists \varepsilon > 0, \quad \forall \lambda \in]-\varepsilon, \varepsilon[, \quad u + \lambda(v - u) \in C. \quad (1.11)$$

When $W = V$, we simply say that u is *internal* to C and the set of all internal points to C , denoted by $\text{core}(C)$, is often called the *algebraic interior* (or *core*) of C . If V is endowed with the structure of a topological vector space, then the topological interior of C is contained in $\text{core}(C)$; and if the topological interior of C is nonempty, they both coincide.

When W is the affine hull of C , i.e. $W = \text{Aff } C$, we say that u belongs to the *relative algebraic interior* of C , or to its *intrinsic core*, which we denote by $u \in \text{rcore}(C)$. From [Kle57, Prop. 2.3], u is in the relative algebraic interior of C if and only if

$$\forall v \in C \setminus \{u\}, \exists z \in C, u \in]v, z[. \quad (1.12)$$

We say that C is *internal* if $\text{rcore}(C) = C$.

Remark 1.1. *Contrary to the finite-dimensional case, the relative algebraic interior of a nonempty convex set might be empty. For instance, let V be the space of Lebesgue integrable functions on $]0, 1[$ and C be the set functions which are nonnegative almost everywhere. For any $u \in C$, it is possible to find $v \in C$ such that for all $\theta > 0$, $(u - \theta v) \notin C$.*

➤ Indeed, let $t_0 \in]0, 1[$ be a Lebesgue point of u and let $A \stackrel{\text{def.}}{=} \{t \in [0, 1] \mid |u(t) - u(t_0)| \geq 1\}$. As $r \rightarrow 0$,

$$\frac{1}{|B(t_0, r)|} |A \cap B(t_0, r)| \leq \frac{1}{|B(t_0, r)|} \int_{B(t_0, r)} |u(t) - u(t_0)| dt \rightarrow 0. \quad (1.13)$$

Now, define $v = 1/|t - t_0|^{1/3}$. For all $\theta > 0$, provided $r > 0$ is small enough, $|t - t_0| < r$ implies $\theta v(t) > u(t_0) + 1$. By (1.13), possibly reducing r , we may also assume that $|B(t_0, r) \setminus A| \geq \frac{1}{2} |B(t_0, r)| > 0$. Hence $u - \theta v < 0$ on the set $B(t_0, r) \setminus A$ which has positive Lebesgue measure.

Thus, for all $\lambda < 0$, setting $\theta = -\lambda/(1-\lambda)$, we have $u + \lambda(v-u) \notin C$, hence $u \notin \text{rcore}(C)$. Since this holds for all $u \in C$, $\text{rcore}(C) = \emptyset$.

Extreme points, extreme rays and faces. A point x of the convex set C is an *extreme point* of C if there is no open interval in C containing x , or equivalently if $C \setminus \{x\}$ is convex. An *extreme ray* ρ of C is a half-line contained in C such that any open interval I which intersects ρ must satisfy $I \subseteq \rho$.

More generally, a subset F of C is said to be a *face* of C if F is convex and, for all $x \in F$ and any open interval $I \subseteq C$ containing x , $I \subset F$. An alternative definition of an extreme point is “a point x such that $\{x\}$ is a face of C ”. Similarly, extreme rays may be defined as the half-lines which are a face of C . One may check that if F is a face of C and F' is a face of F , then F' is a face of C . The dimension of a face, $\dim F$, is defined as the dimension of its affine hull $\text{Aff}(F)$.

Elementary faces. A canonical choice of face is given by the notion of *elementary face*. Given a convex set C and $x \in C$, let us define $\mathcal{F}_C(x)$ as the intersection of all the faces of C which contain x . It is also a face, hence it is the *minimal face* of C (for the inclusion) which contains x . We call such sets the elementary faces of C . It turns out that $\mathcal{F}_C(x)$ is equal to the largest internal subset of C which contains x (see [Dub62, Th. 2.1]), hence it is the union of $\{x\}$ and all the open intervals of C which contain x . Moreover, $y \in \mathcal{F}_C(x)$ if and only if $\mathcal{F}_C(x) = \mathcal{F}_C(y)$, hence the elementary faces yield a *partition* of C .

The behavior of the elementary faces when performing several operations on convex sets is described below.

Intersection. Since the elementary face $\mathcal{F}_C(x)$ is the union of $\{x\}$ and all the open intervals of a convex set which contain x , one may check that if C_1 and C_2 are two convex sets,

$$\mathcal{F}_{C_1 \cap C_2}(x) = \mathcal{F}_{C_1}(x) \cap \mathcal{F}_{C_2}(x). \quad (1.14)$$

Moreover, if $W_{1,2}$, W_1 , W_2 respectively denote the affine hulls of those faces, they consist in the collection of lines through x which respectively intersect $C_1 \cap C_2$, C_1 , C_2 through an open interval. As a consequence,

$$W_{1,2} = W_1 \cap W_2. \quad (1.15)$$

Cartesian product. If C_1 , C_2 are convex subsets of the vector spaces V_1 , V_2 , it is possible to check that $\mathcal{F}_{C_1}(x_1) \times \mathcal{F}_{C_2}(x_2)$ is both a face of $C_1 \times C_2$ and an internal set. As a result,

$$\mathcal{F}_{C_1 \times C_2}((x_1, x_2)) = \mathcal{F}_{C_1}(x_1) \times \mathcal{F}_{C_2}(x_2). \quad (1.16)$$

Moreover, if $W_{1,2}$, W_1 , W_2 respectively denote the affine hulls of the above-mentioned faces, it holds

$$W_{1,2} = W_1 \times W_2. \quad (1.17)$$

Affine map. If $\psi : V_1 \rightarrow V_2$ is an affine bijective map, it preserves the elementary faces:

$$\mathcal{F}_{\psi(C)}(\psi(x)) = \psi(\mathcal{F}_C(x)). \quad (1.18)$$

If W_1 (resp. W_2) denotes the affine hull $\mathcal{F}_C(x)$ (resp. $\mathcal{F}_{\psi(C)}(\psi(x))$),

$$W_2 = \psi(W_1). \quad (1.19)$$

1.2.2 Linearly bounded and linearly closed sets

We say that C is *linearly bounded* if the intersection of C with any line is a bounded set. Similarly, C is *linearly closed* if its intersection with any line yields a closed interval. If V is endowed with the structure of a topological vector space and C is closed for that topology, then, by the continuity of the vector addition and scalar multiplication, C is linearly closed. Obviously, the converse is not true, as any dense proper vector subspace of V is linearly closed but not closed.

If V is finite-dimensional, C is linearly closed if and only if it is closed. If, moreover, C contains no line, its points can be described as a convex combination as explained in [Section 1.1.2](#).

The intersection of all the linearly closed sets which contains C is its *linear closure*. If C is linearly closed and F is a face of C , the linear closure of F is also a face (see [\[Dub62, Prop. 6.1\]](#)).

Example 1.1. Consider the square $C = [0, 1]^2 \subseteq \mathbb{R}^2$. Its elementary faces are $]0, 1[^2$, $]0, 1[\times \{0\}$, $]0, 1[\times \{1\}$, $\{0\} \times]0, 1[$, $\{1\} \times]0, 1[$, $\{(0, 0)\}$, $\{(0, 1)\}$, $\{(1, 0)\}$ and $\{(1, 1)\}$. Their respective linear closures are $[0, 1]^2$, $[0, 1] \times \{0\}$, $[0, 1] \times \{1\}$, $\{0\} \times [0, 1]$, $\{1\} \times [0, 1]$, $\{(0, 0)\}$, $\{(0, 1)\}$, $\{(1, 0)\}$ and $\{(1, 1)\}$. They are also faces of C .

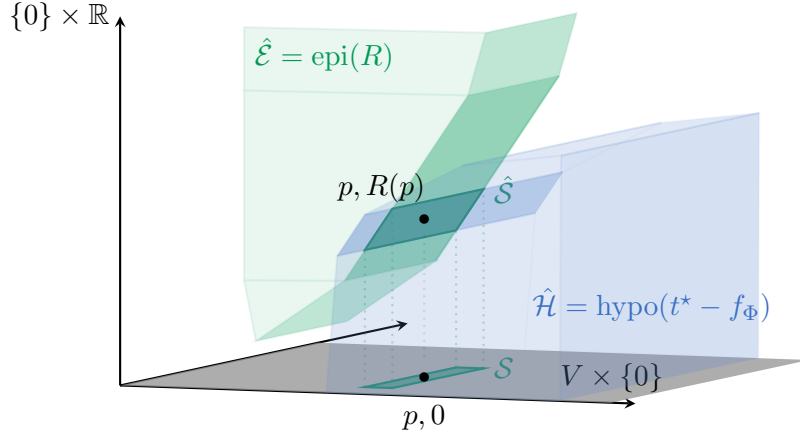


Figure 1.2: The solution set \mathcal{S} is equivalent, up to an affine isomorphism, to the set $\hat{\mathcal{S}}$ (see [Lemma 1.1](#)).

1.3 An epigraphical approach to the representer theorem

Let us consider R, f, Φ as described in [Section 1.1.3](#). Note that, possibly composing Φ with a linear map and reducing the value of M , we may assume that Φ is surjective, i.e. $\text{rank}(\Phi) = M$. For brevity, we define $f_\Phi(u) \stackrel{\text{def.}}{=} f(\Phi u)$. Our goal is to study the problem

$$\min_{u \in V} R(u) + f_\Phi(u). \quad (\mathcal{P})$$

We consider a solution $p \in \mathcal{S}$ (we assume $R(p) < +\infty$ and $f_\Phi(p) < +\infty$).

Instead of directly studying the elementary face of p in \mathcal{S} and in the level sets $\{R \leq R(p)\}, \{f_\Phi \leq f_\Phi(p)\}$, we work with epigraphs and we consider $\hat{\mathcal{S}} \stackrel{\text{def.}}{=} \{(u, R(u)) \mid u \in \mathcal{S}\}$ (see [Fig. 1.2](#) for an illustration). Introducing the epigraph of R and the hypograph of $t^* - f_\Phi$,

$$\hat{\mathcal{E}} \stackrel{\text{def.}}{=} \text{epi}(R) \stackrel{\text{def.}}{=} \{(u, r) \in V \times \mathbb{R} \mid R(u) \leq r\}, \quad (1.20)$$

$$\hat{\mathcal{H}} \stackrel{\text{def.}}{=} \text{hypo}(t^* - f_\Phi) \stackrel{\text{def.}}{=} \{(u, r) \in V \times \mathbb{R} \mid t^* - f_\Phi(u) \geq r\}, \quad (1.21)$$

we note that $\hat{\mathcal{E}}$ and $\hat{\mathcal{H}}$ are convex, with $\hat{\mathcal{S}} = \hat{\mathcal{E}} \cap \hat{\mathcal{H}}$.

➤ Indeed, if $(u, r) \in \hat{\mathcal{E}} \cap \hat{\mathcal{H}}$, then $R(u) \leq r \leq t^* - f_\Phi(u)$, hence

$$R(u) + f_\Phi(u) \leq r + f_\Phi(u) \leq t^*.$$

Since $t^* = \inf(\mathcal{P})$, the left-hand side is bounded below by t^* , hence $u \in \mathcal{S}$ and $r = R(u)$. This proves that $\hat{\mathcal{E}} \cap \hat{\mathcal{H}} \subseteq \hat{\mathcal{S}}$. The converse inclusion is straightforward.

The cornerstone of the epigraphical approach is the observation that \mathcal{S} and $\hat{\mathcal{S}}$ are isomorphic (hence have the same facial structure, see [\(1.18\)](#)).

Lemma 1.1 ([12, Lem. 1]). *There is an affine map $L : \text{Aff}(\mathcal{S}) \rightarrow \mathbb{R}$ such that R coincides with L on \mathcal{S} . Moreover, the map $\hat{L} : \text{Aff}(\mathcal{S}) \rightarrow \text{Aff}(\hat{\mathcal{S}})$ defined by $\hat{L}(v) \stackrel{\text{def.}}{=} (v, L(v))$ is bijective and $\hat{L}(\mathcal{S}) = \hat{\mathcal{S}}$.*

The existence of L in [Lemma 1.1](#) follows from the fact that R should be both convex and concave in \mathcal{S} . The rest of the proof of [Theorem 1.1](#) consists in relating the dimension of the faces in $\hat{\mathcal{E}}$ and $\hat{\mathcal{H}}$, and then converting that relation in terms of the level sets of R and f .

1.3.1 A relation between the faces of the epigraphs

From the description of the elementary faces of an intersection (see (1.14)),

$$\mathcal{F}_{\hat{\mathcal{E}} \cap \hat{\mathcal{H}}}(p, R(p)) = \mathcal{F}_{\hat{\mathcal{E}}}(p, R(p)) \cap \mathcal{F}_{\hat{\mathcal{H}}}(p, R(p)). \quad (1.22)$$

To understand the dimension of the above-mentioned faces, we need to consider their affine hulls. Up to a translation of the origin in $V \times \mathbb{R}$, we assume without loss of generality that $(p, R(p)) = (0, 0)$. In particular, *all the affine hulls of the elementary faces of $p, R(p)$ are now linear hulls*.

Lemma 1.2. *The following relation holds.*

$$\dim \mathcal{F}_{\hat{\mathcal{E}}}(p, R(p)) + \dim \mathcal{F}_{\text{hypo}(t^* - f)}(\Phi p, f(\Phi p)) = M + 1 + j - \text{codim}_{V \times \mathbb{R}}(\hat{E} + \hat{H}) \quad (1.23)$$

where \hat{E} (resp. \hat{H}) denotes the affine hull of $\mathcal{F}_{\hat{\mathcal{E}}}(p, R(p))$ (resp. $\mathcal{F}_{\hat{\mathcal{H}}}(p, R(p))$).

Proof. Let \hat{S} (resp. \hat{E} and \hat{H}) be the linear hull of $\mathcal{F}_{\hat{\mathcal{E}} \cap \hat{\mathcal{H}}}(0, 0)$ (resp. $\mathcal{F}_{\hat{\mathcal{E}}}(0, 0)$ and $\mathcal{F}_{\hat{\mathcal{H}}}(0, 0)$). From (1.15), we note that $\hat{S} = \hat{E} \cap \hat{H}$, and by classical results in linear algebra³,

$$\dim \hat{E} = \dim(\hat{E} \cap \hat{H}) + \text{codim}_{\hat{E}}(\hat{E} \cap \hat{H}), \quad (1.24)$$

$$\text{codim}_{\hat{E}}(\hat{E} \cap \hat{H}) = \text{codim}_{\hat{E} + \hat{H}}(\hat{H}) = \text{codim}_{V \times \mathbb{R}} \hat{H} - \text{codim}_{V \times \mathbb{R}}(\hat{E} + \hat{H}). \quad (1.25)$$

Combining the above equalities, we get

$$\dim \hat{E} = \text{codim}_{V \times \mathbb{R}} \hat{H} + \dim(\hat{S}) - \text{codim}_{V \times \mathbb{R}}(\hat{E} + \hat{H}). \quad (1.26)$$

We note from Lemma 1.1 and (1.18) that $\dim(\hat{S}) = \dim \mathcal{F}_{\hat{\mathcal{S}}}(p, R(p)) = \dim \mathcal{F}_{\mathcal{S}}(p) = j$.

Now, we compute $\text{codim}_{V \times \mathbb{R}} \hat{H}$. Let W be a linear complement to $\ker \Phi$ in V . Since $\text{rank } \Phi = M$, the restriction $\Phi|_W: W \rightarrow \mathbb{R}^M$ is an isomorphism. As a result, the mapping

$$\psi: \begin{array}{ccccc} V \times \mathbb{R} & \longrightarrow & \ker \Phi \times W \times \mathbb{R} & \longrightarrow & (\ker \Phi) \times (\mathbb{R}^M \times \mathbb{R}) \\ (u, r) & \longmapsto & (k, w, r) & \longmapsto & (k, (\Phi w, r)) \end{array}$$

(where (k, w) is the unique element in $\ker \Phi \times W$ such that $u = k + w$) is an isomorphism.

In particular, since ψ maps $\hat{\mathcal{H}}$ to $\ker \Phi \times (\text{hypo}(t^* - f))$,

$$\begin{aligned} \psi(\mathcal{F}_{\hat{\mathcal{H}}}(u, r)) &= \mathcal{F}_{\psi(\hat{\mathcal{H}})}(\psi u, r) \\ &= \mathcal{F}_{\ker \Phi \times (\text{hypo}(t^* - f))}((k, (\Phi w, r))) \\ &= \ker \Phi \times \mathcal{F}_{\text{hypo}(t^* - f)}((\Phi w, r)). \end{aligned}$$

Applying this to $(u, r) = (p, R(p)) = (0, 0)$ and considering the linear spans, we obtain

$$\text{codim}_{V \times \mathbb{R}} \hat{H} = M + 1 - \hat{\ell}, \quad (1.27)$$

where $\hat{\ell}$ is the dimension of $\mathcal{F}_{\text{hypo}(t^* - f)}(0, 0)$. □

³The first equality in (1.25) is a generalization of the Grassmann formula $\dim(F \cap G) + \dim(F + G) = \dim F + \dim G$. It follows from the existence of a linear isomorphism $F/(F \cap G) \approx (F + G)/G$, see for instance [Lan02, Ch. 3, Sec. 1]

1.3.2 From the faces in the epigraphs to the faces in the level sets.

The next step is to relate the elementary faces of p in $\{R \leq R(p)\}$ and $\{f_\Phi \leq f_\Phi(p)\}$ to those of $(p, R(p))$ in $\hat{\mathcal{E}}$ and $\hat{\mathcal{H}}$. Intuitively (see Figure 1.2), when going from epigraphs to level sets, the dimension is reduced if the face is “oblique”, and it does not change if the face is “horizontal”. This is what we formalize now.

The regularizer. Since $\hat{\mathcal{E}} \cap (V \times \{0\}) = \{R \leq 0\} \times \{0\}$, using (1.14) and (1.16) we obtain

$$\mathcal{F}_{\hat{\mathcal{E}}}(0, 0) \cap (V \times \{0\}) = \mathcal{F}_{\hat{\mathcal{E}} \cap (V \times \{0\})}(0, 0) = \mathcal{F}_{\{R \leq 0\}}(0) \times \{0\}. \quad (1.28)$$

Let $E \stackrel{\text{def.}}{=} \text{Span}(\mathcal{F}_{\{R \leq 0\}}(0)) \subseteq V$. From (1.15), we note that the linear spans \hat{E} and E are related through $\hat{E} \cap (V \times \{0\}) = E \times \{0\}$. As a result

$$\dim \hat{E} = \dim E + \text{codim}_{\hat{E}}(E \times \{0\}), \quad (1.29)$$

where $\text{codim}_{\hat{E}}(E \times \{0\}) \in \{0, 1\}$.

➤ This follows from

$$\text{codim}_{\hat{E}}(\hat{E} \cap (V \times \{0\})) = \text{codim}_{\hat{E} + V \times \{0\}}(V \times \{0\}) \leq \text{codim}_{V \times \mathbb{R}}(V \times \{0\}) = 1. \quad (1.30)$$

If $\text{codim}_{\hat{E}}(E \times \{0\}) = 0$, we say that the face $\mathcal{F}_{\hat{\mathcal{E}}}(0, 0)$ is *horizontal*. Otherwise we say that it is *oblique*.

The fidelity term. For similar reasons, with straightforward adaptations,

$$\hat{\ell} \stackrel{\text{def.}}{=} \dim \mathcal{F}_{\text{hypo}(t^*-f)}(0, 0) = \dim \mathcal{F}_{\{f \leq f(0)\}}(0) + \begin{cases} 0 & \text{if } \mathcal{F}_{\text{hypo}(t^*-f)}(0, 0) \text{ is horizontal,} \\ 1 & \text{if } \mathcal{F}_{\text{hypo}(t^*-f)}(0, 0) \text{ is oblique.} \end{cases} \quad (1.31)$$

The obliqueness condition. We are now in position to define the obliqueness condition of Theorem 1.1.

Definition 1.1. We say that p satisfies the double obliqueness condition if both $\mathcal{F}_{\hat{\mathcal{E}}}(p, R(p))$ and $\mathcal{F}_{\text{hypo}(t^*-f)}(\Phi p, f(\Phi p))$ are oblique. In other words,

$$\dim \mathcal{F}_{\hat{\mathcal{E}}}(p, R(p)) = \dim \mathcal{F}_{\{R \leq R(p)\}}(p) + 1 \quad (1.32)$$

$$\text{and } \dim \mathcal{F}_{\text{hypo}(t^*-f)}(\Phi p, f(\Phi p)) = \dim \mathcal{F}_{\{f \leq f(\Phi p)\}}(\Phi p) + 1. \quad (1.33)$$

1.3.3 Proof of the main theorem

The last step is to prove that $\text{codim}_{V \times \mathbb{R}}(\hat{E} + \hat{H})$ is not zero. In other words, $\mathcal{F}_{\hat{\mathcal{E}}}(p, R(p))$ and $\mathcal{F}_{\hat{\mathcal{H}}}(p, R(p))$ do not span the whole space $V \times \mathbb{R}$.

Lemma 1.3 ([12, Lem. 2]). The following inequality holds: $\text{codim}_{V \times \mathbb{R}}(\hat{E} + \hat{H}) \geq 1$.

If both $\mathcal{F}_{\hat{\mathcal{E}}}(p, R(p))$ and $\mathcal{F}_{\hat{\mathcal{H}}}(p, R(p))$ are horizontal and $R(0) > \inf R$ or $f_\Phi(0) > \inf f_\Phi$, then $\text{codim}_{V \times \mathbb{R}}(\hat{E} + \hat{H}) \geq 2$.

We omit the proof and we refer the interested reader to [12]. The idea is that in any case, the union of both faces does not span the vertical line through $(p, R(p))$, otherwise it would contradict the optimality of p . In the special case, one can find, in addition, a horizontal line which is not spanned by the union of $\mathcal{F}_{\hat{\mathcal{E}}}(p, R(p))$ and $\mathcal{F}_{\hat{\mathcal{H}}}(p, R(p))$.

The conclusion of Theorem 1.1 follows by combining Lemma 1.2 with the above results and examining all the possible cases to get an upper-bound on the dimension of the faces. As for Corollary 1.1, it follows from V. Klee's extension of Carathéodory's theorem (see Section 1.1.2): the closure of the k -dimensional convex set $\mathcal{F}_{\{R \leq R(p)\}}(p)$ can be described as a convex combination of k of its extreme points, or $k - 1$ points, each an extreme point or a point in an extreme ray. Moreover those extreme points or extreme rays must also be extremal with respect to $\{R \leq R(p)\}$, which yields the claimed result.

1.3.4 The case of level sets containing lines

The reader might be intrigued by the assumption of Theorem 1.1 that $\{R \leq R(p)\}$ contains no line, since in several applications the regularizer R is invariant by the addition of, *e.g.*, constant functions or low-degree polynomials (see Section 1.4.1). In that case, one is generally interested in the non-constant or non-polynomial part, and it is natural to consider a quotient space in which the constant or polynomial parts are ignored.

Convex sets and their lineality space. Before extending Theorem 1.1 to this more general case, we need to recall several properties of convex sets containing lines (see for instance [Kle57] or [Roc97, Ch.8]). We say that a nonempty convex set $C \subseteq V$ is invariant in the direction $v \in V$ if

$$C + \mathbb{R}v \subseteq C. \quad (1.34)$$

The collection of all vectors $v \in V$ such that (1.34) holds is a vector space called the *lineality space* of C , denoted by $\text{lin}(C)$.

If C is internal or linearly closed, given $v \in V \setminus \{0\}$, it is equivalent to say that C is invariant in the direction v , or to say that C contains a line directed by v , *i.e.* $(x_0 + \mathbb{R}v) \subseteq C$ for some $x_0 \in V$. As a consequence, if C_1, C_2 are two nonempty convex sets, then $\text{lin}(C_1) \cap \text{lin}(C_2) \subseteq \text{lin}(C_1 \cap C_2)$, with equality if C_1 and C_2 are both internal or both linearly closed.

If W is a linear complement⁴ to $\text{lin}(C)$, then $C = \tilde{C} + \text{lin}(C)$ where $\tilde{C} \stackrel{\text{def}}{=} C \cap W$. The corresponding decomposition is unique in the sense that any element of C can be decomposed in a unique way as the sum of an element of \tilde{C} and $\text{lin}(C)$. If C is internal (resp. linearly closed), then \tilde{C} contains no line, and it is internal (resp. linearly closed).

The faces of C are related to those of \tilde{C} by

$$\mathcal{F}_C(p) = \mathcal{F}_{\tilde{C}}(\tilde{p}) + \text{lin}(C), \quad (1.35)$$

where \tilde{p} is the projection of p onto W parallel to $\text{lin}(C)$.

It is sometimes convenient to quotient the ambient space by $\text{lin}(C)$ when the considered properties do not really depend on the choice of W . As the canonical surjection $\pi_{\text{lin}(C)} : V \rightarrow V/\text{lin}(C)$ induces an isomorphism from W to $V/\text{lin}(C)$, it preserves the facial structure of \tilde{C} ,

$$\pi_{\text{lin}(C)}(\mathcal{F}_{\tilde{C}}(\tilde{p})) = \mathcal{F}_{\pi_{\text{lin}(C)}(C)}(\pi_{\text{lin}(C)}(p)), \quad (1.36)$$

and both are equal to $\pi_{\text{lin}(C)}(\mathcal{F}_C(p))$.

⁴In this dissertation, we use freely the axiom of choice, hence any subspace of V admits a complement subspace.

Back to the optimization problem. Let $K = \text{lin}(\{R \leq R(p)\})$ and $N \stackrel{\text{def.}}{=} \ker \Phi$. We note that $\mathcal{F}_S(p)$ is invariant by $K \cap N$.

➤ Indeed, the face of the epigraph $\mathcal{F}_{\hat{\mathcal{E}}}(p, R(p))$ is internal and contains $K \times \{R(p)\}$, hence it is invariant by $\hat{K} \stackrel{\text{def.}}{=} K \times \{0\}$. On the other hand, the hypograph $\hat{\mathcal{H}}$ (hence $\mathcal{F}_{\hat{\mathcal{H}}}(p, R(p))$) is invariant by $\hat{N} \stackrel{\text{def.}}{=} N \times \{0\}$. From (1.22) we deduce that $\mathcal{F}_{\hat{\mathcal{E}} \cap \hat{\mathcal{H}}}(p, R(p))$ is invariant by $\hat{K} \cap \hat{N} = (K \cap N) \times \{0\}$. Since $\mathcal{F}_S(p)$ is its projection onto the horizontal hyperplane (see Lemma 1.1), it is invariant by $K \cap N$.

Therefore, $\pi_{K \cap N}(\mathcal{F}_S(p))$ is an internal set and $\mathcal{F}_S(p)$ is linearly isomorphic to $(K \cap N) \times \pi_{K \cap N}(\mathcal{F}_S(p))$. Instead of considering the dimension of $\mathcal{F}_S(p)$ to describe the point p , the following theorem relies on the dimension of the quotient set $\pi_{K \cap N}(\mathcal{F}_S(p))$.

Theorem 1.2 ([12, Thm. 2]). *Let $R : V \rightarrow \mathbb{R} \cup \{+\infty\}$, $f : \mathbb{R}^M \rightarrow \mathbb{R} \cup \{+\infty\}$ be two convex functions, and let $\Phi : V \rightarrow \mathbb{R}^M$ be linear. Assume that $p \in \mathcal{S}$, with $R(p) + f(\Phi p) < +\infty$, and that $\{R \leq R(p)\}$ is linearly closed. Let $K \stackrel{\text{def.}}{=} \text{lin}(\{R \leq R(p)\})$, $d \stackrel{\text{def.}}{=} \dim \Phi(K)$, and $N \stackrel{\text{def.}}{=} \ker \Phi$.*

If $\dim(\pi_{K \cap N}(\mathcal{F}_S(p))) = j < +\infty$, then $\pi_K(p)$ belongs to a face of $\pi_K(\{R \leq R(p)\})$ with dimension at most k , where

$$k \stackrel{\text{def.}}{=} \begin{cases} M - \ell + j - d - 1 & \text{if } (R(p) > \inf R) \text{ or } (f(\Phi p) > \inf f), \\ M - \ell + j - d & \text{otherwise.} \end{cases} \quad (1.37)$$

and ℓ is the dimension of the minimal face of Φp in $\{f \leq f(\Phi p)\}$.

In particular, $\pi_K(p)$ can be written as a convex combination of (at most):

- $k + 1$ extreme points of $\pi_K(\{R \leq R(p)\})$,
- or k points of $\pi_K(\{R \leq R(p)\})$, each an extreme point or a point in an extreme ray.

If, moreover, p satisfies the obliqueness condition described in Definition 1.1, the number k can be reduced to $M - \ell + j - d - 2$.

In particular, if $p_1, \dots, p_r \in \{R \leq R(p)\}$ are such that $\pi_K(p_1), \dots, \pi_K(p_r)$ denote those extreme points (or points in extreme rays),

$$p = \sum_{i=1}^r \theta_i p_i + u_K, \quad \text{where } \theta_i \geq 0, \sum_{i=1}^r \theta_i = 1, \quad \text{and } u_K \in K. \quad (1.38)$$

The interested reader may consult [12, Thm. 2] for the proof of Theorem 1.2. It relies again on linear algebra arguments so as to compute the dimensions of the relevant spaces.

Remark 1.2. *In practice, if $\hat{\mathcal{E}}$ is linearly closed (e.g. if R is lower semi-continuous for some topology), then the whole solution set \mathcal{S} is invariant by $(K \cap N)$, and $\pi_{K \cap N}(\mathcal{F}_S(p)) = (\mathcal{F}_{\pi_{K \cap N}(\mathcal{S})}(\pi_{K \cap N}(p)))$. However, the solution set \mathcal{S} may have more invariant directions than just $(K \cap N)$.*

1.4 Examples

1.4.1 Point source reconstruction

Following the pioneering works [BP13, dCG12, CFG14], variational models in the space of measures for point source reconstruction have recently drawn a lot of attention.

As in (1.2), the idea is to solve

$$\min_{m \in \mathcal{M}(X)} |m|(X) \quad \text{s.t.} \quad \Phi m = y \quad (1.39)$$

where $\mathcal{M}(X)$ is the space of bounded Radon measures on X , $\Phi m = \int_X \varphi(x) dm(x)$ where $\varphi \in \mathcal{C}_c(X; \mathbb{R}^M)$, and $|\cdot|(X)$ denotes the total variation of measures,

$$|m|(X) \stackrel{\text{def.}}{=} \sup \left\{ \int_X \psi(x) dm(x) \mid \psi \in \mathcal{C}_c(X), \sup_{x \in X} |\psi(x)| \leq 1 \right\}. \quad (1.40)$$

Since Theorem 1.1 treats strictly convex functions f equally, our discussion also concerns formulations like the BLASSO,

$$\min_{m \in \mathcal{M}(X)} \lambda |m|(X) + \frac{1}{2} \|\Phi m - y\|_2^2,$$

but we focus on (1.39) to fix ideas.

The total variation unit-ball. It is possible to prove (see for instance [BC19]) that the extreme points of $C_{\mathcal{M}} \stackrel{\text{def.}}{=} \{m \in \mathcal{M}(X) \mid |m|(X) \leq 1\}$ are precisely the measures of the form $\varepsilon \delta_x$ for $\varepsilon \in \{-1, +1\}$, $x \in X$. In fact, applying similar arguments as in [BC19] and Chapter 2, one may even show that the k -dimensional elementary faces of $C_{\mathcal{M}}$ are in one-to-one correspondence with the collections $\{(\varepsilon_i, x_i)\}_{i=0}^k$ where, for each i , $\varepsilon_i \in \{-1, +1\}$, $x_i \in X$ and $x_i \neq x_j$ for $j \neq i$. Each elementary face is then described by the convex combinations

$$\sum_{i=0}^k \theta_i \varepsilon_i \delta_{x_i}, \quad \text{with} \quad \sum_{i=0}^k \theta_i = 1 \quad \text{and} \quad \forall i \in \{0, \dots, k\}, \theta_i > 0. \quad (1.41)$$

In other words, the total variation unit ball is one of the simplest infinite-dimensional convex sets: *its k -dimensional faces are the simplices determined by $k+1$ extreme points* (corresponding to distinct positions). The cone $\mathcal{M}^+(X)$ of non-negative Radon measures has a similar structure, with straightforward adaptations.

Generalized splines. Following S.D. Fisher and J.W. Jerome [FJ75], we may consider more elaborate models involving functions whose “derivatives” are measures. Let L be a linear operator $L : \mathcal{D}'(X) \rightarrow \mathcal{D}'(X)$ and define $V \stackrel{\text{def.}}{=} L^{-1}(\mathcal{M}(X))$. The problem considered in [FJ75] (and later in [UFW17, FW19]) is

$$\min_{u \in V} |Lu|(X) \quad \text{s.t.} \quad \Phi u = y. \quad (1.42)$$

Typical examples include $L = D^m$ (in dimension $d = 1$) or $(-\Delta)^\gamma$ for $\gamma \geq d$. The main difficulty with (1.42) is to define a suitable topology which ensures some compactness, hence the existence of solutions and extreme points. We leave this delicate matter aside and we refer to [UFW17, FW19, GFU18] for more detail.

Assuming the existence of solutions and extreme points, let us discuss the geometric side. Let $C_{FJ} \stackrel{\text{def.}}{=} \{u \in V \mid |Lu|(X) \leq 1\}$. We assume that $L|_V : V \rightarrow \mathcal{M}(X)$ is *surjective*. In that case, with the notation of Section 1.3.4, the first isomorphism theorem ensures that $V/K \approx \mathcal{M}(X)$ where $K \stackrel{\text{def.}}{=} \ker L$, and $\pi_K(C_{FJ})$ is mapped isomorphically to $C_{\mathcal{M}}$. By Theorem 1.2, the extreme points of the solution set to (1.42) can be described as

$$u = \sum_{i=1}^M \theta_i u_i + u_K, \quad (1.43)$$

where $\sum_i \theta_i = |Lu|(X)$, $u_K \in K$ and for all i there exists $\varepsilon_i \in \{-1, +1\}$, $x_i \in X$ such that $Lu_i = \varepsilon_i \delta_{x_i}$. If a suitable pseudo-inverse $L^+ : \mathcal{M}(X) \rightarrow V$ has been defined, one may choose $u_i = \varepsilon_i L^+ \delta_{x_i}$ (see [FW19]).

For instance, if $L = D^m$, $\Omega = \mathbb{R}$, the solutions are *generalized splines*: for a.e. $t \in \mathbb{R}$,

$$u(t) = \sum_{i=1}^M \theta_i \rho(t - x_i) + a_0 + a_1 t + \dots + a_{m-1} t^{m-1}, \quad (1.44)$$

where $\rho(t) = \mathbb{1}_{]0, +\infty[}(t) \frac{t^{m-1}}{(m-1)!}$. See [GFU18] for more examples.

1.4.2 Semi-definite programs

Several optimization problems involve the reconstruction of positive semi-definite matrices (see for instance Section 7.3). Interestingly, the positive semi-definite cone $\mathcal{S}_n^+(\mathbb{R})$ has a special structure which shows that the number of points in the representation provided by Corollary 1.1 is sometimes too pessimistic.

Consider for instance the following constrained problem

$$\inf_{Q \in \mathcal{S}_n^+(\mathbb{R})} f(\Phi Q - y), \quad (1.45)$$

where $f : \mathbb{R}^M \rightarrow \mathbb{R} \cup \{+\infty\}$, and assume that a solution to (1.45) exists. As the extreme rays of the positive semi-definite cone $\mathcal{S}_n^+(\mathbb{R})$ are the p.s.d. matrices of rank 1 (see for instance [Dat05, Sec. 2.9.2.7]), we may deduce from Corollary 1.1 that there is also a solution which has rank (at most) M . However, that conclusion is not optimal, as a theorem by Barvinok [Bar95, Th. 2.2] ensures that, provided (1.45) has a solution, there is a solution Q with

$$\text{rank}(Q) \leq \frac{1}{2} \left(\sqrt{8M + 1} - 1 \right). \quad (1.46)$$

To understand the gap with Barvinok's result, we need to describe the faces of $\mathcal{S}_n^+(\mathbb{R})$ and to see how the Minkowski-Carathéodory theorem (or its extension by Klee) is too pessimistic in that case.

The faces of $\mathcal{S}_n^+(\mathbb{R})$. Let $Q \in \mathcal{S}_n^+(\mathbb{R}) \setminus \{0\}$ and assume that $R \in \mathcal{F}_{\mathcal{S}_n^+(\mathbb{R})}(Q) \setminus \{Q\}$. Since $\mathcal{F}_{\mathcal{S}_n^+(\mathbb{R})}(Q)$ is an elementary face, it is internal: there exists $S \in \mathcal{F}_{\mathcal{S}_n^+(\mathbb{R})}(Q)$, such that $Q \in]R, S[$ (see (1.12)). Let $\theta \in]0, 1[$ such that $Q = \theta R + (1 - \theta)S$. For all $x \in \ker Q$,

$$0 = x^\top Q x = \theta \underbrace{x^\top R x}_{\geq 0} + (1 - \theta) \underbrace{x^\top S x}_{\geq 0}, \quad (1.47)$$

hence $x \in \ker R \cap \ker S$. As a result, if a matrix R belongs to $\mathcal{F}_{\mathcal{S}_n^+(\mathbb{R})}(Q)$, then $\ker Q \subseteq \ker R$. Since $\mathcal{F}_{\mathcal{S}_n^+(\mathbb{R})}(Q) = \mathcal{F}_{\mathcal{S}_n^+(\mathbb{R})}(R)$, we may swap the roles of Q and R to obtain the converse inclusion, hence $\ker Q = \ker R$.

Conversely, assume that $R \in \mathcal{S}_n^+(\mathbb{R})$ has the same kernel as Q . The open interval

$$\{Q + t(R - Q) \mid t \in \mathbb{R}, -\delta < t < 1 + \delta\}$$

lies in $\mathcal{S}_n^+(\mathbb{R})$ for $\delta > 0$ sufficiently small. As it contains both Q and R , we deduce that $R \in \mathcal{F}_{\mathcal{S}_n^+(\mathbb{R})}(Q)$.

To summarize, *each elementary face of $\mathcal{S}_n^+(\mathbb{R})$ is uniquely determined by a vector subspace of \mathbb{R}^n which represents the common kernel of its elements.*

Carathéodory's theorem is not optimal for $\mathcal{S}_n^+(\mathbb{R})$. Fixing a basis of \mathbb{R}^n adapted to that subspace and its orthogonal complement, we see that a matrix Q is only determined by its entries corresponding to $\text{Im } Q$, that is $\frac{1}{2}r(r+1)$ coefficients, where $r = \text{rank } Q$. Taking small variations around Q , we deduce that

$$\dim \mathcal{F}_{\mathcal{S}_n^+(\mathbb{R})}(Q) = \frac{1}{2}r(r+1). \quad (1.48)$$

Inverting Eq. (1.48), we see that the rank of Q is $r = \frac{1}{2}(\sqrt{8d+1} - 1)$, where $d \stackrel{\text{def.}}{=} \dim \mathcal{F}_{\mathcal{S}_n^+(\mathbb{R})}(Q)$. As a result, Q is a convex combination of $\frac{1}{2}(\sqrt{8d+1} - 1)$ points in extreme rays, a value which is less than the value d predicted by Klee's extension of Carathéodory's theorem, but coincides with Barvinok's result.

More generally, Carathéodory's theorem only provides an upper bound on the number of extreme points (or points in extreme rays) needed to describe every point of a convex set. When the convex set has infinitely many extreme points (like the Euclidean ball, for instance), fewer extreme points might be sufficient in the convex combinations (*e.g.* 2, in the case of the Euclidean ball). The minimal number of elements in convex combinations need to describe all the points of a convex set, is called the *Carathéodory number* of that set (and it is bounded by $d+1$, where d is the dimension of the convex set). On the other hand, if the convex set has a finite number of extreme points, that upper bound is sharp (see the discussion in Section 2.3.3 in the context of the total gradient variation).

1.4.3 Interactions between the regularizer and the sensing operator

In Section 1.4.1, we have described the faces of $C_{\mathcal{M}}$ and $\mathcal{M}^+(X)$, and we have seen that the number of atoms needed to describe the elements of each face matches the bound given by the Carathéodory-Klee theorem. It is not difficult, at least when X is finite, to construct sensing operators Φ such that the bounds given in Corollary 1.1 are matched. On the other hand, we have seen in Section 1.4.2 that one needs fewer atoms than predicted by the Carathéodory-Klee theorem to describe the faces of cone $\mathcal{S}_n^+(\mathbb{R})$. That is a structural property of the convex set $\mathcal{S}_n^+(\mathbb{R})$ which is related to its having a continuous family of extreme rays (as opposed to a polyhedron for instance).

Now, we discuss another case where the prediction of Theorem 1.1 is not optimal, due to the interaction of the linear operator Φ and the level sets of the regularizer.

The truncated trigonometric moment problem. We consider the problem

$$\min_m \chi_{\mathcal{M}^+(\mathbb{T})}(m) \quad \text{s.t.} \quad \int_{\mathbb{T}} \varphi_k(t) dm(t) = y_k \quad (0 \leq k \leq 2f_c), \quad (1.49)$$

where $\mathcal{M}^+(\mathbb{T})$ is the set of nonnegative measures on the torus $\mathbb{T} = \mathbb{R}/\mathbb{Z}$, $y \in \mathbb{R}^{2f_c+1}$, and $\varphi_0(t) = 1$, $\varphi_{2j-1}(t) = \cos(j2\pi t)$ and $\varphi_{2j}(t) = \sin(j2\pi t)$ for $1 \leq j \leq f_c$.

The Carathéodory-Toeplitz theorem [Car07, Toe11] states that there is a solution to (1.49) if and only if the Hermitian matrix

$$T(c) \stackrel{\text{def.}}{=} \begin{pmatrix} c_0 & c_1 & \cdots & c_{f_c} \\ c_1^* & c_0 & \ddots & \vdots \\ \vdots & \ddots & \ddots & c_1 \\ c_{f_c}^* & \cdots & c_1^* & c_0 \end{pmatrix}, \quad \text{where} \quad c_j \stackrel{\text{def.}}{=} y_{2j-1} - iy_{2j}, \quad c_0 \stackrel{\text{def.}}{=} y_0,$$

is positive semi-definite. If $r \stackrel{\text{def.}}{=} \text{rank } T(c) \leq f_c$, the solution m is unique, and its support has cardinality r . If $T(c)$ is invertible, there are infinitely many solutions with cardinality

$f_c + 1$ (and more). In particular for any $t_0 \in \mathbb{T}$ there is a solution which charges $\{t_0\}$. Note that similar results hold for T-systems on an interval [KN77, Ch. 4, Sec. 4].

That result contrasts with Corollary 1.1 which would predict a sum of at most $2f_c + 1$ Dirac masses. Here, the situation is different from the case of $\mathcal{S}_n^+(\mathbb{R})$, since any measure belonging to a d -dimensional elementary face of $\mathcal{M}^+(\mathbb{T})$ is a sum of *exactly* d Dirac masses. As a result Carathéodory's theorem is sharp. Therefore, we must have $\dim \mathcal{F}_{\mathcal{M}^+(\mathbb{T})}(m) < 2f_c + 1$ and, recalling (1.23), we deduce that the lower bound on $\text{codim}_{V \times \mathbb{R}}(\hat{E} + \hat{H})$ provided by Lemma 1.3 is far too pessimistic. In other words, the affine spaces determined by the Fourier coefficients only intersect very specific faces of the cone $\mathcal{M}^+(\mathbb{T})$.

An intuitive explanation consists in counting the “degrees of freedom” of the problem (we do not consider the statistical notion used in [PP19], but simply the “number of variables that should be fixed”). Informally, to fix the positions and amplitudes of k Dirac masses, that is $2k$ variables, we need at least $2k$ equations, *i.e.* $2k \leq 2f_c + 1$.

With total variation regularization. Surprisingly, things are different if one replaces the nonnegativity constraint with the total variation regularization,

$$\min_{m \in \mathcal{M}(\mathbb{T})} |m|(\mathbb{T}) \quad \text{s.t.} \quad \int_{\mathbb{T}} \varphi_k(t) dm(t) = y_k \quad (0 \leq k \leq 2f_c), \quad (1.50)$$

(and $\{\varphi_k\}_{k=0}^{2f_c}$ is again the trigonometric system). Following an observation of L. Condat in [Con20], we have proved in [12] that the unique solution to (1.50) when y is the Fourier coefficient vector of two opposite close spikes is given by a Dirac comb with $2f_c$ masses (see Section 6.1.2 and in particular (6.5) for more detail).

As a consequence, the number of Dirac masses predicted by Theorem 1.1 is *almost optimal* ($2f_c + 1$ Dirac masses are predicted whereas $2f_c$ actually appear). In fact, one cannot do “better”: it is proved in [Con20] that for every $y \in \mathbb{R}^{2f_c+1}$, there is a solution to (1.50) which is a sum of at most $2f_c$ Dirac masses.

Arguing informally in terms of “degrees of freedom”, we note that the above situation is quite peculiar: the relative positions of the Dirac masses are fixed (see (6.5)), they can only move by a global translation. As a result, the $2f_c + 1$ variables determine the $2f_c$ amplitudes of the spikes and the last degree of freedom which is a global shift of the Dirac comb.

1.5 Conclusion

1.5.1 Summary

We have proposed in this chapter a representer theorem for convex variational problems. Given some solution p , it relates the dimension of the face of p in the solution set to the dimension of its face in the level set of the regularizer $\{R \leq R(p)\}$. Using a Carathéodory-type theorem, it is then possible to describe the solution as a combination of “atoms”. That representation principle allows to recover several known results in the literature.

1.5.2 Discussion with respect to prior works and extensions

Topological issues. Theorem 1.1 does not assert the existence of solutions ($\mathcal{S} \neq \emptyset$) nor the existence of finite-dimensional faces in \mathcal{S} . Those are assumptions we make (but the theorem *does* imply that $\{R \leq R(p)\}$ has extreme points).

The philosophy here (and in [3]) is to leave aside the existence issues so as to emphasize the geometrical nature of the result: the notions of extreme point or dimension of a face stem from linear algebra, they are independent from any choice of topology. In practice, one should always complement [Theorem 1.1](#) with some argument ensuring that $\mathcal{S} \neq \emptyset$ and that \mathcal{S} has finite-dimensional faces. For that purpose, topological arguments are useful. If V is endowed with the topology of a locally convex (Hausdorff) vector space, the theorems [\[Kle57, 3.3 and 3.4\]](#) which generalize the celebrated Krein-Milman theorem, state that \mathcal{S} has an extreme point provided:

- \mathcal{S} is nonempty, convex,
- \mathcal{S} contains no line,
- and \mathcal{S} is closed, locally compact.

The last two conditions hold in particular if \mathcal{S} is compact. Moreover, as in [Theorem 1.2](#), the second condition can be ensured by considering a suitable quotient map, provided it preserves the other topological properties (*e.g.* if $\text{lin}(\mathcal{S})$ has a topological complement). Choosing a suitable topology which provides those properties can be highly nontrivial, see for instance [\[UFW17\]](#).

Representer theorems in Machine Learning. To our knowledge, the name “*representer theorem*” in the general field of inverse problems was introduced by M. Unser, J. Fageot, and J.P. Ward in [\[UFW17\]](#), in reference to the famous theorem in the field of machine learning and kernel methods [\[SS02\]](#). A typical example is the following⁵. Let $\Phi : \mathbb{R}^n \rightarrow \mathbb{R}^M$ be a finite dimensional measurement operator and $L : \mathbb{R}^n \rightarrow \mathbb{R}^p$ be a linear transform. Solving an inverse problem using Tikhonov regularization amounts to finding the minimizers of

$$\min_{u \in \mathbb{R}^n} \frac{1}{2} \|\Phi u - y\|_2^2 + \frac{1}{2} \|Lu\|_2^2. \quad (1.51)$$

Provided that $\ker \Phi \cap \ker L = \{0\}$, it is possible to show that, whatever the data y is, solutions are always of the form

$$u^* = \sum_{i=1}^m \alpha_i \psi_i + u_K, \quad (1.52)$$

where $u_K \in \ker(L)$ and $\psi_i = (\Phi^T \Phi + L^T L)^{-1}(\varphi_i)$, where $\varphi_i^T \in \mathbb{R}^n$ is the i -th row of Φ . This result characterizes structural properties of the minimizers without actually needing to solve the problem. Like the representer theorem of this chapter, [Eq. \(1.52\)](#) sometimes allows us to tackle infinite dimensional problems, simply by solving a finite dimensional linear system. This is a critical observation that explains the practical success of kernel methods and radial basis functions [\[Wen05\]](#). Representation properties like [\(1.52\)](#) have been generalized to the case of reflexive strictly convex Banach spaces by M. Unser in [\[Uns21\]](#).

However, let us stress that the representer theorem [\(1.52\)](#) (and the one in [\[Uns21\]](#)) is essentially different from the one presented in this chapter, since it relies on a finer analysis which exploits the optimality conditions. [Theorem 1.2](#) applied to [Eq. \(1.51\)](#) would not provide any information, as the optimal level set $\{R \leq R(p)\}$ is of the form $\tilde{C} + \ker(L)$ with \tilde{C} strictly convex! The theorems of this chapter rely on a sparsity principle: they are only useful when the boundary of $\{R \leq R(p)\}$ has flat regions.

⁵Here, we follow the presentation of [\[GFU18\]](#).

Generalized splines and the surjectivity assumption. While discussing the Fisher-Jerome problem (1.42), we have insisted that $L|_V$ should be surjective. Without that assumption, the extreme points and faces of C are difficult to relate to those of $C_{\mathcal{M}}$.

More generally, when composing R with a non-surjective operator L , it is not straightforward to deduce the extreme points of $\{R \circ L \leq 1\}$ from those of $\{R \leq 1\}$. An elementary example is displayed in Figure 1.3 with the ℓ^1 -unit ball in \mathbb{R}^3 . The unit ball corresponding to $\|L \cdot\|_1$ (we assume that L is injective for the sake of simplicity) is isomorphic to the intersection of the ℓ^1 -unit ball with $\text{Im } L$. In order to predict its facial structure, one has to study the direction of all the faces of the original ball and compute their intersection with $\text{Im } L$, which is not trivial.

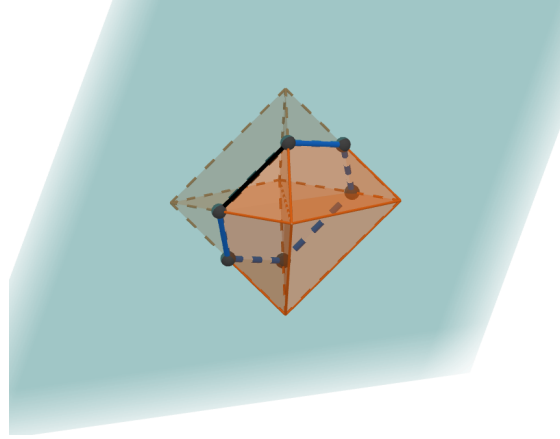


Figure 1.3: The ℓ^1 unit ball and an ℓ^1 analysis unit ball (that is, the unit ball of $\|L \cdot\|_1$) which can be obtained by intersecting the former with $\text{Im } L$. Predicting the extreme points of the intersection is not straightforward.

Things are even more involved in infinite dimension. To come back to the Fisher-Jerome problem (1.42), we discuss the case of the total gradient variation. The vector total variation of vector measures can be defined as

$$\forall g \in (\mathcal{M}(X))^d, |g|(X) \stackrel{\text{def.}}{=} \sup \left\{ \int_X \langle \psi(x), dg(x) \rangle \mid \psi \in \mathcal{C}_c(X; \mathbb{R}^d), \sup_{x \in X} |\psi(x)| \leq 1 \right\}. \quad (1.53)$$

It can be shown that the extreme points of its unit ball are of the form $a\delta_x$ where $x \in X$, $a \in \mathbb{R}^d$ and $|a|_2 = 1$. On the other hand, let $X = \mathbb{R}^d$, if Du denotes the distributional gradient of u and $Du \in (\mathcal{M}(\mathbb{R}^d))^d$, the total gradient variation is defined as $|Du|(\mathbb{R}^d)$. The faces and extreme points of its unit ball have a much richer structure than those corresponding to (1.53), and we study them in Chapter 2.

Chapter 2

The faces of the total gradient variation unit ball

Contents

2.1	A representation using only the extreme points	40
2.1.1	Functional setting	40
2.1.2	Fleming's result	41
2.1.3	Numerical experiments	41
2.2	Structural properties of the faces of C_{BV}	42
2.2.1	Set "algebra"	43
2.2.2	Decomposability	45
2.3	The finite-dimensional faces of C_{BV} are polytopes	46
2.3.1	Chains in \mathcal{E}	46
2.3.2	Maximal chains	48
2.3.3	Extreme points of finite-dimensional faces	49
2.4	The tree of shapes of a function	50
2.4.1	A decomposition of u using simple sets	50
2.4.2	The tree structure of the decomposition	51
2.5	Examples of finite dimensional faces	53
2.6	Conclusion	56
2.6.1	Summary	56
2.6.2	Discussion with respect to prior works and extensions	56

In [Chapter 1](#), we have seen that understanding the extreme points and the faces of the level sets of a regularizer provides insightful information on the structure of the solution set of a variational problem. Indeed, the extreme points of the solution set belong to low-dimensional faces of those level sets (provided one observes a finite number of measurements). The present chapter is devoted to the study of the faces corresponding to the *total variation of the gradient*, a convex regularizer which has been widely used in image restoration since the seminal work of Rudin, Osher and Fatemi [\[ROF92\]](#).

Given a locally integrable function $u : \mathbb{R}^d \rightarrow \mathbb{R}$, its *total (gradient) variation* is defined as

$$R^{(BV)}(u) \stackrel{\text{def.}}{=} \sup \left\{ \int_{\mathbb{R}^d} u \operatorname{div}(\varphi) \mid \varphi \in \mathcal{C}_c^1(\mathbb{R}^d; \mathbb{R}^d), \sup_{x \in \mathbb{R}^d} |\varphi(x)|_2 \leq 1 \right\}. \quad (2.1)$$

By the Radon-Riesz representation theorem, $R^{(\text{BV})}(u)$ is finite if and only if its distributional derivative Du is a bounded (vector) Radon measure, in which case $R^{(\text{BV})}(u)$ is the (vector) total variation of the measure Du . In any case, we commonly write $|Du|(\mathbb{R}^d)$ for $R^{(\text{BV})}(u)$. If $F \subseteq \mathbb{R}^d$ is a measurable set¹, its (distributional) perimeter is defined as $P(F) \stackrel{\text{def.}}{=} R^{(\text{BV})}(\mathbf{1}_F)$. The basic properties of functions with bounded variation and sets of finite perimeter which are necessary for this chapter are gathered in [Appendix A](#), but we refer to [\[AFP00, Mag12\]](#) for a comprehensive treatment of the topic.

The main reason for using the (gradient²) total variation as a regularizer is that it allows for solutions with discontinuities, a property which is crucial when modelling images, because of the *occlusion* phenomenon. In fact, it is well known that the total gradient variation *tends to promote piecewise constant functions*, and one informal explanation is that minimizing $R^{(\text{BV})}(u)$ plus some fidelity term yields solutions u with sparse gradient. Relying on the representation theorem of [Chapter 1](#), this chapter provides a more rigorous argument which accounts for the appearance of piecewise constant solutions.

Collaboration. This chapter originates from an unpublished work with Claire Boyer, Antonin Chambolle, Yohann De Castro, Frédéric de Gournay, and Pierre Weiss.

2.1 A representation using only the extreme points

2.1.1 Functional setting

If u has finite total variation, then, up to a unique additive constant, $u \in L^{d/(d-1)}(\mathbb{R}^d)$ (see for instance [\[AFP00, Thm. 3.47\]](#)). It is thus natural to choose $L^{d/(d-1)}(\mathbb{R}^d)$ as ambient space on which $R^{(\text{BV})}$ defines a convex functional, together with linear measurements of the form

$$\Phi : u \mapsto \left(\int_{\mathbb{R}^d} u(x) \varphi_i(x) dx \right)_{1 \leq i \leq M} \quad (2.2)$$

where $\varphi_i \in L^d(\mathbb{R}^d)$ for all i . As $R^{(\text{BV})}$ is lower semi-continuous and coercive (for the weak topology of $L^{d/(d-1)}(\mathbb{R}^d)$), the problem

$$\min_u R^{(\text{BV})}(u) \quad \text{s.t.} \quad \Phi u = y \quad (\mathcal{P}_{\text{BV}})$$

has a solution provided there is a feasible point. The existence of extreme points (or finite dimensional faces) of the solution set is guaranteed by its compactness (since $R^{(\text{BV})}$ is coercive).

As a result, [Corollary 1.1](#) ensures that the extreme points of the solution set are convex combinations of at most M extreme points of the level set $\{u \in L^{d/(d-1)}(\mathbb{R}^d) \mid R^{(\text{BV})}(u) \leq \min(\mathcal{P}_{\text{BV}})\}$.

¹All the subsets of \mathbb{R}^d considered in this chapter are Lebesgue measurable. In the following, we omit this mention.

²The common use in Analysis is to refer to $R^{(\text{BV})}(u)$ as the *total variation* of u , and we follow this convention whenever the context is clear. However, as the present dissertation alternatively considers measures and functions as signals of interest, we occasionally use the term *total gradient variation* to disambiguate the fact that we use [Eq. \(2.1\)](#) as a regularizer and that we try to reconstruct is a function (as opposed to a measure). That terminology is inspired from the one used by W. Fleming and R. Rishel in [\[FR60\]](#).

2.1.2 Fleming’s result

As $R^{(\text{BV})}$ is positively homogeneous, it suffices to characterize the extreme points (and the faces) of the “unit ball”

$$C_{\text{BV}} \stackrel{\text{def.}}{=} \left\{ u \in L^{d/(d-1)}(\mathbb{R}^d) \mid R^{(\text{BV})}(u) \leq 1 \right\}. \quad (2.3)$$

That problem was solved by Fleming in [Fle57] in the framework of generalized surfaces. A variant of that result in terms of functions with bounded variation is provided in [ACMM01].

Let $A \subseteq \mathbb{R}^d$ be a set with finite perimeter. Following [ACMM01], we say that A is *decomposable* if there exists a partition (A_1, A_2) of A such that $P(A) = P(A_1) + P(A_2)$ and $|A_1| > 0$, $|A_2| > 0$, where $P(A)$ denotes the perimeter of A (see Appendix A). We say that A is *indecomposable*³ (or *M-connected*) if it is not decomposable. Additionally, we say that A is *simple* if it is indecomposable and its complement A^c is indecomposable. Informally, simple sets are the simply connected sets in the measure-theoretic sense (*i.e.* they consist of one connected component and they have no holes).

Proposition 2.1 ([Fle57, ACMM01]). *The extreme points of C_{BV} are the functions $u = \pm \mathbb{1}_F / P(F)$, where F is a simple set, $0 < |F| < +\infty$ and $P(F) < +\infty$.*

Let us mention that, while we restrict our discussion to the domain \mathbb{R}^d , the notion of indecomposable and simple sets was extended by K. Bredies and M. Carioni in [BC19] to the case of a bounded domain Ω with Neumann boundary condition (actually we have used their definition of simple set, which is equivalent to the one in [ACMM01] when $\Omega = \mathbb{R}^d$). They have proved that Proposition 2.1 also holds in that case (where functions are considered modulo an additive constant).

In view of Proposition 2.1, the representer theorem states that there is (at least) one solution to $(\mathcal{P}_{\text{BV}})$ which is a linear combination of at most M indicator functions. This result explains the so-called *staircasing effect*⁴ when using a finite number of measurements M , *i.e.* the appearance of regions where the reconstructed signal is flat whereas the image to recover has smooth gradations. In addition, it gives some insight on the family of functions that can be exactly recovered by total gradient variation minimization.

2.1.3 Numerical experiments

The above discussion states that some solution to $(\mathcal{P}_{\text{BV}})$ can be written as

$$u = \sum_{i=1}^M \alpha_i \mathbb{1}_{E_i}$$

where each E_i is a simple set. Depending on the intersections of the E_i ’s and the values α_i , this implies that u may take up to $2^M - 1$ nonzero values. However, the following numerical experiment suggests that this bound is too pessimistic.

³In [Bac13, Fuj05], that notion is called *inseparable*.

⁴At least when the number of measurements M is small. In practice, even when M is large, the staircasing appears because a strong regularization parameter tends to produce solutions on low-dimensional faces.

Consider an image $u \in \mathbb{R}^{N_1 \times N_2}$ and define the following discretization of the gradient:

$$(\nabla_1 u)_{i,j} = \begin{cases} u_{i,j} & \text{for } i = 1, 1 \leq j \leq N_2, \\ u_{i,j} - u_{i-1,j} & \text{for } 2 \leq i \leq N_1, 1 \leq j \leq N_2, \\ -u_{i-1,j} & \text{for } i = N_1 + 1, 1 \leq j \leq N_2, \\ 0 & \text{for } 1 \leq i \leq N_1 + 1, j = N_2 + 1, \end{cases} \quad (2.4)$$

$$(\nabla_2 u)_{i,j} = \begin{cases} u_{i,j} & \text{for } 1 \leq i \leq N_1, j = 1 \\ u_{i,j} - u_{i,j-1} & \text{for } 1 \leq i \leq N_1, 2 \leq j \leq N_2, \\ -u_{i,j-1} & \text{for } i = N_1 + 1, 1 \leq j \leq N_2, \\ 0 & \text{for } i = N_1 + 1, 1 \leq j \leq N_2 + 1. \end{cases} \quad (2.5)$$

A discrete scheme for the total variation with Dirichlet boundary condition is given by

$$R_{\text{BVdisc}}(u) = \|\nabla u\|_1 = \sum_{\substack{1 \leq i \leq N_1+1 \\ 1 \leq j \leq N_2+1}} \sqrt{((\nabla_2 u)_{i,j})^2 + ((\nabla_1 u)_{i,j})^2} \quad (2.6)$$

The sensing operator Φ is discretized by a matrix $\mathbb{R}^{M \times (N_1 N_2)}$. The resulting discretization of $(\mathcal{P}_{\text{BV}})$ is a problem of the form $\min_u F(Ku) + G(u)$ where F is the ℓ^1 norm, $K = \nabla$, G is the indicator function of the affine space $\Phi^{-1}(\{y\})$. An instance of the Chambolle-Pock algorithm [CP11] yields

$$\begin{cases} p^{n+1} &= \text{Proj}_{\mathcal{B}}(p^n + \sigma \nabla \bar{u}^n) \\ u^{n+1} &= \text{Proj}_{\Phi^{-1}(\{y\})}(u^n - \tau (\nabla)^* p^{n+1}) \\ \bar{u}^{n+1} &= 2u^{n+1} - u^n \end{cases}$$

where $\mathcal{B} = \{u \in \mathbb{R}^{N_1 \times N_2} \mid \forall i, j, |u_{i,j}|_2 \leq 1\}$. It provides a convergent iterative method for the minimization of our discretized problem, provided $\tau, \sigma > 0$ and $\tau\sigma \leq 1/8$. The projections onto \mathcal{B} and $\Phi^{-1}(\{y\})$ have closed form expressions.

We choose $M = 3$ sensing functions $\varphi_i = \Phi_{i,\cdot}$ for $1 \leq i \leq M$ (see Figure 2.1), $N_1 = N_2 = 200$, and we run the algorithm for 40.000 iterations. The result is shown in Figure 2.2. As expected, the solution is a convex combination of 3 simple shapes, but the function only takes 3 nonzero values (if we neglect the discretization and convergence artifacts): the relative positions of the simple sets are not arbitrary. Precisely, we distinguish three simple sets:

$$E_1 = \{u = 4.04\}, E_2 = \{u = -13.4\} \quad \text{and} \quad E_3 = \{u = -13.4\} \cup \{u = -8.03\},$$

with the remarkable properties that $E_2 \subseteq E_3$ and the boundaries of E_1 and E_3 have a nontrivial intersection, *i.e.* $\mathcal{H}^1((\partial^* E_1) \cap (\partial^* E_3)) > 0$.

That experiment suggests that describing the solutions of $(\mathcal{P}_{\text{BV}})$ as linear convex combinations of the extreme points of C_{BV} is too rough. Similarly to the positive semi-definite cone (see Section 1.4.2), we need to understand the (low-dimensional) faces of C_{BV} , which have more structure than just arbitrary convex hulls of extreme points.

2.2 Structural properties of the faces of C_{BV}

In this section and in the rest of the chapter, we consider a linearly closed face \mathcal{F} of C_{BV} (for instance, the linear closure of an elementary face, see [Dub62, Thm. 6.1]), and we try to describe its structure.



Figure 2.1: The three sensing functions $(\varphi_i)_{i=1}^M$.

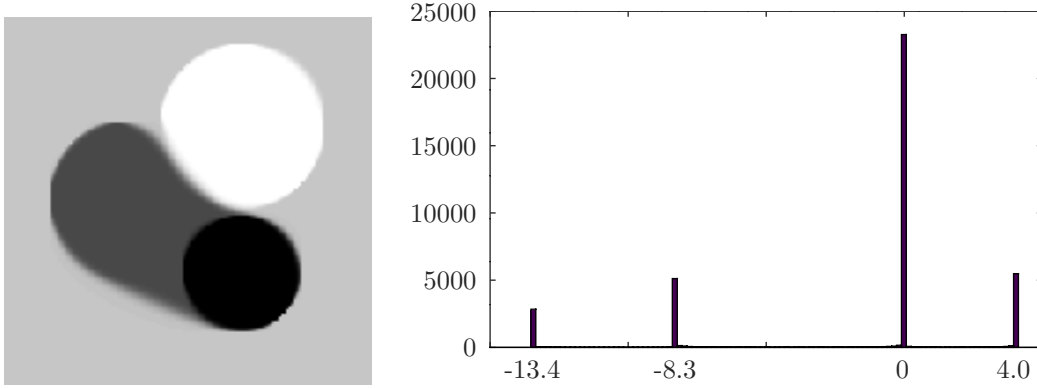


Figure 2.2: (Left) Solution of $(\mathcal{P}_{\text{BV}})$. Three shapes appear. (Right) Histogram of the corresponding image. Up to the discretization and convergence errors, the image takes three nonzero values.

The following observation is elementary but quite useful to our discussion: if $u \in \mathcal{F}$, and there exists $\theta \in]0, 1[$, $u_1, u_2 \in C_{\text{BV}}$ such that $u = \theta u_1 + (1 - \theta)u_2$, then $u_1 \in \mathcal{F}$ and $u_2 \in \mathcal{F}$. We refer to it as the *closed face property*⁵.

Another useful remark is that, if \mathcal{F} contains 0, then $\mathcal{F} = C_{\text{BV}}$.

2.2.1 Set “algebra”

Let us focus on the elements of \mathcal{F} which are (signed) indicators of sets, *i.e.* there exists $E \subseteq \mathbb{R}^d$ such that $u = \varepsilon \mathbb{1}_E / P(E)$ for some $\varepsilon \in \{+1, -1\}$. Let us define

$$\mathcal{E} \stackrel{\text{def.}}{=} \mathcal{E}_+ \cup \mathcal{E}_- \cup \{\emptyset, \mathbb{R}^d\}, \quad \text{where} \quad (2.7)$$

$$\mathcal{E}_+ \stackrel{\text{def.}}{=} \left\{ E \subset \mathbb{R}^d \mid |E| < +\infty, 0 < P(E) < +\infty \text{ and } \frac{\mathbb{1}_E}{P(E)} \in \mathcal{F} \right\}, \quad (2.8)$$

$$\mathcal{E}_- \stackrel{\text{def.}}{=} \left\{ E \subset \mathbb{R}^d \mid |E^c| < +\infty, 0 < P(E^c) < +\infty \text{ and } \frac{(-\mathbb{1}_{E^c})}{P(E^c)} \in \mathcal{F} \right\}. \quad (2.9)$$

Proposition 2.2. The collection \mathcal{E} is a ring of sets⁶.

In other words, for all $A, B \in \mathcal{E}$, $(A \cap B) \in \mathcal{E}$ and $(A \cup B) \in \mathcal{E}$.

As an immediate consequence, if \mathcal{E} contains E_1, \dots, E_n , it must also contain all the

⁵More generally, by induction, if we can write $u = \sum_{i=1}^n \theta_i u_i \in \mathcal{F}$ with $\sum_i \theta_i = 1$, $\theta_i > 0$ and $u_i \in C_{\text{BV}}$ for all i , then $\{u_i\}_{i=1}^n \subseteq \mathcal{F}$.

⁶In the sense of [MLB99]. In particular \mathcal{E} is a distributive lattice.

sets E of the form

$$E = \bigcup_{J \in \{J_1, \dots, J_\ell\}} \left(\bigcap_{j \in J} E_j \right), \quad J_1, \dots, J_\ell \subseteq \{1, \dots, n\},$$

that is, all (finite) unions of (finite) intersections of the E_j 's.

[Proposition 2.2](#) follows from the next two lemmas.

Lemma 2.1. *Let $A, B \in \mathcal{E}_+$. Then,*

- $(A \cup B) \in \mathcal{E}_+$,
- $(A \cap B) \in \mathcal{E}_+$ provided that $|A \cap B| > 0$.

Moreover, the same holds when replacing \mathcal{E}_+ with \mathcal{E}_- .

Proof. Let $\theta \stackrel{\text{def.}}{=} P(A)/(P(A) + P(B)) \in]0, 1[$ and let $u \stackrel{\text{def.}}{=} \theta \frac{\mathbb{1}_A}{P(A)} + (1 - \theta) \frac{\mathbb{1}_B}{P(B)}$.

Then, $u \in \mathcal{F}$ and $u = \frac{1}{P(A) + P(B)}(\mathbb{1}_A + \mathbb{1}_B) = \frac{1}{P(A) + P(B)}(\mathbb{1}_{A \cup B} + \mathbb{1}_{A \cap B})$.

First, let us assume that $|A \cap B| > 0$, hence $P(A \cap B) > 0$. We have

$$u = \sigma \frac{\mathbb{1}_{A \cup B}}{P(A \cup B)} + \delta \frac{\mathbb{1}_{A \cap B}}{P(A \cap B)} \quad \text{with } \sigma \stackrel{\text{def.}}{=} \frac{P(A \cup B)}{P(A) + P(B)}, \quad \delta \stackrel{\text{def.}}{=} \frac{P(A \cap B)}{P(A) + P(B)},$$

and by submodularity of the perimeter

$$\sigma + \delta \leq 1. \tag{2.10}$$

If (2.10) is an equality, we have written u as a convex combination of elements in C_{BV} , and by the closed face property $\left\{ \frac{\mathbb{1}_{A \cup B}}{P(A \cup B)}, \frac{\mathbb{1}_{A \cap B}}{P(A \cap B)} \right\} \subseteq \mathcal{F}$. If (2.10) is strict, we write $u = \sigma \frac{\mathbb{1}_{A \cup B}}{P(A \cup B)} + \delta \frac{\mathbb{1}_{A \cap B}}{P(A \cap B)} + (1 - \sigma - \delta)0$, and the closed face property implies that $\left\{ \frac{\mathbb{1}_{A \cup B}}{P(A \cup B)}, \frac{\mathbb{1}_{A \cap B}}{P(A \cap B)}, 0 \right\} \subseteq \mathcal{F}$.

Now, if $|A \cap B| = 0$, we have $u = \sigma \frac{\mathbb{1}_{A \cup B}}{P(A \cup B)}$ with $0 < \sigma \leq 1$ and we conclude similarly that $\frac{\mathbb{1}_{A \cup B}}{P(A \cup B)} \in \mathcal{F}$ (and $0 \in \mathcal{F}$ too if $\sigma < 1$). \square

Lemma 2.2. *Let $A \in \mathcal{E}_+$ and $B \in \mathcal{E}_-$. Then*

- $(A \cup B) \in \mathcal{E}_-$ provided that $|\mathbb{R}^d \setminus (A \cup B)| > 0$,
- $(A \cap B) \in \mathcal{E}_+$ provided that $|A \cap B| > 0$.

Proof. Let $\theta \stackrel{\text{def.}}{=} P(A)/(P(A) + P(B^c)) \in]0, 1[$ and let $u \stackrel{\text{def.}}{=} \theta \frac{\mathbb{1}_A}{P(A)} + (1 - \theta) \frac{(-\mathbb{1}_{B^c})}{P(B^c)}$. Observing that $u = \frac{1}{P(A) + P(B^c)}(\mathbb{1}_{A \cap B} - \mathbb{1}_{A^c \cap B^c})$, we argue similarly as in the proof of [Lemma 2.1](#) to deduce that $\frac{\mathbb{1}_{A \cap B}}{P(A \cap B)}$, $\frac{(-\mathbb{1}_{A^c \cap B^c})}{P(A^c \cap B^c)}$ and possibly 0 belong to \mathcal{F} . The only difference which is worth mentioning is that to obtain the inequality

$$P(A \cap B) + P(A^c \cap B^c) \leq P(A) + P(B^c),$$

we use the submodularity of the perimeter and the fact that $P(A^c \cap B^c) = P(A \cup B)$ and $P(B^c) = P(B)$. \square

Eventually, we note from the proofs of [Lemma 2.1](#) and [Lemma 2.2](#) the following property.

Proposition 2.3 (Modularity in the proper faces). *If $\mathcal{F} \subset C_{\text{BV}}$ is a linearly closed face of C_{BV} which does not contain 0, then, for all $A, B \in \mathcal{E}$,*

$$P(A \cup B) + P(A \cap B) = P(A) + P(B). \quad (2.11)$$

It is simply the equality case in (2.10).

Remark 2.1. *In particular, if $A, B \in \mathcal{E}$ are such that $|A \cap B| = 0$, then $P(A \cup B) = P(A) + P(B)$. By [ACMM01, Prop. 1], that is equivalent to $\mathcal{H}^{d-1}(\partial^* A \cap \partial^* B) = 0$, that is, the reduced boundaries of A and B “do not touch” (except on a \mathcal{H}^{d-1} -negligible set).*

2.2.2 Decomposability

Besides the union and intersection operations, the collection \mathcal{E} is stable by taking the M -connected components.

Proposition 2.4. *Let $A, B \in \mathcal{E}$ such that $B \subset A$. If there exist $C_1, C_2 \subset \mathbb{R}^d$ such that $A \setminus B = C_1 \cup C_2$ with $|C_1| > 0$, $|C_2| > 0$ and $P(A \setminus B) = P(C_1) + P(C_2)$, then $(B \cup C_1) \in \mathcal{E}$ and $(B \cup C_2) \in \mathcal{E}$.*

Proof. First, we note that the case ($A = \mathbb{R}^d$ and $B = \emptyset$) is impossible since \mathbb{R}^d is indecomposable. Hence, $C_1 \subsetneq \mathbb{R}^d$, $C_2 \subsetneq \mathbb{R}^d$, and [ACMM01, Prop. 3] ensures that $|C_1 \cap C_2| = 0$ and $\mathcal{H}^{d-1}(\partial^* C_1 \cap \partial^* C_2) = 0$.

Now, let us recall [ACMM01, Prop. 1] which states that for all sets of finite perimeter E_1 and E_2 with $|E_1 \cap E_2| = 0$,

$$P(E_1 \cup E_2) = P(E_1) + P(E_2) - 2\mathcal{H}^{d-1}(\partial^* E_1 \cap \partial^* E_2). \quad (2.12)$$

Applying that property twice, we get

$$\begin{aligned} P(A) + P(B) &= 2P(B) + P(A \setminus B) - 2\mathcal{H}^{d-1}(\partial^* B \cap \partial^*(A \setminus B)) \\ &= 2P(B) + P(A \setminus B) - 2\mathcal{H}^{d-1}(\partial^* B \cap (\partial^*(C_1 \cup C_2))) \\ &= \left(P(B) + P(C_1) - 2\mathcal{H}^{d-1}(\partial^* B \cap \partial^* C_1) \right) \\ &\quad + \left(P(B) + P(C_2) - 2\mathcal{H}^{d-1}(\partial^* B \cap \partial^* C_2) \right) \\ &= P(Y_1) + P(Y_2) \end{aligned} \quad (2.13)$$

where we have defined $Y_1 = B \cup C_1$, $Y_2 = B \cup C_2$, and we have used the fact that $|B \cap C_i| = 0$ for $i \in \{1, 2\}$. Observing that $A = Y_1 \cup Y_2$ and $B = Y_1 \cap Y_2$, we also note that

$$\mathbb{1}_A + \mathbb{1}_B = \mathbb{1}_{Y_1} + \mathbb{1}_{Y_2} \quad (2.14)$$

$$\text{and } (\mathbb{1}_A - \mathbb{1}_B) + \mathbb{1}_B = (\mathbb{1}_{Y_1} - \mathbb{1}_B) + \mathbb{1}_{Y_2}. \quad (2.15)$$

If $A \in \mathcal{E}_+$ and $B \in \mathcal{E}_+$, we combine (2.13) and (2.14) to get

$$\frac{P(A)}{P(A) + P(B)} \frac{\mathbb{1}_A}{P(A)} + \frac{P(B)}{P(A) + P(B)} \frac{\mathbb{1}_B}{P(B)} = \frac{P(Y_1)}{P(Y_1) + P(Y_2)} \frac{\mathbb{1}_{Y_1}}{P(Y_1)} + \frac{P(Y_2)}{P(Y_1) + P(Y_2)} \frac{\mathbb{1}_{Y_2}}{P(Y_2)}.$$

Since the left-hand side is an element of \mathcal{F} , we deduce by the closed face property that $\frac{\mathbb{1}_{Y_1}}{P(Y_1)}$ and $\frac{\mathbb{1}_{Y_2}}{P(Y_2)}$ are elements of \mathcal{F} , that is $Y_1, Y_2 \in \mathcal{E}$. The case where $A \in \mathcal{E}_-$ and $B \in \mathcal{E}_-$ is dealt with similarly.

If $A \in \mathcal{E}_-$ and $B \in \mathcal{E}_+$, then one (and exactly one, by the isoperimetric inequality) of the Y_i 's has infinite Lebesgue measure. Let us assume that it is Y_1 . By (2.13) and (2.15),

$$\frac{P(A)}{P(A)+P(B)} \frac{(-\mathbb{1}_{A^c})}{P(A^c)} + \frac{P(B)}{P(A)+P(B)} \frac{\mathbb{1}_B}{P(B)} = \frac{P(Y_1)}{P(Y_1)+P(Y_2)} \frac{(-\mathbb{1}_{Y_1^c})}{P(Y_1^c)} + \frac{P(Y_2)}{P(Y_1)+P(Y_2)} \frac{\mathbb{1}_{Y_2}}{P(Y_2)},$$

and we deduce again that $Y_1, Y_2 \in \mathcal{E}$ by the closed face property.

If $B = \emptyset$, we argue similarly, using $\frac{\mathbb{1}_A}{P(A)} = \frac{P(Y_1)}{P(Y_1)+P(Y_2)} \frac{\mathbb{1}_{Y_1}}{P(Y_1)} + \frac{P(Y_2)}{P(Y_1)+P(Y_2)} \frac{\mathbb{1}_{Y_2}}{P(Y_2)}$ or $\frac{(-\mathbb{1}_{A^c})}{P(A^c)} = \frac{P(Y_1)}{P(Y_1)+P(Y_2)} \frac{(-\mathbb{1}_{Y_1^c})}{P(Y_1^c)} + \frac{P(Y_2)}{P(Y_1)+P(Y_2)} \frac{\mathbb{1}_{Y_2}}{P(Y_2)}$.
 If $A = \mathbb{R}^d$, we use $\frac{\mathbb{1}_B}{P(B)} = \frac{P(Y_1)}{P(Y_1)+P(Y_2)} \frac{(-\mathbb{1}_{Y_1^c})}{P(Y_1^c)} + \frac{P(Y_2)}{P(Y_1)+P(Y_2)} \frac{\mathbb{1}_{Y_2}}{P(Y_2)}$ or $\frac{(-\mathbb{1}_{B^c})}{P(B^c)} = \frac{P(Y_1)}{P(Y_1)+P(Y_2)} \frac{\mathbb{1}_{Y_1}}{P(Y_1)} + \frac{P(Y_2)}{P(Y_1)+P(Y_2)} \frac{\mathbb{1}_{Y_2}}{P(Y_2)}$, and this concludes the proof. \square

Let us examine more concretely the consequences of Proposition 2.4.

Remark 2.2 (Connected components of the increments). *By iteratively decomposing $B \setminus A = C_1 \cup (\bigcup_{i \in I} C_i)$, we deduce that for any M -connected component C of $A \setminus B$, it holds $(B \cup C) \in \mathcal{E}$.*

Remark 2.3 (Connected components and holes). *Choosing $B = \emptyset$ in Proposition 2.4, we see that any M -connected component of $A \in \mathcal{E}$ is also in \mathcal{E} . Conversely, choosing $A = \mathbb{R}^d$, we see that we can “fill” any hole of $B \in \mathcal{E}$ (i.e. any M -connected component of B^c which has finite Lebesgue measure): if $Y \subseteq \mathbb{R}^d$ is a hole of B , $B \cup Y \in \mathcal{E}$.*

2.3 The finite-dimensional faces of C_{BV} are polytopes

As the collection \mathcal{E} has the structure of a ring of sets (or a distributive lattice), it is natural to study the chains of \mathcal{E} . It turns out that they are intimately connected to the dimension of the face \mathcal{F} .

2.3.1 Chains in \mathcal{E}

Let \mathcal{G} be a collection of subsets of \mathbb{R}^d . We say that \mathcal{G} is a *chain* if for all $E, E' \in \mathcal{G}$, $E \subseteq E'$ or $E' \subseteq E$. We call its cardinal the length of \mathcal{G} .

Please note that we identify sets which differ up to a Lebesgue negligible set, and we write $A \subsetneq B$ to mean that $|A \setminus B| = 0$ and $|B \setminus A| > 0$.

Proposition 2.5. *Let $\mathcal{G} \subseteq \mathcal{E} \setminus \{\emptyset, \mathbb{R}^d\}$ be a chain. If $\dim \mathcal{F} = k$, then \mathcal{G} has length at most $k + 1$.*

Proof. Assume that \mathcal{G} contains (at least) m elements E_i , $1 \leq i \leq m$, with

$$\emptyset \subsetneq E_1 \subsetneq E_2 \subsetneq \dots \subsetneq E_m \subsetneq \mathbb{R}^d.$$

Let i_0 be the number of elements of \mathcal{G} in \mathcal{E}_+ . We assume that $1 \leq i_0 \leq m - 1$ (otherwise the argument is similar but simpler). In other words, $E_i \in \mathcal{E}_+$ for $1 \leq i \leq i_0$, and $E_i \in \mathcal{E}_-$ for $i_0 + 1 \leq i \leq m$.

Let $(u_1, \dots, u_{i_0}, u_{i_0+1}, \dots, u_m) \stackrel{\text{def.}}{=} \left(\frac{\mathbb{1}_{E_1}}{P(E_1)}, \dots, \frac{\mathbb{1}_{E_{i_0}}}{P(E_{i_0})}, \frac{(-\mathbb{1}_{E_{i_0+1}^c})}{P(E_{i_0+1}^c)}, \dots, \frac{(-\mathbb{1}_{E_m^c})}{P(E_m^c)} \right)$. The family $\{u_1, \dots, u_m\}$ is linearly independent. Indeed, if

$$\sum_{i=1}^{i_0} \alpha_i \frac{\mathbb{1}_{E_i}}{P(E_i)} + \sum_{i=i_0+1}^m \alpha_i \frac{(-\mathbb{1}_{E_i^c})}{P(E_i^c)} = 0, \quad (2.16)$$

we integrate on $E_1, E_2 \setminus E_1, \dots, E_{i_0} \setminus E_{i_0-1}$, to get

$$\sum_{i=1}^{i_0} \alpha_i = 0, \quad \sum_{i=2}^{i_0} \alpha_i = 0, \quad \dots, \quad \alpha_{i_0} = 0.$$

Integrating on $E_m^{\mathbb{C}}, E_{m-1}^{\mathbb{C}} \setminus E_m^{\mathbb{C}}, \dots, E_{i_0+1}^{\mathbb{C}} \setminus E_{i_0+2}^{\mathbb{C}}$, we also get

$$\sum_{i=i_0+1}^m \alpha_i = 0, \quad \sum_{i=i_0+1}^{m-1} \alpha_i = 0, \quad \dots, \quad \alpha_{i_0+1} = 0.$$

As a result, $\alpha_1 = \dots = \alpha_m = 0$ and the family has rank m . Hence, the family $\{u_2 - u_1, \dots, u_m - u_1\}$ has rank $m - 1$ and since it is contained in the direction space of \mathcal{F} , we get $m - 1 \leq \dim \mathcal{F} = k$. \square

Corollary 2.1. *Assume that $\dim \mathcal{F} = k$ and $u \in \mathcal{F}$. Then, u takes a finite number of values and the number of nonzero values of u is at most $k + 1$.*

Proof. By Carathéodory's theorem, we may write $u = \sum_{i=1}^{k+1} \theta_i \varepsilon_i \frac{\mathbb{1}_{A_i}}{P(A_i)}$, where $\theta_i \geq 0$, $\sum \theta_i = 1$, $\varepsilon_i \in \{-1, +1\}$ and A_i is a simple set. Hence u takes a finite number of nonzero values.

Assume that u takes the values⁷ $t_1 > \dots > t_{i_0} > 0 > t_{i_0+1} > \dots > t_m$, and let $E_i = \{u \geq t_i\}$ for $1 \leq i \leq m$, $E_{i_0+1} = \{u \geq 0\}$ and $E_i = \{u \geq t_{i-1}\}$ for $i_0 + 2 \leq i \leq m$.

This yields the level set decomposition $u = \sum_{i=1}^{i_0} \alpha_i \mathbb{1}_{E_i} + \sum_{i=i_0+1}^m \alpha_i (-\mathbb{1}_{E_i^{\mathbb{C}}})$ where $\alpha_i > 0$ and $E_i \subsetneq E_{i+1}$. By the coarea formula (see [Theorem A.1](#)),

$$1 \geq |Du|(\mathbb{R}^d) = \sum_{i=1}^{i_0} \alpha_i P(E_i) + \sum_{i=i_0+1}^m \alpha_i P(E_i^{\mathbb{C}}).$$

The case $1 > |Du|(\mathbb{R}^d)$ is impossible since it implies $0 \in \mathcal{F}$, hence $\mathcal{F} = C_{\text{BV}}$, which contradicts $\dim \mathcal{F} = k$. Hence, $1 = \sum_{i=1}^{i_0} \alpha_i P(E_i) + \sum_{i=i_0+1}^m \alpha_i P(E_i^{\mathbb{C}})$, and we may write u as a convex combination,

$$u = \sum_{i=1}^{i_0} \alpha_i P(E_i) \frac{\mathbb{1}_{E_i}}{P(E_i)} + \sum_{i=i_0+1}^m \alpha_i P(E_i^{\mathbb{C}}) \frac{(-\mathbb{1}_{E_i^{\mathbb{C}}})}{P(E_i^{\mathbb{C}})}.$$

The closed face property implies that $\frac{\mathbb{1}_{E_i}}{P(E_i)} \in \mathcal{F}$ (resp. $\frac{(-\mathbb{1}_{E_i^{\mathbb{C}}})}{P(E_i^{\mathbb{C}})} \in \mathcal{F}$) for all $1 \leq i \leq i_0$ (resp. $i_0 + 2 \leq i \leq m$).

As a result, we obtain a chain in \mathcal{E} with length m , and [Proposition 2.5](#) implies that $m \leq k + 1$. \square

Remark 2.4. *In [Corollary 2.1](#), we have used the fact that given a function u , its non-trivial upper level sets yield a chain in $\mathcal{E} \setminus \{\emptyset, \mathbb{R}^d\}$ with same cardinality. Conversely, given a chain of $\mathcal{E} \setminus \{\emptyset, \mathbb{R}^d\}$, say $G_1 \subsetneq \dots \subsetneq G_m$, the function u defined by*

$$u = \sum_{i=1}^{i_0} \theta_i \frac{\mathbb{1}_{G_i}}{P(G_i)} + \sum_{i=i_0+1}^m \theta_i \frac{(-\mathbb{1}_{G_i^{\mathbb{C}}})}{P(G_i^{\mathbb{C}})} \quad (2.17)$$

with $\theta_i > 0$, $\sum_i \theta_i = 1$, yields a function $u \in C_{\text{BV}}$ with level sets G_1, \dots, G_m .

⁷The simpler case where u takes only positive or only negative values is left to the reader.

2.3.2 Maximal chains

We say that a collection \mathcal{G} of elements of \mathcal{E} is a *maximal chain* (in \mathcal{E}) if it is a chain and there is no $G \in \mathcal{E} \setminus \mathcal{G}$ such that $\mathcal{G} \cup \{G\}$ is a chain. We note that, if \mathcal{G} is a maximal chain, then it must contain \emptyset (as its smallest element) and \mathbb{R}^d (as its greatest one).

Observe that, by Proposition 2.5, if \mathcal{F} is any linearly closed face with dimension $k < +\infty$, then \mathcal{E} has at least a maximal chain (and its length is at most $k + 3$).

Proposition 2.6. *Let \mathcal{F} be a linearly closed face, and assume that \mathcal{G} is a maximal chain of \mathcal{E} with finite length, say $\mathcal{G} = \{G_i\}_{i=0}^m$ with*

$$\emptyset = G_0 \subset G_1 \subset \dots \subset G_m = \mathbb{R}^d.$$

Then, the following properties hold.

1. *For all $i \in \{1, \dots, m\}$, the set $(G_i \setminus G_{i-1})$ is indecomposable.*
2. *For any $A \in \mathcal{E}$, there exists $I \subseteq \{1, \dots, m\}$ such that $A = \bigcup_{i \in I} (G_i \setminus G_{i-1})$.*
3. *Any function $u \in \mathcal{F}$ is constant on the sets $(G_i \setminus G_{i-1})$, for all $i \in \{1, \dots, m\}$.*

Proof. Assume for contradiction that $G_i \setminus G_{i-1} = C_1 \cup C_2$ with $|C_1| > 0$, $|C_2| > 0$ and $P(G_i \setminus G_{i-1}) = P(C_1) + P(C_2)$. Let us define $G_{i-1/2} \stackrel{\text{def.}}{=} (G_{i-1} \cup C_1)$. By Proposition 2.4, $G_{i-1/2} \in \mathcal{E}$, and we are thus able to insert it in \mathcal{G} , yielding a longer chain,

$$\emptyset = G_0 \subset \dots \subset G_{i-1} \subset G_{i-1/2} \subset G_i \subset \dots \subset G_m = \mathbb{R}^d,$$

which contradicts the maximality of \mathcal{G} .

For the second point, let us observe that the collection $\{H_i\}_{i=1}^m$, where $H_i \stackrel{\text{def.}}{=} G_i \setminus G_{i-1}$, is a partition of \mathbb{R}^d . Let $A \in \mathcal{E}$, $A \neq \emptyset$, and write $A = \bigcup_{i=1}^m (H_i \cap A)$ (disjoint union). We claim that for all $i \in \{1, \dots, m\}$, either $|H_i \cap A| = 0$ or $|H_i \setminus A| = 0$. For, if it were not the case, there would exist $i \in \{1, \dots, m\}$ such that $0 < |H_i \cap A|$ and $|H_i \setminus A| > 0$, hence the set $G_{i-1/2} \stackrel{\text{def.}}{=} G_{i-1} \cup (H_i \cap A)$ would satisfy $G_{i-1} \subsetneq G_{i-1/2} \subsetneq G_i$. Since $G_{i-1/2} = G_{i-1} \cup (G_i \cap A)$, it is an element of \mathcal{E} , hence we would have a new chain

$$\emptyset = G_0 \subset \dots \subset G_{i-1} \subset G_{i-1/2} \subset G_i \subset \dots \subset G_m = \mathbb{R}^d,$$

which would contradict the maximality of \mathcal{G} . As a result $A = \bigcup_{i \in I} H_i$, where $I \subseteq \{1, \dots, m\}$.

The last point is a straightforward consequence of the second one, since the sublevel sets of u belong to \mathcal{E} (see Corollary 2.1). \square

Though a (finite-dimensional) face \mathcal{F} may have several maximal chains, it is remarkable that they all share the same collection of increments (see Figure 2.3). In particular they all have the same length.

Proposition 2.7. *Assume that \mathcal{F} is finite dimensional. Let $\mathcal{G} = \{G_i\}_{i=0}^m$ and $\mathcal{G}' = \{G'_i\}_{i=0}^{m'}$ be two maximal chains in \mathcal{E} . Then $m = m' = \dim \mathcal{F} + 2$ and*

$$\{G_i \setminus G_{i-1}\}_{i=1}^m = \{G'_i \setminus G'_{i-1}\}_{i=1}^{m'}. \quad (2.18)$$

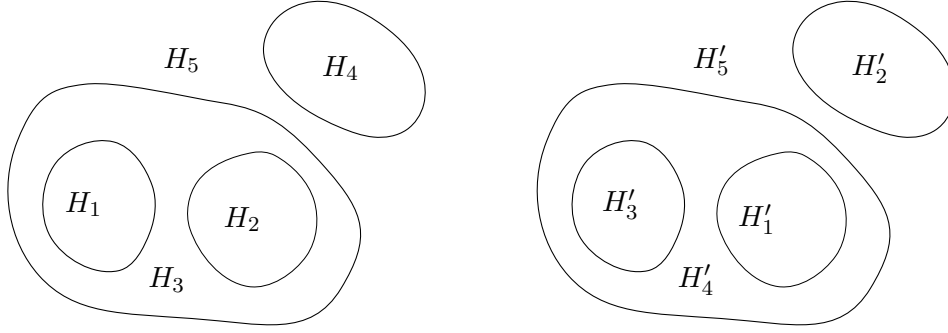


Figure 2.3: Example of two maximal chains \mathcal{G} and \mathcal{G}' corresponding to the same partition (we display the increments $H_i \stackrel{\text{def.}}{=} G_i \setminus G_{i-1}$)

Proof. As in the proof of Proposition 2.6, let us define $H_i \stackrel{\text{def.}}{=} G_i \setminus G_{i-1}$ for $1 \leq i \leq m$. The collection $\{H_i\}_{1 \leq i \leq m}$ defines a partition of \mathbb{R}^d .

By Proposition 2.6, for all $j \in \{1, \dots, m'\}$, since $G'_j \in \mathcal{E}$, there exists $I(j) \subseteq \{1, \dots, m\}$ such that $G'_j = \bigcup_{i \in I(j)} H_i$. Since $G'_{j-1} \subsetneq G'_j$, we must have $\text{Card } I(j) \geq \text{Card } I(j-1) + 1$ (with the convention that $I(0) = \emptyset$). As a result,

$$m \geq \text{Card } I(m') \geq m'.$$

Swapping the roles of $\{G_i\}_{i=0}^m$ and $\{G'_j\}_{j=0}^{m'}$, we deduce similarly that $m' \geq m$. Hence, by cardinality, each $G'_j \setminus G'_{j-1}$ is actually made of a single H_i , and there is a permutation $\sigma : \{1, \dots, m\} \rightarrow \{1, \dots, m'\}$ such that

$$\forall j \in \{1, \dots, m'\}, \quad G'_j \setminus G'_{j-1} = G_{\sigma(j)} \setminus G_{\sigma(j)-1}.$$

Now let $u \in \mathcal{F}$. By Proposition 2.6, u is constant on each H_i , hence

$$u = \sum_{i=1}^m \alpha_i \mathbb{1}_{H_i},$$

for some coefficients $(\alpha_i)_{1 \leq i \leq m} \in \mathbb{R}^m$.

However, there is one (and exactly one, by the isoperimetric inequality) index $i_0 \in \{1, \dots, m\}$ such that $|H_{i_0}| = +\infty$. Since u is integrable, we must have $\alpha_{i_0} = 0$, so that in fact $\text{Vect}(\mathcal{F}) \subseteq \text{Vect}(\{H_i\}_{1 \leq i \leq m, i \neq i_0})$ and $\dim \text{Vect}(\mathcal{F}) \leq m - 1$. Moreover, since \mathcal{F} is finite-dimensional, it does not contain 0, hence $\text{Aff}(\mathcal{F})$ does not contain 0 either and

$$\dim(\text{Aff}(\mathcal{F})) = \dim(\text{Vect}(\mathcal{F})) - 1 \leq m - 2.$$

The converse inequality readily follows from Proposition 2.5 since the length of the chain $\mathcal{G} \setminus \{\emptyset, \mathbb{R}^d\} = \{G_i\}_{i=1}^{m-1}$ is at most $\dim \mathcal{F} + 1$. \square

2.3.3 Extreme points of finite-dimensional faces

Gathering the previous results, we may now state the main theorem of this section.

Theorem 2.1. *Let \mathcal{F} be a closed k -dimensional face of C_{BV} . Then the collection \mathcal{E} is finite, with at most 2^{k+2} elements.*

In particular, \mathcal{F} has finitely many extreme points, it is a polytope.

As a consequence of Theorem 2.1 and the previous results, we deduce that if \mathcal{F} is a k -dimensional face of C_{BV} , almost every point of \mathcal{F} (in the sense of the Lebesgue or k -dimensional Hausdorff measure on its affine hull)

- is a convex combination of exactly $k + 1$ indicators of simple sets
- and takes exactly $k + 1$ nonzero values.

➤ Indeed, the collection of points that can be written as a convex combination of k or fewer extreme points is given by

$$S = \bigcup_{\substack{J \subseteq \text{extr}(\mathcal{F}), \\ |J|=k}} \text{conv}(J),$$

hence it is a finite union of $(k - 1)$ -dimensional convex sets. Therefore it is \mathcal{H}^k -negligible.

That result tends to explain the observations of Figure 2.2, where 3 measurements yield an element in a 2-dimensional face, hence (generically) 3 non-zero values.

2.4 The tree of shapes of a function

Whereas the use of chains in \mathcal{E} is a way of describing the functions in \mathcal{F} using their upper level sets, we discuss in this section an alternative description of \mathcal{F} , related to the tree of shapes of images used in image processing [BCM03].

Throughout this section, \mathcal{F} is a linearly closed face with finite dimension. As the collection \mathcal{E} is finite, and in view of the remarks of Section 2.2.2, we note that each element of \mathcal{E} has a finite number of M -connected components, as well as a finite number of holes.

2.4.1 A decomposition of u using simple sets

Let $C \in \mathcal{E}$ be an indecomposable set, and let $\{Y_k\}_{k \in K}$ denote its holes. Following [ACMM01], we define its saturation as $\text{sat}(C) \stackrel{\text{def}}{=} C \cup \bigcup_{k \in K} Y_k$. From [ACMM01, Prop. 9], we know that

$$\mathbb{1}_C = \mathbb{1}_{\text{sat}(C)} - \sum_{k \in K} \mathbb{1}_{Y_k} \quad \text{and} \quad P(C) = P(\text{sat}(C)) + \sum_{k \in K} P(Y_k). \quad (2.19)$$

Now, let $E \in \mathcal{E}$, and let $\{C_j\}_{j \in J}$ denote its M -connected components. Since $\mathbb{1}_E = \sum_{j \in J} \mathbb{1}_{C_j}$ and $P(E) = \sum_{j \in J} P(C_j)$, Eq. (2.19) with $C = C_j$ implies

$$\mathbb{1}_E = \sum_{j \in J} \left(\mathbb{1}_{\text{sat}(C_j)} - \sum_{k \in K(j)} \mathbb{1}_{Y_{k,j}} \right), \quad \text{and} \quad P(E) = \sum_{j \in J} \left(P(\text{sat}(C_j)) + \sum_{k \in K(j)} P(Y_{k,j}) \right) \quad (2.20)$$

where $\{Y_{k,j}\}_{k \in K(j)}$ denotes the holes of C_j . Note that if $|E| = +\infty$, there is exactly one j such that $|C_j| = +\infty$, say, for $j = j_0$. In that case, $\text{sat}(C_{j_0}) = \mathbb{R}^d$ and we may alternatively write

$$\underbrace{(\mathbb{1}_E - 1)}_{=-\mathbb{1}_{E^c}} = - \sum_{k \in K(j_0)} \mathbb{1}_{Y_{k,j_0}} + \sum_{j \in J \setminus \{j_0\}} \left(\mathbb{1}_{\text{sat}(C_j)} - \sum_{k \in K(j)} \mathbb{1}_{Y_{k,j}} \right) \quad (2.21)$$

Eventually, let $u \in \mathcal{F}$. Using a level set decomposition as in [Corollary 2.1](#), we may write

$$u = \sum_{i=1}^{i_0} \beta_i \mathbb{1}_{E_i} + \sum_{i=i_0+1}^m \beta_i (-\mathbb{1}_{E_i^c}) \quad (2.22)$$

$$\text{where } E_1 \subsetneq \dots \subsetneq E_{i_0} \subsetneq \dots \subsetneq E_m, \quad \text{and } |E_i| < +\infty \text{ iff } i \leq i_0, \quad (2.23)$$

$$\forall i \in \{1, \dots, m\}, \beta_i > 0, \quad \text{and } \sum_{1 \leq i \leq m} \beta_i P(E_i) = 1. \quad (2.24)$$

Combining [\(2.20\)](#) and [\(2.21\)](#), we obtain the decomposition:

$$u = \sum_{\ell} \gamma_{\ell} \mathbb{1}_{S_{\ell}} \quad (2.25)$$

where each S_{ℓ} is a simple set, $\gamma_{\ell} \in \mathbb{R}$, and $\sum_{\ell} |\gamma_{\ell}| P(S_{\ell}) = 1$. This looks like the mere conclusion of Carathéodory's theorem, but as we show below, we can now track the relations between the S_{ℓ} 's.

2.4.2 The tree structure of the decomposition

In the decomposition [\(2.25\)](#), each S_{ℓ} is of the form $\text{sat}(C_j)$ or $Y_{k,j}$, that is, the saturation or a hole of some level set. If S_{ℓ} and $S_{\ell'}$ stem from two different level sets, say E and E' with $E \subseteq E'$, it is possible to compare them, using the following observations.

If C is an indecomposable set, we define the exterior of C , denoted by $\text{ext}(C)$, as the unique M -connected component of C^c with infinite measure (if it exists). In particular, the M -connected components of C^c are exactly the holes of C and its exterior.

Connected components of nested sets. If E, E' are sets with finite perimeter with $E \subseteq E'$, then any M -connected component of E is contained in some (unique) M -connected component of E' , see [\[ACMM01, Thm. 1\]](#).

Saturations of nested sets. Let C, C' be indecomposable sets with $C \subseteq C'$. Then $\text{sat}(C) \subseteq \text{sat}(C')$, see [\[ACMM01, Prop. 6\]](#).

Holes of nested sets. Let C, C' be indecomposable sets with $C \subseteq C'$. If Y is a hole of C , then $Y \subseteq \text{sat}(C) \subseteq \text{sat}(C')$. If Y' is a hole of C' , then $Y' \subset \text{ext}(C)$ or $Y' \subseteq Y$ for some hole Y of C (this is a consequence of [\[ACMM01, Thm. 1\]](#)).

Saturations of disjoint sets. If C, C' are indecomposable sets with $|C \cap C'| = 0$, then $|\text{sat}(C) \cap \text{sat}(C')| = 0$ or $\text{sat}(C) \subseteq \text{sat}(C')$ (or conversely), see [\[ACMM01, Prop. 6\]](#).

Holes of disjoint sets. If C, C' are indecomposable sets with $|C \cap C'| = 0$, then C' is included in the exterior of C or in a hole of C .

The different possibilities are summarized in [Table 2.1](#). The conclusion is that $S_{\ell} \cap S_{\ell'} = \emptyset$, $S_{\ell} \subseteq S_{\ell'}$ or $S_{\ell'} \subseteq S_{\ell}$.

Theorem 2.2 (The tree of shapes of an image). *Let \mathcal{F} be a closed k -dimensional face of C_{BV} . Then, for all $u \in \mathcal{F}$, there exists a family $\{S_{\ell}\}_{\ell \in \mathcal{L}} \subseteq \mathcal{E}$ such that each S_{ℓ} is simple, $0 < |S_{\ell}| < +\infty$,*

$$u = \sum_{\ell \in \mathcal{L}} \gamma_{\ell} \mathbb{1}_{S_{\ell}}, \quad (2.26)$$

Connected component	$C_j \subseteq C'_{j'}$		$C_j \cap C'_{j'} = \emptyset$	
Saturation	$\text{sat}(C_j) \subseteq \text{sat}(C'_{j'})$		$\text{sat}(C_j) \subseteq \text{sat}(C'_{j'})$	$\text{sat}(C'_{j'}) \subseteq \text{sat}(C_j)$
For each hole $Y'_{k',j'}$ of $C'_{j'}$,	$(\exists k_\star, Y_{k',j'} \subseteq Y_{k_\star,j} \subset \text{sat}(C_j))$ hence $(\forall k \neq k_\star, Y'_{k',j'} \cap Y_{k,j} = \emptyset)$	$(Y'_{k',j} \subset \text{ext}(C_j) = (\text{sat}(C_j))^c)$ hence $(\forall k, Y_{k',j'} \cap Y_{k,j} = \emptyset)$	$(\forall k, Y_{k,j} \subset \text{sat}(C_j) \subseteq Y'_{k',j'})$ or $(\text{sat}(C_j) \cap Y'_{k',j'} = \emptyset)$ hence $\forall k, Y_{k,j} \cap Y'_{k',j'} = \emptyset$	$(\exists k_\star \text{ (independent of } k'),$ $Y'_{k',j'} \subset \text{sat}(C'_{j'}) \subseteq Y_{k_\star,j})$ hence $(\forall k \neq k_\star, Y_{k,j} \cap Y'_{k',j'} = \emptyset)$
For each hole $Y_{k,j}$ of C_j	$\forall k', (Y'_{k',j'} \subseteq Y_{k,j}) \text{ or } (Y'_{k',j'} \cap Y_{k,j} = \emptyset)$		$(\exists k'_\star \text{ (independent of } k),$ $Y_{k,j} \subset \text{sat}(C_j) \subseteq Y'_{k'_\star,j'})$ hence $(\forall k' \neq k'_\star, Y_{k,j} \cap Y'_{k',j'} = \emptyset)$	$(\forall k', Y'_{k',j'} \subset \text{sat}(C'_{j'}) \subseteq Y_{k,j})$ or $(\text{sat}(C'_{j'}) \cap Y_{k,j} = \emptyset \text{ hence } \forall k', Y'_{k',j'} \cap Y_{k,j} = \emptyset)$

Table 2.1: The different relations between the M -connected components and holes of E with respect to those of E' (where $E \subseteq E'$). Each column corresponds to an alternative. Together with the relations which always hold $Y_{k,j} \subset \text{sat}(C_j)$, $Y_{k_1,j} \cap Y_{k_2,j} = \emptyset$ for $k_1 \neq k_2$, this implies that the sets S_ℓ in Eq. (2.25) always disjoint or nested.

and for all $\ell, \ell' \in \mathcal{L}$, the sets S_ℓ and $S_{\ell'}$ are either disjoint or nested.

The collection $\{\mathbb{R}^d\} \cup \{S_\ell\}_{\ell \in \mathcal{L}}$ has a tree structure (for the inclusion relation), $\text{card } \mathcal{L} \leq k + 1$, and:

- If $\text{sign}(\gamma_\ell) = \text{sign}(\gamma_{\ell'})$ and $S_\ell \cap S_{\ell'} = \emptyset$, then $\mathcal{H}^{d-1}(\partial^* S_\ell \cap \partial^* S_{\ell'}) = 0$.
- If $\text{sign}(\gamma_\ell) = -\text{sign}(\gamma_{\ell'})$ and $S_\ell \subseteq S_{\ell'}$, then $\mathcal{H}^{d-1}(\partial^* S_\ell \cap \partial^* S_{\ell'}) = 0$.

Proof. The collection built in (2.25) is almost the one we need, except that it may contain redundant shapes. If $S_{\ell_1} = S_{\ell_2}$, we must have $\text{sign}(\gamma_{\ell_1}) = \text{sign}(\gamma_{\ell_2})$, otherwise $|Du|(\mathbb{R}^d) < \sum_\ell |\gamma_\ell| P(S_\ell) = 1$, which would imply $\mathcal{F} = C_{\text{BV}}$ and would contradict $\dim \mathcal{F} = k$. Therefore if $S_{\ell_1} = \dots = S_{\ell_n}$, we replace them with a single occurrence of S_{ℓ_1} with weight $\sum_{i=1}^n \gamma_{\ell_i}$, which preserves the property $\sum_\ell |\gamma_\ell| P(S_\ell) = 1$.

Note that $S_\ell \in \mathcal{E}$ for each ℓ such that $\gamma_\ell > 0$, and $S_\ell^c \in \mathcal{E}$ for each ℓ such that $\gamma_\ell < 0$. Indeed, the decomposition

$$u = \sum_\ell |\gamma_\ell| P(S_\ell) \frac{(\text{sign}(\gamma_\ell) \mathbb{1}_{S_\ell})}{P(S_\ell)} \quad (2.27)$$

describes $u \in \mathcal{F}$ as a convex combination of the functions $\frac{(\text{sign}(\gamma_\ell) \mathbb{1}_{S_\ell})}{P(S_\ell)}$, hence $\frac{(\text{sign}(\gamma_\ell) \mathbb{1}_{S_\ell})}{P(S_\ell)} \in \mathcal{F}$.

Now, we have have a collection such that, if $\ell \neq \ell'$, S_ℓ and $S_{\ell'}$ are disjoint or nested. This provides a tree structure, and implies that the family $\{\text{sign}(\gamma_\ell) \frac{\mathbb{1}_{S_\ell}}{P(S_\ell)}\}_{\ell \in \mathcal{L}}$ is linearly independent. Since this collection is included in \mathcal{F} , we deduce that $\text{card}(\mathcal{L}) \leq k + 1$.

To conclude the proof, we note that the conclusions $\mathcal{H}^{d-1}(\partial^* S_\ell \cap \partial^* S_{\ell'}) = 0$ follow from Remark 2.1. \square

2.5 Examples of finite dimensional faces

To illustrate the results of the previous sections, we describe the closed 1-faces of C_{BV} . As C_{BV} is bounded and any extreme point of a 1-face is an extreme point of C_{BV} , those must be of the form $\left[\varepsilon_A \frac{\mathbb{1}_A}{P(A)}, \varepsilon_B \frac{\mathbb{1}_B}{P(B)} \right]$ where A and B are simple sets and $\{\varepsilon_A, \varepsilon_B\} \subseteq \{-1, +1\}$.

Proposition 2.8. *Let $A, B \subseteq \mathbb{R}^d$ be two distinct simple sets with $0 < |A|, |B| < +\infty$.*

Then, the line segment $\left[\frac{\mathbb{1}_A}{P(A)}, \frac{\mathbb{1}_B}{P(B)} \right]$ is a face of C_{BV} if and only if one of the following holds:

- $B \subseteq A$ and $A \setminus B$ is indecomposable (or similarly, exchanging the roles of A and B)
- $A \cap B = \emptyset$, $\mathcal{H}^{d-1}(\partial^* A \cap \partial^* B) = 0$ and $\mathbb{R}^d \setminus (A \cup B)$ is indecomposable.

Proof. Let $\mathcal{F} = \left[\frac{\mathbb{1}_A}{P(A)}, \frac{\mathbb{1}_B}{P(B)} \right]$, and assume that \mathcal{F} is a face. Then $A, B \in \mathcal{E}_+$, and, since $0 \notin \mathcal{F}$ (otherwise we would have $\mathcal{F} = C$), Proposition 2.3 implies $P(A \cup B) + P(A \cap B) = P(A) + P(B)$.

First, assume that $|A \cap B| = 0$. Then $P(A \cup B) = P(A) + P(B)$, which is equivalent to $\mathcal{H}^{d-1}(\partial^* A \cap \partial^* B) = 0$. Moreover, consider the chain

$$\emptyset \subset A \subset A \cup B \subset \mathbb{R}^d.$$

If $\mathbb{R}^d \setminus (A \cup B)$ were decomposable, then that chain would not be maximal (since, by Proposition 2.6, $A \cup B \subsetneq A \cup B \cup C \subsetneq \mathbb{R}^d$ for any M -connected component of $\mathbb{R}^d \setminus$

$(A \cup B)$). That would contradict the fact that $\dim \mathcal{F} = 1$. As a result, $\mathbb{R}^d \setminus (A \cup B)$ is indecomposable.

Now, if $|A \cap B| > 0$, we have $A \cap B \in \mathcal{E}_+$ and

$$(A \cap B) \subseteq A \subseteq (A \cup B) \quad (2.28)$$

yields a chain in \mathcal{E}_+ . Since $\dim \mathcal{F} = 1$, this chain has at most two distinct elements, hence, modulo a Lebesgue negligible set, $A \cap B = A$ (*i.e.* $A \subseteq B$) or $A = A \cup B$ (*i.e.* $B \subseteq A$). Assume without loss of generality that $B \subseteq A$. By contradiction, if $A \setminus B$ is decomposable, the chain

$$\emptyset \subset B \subset A \subset \mathbb{R}^d$$

is not maximal, which contradicts $\dim \mathcal{F} = 1$. Hence $A \setminus B$ is indecomposable.

For the converse implication, the proof follows the same line as the proof in [BC19] that the (renormalized) indicators of the simple sets are the extreme points of C_{BV} . We only sketch it for brevity.

Let A, B satisfy one the above assumptions, let $\theta \in]0, 1[$, and define $u = \theta \mathbf{1}_A / P(A) + (1 - \theta) \mathbf{1}_B / P(B)$. Note that, in both cases, $|Du|(\mathbb{R}^d) = 1$. Assume that there exist $u_1, u_2 \in C_{\text{BV}}$ such that $u = \rho u_1 + (1 - \rho) u_2$ for some $\rho \in]0, 1[$. The goal is to prove necessarily u_1 and u_2 are in $[\frac{\mathbf{1}_A}{P(A)}, \frac{\mathbf{1}_B}{P(B)}]$. By defining $S := \partial^* A \cup \partial^* B$, remark that

$$1 = |Du|(S) \leq \rho \underbrace{|Du_1|(S)}_{\leq 1} + (1 - \rho) \underbrace{|Du_2|(S)}_{\leq 1} \leq 1 \quad (2.29)$$

where the last inequality comes from $u_1, u_2 \in C_{\text{BV}}$. Therefore, $|Du_i|(S) = 1$, and in particular $|Du_i|(\mathbb{R}^d \setminus S) = 0$ for $i = 1, 2$. Thus, for any indecomposable set C such that $\overset{\circ}{C}^M \subseteq \mathbb{R}^d \setminus S$ (where $\overset{\circ}{C}^M$ denotes the measure-theoretic interior of C , *i.e.* its set of Lebesgue points), we have $|Du|(\overset{\circ}{C}^M) = 0$, and by a result of G. Dolzmann and S. Müller [DM95], u_i is constant on C .

If $A \cap B = \emptyset$, we apply this principle to A , B and $\mathbb{R}^d \setminus (A \cup B)$. Indeed, their measure-theoretic interior does not intersect S , since, denoting by E^t the points of E of Lebesgue density t ,

$$\overset{\circ}{A}^M \cap S = A^1 \cap (\partial^* A \cup \partial^* B) \subseteq A^1 \cap (A^{1/2} \cup B^{1/2}) = A^1 \cap B^{1/2} = \emptyset \quad \text{since } |A \cap B| = 0, \quad (2.30)$$

$$\overbrace{\mathbb{R}^d \setminus (A \cup B)}^{\circ}{}^M \cap S \subseteq A^0 \cap B^0 \cap (A^{1/2} \cup B^{1/2}) = \emptyset. \quad (2.31)$$

Hence each u_i is constant on those sets. On the other hand, if $B \subseteq A$, we apply it to $\mathbb{R}^d \setminus A$, $A \setminus B$ and A , and we obtain similarly that u_i is constant on those sets.

In both cases, by integrability, u_i must vanish on $\mathbb{R}^d \setminus (A \cup B)$. Thus, there exist $\alpha_1, \alpha_2, \beta_1, \beta_2$ such that

$$\begin{cases} u_1 &= \alpha_1 \mathbf{1}_A + \beta_1 \mathbf{1}_B \\ u_2 &= \alpha_2 \mathbf{1}_A + \beta_2 \mathbf{1}_B. \end{cases}$$

To write u_i as a convex combination of $\mathbf{1}_A / P(A)$ and $\mathbf{1}_B / P(B)$, it remains to prove that $\alpha_i \geq 0$, $\beta_i \geq 0$ with $\alpha_i P(A) + \beta_i P(B) = 1$, for $i \in \{1, 2\}$. To this end, we recall from Eq. (2.29) that

$$|Du|(\mathbb{R}^d) = \rho |Du_1|(\mathbb{R}^d) + (1 - \rho) |Du_2|(\mathbb{R}^d), \quad (2.32)$$

and we make each term explicit.

First, consider the case $A \cap B = \emptyset$. As $u = \theta \mathbf{1}_A / P(A) + (1 - \theta) \mathbf{1}_B / P(B) = \rho u_1 + (1 - \rho) u_2$, we observe the values in A and B to get

$$\begin{cases} \theta / P(A) &= \rho \alpha_1 + (1 - \rho) \alpha_2, \\ (1 - \theta) / P(B) &= \rho \beta_1 + (1 - \rho) \beta_2. \end{cases} \quad (2.33)$$

By the coarea formula (see [Theorem A.1](#)), the left-hand side of (2.32) is

$$\begin{aligned} |Du|(\mathbb{R}^d) &= \frac{\theta}{P(A)} P(A) + \frac{(1 - \theta)}{P(B)} P(B) \\ &= (\rho \alpha_1 + (1 - \rho) \alpha_2) P(A) + (\rho \beta_1 + (1 - \rho) \beta_2) P(B) \\ &= \rho(\alpha_1 P(A) + \beta_1 P(B)) + (1 - \rho)(\alpha_2 P(A) + \beta_2 P(B)). \end{aligned}$$

On the other hand, we have

$$\begin{aligned} \rho |Du_1|(\mathbb{R}^d) + (1 - \rho) |Du_2|(\mathbb{R}^d) &= \rho(|\alpha_1| P(A) + |\beta_1| P(B)) \\ &\quad + (1 - \rho)(|\alpha_2| P(A) + |\beta_2| P(B)). \end{aligned}$$

Hence, (2.32) implies that $|\alpha_i| P(A) + |\beta_i| P(B) = \alpha_i P(A) + \beta_i P(B)$, which implies that $\alpha_i = |\alpha_i|$, $\beta_i = |\beta_i|$ and the desired result holds.

Now, we deal with the case $B \subseteq A$. We note that (2.33) also holds (but the second line is the value in B minus the value in A). Let ν_A and ν_B be the measure-theoretic inner unit normals of A and B (respectively defined on $\partial^* A$ and $\partial^* B$). As a consequence of $B \subseteq A$, ν_A and ν_B must coincide in $\partial^* A \cap \partial^* B$. Hence, for $i = 1, 2$,

$$Du_i = \alpha_i \nu_A \mathcal{H}^{d-1} \llcorner (\partial^* A \setminus \partial^* B) + \beta_i \nu_B \mathcal{H}^{d-1} \llcorner (\partial^* B \setminus \partial^* A) + (\alpha_i + \beta_i) \nu_A \mathcal{H}^{d-1} \llcorner (\partial^* A \cap \partial^* B)$$

and

$$\begin{aligned} Du &= \frac{\theta}{P(A)} \nu_A \mathcal{H}^{d-1} \llcorner (\partial^* A \setminus \partial^* B) + \frac{(1 - \theta)}{P(B)} \nu_B \mathcal{H}^{d-1} \llcorner (\partial^* B \setminus \partial^* A) \\ &\quad + \left(\frac{\theta}{P(A)} + \frac{(1 - \theta)}{P(B)} \right) \nu_A \mathcal{H}^{d-1} \llcorner (\partial^* A \cap \partial^* B). \end{aligned}$$

As a result, the left-hand side of (2.32) is

$$\begin{aligned} |Du|(\mathbb{R}^d) &= \frac{\theta}{P(A)} \mathcal{H}^{d-1}(\partial^* A \setminus \partial^* B) + \frac{(1 - \theta)}{P(B)} \mathcal{H}^{d-1}(\partial^* B \setminus \partial^* A) \\ &\quad + \left(\frac{\theta}{P(A)} + \frac{(1 - \theta)}{P(B)} \right) \mathcal{H}^{d-1}(\partial^* A \cap \partial^* B) \\ &= (\rho \alpha_1 + (1 - \rho) \alpha_2) \mathcal{H}^{d-1}(\partial^* A \setminus \partial^* B) + (\rho \beta_1 + (1 - \rho) \beta_2) \mathcal{H}^{d-1}(\partial^* B \setminus \partial^* A) \\ &\quad + (\rho(\alpha_1 + \beta_1) + (1 - \rho)(\alpha_2 + \beta_2)) \mathcal{H}^{d-1}(\partial^* A \cap \partial^* B) \end{aligned}$$

On the other hand, we have

$$\begin{aligned} \rho |Du_1|(\mathbb{R}^d) + (1 - \rho) |Du_2|(\mathbb{R}^d) &= \rho(|\alpha_1| \mathcal{H}^{d-1}(\partial^* A \setminus \partial^* B) + |\beta_1| \mathcal{H}^{d-1}(\partial^* B \setminus \partial^* A) \\ &\quad + |\alpha_1 + \beta_1| \mathcal{H}^{d-1}(\partial^* A \cap \partial^* B)) \\ &\quad + (1 - \rho)(|\alpha_2| \mathcal{H}^{d-1}(\partial^* A \setminus \partial^* B) + |\beta_2| \mathcal{H}^{d-1}(\partial^* B \setminus \partial^* A) \\ &\quad + |\alpha_2 + \beta_2| \mathcal{H}^{d-1}(\partial^* A \cap \partial^* B)). \end{aligned}$$

Thus, provided that $\mathcal{H}^{d-1}(\partial^* A \setminus \partial^* B) > 0$ and $\mathcal{H}^{d-1}(\partial^* B \setminus \partial^* A) > 0$, [Eq. \(2.32\)](#) implies that $|\alpha_i| = \alpha_i$, $|\beta_i| = \beta_i$, hence $|\alpha_i + \beta_i| = \alpha_i + \beta_i$. We deduce that $\alpha_i P(A) + \beta_i P(B) = 1$ for $i \in \{1, 2\}$, and the claimed result follows.

Therefore, to complete the proof, we need to show that $\mathcal{H}^{d-1}(\partial^* A \setminus \partial^* B) > 0$ and $\mathcal{H}^{d-1}(\partial^* B \setminus \partial^* A) > 0$. We apply [ACMM01, Prop. 4]: since A is indecomposable and $B \subseteq A$, if we had $\partial^* B \subseteq \partial^* A \pmod{\mathcal{H}^{d-1}}$ we would have $B = A$ (since $|B| > 0$ by hypothesis), a contradiction. Arguing similarly for $A^\complement \subseteq B^\complement$ with B^\complement indecomposable, we deduce that $\partial^* A \not\subseteq \partial^* B \pmod{\mathcal{H}^{d-1}}$. The proof is complete. \square

A similar result holds for opposite signs, we omit the proof for the sake of brevity.

Proposition 2.9. *Let $A, B \subseteq \mathbb{R}^d$ be two distinct simple sets with $0 < |A|, |B| < +\infty$.*

Then, the line segment $\left[\frac{\mathbf{1}_A}{P(A)}, \frac{(-\mathbf{1}_B)}{P(B)} \right]$ is a face of C_{BV} if and only if one of the following holds:

- $B \subseteq A$, $\mathcal{H}^{d-1}(\partial^* A \cap \partial^* B) = 0$, and $A \setminus B$ is indecomposable (or similarly, exchanging the roles of A and B)
- $A \cap B = \emptyset$, and $\mathbb{R}^d \setminus (A \cup B)$ is indecomposable.

2.6 Conclusion

2.6.1 Summary

In this chapter, we have studied the extreme points of the faces of the total variation unit ball. Considering only the extreme points of that ball, *i.e.* renormalized indicators of simple sets, yields only a representation of the solutions to $(\mathcal{P}_{\text{BV}})$ as a sum of M indicator functions, having at most $2^M - 1$ nonzero values. However, a closer inspection of the faces of finite dimension shows that there is a strong structure in the family of simple sets involved in each face. In particular, an extreme point of the solutions to $(\mathcal{P}_{\text{BV}})$ can only take at most M nonzero values. Eventually, we show that the (finite-dimensional) faces of C_{BV} encode the tree of shape of its elements u . More precisely, there is a representation of u as a convex combination of (renormalized) indicators of simple sets, and that family has the same properties as the *tree of shapes decomposition* of an image introduced in [MG00].

2.6.2 Discussion with respect to prior works and extensions

Case of a bounded domain. While this chapter focuses on the domain \mathbb{R}^d for simplicity, let us mention that the case of a bounded domain with Dirichlet or Neumann boundary conditions is also interesting (and, admittedly, more relevant to image processing). The Neumann case has been considered by K. Bredies and M. Carioni in [BC19], who define a suitable notion of simple set and extend W. Fleming's result stating that the extreme point of the unit ball are the (signed and normalized) indicator functions of simple sets (modulo constant functions). To our knowledge, the higher dimensional faces have not been studied in the literature. However, it seems likely that the properties described in the present chapter extend to that case as well.

Submodular functions and faces of the unit ball. Describing the faces of the total variation unit ball is a particular case of understanding the unit ball of a submodular regularization. That problem has received a lot of attention and the monographs by S. Fujishige [Fuj05] and F. Bach [Bac13] (see also [Bac11]) provide comprehensive studies of submodular functions defined on a finite set. For instance, the description of faces using partitions and maximal chains in Section 2.3 are inspired from [Fuj05, Sec. 3.2]. However, please note that, as they work on a finite graph, the above-mentioned references

usually exploit the polyhedral nature of the convex set C . In particular, the description of the faces of C in [Bac11] is obtained by a duality argument from the description provided in [Fuj05] of the faces of its polar set. In our continuous setting, C is not a polyhedron, and we cannot assume that every face of C is an exposed face.

If we relied on a duality argument we would only be able to describe the exposed faces (which would depend on the chosen duality pairing). This has some striking consequences on the description that one may obtain. For instance, with $d = 2$, W. Fleming's result (Proposition 2.1) states that the (normalized) indicator function of a square is an extreme point of C_{BV} . However, it is not an exposed point for the natural choice of a dual space $(L^{d/(d-1)}(\mathbb{R}^d))' = L^2(\mathbb{R}^2)$, otherwise the square would have a variational curvature⁸ in $L^2(\mathbb{R}^2)$, which is known to be false (see [Mey01]).

As a result, in continuation of W. Fleming's result, we have chosen to describe the (not necessarily exposed) faces of C_{BV} .

Submodular functions and contractions. In standard references on submodular functions [Fuj05, Bac13], it is important, when describing the faces of the unit ball, to consider the indecomposability for the *contraction*, that is the submodular function

$$P_B : E \longmapsto P(E \cup B) - P(B) \quad (2.34)$$

defined on the measurable subsets of $\mathbb{R}^d \setminus B$. In particular, given a chain $G_0 \subset \dots \subset G_m$, one states that $G_{i+1} \setminus G_i$ is indecomposable for P_{G_i} . With the total variation, we need not consider such perimeters since both notions coincide. Indeed, it is possible to prove:

Proposition 2.10. *Let $A, B \subseteq \mathbb{R}^d$ be two sets of finite perimeter such that $B \subset A$. Then $A \setminus B$ is indecomposable (for P) if and only if it is indecomposable for P_B .*

The tree of shapes of an image. A fundamental principle of Mathematical Morphology is the idea that images are equivalent through contrast changes (say, $v = g \circ u$ with g Lipschitz strictly increasing), hence image analysis operations should respect that invariance [SC82]. Under suitable assumptions, it is equivalent to working on the upper level sets $(E_t)_{t \in \mathbb{R}}$ of images and reconstructing it using the formula

$$u(x) = \sup \{ t \in \mathbb{R} \mid x \in E_t \}. \quad (2.35)$$

However, the level set representation is redundant. Moreover, many interesting image processing operations focus on the connected components of E_t rather than E_t itself. As it is desirable to handle dark objects in the same way as one handles the clear objects (this property is called *self-duality* in imaging), one has to deal with two trees of connected components (one for the upper and one for the lower level sets), and modifying the former impacts the latter. To overcome such limitations, P. Monasse and F. Guichard define a shape by filling-in the holes of the connected components of upper or lower level sets, organizing them into a single tree structure which can be efficiently computed using a fast transform [MG00]. In [BCM03], C. Ballester *et al.* extend it to images having a continuum of gray levels. The tree of shapes is a convenient tool which can be used in image registration [Mon99], denoising [DK00], or scale analysis [LAG09] methods.

It is worth noting that the tree of shapes constructed in the present chapter slightly differs from the one in [MG00, BCM03] insofar as we use measure theoretic notions (M -connectedness, functions with bounded variation) as opposed to topological ones

⁸A locally integrable function v is a variational curvature of $A \subseteq \mathbb{R}^d$ if A is a solution to the problem $\min_{E \subseteq \mathbb{R}^d} \int_E v - P(E)$.

(connectedness, semi-continuous functions), see [BC01] for a comparison of the two notions. However, the similarity between the two constructions is striking: the filling of the holes as introduced by P. Monasse and F. Guichard naturally leads to the simple sets (*i.e.* the extreme points of the total variation unit ball) and, in some sense, the tree of shapes of images is encoded in the faces of the TV unit ball.

Choquet's integral and the coarea formula. In this chapter, we have often written a function with finite range as a convex combination of the (renormalized) indicator functions of its level sets. More generally, if $u \in L^{d/(d-1)}(\mathbb{R}^d)$, we may write for a.e. $x \in \mathbb{R}^d$ (compare with (2.35)),

$$u(x) = \int_0^{+\infty} \mathbb{1}_{\{u(x) \geq t\}} dt + \int_{-\infty}^0 (\mathbb{1}_{\{u(x) \geq t\}} - 1) dt. \quad (2.36)$$

On the other hand, for $|Du|(\mathbb{R}^d) = 1$, the coarea formula states that

$$1 = \int_{-\infty}^{+\infty} P(\{u \geq t\}) dt \quad (2.37)$$

so that, at least formally, we may define a probability measure by $d\omega(t) = P(\{u \geq t\}) dt$ and (2.36) becomes

$$u = \int_0^{+\infty} \frac{\mathbb{1}_{\{u \geq t\}}}{P(\{u \geq t\})} d\omega(t) + \int_{-\infty}^0 \frac{(\mathbb{1}_{\{u \geq t\}} - 1)}{P(\{u \geq t\})} d\omega(t). \quad (2.38)$$

In other words, u is expressed as a weighted average of the (renormalized) indicator functions of its level sets. Now, each level set $\{u \geq t\}$ may be decomposed as in Section 2.4, expressing u as a weighted combination of indicators of simple sets. Such expression might be interpreted as a Choquet integral, which describes the points of a closed convex set using a probability measure on the set of extreme points. Such a connection was already pointed out in [Fle57]. It seems the right way to study the faces of infinite dimension, but its manipulation is not trivial. We leave such investigations for future work.

Chapter 3

Sensitivity analysis in inverse problems

Contents

3.1	General results	60
3.1.1	Regularized inverse problems	60
3.1.2	Duality for face identification	60
3.1.3	The positively homogeneous case	61
3.2	Examples	62
3.2.1	Inverse problems in the space of measures	62
3.2.2	Finite-dimensional ℓ^1 -regularized inverse problems	64
3.2.3	Inverse problems involving the total gradient variation	64
3.3	Strong duality and existence of dual solutions	66
3.3.1	The case $\lambda > 0$	66
3.3.2	The case $\lambda = 0$	67
3.4	Identifiability, source condition and low noise regimes	69
3.4.1	The source condition to ensure identifiability	69
3.4.2	Convergence for $\lambda \rightarrow 0^+$ and minimal norm certificate	71
3.5	Conclusion	73

In [Chapter 1](#), we have described the solutions u_τ of inverse problems of the form

$$\inf_{u \in V} R(u) + f(\Phi u, \tau) \quad (3.1)$$

as convex combinations of extreme points, or points in extreme rays of the level sets $\{R \leq R(u_\tau)\}$. Our goal is now to discuss *the stability of this representation* as the parameter τ varies (typically τ encodes the input data or the regularization parameter).

The main difficulty is that, when τ varies, the value $R(u_\tau)$ is very likely to change. Hence, there is hardly any hope that u_τ stays on the same face of $\{R \leq R(u_\tau)\}$, since the convex set $\{R \leq R(u_\tau)\}$ itself may change! However, one could expect that $u_\tau, R(u_\tau)$ stays on the same face of *the epigraph of R* . In that case, one could represent $u_\tau, R(u_\tau)$ as a convex combination using extreme points (or points in extreme rays) of that face. It is one of the reasons why in [Chapter 1](#) we have promoted the epigraphical approach. Alternatively, if there is a simple way to “track” the extreme points of $\{R \leq t\}$ as t varies (*e.g.* if R is positively homogeneous), we could also rely on the extreme points of $\{R \leq R(u_\tau)\}$, using a constant number of points.

As often in the calculus of variations, the study of optimality conditions is the heart of the matter. We explain below how they provide information on the face of the solution $\mathcal{F}_{\text{epi } R}(u, R(u))$, and how they vary with τ .

Collaboration. Part of this chapter is related to the work [13] with Gabriel Peyré. The influence of discussions with Jalal Fadili, Samuel Vaiter and Charles Dossal should also be acknowledged.

3.1 General results

3.1.1 Regularized inverse problems

Throughout the present chapter, we assume we are given an observation $y \in \mathcal{H}$, where \mathcal{H} is a separable Hilbert space, and we focus on energies of the form (3.1) where f is a quadratic fidelity term or an exact penalty term. In other words, given $\lambda > 0$, $y \in \mathcal{H}$, we consider the problems

$$\begin{aligned} \inf_{u \in V} R(u) + \frac{1}{2\lambda} \|\Phi u - y\|_{\mathcal{H}}^2 & \quad (\mathcal{P}(\lambda, y)) \\ \inf_{u \in V} R(u) \quad \text{s.t.} \quad \Phi u = y. & \quad (\mathcal{P}(0, y)) \end{aligned}$$

Typical instances of such energies include the BASIS PURSUIT or the LASSO [CDS99, Tib96] or total-variation regularized problems [ROF92, CL97]. The choice of the fidelity term f depends on the presence and structure of the noise. Our discussion could be extended to more general fidelity terms f , but the current setting is quite typical and allows for geometric interpretations.

Remark 3.1. Problems $(\mathcal{P}(\lambda, y))$ and $(\mathcal{P}(0, y))$ belong to the same family of problems (3.1) with $\tau = (\lambda, y)$ and $f(q, \tau) \stackrel{\text{def.}}{=} g(q - y, \lambda)$, where

$$\forall q \in \mathcal{H}, \quad g(q, \lambda) \stackrel{\text{def.}}{=} \begin{cases} \frac{1}{2\lambda} \|q\|_{\mathcal{H}}^2 & \text{if } \lambda > 0, \\ 0 & \text{if } (\lambda, q) = (0, 0), \\ +\infty & \text{otherwise.} \end{cases} \quad (3.2)$$

It turns out that g is a convex function of (q, λ) (see [BB00]). Besides, a monotonicity argument [DM93, Prop. 5.4] shows that the problems $(\mathcal{P}(\lambda, y))$ Γ -converge towards $(\mathcal{P}(0, y))$, provided R is lower semi-continuous and Φ is continuous (see below for the precise topological assumptions of the chapter).

In the rest of the chapter, we denote the problem parameter by $\tau \stackrel{\text{def.}}{=} (\lambda, y)$, where $\lambda \geq 0$, $y \in \mathcal{H}$, and we study the properties of the solutions u_τ of $(\mathcal{P}(\tau))$ as τ varies. Pushing the study of the previous chapters further, we try to estimate the face of $u_\tau, R(u_\tau)$ in the epigraph of R using *duality arguments*.

3.1.2 Duality for face identification

As we highlight in Appendix B, the duality theory is intimately related to the description in terms of faces used in the previous chapters. Though the results described in Appendix B are fairly standard, the geometric perspective is somewhat different from the literature. In a nutshell,

- Finding a normal to a convex set C at some point x provides a superset of the elementary face $\mathcal{F}_C(x)$,

- That superset is the sharpest when the normal is in the relative algebraic interior of the normal cone.
- In the case of an epigraph, $C = \text{epi } R$, that amounts to finding a subgradient at u_τ , and again, the sharpest estimation is provided by subgradients in the relative algebraic interior of the subdifferential.
- Solving the dual problem gives access to a subgradient of R at the primal solution.

To exploit the Fenchel-Rockafellar duality described in [Appendix B.4](#) and state convergence properties, it is necessary to specify the topologies and the dual spaces that we use. We resort to the theory of *paired spaces* which we recap in [Appendix B.1.1](#), but we refer to [\[Roc89\]](#) for further detail.

Assumptions 3.1. *With the notation of [Appendix B.1.1](#) we make the following assumptions throughout the chapter.*

- V and Υ are two linear spaces endowed with a duality pairing $\langle \cdot, \cdot \rangle$ which is separating.
- $R: V \rightarrow \mathbb{R} \cup \{+\infty\}$ is convex proper, lower semi-continuous for some (hence any) compatible topology.
- Π and P are equal to some linear space \mathcal{H} which can be equipped with the topology of a separable Hilbert space, and they are paired with the corresponding scalar product,
- $\Phi: V \rightarrow \Pi$ is linear continuous from $\sigma(V, \Upsilon)$ to $\sigma(\Pi, P)$ (the latter being simply the weak topology of \mathcal{H}).

With the perturbations considered in [Appendix B.4.2](#), the dual problems are respectively given by

$$\begin{aligned} \sup_{p \in \mathcal{H}} \left(\langle p, y \rangle - \frac{\lambda}{2} \|p\|_{\mathcal{H}}^2 - R^*(\Phi^* p) \right) & \quad (\mathcal{D}(\lambda, y)) \\ \sup_{p \in \mathcal{H}} (\langle p, y \rangle - R^*(\Phi^* p)) & \quad (\mathcal{D}(0, y)) \end{aligned}$$

Provided strong duality holds (*i.e.* $\inf \mathcal{P}(\tau) = \sup \mathcal{D}(\tau)$, see [Section 3.3](#)), given a pair $(u, p) \in V \times P$, u is a solution to $\mathcal{P}(\tau)$ and p is a solution to $\mathcal{D}(\tau)$ if and only if

$$p = \frac{1}{\lambda} (y - \Phi u) \quad \text{and} \quad \Phi^* p \in \partial R(u) \quad (\text{for } \lambda > 0), \quad (3.3)$$

$$y = \Phi u \quad \text{and} \quad \Phi^* p \in \partial R(u) \quad (\text{for } \lambda = 0). \quad (3.4)$$

3.1.3 The positively homogeneous case

Very often in the literature [\[CDS99, Tib96, ROF92\]](#), the regularizer R is a *positively homogeneous function*, *i.e.*

$$\forall \alpha > 0, \forall u \in V, R(\alpha u) = \alpha R(u). \quad (3.5)$$

Under that assumption (together with [Assumptions 3.1](#)), the dual problem gets an interesting geometric interpretation. One may check that R is the support function of the closed convex set $\partial R(0)$ (see [\[Roc89, Sec. 6\]](#)) and that

$$\partial R(u) = \{ \eta \in \partial R(0) \mid \langle u, \eta \rangle = R(u) \}, \quad (3.6)$$

$$R^*(\eta) = \chi_{\partial R(0)}(\eta) \stackrel{\text{def.}}{=} \begin{cases} 0 & \text{if } \eta \in \partial R(0) \\ +\infty & \text{otherwise.} \end{cases} \quad (3.7)$$

The dual problems become respectively

$$\begin{aligned} \sup_{p \in \mathcal{H}} \left(\langle p, y \rangle - \frac{\lambda}{2} \|p\|_{\mathcal{H}}^2 \right) \quad \text{s.t. } \Phi^* p \in \partial R(0), & \quad (\mathcal{D}^{(\text{PH})}(\lambda, y)) \\ \sup_{p \in \mathcal{H}} (\langle p, y \rangle) \quad \text{s.t. } \Phi^* p \in \partial R(0). & \quad (\mathcal{D}^{(\text{PH})}(0, y)) \end{aligned}$$

Introducing the closed convex set

$$K \stackrel{\text{def.}}{=} (\Phi^*)^{-1}(\partial R(0)) = \{ p \in \mathcal{H} \mid \forall u \in V, \langle \Phi u, p \rangle \leq R(u) \}, \quad (3.8)$$

we see that $(\mathcal{D}^{(\text{PH})}(\lambda, y))$ is equivalent to the projection of y/λ onto K , whereas $(\mathcal{D}^{(\text{PH})}(0, y))$ amounts to finding the face of K which is exposed by y . Alternatively, if $y = \Phi u_0$ and strong duality holds, the solution set to $(\mathcal{D}^{(\text{PH})}(0, y))$ is $(\Phi^*)^{-1}(\partial R(u_0))$.

3.2 Examples

3.2.1 Inverse problems in the space of measures

Let (X, d_X) be a locally compact separable metric space and denote by $\mathcal{M}(X)$ (resp. $\mathcal{M}^+(X)$) the set of finite signed (resp. nonnegative) Radon measures. Let $\mathcal{C}_0(X)$ be the set of real-valued continuous functions on X which vanish at infinity, *i.e.*

$$\forall \varepsilon > 0, \exists K \subseteq X \text{ compact, } \forall x \in X \setminus K, |\varphi(x)| \leq \varepsilon. \quad (3.9)$$

With the notation of [Appendix B.1.1](#), we set $V = \mathcal{M}(X)$, $\Upsilon = \mathcal{C}_0(X)$ (and $\Pi = P = \mathcal{H}$ as already mentioned).

The assumption that Φ is continuous from $\sigma(V, \Upsilon)$ to $\sigma(\Pi, P)$ means that $\Phi: \mathcal{M}(X) \rightarrow \mathcal{H}$ is weak-* to weak continuous. It is equivalent to assuming that it has the form of a Bochner integral [\[Bou07a, Sec. III.3.1\]](#)

$$\Phi m \stackrel{\text{def.}}{=} \int_X \varphi(x) dm(x), \quad (3.10)$$

where $\varphi: X \rightarrow \mathcal{H}$ is weakly continuous and weakly vanishing at infinity, *i.e.* such that $(x \mapsto \langle q, \varphi(x) \rangle_{\mathcal{H}}) \in \mathcal{C}_0(X)$ for all $q \in \mathcal{H}$.

Remark 3.2. In general, the function φ does not vanish at infinity in the norm topology of \mathcal{H} . For instance, in the case of a convolution operator, $\varphi(x) = \tilde{\varphi}(\cdot - x)$, where $\tilde{\varphi} \in \mathcal{H} \stackrel{\text{def.}}{=} L^2(\mathbb{R}^d)$ is the impulse response, φ has constant norm.

However, by the Banach-Steinhaus theorem, since

$$\forall q \in \mathcal{H}, \sup_{x \in X} |\langle q, \varphi(x) \rangle_{\mathcal{H}}| < +\infty, \quad (3.11)$$

we note that $(x \mapsto \|\varphi(x)\|_{\mathcal{H}})$ is bounded on X .

Typical examples include the case where $\varphi = (\varphi_1, \dots, \varphi_M)$ is a collection of sensing functions, such as the trigonometric system

$$\varphi(x) = (1, \cos(2\pi x), \sin(2\pi x), \dots, \cos(2f_c \pi x), \sin(2f_c \pi x)) \quad (X = \mathbb{T}) \quad (3.12)$$

or an exponential system

$$\varphi(x) = (e^{-s_1 x}, \dots, e^{-s_M x}) \quad (X = [a, +\infty[). \quad (3.13)$$

Alternatively, φ might be the impulse response of a convolution,

$$\varphi(x) = \tilde{\varphi}(\cdot - x) \quad (X = \mathbb{R}^d \text{ or } \mathbb{T}^d). \quad (3.14)$$

for some function $\tilde{\varphi} \in \mathcal{H} \stackrel{\text{def.}}{=} L^2(X)$. It is standard that the mapping $x \mapsto \tilde{\varphi}(\cdot - x)$ is strongly (hence weakly) continuous from X to $L^2(X)$ and weakly vanishes at infinity. More general operators $\tilde{\varphi}(\cdot, x)$ might be considered, with suitable integrability properties (see [Section 7.3.1](#) for more detail on spatially varying filters).

The generalized moment problem

The generalized moment problem consists in finding a nonnegative measure with given prescribed moment. We let

$$R^{(\text{GM})}(m) \stackrel{\text{def.}}{=} \chi_{\mathcal{M}^+(X)}(m) = \begin{cases} 0 & \text{if } m \in \mathcal{M}^+(X), \\ +\infty & \text{otherwise.} \end{cases} \quad (3.15)$$

The corresponding problems are respectively

$$\begin{aligned} \min_{m \in \mathcal{M}(X)} \chi_{\mathcal{M}^+(X)}(m) + \frac{1}{2\lambda} \|\Phi m - y\|_{\mathcal{H}}^2 & \quad (\mathcal{P}^{(\text{GM})}(\lambda, y)) \\ \min_{m \in \mathcal{M}(X)} \chi_{\mathcal{M}^+(X)}(m) \quad \text{s.t. } \Phi m = y & \quad (\mathcal{P}^{(\text{GM})}(0, y)) \end{aligned}$$

The existence of a solution to $\mathcal{P}^{(\text{GM})}(0, y)$ depends on whether or not $y \in \Phi(\mathcal{M}^+(X))$. A solution to $\mathcal{P}^{(\text{GM})}(\lambda, y)$ exists provided $\Phi(\mathcal{M}^+(X))$ is closed, which is guaranteed in particular if X is compact and there exists a (strictly) positive “polynomial” (see [\[KN77, Ch. I, sec 3\]](#)), *i.e.*

$$\exists p \in \mathcal{H}, \forall x \in X, \quad \langle \varphi(x), p \rangle = (\Phi^* p)(x) > 0. \quad (3.16)$$

Since $R = \chi_{\mathcal{M}^+(X)}$ is positively homogeneous, the dual problem has the form $(\mathcal{D}^{(\text{PH})}(\lambda, y))$ with

$$\partial R^{(\text{GM})}(0) = \mathcal{C}_0^+(X) \stackrel{\text{def.}}{=} \{ \eta \in \mathcal{C}_0(X) \mid \forall x \in X, \eta(x) \geq 0 \}. \quad (3.17)$$

In view of [\(3.6\)](#), the subdifferential is characterized by

$$\eta \in \partial R(m) \iff (\forall x \in X, \eta(x) \geq 0, \quad \text{and} \quad \forall x \in \text{supp}(m), \eta(x) = 0). \quad (3.18)$$

Total variation minimization

One may also regularize using the total variation of measures,

$$R^{(\text{TV})}(m) \stackrel{\text{def.}}{=} |m|(X) = \sup \left\{ \int_X \eta dm \mid \eta \in \mathcal{C}_0(X), \|\eta\|_{\infty} \leq 1 \right\}. \quad (3.19)$$

The variational problems then read

$$\begin{aligned} \min_{m \in \mathcal{M}(X)} |m|(X) + \frac{1}{2\lambda} \|\Phi m - y\|_{\mathcal{H}}^2, & \quad (\mathcal{P}^{(\text{TV})}(\lambda, y)) \\ \min_{m \in \mathcal{M}(X)} |m|(X) \quad \text{s.t. } \Phi m = y. & \quad (\mathcal{P}^{(\text{TV})}(0, y)) \end{aligned}$$

Since the total variation of measures is coercive for the weak-* topology of measures, a solution to $\mathcal{P}^{(\text{TV})}(\lambda, y)$ always exists. On the other hand, a solution to $\mathcal{P}^{(\text{TV})}(0, y)$ exists if and only if $y \in \Phi(\mathcal{M}(X))$.

Since the total variation of measures is the support function of the closed convex set

$$\partial R^{(\text{TV})}(0) = \{ \eta \in \mathcal{C}_0(X) \mid \forall x \in X, |\eta(x)| \leq 1 \}, \quad (3.20)$$

the subdifferential is characterized by

$$\eta \in \partial R(m) \iff (\forall x \in X, |\eta(x)| \leq 1, \quad \text{and} \quad \forall x \in \text{supp}(m_{\pm}), \eta(x) = \pm 1), \quad (3.21)$$

where $m = (m_+ - m_-)$ is the Hahn-Jordan decomposition of m .

Therefore, the dual problems read

$$\begin{aligned} \sup_{p \in \mathcal{H}} \left(\langle p, y \rangle - \frac{\lambda}{2} \|p\|_{\mathcal{H}}^2 \right) \quad \text{s.t.} \quad \|\Phi^* p\|_{\infty} \leq 1, & \quad (\mathcal{D}^{(\text{TV})}(\lambda, y)) \\ \sup_{p \in \mathcal{H}} (\langle p, y \rangle) \quad \text{s.t.} \quad \|\Phi^* p\|_{\infty} \leq 1. & \quad (\mathcal{D}^{(\text{TV})}(0, y)) \end{aligned}$$

Remark 3.3. In addition, it is possible to combine the total variation of measures with the positivity constraint, $R^{(\text{TV}^+)}(m) = |m|(X) + \chi_{\mathcal{M}^+(X)}(m)$, which corresponds to

$$\partial R^{(\text{TV}^+)}(0) = \{ \eta \in \mathcal{C}_0(X) \mid \forall x \in X, \eta(x) \leq 1 \}. \quad (3.22)$$

3.2.2 Finite-dimensional ℓ^1 -regularized inverse problems

Let $\mathcal{G} \subseteq X$ be a finite set (typically \mathcal{G} is a grid of points). We consider the same functional spaces as above, and we define the ℓ^1 -norm on \mathcal{G} as

$$\forall m \in \mathcal{M}(X), \quad R^{\ell^1(\mathcal{G})}(m) \stackrel{\text{def.}}{=} \|m\|_{\ell^1(\mathcal{G})} \stackrel{\text{def.}}{=} \sup \left\{ \int_X \eta dm \mid \eta \in \mathcal{C}_0(X), \forall x \in \mathcal{G}, |\eta(x)| \leq 1 \right\}. \quad (3.23)$$

The above quantity is equal to the ℓ^1 -norm, $\|a\|_1 = \sum_{x \in \mathcal{G}} |a_x|$, if $m = \sum_{x \in \mathcal{G}} a_x \delta_x$, and $+\infty$ otherwise. The corresponding problems are the celebrated LASSO and BASIS PURSUIT problems [CDS99, Tib96]:

$$\begin{aligned} \min_{m \in \mathcal{M}(X)} \|m\|_{\ell^1(\mathcal{G})} + \frac{1}{2\lambda} \|\Phi m - y\|_{\mathcal{H}}^2 & \quad (\mathcal{P}^{(\ell^1(\mathcal{G}))}(\lambda, y)) \\ \min_{m \in \mathcal{M}(X)} \|m\|_{\ell^1(\mathcal{G})} \quad \text{s.t.} \quad \Phi m = y & \quad (\mathcal{P}^{(\ell^1(\mathcal{G}))}(0, y)) \end{aligned}$$

Though it might look overly sophisticated to write an ℓ^1 -minimisation problem using (3.23), that formulation is useful to embed the discrete problem into a continuous one. While many imaging problems aim at capturing a physical signal which is defined on a continuous domain, the common practice is to try to reconstruct the signal on a grid, where it is possible to handle computations. Embedding the discrete problems into a continuous one allows to study the convergence of the approximation (see Section 5.3).

3.2.3 Inverse problems involving the total gradient variation

Let $X \stackrel{\text{def.}}{=} \mathbb{R}^d$, $d \geq 2$. Since the seminal work of L. Rudin, S. Osher and E. Fatemi [ROF92], it is common in image processing to use the total variation of the gradient as a regularizer,

$$R^{(\text{BV})}(u) = \int_X |Du| \stackrel{\text{def.}}{=} \sup \left\{ \int_X u \text{div} z \mid z \in \mathcal{C}_c^1(X; \mathbb{R}^d), \sup_{x \in X} |z(x)|_2 \leq 1 \right\}, \quad (3.24)$$

for u locally integrable in X . Typical applications of total variation regularization include: deblurring in satellite imaging [DMR00], inverse problems in microscopy [DBFZ⁺06, BGM⁺14], magnetic resonance imaging (MRI) [BV19], or structure-texture decomposition [AABFC05, Had07], but this list is far from being exhaustive.

Using the notation of Appendix B.1.1, we set $V = L^{d/(d-1)}(\mathbb{R}^d)$, $\Upsilon = L^d(\mathbb{R}^d)$. That choice is dictated by the Poincaré-type inequality [AFP00, Thm. 3.47],

$$\|u\|_{L^{d/(d-1)}(\mathbb{R}^d)} \leq C \int_{\mathbb{R}^d} |Du| \quad (3.25)$$

which makes $R^{(\text{BV})}$ coercive on V for the weak topology $\sigma(V, \Upsilon)$, hence provides existence of minimizers in variational problems.

We consider as before $\Pi = P = \mathcal{H}$ for some separable Hilbert space \mathcal{H} , and a linear map $\Phi: L^{d/(d-1)}(\mathbb{R}^d) \rightarrow \mathcal{H}$ which is continuous for the weak topologies. Typically, Φ may be a convolution operator, *i.e.*

$$(\Phi u)(x) = \int_{\mathbb{R}^d} u(t) \tilde{\varphi}(x-t) dt \quad (3.26)$$

for some function $\tilde{\varphi} \in L^q(X)$ with $q = (2d)/(d+2)$. One may check¹ that Φ maps $L^{d/(d-1)}(\mathbb{R}^d)$ into $\mathcal{H} = L^2(X)$ with the desired continuity.

Let us mention that this is only one example of functional framework. Several other variants are possible *e.g.* considering bounded domains together with different boundary conditions (see for instance [CL97, IMS17, IM20a]). In this manuscript, we mainly focus on the case where $d = 2$, and the domain is $X = \mathbb{R}^2$. In Section 4.4, we even narrow down the discussion to the case where $\Phi: L^2(\mathbb{R}^2) \rightarrow L^2(\mathbb{R}^2)$ is the identity operator.

We consider an inverse problem of the form

$$\min_{u \in L^{d/(d-1)}(\mathbb{R}^d)} \int_{\mathbb{R}^d} |Du| + \frac{1}{2\lambda} \|\Phi u - y\|_{\mathcal{H}}^2, \quad (\mathcal{P}^{(\text{BV})}(\lambda, y))$$

and its limit problem

$$\min_{u \in L^{d/(d-1)}(\mathbb{R}^d)} \int_{\mathbb{R}^d} |Du| \quad \text{s.t. } \Phi u = y. \quad (\mathcal{P}^{(\text{BV})}(0, y))$$

Typically, $y = \Phi f + w$, where $f \in L^{d/(d-1)}(\mathbb{R}^d)$ is some function to recover and $w \in \mathcal{H}$ is some noise.

To write $R^{(\text{BV})}$ as a support function of some closed convex set, we need to take the closure of the set of divergences in (3.24). It is thus the support function of

$$\partial R^{(\text{BV})}(0) = \left\{ \operatorname{div} z \mid z \in L^\infty(\mathbb{R}^d; \mathbb{R}^d), \|z\|_\infty \leq 1 \text{ and } \operatorname{div} z \in L^d(\mathbb{R}^d) \right\} \quad (3.27)$$

where the divergence should be understood in the sense of distributions.

The optimality $R^{(\text{BV})}(u) = \int u \operatorname{div} z$ which characterizes $\operatorname{div} z \in \partial R^{(\text{BV})}(u)$ can be interpreted informally as z being orthogonal to the level lines of u (and pointing outward from the lower level sets), and its saturation points contains the support of Du . However, giving a precise meaning to z on small sets such as \mathcal{H}^{d-1} -rectifiable sets is not trivial, and we refer to [BH16, CGN15] for rigorous statements.

Still, it is useful to characterize the subdifferential using the level sets of the function u . For $t \geq 0$, we define $U^{(t)} \stackrel{\text{def.}}{=} \{u \geq t\}$, and for $t < 0$, we define $U^{(t)} \stackrel{\text{def.}}{=} \{u \leq t\}$.

¹Using the inequality $\|f * g\|_r \leq \|f\|_p \|g\|_q$ provided $1 \leq p, q \leq +\infty$ and $1/r = 1/p + 1/q - 1 \geq 0$ (see for instance [Sch66, Sec. VI.2]).

Proposition 3.1 ([KOX06],[6]). Let $u \in L^{d/(d-1)}(\mathbb{R}^d)$, $R^{(\text{BV})}(u) < +\infty$, and $\eta \in L^d(\mathbb{R}^d)$. The following conditions are equivalent.

(i) $\eta \in \partial R^{(\text{BV})}(u)$.

(ii) $\eta \in \partial R^{(\text{BV})}(0)$ and the level sets of u satisfy

$$\forall t > 0, \quad P(U^{(t)}) = \int_{U^{(t)}} \eta, \quad \forall t < 0, \quad P(U^{(t)}) = - \int_{U^{(t)}} \eta. \quad (3.28)$$

(iii) The level sets of u satisfy

$$\forall t > 0, \quad \forall G \subset \mathbb{R}^d, |G| < +\infty, \quad P(G) - \int_G \eta \geq P(U^{(t)}) - \int_{U^{(t)}} \eta, \quad (3.29)$$

$$\forall t < 0, \quad \forall G \subset \mathbb{R}^d, |G| < +\infty, \quad P(G) + \int_G \eta \geq P(U^{(t)}) + \int_{U^{(t)}} \eta. \quad (3.30)$$

where $U^{(t)} \stackrel{\text{def.}}{=} \{x \in \mathbb{R}^d \mid u(x) \geq t\}$ for $t > 0$, and $U^{(t)} \stackrel{\text{def.}}{=} \{x \in \mathbb{R}^d \mid u(x) \leq t\}$ for $t < 0$.

3.3 Strong duality and existence of dual solutions

Of course, considering $(\mathcal{P}(\tau))$ to solve an inverse problem only makes sense if one can prove the existence of a solution. As mentioned in [Section 3.2](#), our typical regularizers usually have the coercivity properties which provide the existence of a solution, at least for $\lambda > 0$. We discuss here the existence of a solution for the dual problems.

3.3.1 The case $\lambda > 0$

For $\lambda > 0$, the existence of a dual solution and strong duality hold under mild assumptions.

Proposition 3.2. If [Assumptions 3.1](#) hold, $y \in \mathcal{H}$ and $\lambda > 0$, then strong duality holds between $(\mathcal{P}(\lambda, y))$ and $(\mathcal{D}(\lambda, y))$, i.e.

$$\sup (\mathcal{D}(\lambda, y)) = \inf (\mathcal{P}(\lambda, y)). \quad (3.31)$$

Moreover, the above quantity is finite iff $(\text{Im } \Phi^*) \cap (\text{dom } R^*) \neq \emptyset$, in which case there is a unique solution to $\mathcal{D}(\lambda, y)$, and it depends continuously on $(\lambda, y) \in]0, +\infty[\times \mathcal{H}$.

Proof. Note that $\inf \mathcal{P}(\lambda, y) < +\infty$, and that $\sup \mathcal{D}(\lambda, y) > -\infty$ iff $(\text{Im } \Phi^*) \cap (\text{dom } R^*) \neq \emptyset$.

If $\inf \mathcal{P}(\lambda, y) = -\infty$ there is nothing to prove since the weak duality ensures $\sup \mathcal{D}(\lambda, y) \leq \inf \mathcal{P}(\lambda, y)$ (see [Appendix B.4.1](#)). Otherwise, $-\infty < \inf \mathcal{P}(\lambda, y) < +\infty$ and it suffices to apply the first point of [Corollary B.1](#) with $f = \frac{1}{2} \|\cdot - y\|_{\mathcal{H}}^2$ and τ_{Π} the norm topology of \mathcal{H} . As it ensures the stability of $\mathcal{P}(\lambda, y)$, we obtain the strong duality and the existence of a solution to $\mathcal{D}(\lambda, y)$ by [Lemma B.1](#).

Now, if $(\text{Im } \Phi^*) \cap (\text{dom } R^*) \neq \emptyset$, the convex l.s.c. function $g: p \mapsto R^*(\Phi^* p)$ is proper. Solving $(\mathcal{D}(\lambda, y))$ is equivalent to computing $\text{prox}_{g/\lambda}(\frac{y}{\lambda})$, the proximity operator of g/λ at y/λ , which is then well-defined and unique. The continuity follows from the nonexpansiveness of proximity operators, the triangle inequality

$$\begin{aligned} \left\| \text{prox}_{g/\lambda'}\left(\frac{y'}{\lambda'}\right) - \text{prox}_{g/\lambda}\left(\frac{y}{\lambda}\right) \right\|_{\mathcal{H}} &\leq \left\| \text{prox}_{g/\lambda'}\left(\frac{y'}{\lambda'}\right) - \text{prox}_{g/\lambda'}\left(\frac{y}{\lambda}\right) \right\|_{\mathcal{H}} \\ &\quad + \left\| \text{prox}_{g/\lambda'}\left(\frac{y}{\lambda}\right) - \text{prox}_{g/\lambda}\left(\frac{y}{\lambda}\right) \right\|_{\mathcal{H}} \\ &\leq \left\| \frac{y'}{\lambda'} - \frac{y}{\lambda} \right\|_{\mathcal{H}} + \left\| \text{prox}_{g/\lambda'}\left(\frac{y}{\lambda}\right) - \text{prox}_{g/\lambda}\left(\frac{y}{\lambda}\right) \right\|_{\mathcal{H}} \end{aligned}$$

and the fact that the last term vanishes as $\lambda' \rightarrow \lambda$ (see for instance [Bré73, Prop. II.8]). \square

3.3.2 The case $\lambda = 0$

On the other hand, even under mild assumptions, a solution to $(\mathcal{D}(0, y))$ may fail to exist.

Example 3.1 (No solution to $(\mathcal{D}(0, y))$). Consider the Gaussian deconvolution problem $(\mathcal{P}^{(\text{TV})}(0, y))$ on the real line, i.e. set $X = \mathbb{R}$, $\mathcal{H} = L^2(X)$, and

$$(\Phi m)(x) = \int_{\mathbb{R}} g(y - x) dm(y) \quad \text{with } g(x) \stackrel{\text{def.}}{=} e^{-\frac{1}{2}|x|^2}. \quad (3.32)$$

Since Gaussian filtering is injective on $\mathcal{M}(X)$, the measure m_0 defined by

$$dm_0 \stackrel{\text{def.}}{=} (\mathbb{1}_{[0,1]} - \mathbb{1}_{[-1,0]}) d\mathcal{L}, \quad (3.33)$$

where \mathcal{L} is the Lebesgue measure, is obviously the unique solution to $(\mathcal{P}(0, y_0))$ for $y_0 = \Phi m_0$. However, there is no function $p \in L^2(X)$ which maximizes $\langle y_0, p \rangle$ under the constraint $\|\Phi^* p\|_{\infty} \leq 1$, hence no solution to $(\mathcal{D}^{(\text{PH})}(0, y))$.

➤ Indeed, using Fubini's theorem, one may check that $\Phi^* p = p * g$ where $*$ is the convolution product, so that

$$\langle y_0, p \rangle_{\mathcal{H}, \mathcal{H}} = \int_X \left(\int_X p(x - x') g(x') dm_0(x) \right) dx' = \langle m_0, p * g \rangle_{\mathcal{M}(X), \mathcal{C}_0(X)}. \quad (3.34)$$

It is possible to prove that $\text{Im } \Phi^*$ is dense in $\mathcal{C}_0(X)$, so that the supremum of (3.34) for $\|\Phi^* p\|_{\infty} \leq 1$ is $|m_0|(X)$. However, that supremum is not reached, since it would imply that $(\Phi^* p)(x) = 1$ for $x \in]0, 1[$ and -1 for $x \in]-1, 0[$, which is impossible by continuity.

Still, the strong duality holds under the following condition.

Proposition 3.3. *Suppose that Assumptions 3.1 hold and that $y \in \Phi(\text{dom } R)$. If there exists a point $p \in \mathcal{H}$ such that R^* is finite and continuous at $\Phi^* p \in \Upsilon$ for some topology τ_{Υ} compatible with the pairing, then strong duality holds between $(\mathcal{P}(0, y))$ and $(\mathcal{D}(0, y))$, and there is a solution to $(\mathcal{P}(0, y))$.*

Proof. We note that

$$-\infty < \sup(\mathcal{D}(0, y)) \leq \inf(\mathcal{P}(0, y)) < +\infty$$

where the first inequality follows from $\langle y, p \rangle - R^*(\Phi^* p) > -\infty$, the second one is the weak duality and the last one follows from $y \in \Phi(\text{dom } R)$. As a result, $\sup(\mathcal{D}(0, y))$ is finite and the second point of Corollary B.1 ensures that strong duality holds and that there is a solution to $(\mathcal{P}(0, y))$. \square

Example 3.2 (Strong duality for inverse problems in the space of measures). In the setting of Section 3.2.1, for $R = R^{(\text{TV})}$ or $R^{(\text{TV}^+)}$, since $R^* = \chi_{\partial R(0)}$ we note that $R^*(\eta) = 0$ for all η in the open set $\{\tilde{\eta} \in \mathcal{C}_0(X) \mid \|\tilde{\eta}\|_{\infty} < 1\}$ (for the topology of the uniform convergence). As a result, R^* is continuous at $\Phi^* 0 \in \mathcal{C}_0(X)$, and by Proposition 3.3 strong duality holds provided $y \in \Phi(\text{dom } R)$. However, as shown by Example 3.1, a solution to the dual problem might not exist. The criterion for strong duality applies similarly to ℓ^1 -regularization on a grid (Section 3.2.2), and since the dual problem is

essentially a linear program in finite dimension, a solution exists provided its value is finite, see also [Corollary 3.1](#) below.

For the positivity constraint ($R = R^{(\text{GM})}$), it is usually assumed that X is compact and that there exists $p \in \mathcal{H}$ such that $\Phi^*p > 0$ on X (see [\[KN77, Sec. I.3.2\]](#)). With that assumption, $R^*(\eta) = 0$ for all η in an open neighborhood of Φ^*p (in the topology of the uniform convergence), hence by [Proposition 3.3](#) *strong duality holds for $y \in \Phi(\text{dom } R)$* .

Example 3.3 (Strong duality for total gradient variation regularization). The same argument as above can be applied to the total gradient variation ([Section 3.2.3](#)), by observing that $\partial R^{(\text{BV})}(0)$ contains an open neighborhood of $0 = \Phi^*0$ in the strong $L^d(\mathbb{R}^d)$ topology. That point is not obvious when looking at [\(3.27\)](#), but the Poincaré-type inequality [\(3.25\)](#) can be interpreted as an inequality between support functions,

$$\forall u \in L^{d/(d-1)}(\mathbb{R}^d), \quad \sigma_{\partial R(0)}(u) \geq \sigma_{\overline{B_d(0,C)}}(u),$$

where $\sigma_{\partial R(0)}$ and $\sigma_{\overline{B_d(0,C)}}$ denote the support functions of $\partial R(0)$ and the closed $L^d(\mathbb{R}^d)$ ball with center 0 and radius C respectively. An inequality between support functions of closed convex sets implies the inclusion of those sets, hence² $\overline{B_d(0,C)} \subseteq \partial R^{(\text{BV})}(0)$ so that $R^{(\text{BV})^*}$ vanishes in a neighborhood of 0 and *strong duality holds by Proposition 3.3*.

As we can see, the existence of a solution for $(\mathcal{D}(0, y))$ is not granted. Nor is its uniqueness. However, both hold generically in the following sense.

Proposition 3.4. *Suppose that [Assumptions 3.1](#) hold with $\dim \mathcal{H} < +\infty$, and let $\omega \stackrel{\text{def.}}{=} \text{int}(\Phi(\text{dom } R))$.*

If there exists $y_0 \in \omega$ such that $\inf(\mathcal{P}(0, y_0)) > -\infty$, then

- *for every $y \in \omega$, strong duality holds between $(\mathcal{P}(0, y))$ and $(\mathcal{D}(0, y))$, and $(\mathcal{D}(0, y))$ has solutions.*
- *for (Lebesgue) almost every $y \in \omega$, the solution to $(\mathcal{D}(0, y))$ is unique.*

Proof. We use the notations of [Appendix B.4.3](#), considering the value function $\varphi_0: y \mapsto \inf \mathcal{P}(0, y)$. For every $y \in \omega$, there exists $u \in \text{dom } R$ such that $y = \Phi u$, so that $\varphi_0(y) \leq R(u) < +\infty$. Moreover $\varphi_0(y_0) > -\infty$, hence, by convexity, the function φ_0 cannot take the value $-\infty$ on ω . Thus, [Proposition B.4](#) applies and yields the claimed result. □

Remark 3.4. *Up to a minor adaptation, [Proposition 3.4](#) also holds when considering the relative interior instead of the interior, i.e. setting $\omega \stackrel{\text{def.}}{=} \text{rint}(\Phi(\text{dom } R))$. That allows to remove the implicit assumption that the topological interior is nonempty. The minor adaptation is that the uniqueness of the solution then holds modulo some vector space.*

➤ *Indeed, replacing the perturbation space \mathcal{H} with $\hat{\mathcal{H}} \stackrel{\text{def.}}{=} \text{Vect}(\Phi(\text{dom } R) - y_0)$, we see that $\omega - y_0$ is open in $\hat{\mathcal{H}}$, thus we may apply [Proposition 3.4](#) to obtain the strong duality and the existence of a solution to the “restricted” dual problem*

$$\sup_{\hat{p} \in \hat{\mathcal{H}}} (\langle \hat{p}, y \rangle - R^*(\Phi^* \hat{p})). \quad (3.35)$$

Moreover, the solution is unique for almost every³ $y \in \omega$.

²An alternative formulation, for $d = 2$, is that the G -norm is controlled by the $L^2(\mathbb{R}^2)$ norm (see [\[HM07\]](#)).

³For the Lebesgue measure on the affine hull of ω .

Since replacing \hat{p} with $p = \hat{p} + q$, where $q \in \hat{\mathcal{H}}^\perp$, does not change the objective, we note that the values of (3.35) and $(\mathcal{D}(0, y))$ are equal. Hence the stability property also holds for the original dual $(\mathcal{D}(0, y))$, and for almost every $y \in \text{rint}(\Phi(\text{dom } R))$, the solution set is $\hat{p} + \hat{\mathcal{H}}^\perp$, where \hat{p} is the unique solution to (3.35).

As a consequence of Remark 3.4, if R is lower-bounded and \mathcal{H} is finite-dimensional, the existence of a solution to $(\mathcal{D}(0, y))$ is essentially guaranteed. More precisely:

Corollary 3.1. *Suppose that Assumptions 3.1 hold with $\dim \mathcal{H} < +\infty$, and $R : V \rightarrow [0, +\infty]$. Then, for all $y \in \text{rint}(\Phi(\text{dom } R))$ strong duality holds between $(\mathcal{P}(0, y))$ and $(\mathcal{D}(0, y))$, and $(\mathcal{D}(0, y))$ has solutions.*

As we have seen with Example 3.1, if $\dim \mathcal{H} = +\infty$, the existence of a solution to $(\mathcal{D}(0, y))$ does not always hold, even if R is lower-bounded. However, the following analog of Proposition 3.4 holds.

Proposition 3.5. *Let $R : V \rightarrow \mathbb{R} \cup \{+\infty\}$ be convex, proper, lower semi-continuous and let $\omega \stackrel{\text{def.}}{=} \text{int}(\Phi(\text{dom } R))$ (where the interior is in the strong topology of \mathcal{H}).*

If there exists $y_0 \in \omega$ such that $\inf(\mathcal{P}(0, y_0)) > -\infty$, then

- *for every $y \in \omega$, strong duality holds between $(\mathcal{P}(0, y))$ and $(\mathcal{D}(0, y))$, and $(\mathcal{D}(0, y))$ has solutions.*
- *the set of points $y \in \omega$ for which the solution to $(\mathcal{D}(0, y))$ is unique is a dense G_δ subset of \mathcal{H} (in the strong topology).*

Proof. The proof follows the same lines as Proposition 3.4, but we apply Proposition B.5 instead of Proposition B.4. \square

Remark 3.5. *The generic uniqueness results of Proposition 3.4 and Proposition 3.5 seem to be new in the context of sparse inverse problems. We have drawn inspiration from [BCC07] which establishes the uniqueness of the solution to the Cheeger problem for generic weights on the area and the perimeter. However, it should be noted that, in sparse recovery, one is usually interested in analyzing data which lie in a very small specific set, in which uniqueness in the dual problem is rather the exception than the rule.*

3.4 Identifiability, source condition and low noise regimes

For the rest of the chapter, we assume that Assumptions 3.1 and strong duality hold.

3.4.1 The source condition to ensure identifiability

First, we consider the noiseless setting. Given $u_0 \in V$, we ask whether we can recover it from the observation $y_0 = \Phi u_0$. In other words, is u_0 the solution to $(\mathcal{P}(0, y))$ for $y = y_0 = \Phi u_0$?

Definition 3.1 (Source condition [BO04]). *We say that $u_0 \in V$ satisfies the source condition if there exists $p \in \Upsilon$ such that $\Phi^* p \in \partial R(u_0)$.*

The source condition is simply the extremality relation (B.13), hence it implies that u_0 is a solution to $(\mathcal{P}(0, y))$. Since any other solution v to $(\mathcal{P}(0, y))$ must satisfy the extremality relation (B.13) with the same p , we have:

Proposition 3.6. *If the source condition holds, u_0 is a solution to $(\mathcal{P}(0, y))$. If, moreover, Φ is injective on $\text{Aff}(\partial R^*(\Phi^*p))$, that solution is the unique one.*

Proof. The fact that u_0 is a solution has already been discussed. For the second point, we note that any other solution $v \in V$ must satisfy $\Phi^*p \in \partial R(v)$, which is equivalent to $v \in \partial R^*(\Phi^*p)$. The injectivity of Φ on $\text{Aff}(\partial R^*(\Phi^*p))$ then implies $v = u_0$. \square

Remark 3.6. *The injectivity of Φ on $\text{Aff}(\partial R^*(\Phi^*p))$ is equivalent to injectivity on its direction space $\text{Span}(\partial R^*(\Phi^*p) - u_0)$.*

Proposition 3.6 is a folklore result and the cornerstone of identifiability results in the context of ℓ^1 reconstruction (see [FR13, Th. 4.26]). For Radon measures, an emblematic result, proved by E. Candès and C. Fernandez-Granda in [CFG14] and refined in [FG16], ensures the identifiability of a combination of “well-separated” spikes in the case of the ideal low-pass filter (see also [dCG12] for an earlier result on M-systems). In the theorem below, $d_{\mathbb{T}}$ denotes the canonical distance on the torus.

Theorem 3.1 ([CFG14, FG16]). *Let $X = \mathbb{T}$, $(x, a) \in X^s \times \mathbb{R}^s$, $m_0 \stackrel{\text{def.}}{=} \sum_{i=1}^s a_i \delta_{x_i} \in \mathcal{M}(X)$ and let $y_0 \stackrel{\text{def.}}{=} \Phi m_0$ where Φ is defined by (3.12). If $\min_{i \neq j} d_{\mathbb{T}}(x_i, x_j) \geq 1.26/f_c$ and⁴ $f_c \geq 10^3$, then m_0 is the unique solution to the problem*

$$\min_{m \in \mathcal{M}(X)} |m|(X) \quad \text{s.t. } \Phi m = y_0. \quad (3.36)$$

The main ingredient in the proof of Theorem 3.1 is the construction of a “dual certificate” for m_0 , i.e. an element $\eta \in (\text{Im } \Phi^*) \cap \partial R^{(\text{TV})}(m_0)$ as in Proposition 3.6. More precisely, they build a trigonometric polynomial η such that $\|\eta\|_{\infty} \leq 1$, $\eta(x) = 1$ iff $x \in \text{supp}(m_{0,+})$, and $\eta(x) = -1$ iff $x \in \text{supp}(m_{0,-})$, see (3.21). The uniqueness follows from the injectivity of the restriction of Φ to the space of measures with the same support as m_0 : it corresponds to a Vandermonde system.

Relying on the above theorem (or its proof), several authors have extended it to random settings, different geometries or acquisition operators (see [TBSR13, BDF16, PKP20]). In [10] we have proposed an identifiability in the case of radial Fourier measurements,

$$\Phi m = [(\mathcal{F}m)(k\theta)]_{k \in \Gamma, \theta \in \Theta}. \quad (3.37)$$

where $\mathcal{F}m$ is the Fourier transform on \mathbb{R}^d , i.e. $(\mathcal{F}m)(\xi) = \int_{\mathbb{R}^d} e^{-2i\pi \langle \xi, x \rangle} dm(x)$, Θ is a set of directions, and $\Gamma \subseteq \mathbb{Z}$ is a set of radial frequencies.

Theorem 3.2 ([10, Thm. 1]). *Let $X = B(0, 1/2) \subseteq \mathbb{R}^d$, $(x, a) \in X^s \times \mathbb{C}^s$, and let $m_0 = \sum_{j=1}^s a_j \delta_{x_j}$. Let $S \subset \mathbb{S}^{d-1}$ be a set of non-zero \mathcal{H}^{d-1} -measure such that*

$$\nu_{\min} \stackrel{\text{def.}}{=} \inf_{\theta \in S} \left(\min_{i \neq j} d_{\mathbb{T}}(\langle \theta, x_i \rangle, \langle \theta, x_j \rangle) \right) > 0.$$

Let Θ be a set of $d+1$ distinct elements drawn uniformly at random from S and let $f_c = \lceil 2/\nu_{\min} \rceil$. Then, the following holds:

1. *If $\Gamma = \{-f_c, \dots, f_c\}$, then m_0 is the unique solution to*

$$\min_{m \in \mathcal{M}(X)} |m|(X) \quad \text{s.t. } \Phi m = y_0. \quad (3.38)$$

⁴More precisely, in [CFG14], the condition $f_c \geq 10^3$ is not required, but the separation constant is larger: 1.87 instead of 1.26.

2. If Γ consists of k indices drawn uniformly at random from $\{-N, \dots, N\}$, where

$$k \gtrsim \max\{\log^2(f_c/\delta), s \log(s/\delta) \log(f_c/\delta)\},$$

and $\{\text{sign}(a_j)\}_{j=1}^{f_c}$ are drawn i.i.d. from the uniform distribution on the complex unit circle, then with probability exceeding $1 - (d+1)\delta$, m_0 is the unique solution to (3.38).

The main “trick” in the proof of Theorem 3.2 is to use Theorem 3.1 to build a one-dimensional dual certificate in each direction $\theta \in \Theta$. Then by taking a convex combination of them, one obtains a dual certificate whose saturation set (i.e. $\{x \mid \eta(x) = \pm 1\}$) is the intersection of all the saturation sets, i.e. $\text{supp}(m_0)$.

Remark 3.7. Constructing a dual certificate is not the only way to ensure identifiability. For instance, in [BV19], a perfect reconstruction result is obtained by analyzing the kernel of Φ .

Conversely, in cases where $(\mathcal{P}(0, y_0))$ is stable (which does not always hold in infinite dimension), the source condition must hold for all solution of $(\mathcal{P}(0, y_0))$. Hence it can be used to ensure that a signal u_0 cannot be recovered using $(\mathcal{P}(0, y_0))$. For instance, with total variation regularization (3.19), this implies that, at least for signed measures, a separation condition as in Theorem 3.1 must hold (see Section 6.1).

3.4.2 Convergence for $\lambda \rightarrow 0^+$ and minimal norm certificate

We have seen that the solutions to $(\mathcal{D}(\lambda, y))$ vary continuously as (λ, y) varies in $]0, +\infty[\times \mathcal{H}$. The case $\lambda \rightarrow 0^+$ is more subtle as there can be many solutions to $(\mathcal{D}(0, y_0))$ or none. Moreover, for the convergence of the primal problem, the parameter λ should decay sufficiently fast.

To that end, we fix $C > 0$ and an observation y_0 . We consider a domain of parameters called *low noise regime*,

$$\Omega_C \stackrel{\text{def.}}{=} \{(\lambda, y) \in \mathbb{R} \times \mathcal{H} \mid \|y - y_0\|_{\mathcal{H}} \leq C\lambda\}. \quad (3.39)$$

and we deal with the non-uniqueness using the notion of Γ -convergence (see Appendix C for a reminder of the definition and its main properties). The following proposition is a reformulation of [HKPS07, Thm. 3.5].

Proposition 3.7 (Low noise convergence). *As $(\lambda, y) \rightarrow (0, y_0)$ in Ω_C the problems $(\mathcal{P}(\lambda, y))$ Γ -converge towards $(\mathcal{P}(0, y_0))$, for any compatible topology on V .*

Proof. We write $\tau = (\lambda, y)$, $\tau_0 = (0, y_0)$, and

$$\mathcal{E}_\tau(u) \stackrel{\text{def.}}{=} R(u) + \frac{1}{2\lambda} \|\Phi u - y\|_{\mathcal{H}}^2, \quad (3.40)$$

$$\mathcal{E}_{\tau_0}(u) \stackrel{\text{def.}}{=} \begin{cases} R(u) & \text{if } \Phi u = y_0, \\ +\infty & \text{otherwise.} \end{cases} \quad (3.41)$$

Let $\tilde{u} \in V$. We prove that the Γ -limit inferior and Γ -limit superior at \tilde{u} is equal to $\mathcal{E}_{\tau_0}(\tilde{u})$.

First, we note that by lower semi-continuity of R and $u \mapsto \|\Phi u - y_0\|_{\mathcal{H}}$, for all $r < R(\tilde{u})$ and $t < \|\Phi \tilde{u} - y_0\|_{\mathcal{H}}$, there is a neighborhood $U \subseteq V$ of \tilde{u} such that for all $u \in U$,

$$R(u) \geq r, \quad \text{and} \quad \|\Phi u - y_0\|_{\mathcal{H}} \geq t. \quad (3.42)$$

As a result of the first inequality, we obtain

$$\liminf_{\substack{\tau \rightarrow \tau_0 \\ \tau \in \Omega_C}} \left(\inf_{u \in U} \left(R(u) + \frac{1}{2\lambda} \|\Phi u - y\|_{\mathcal{H}}^2 \right) \right) \geq r. \quad (3.43)$$

and taking the supremum over r we deduce that $\Gamma - \liminf_{\substack{\tau \rightarrow \tau_0 \\ \tau \in \Omega_C}} \mathcal{E}_\tau(\tilde{u}) \geq R(\tilde{u})$.

Now, if $\Phi \tilde{u} \neq y_0$, we may assume in (3.42) that $t > 0$. Then, for all $u \in U$,

$$\begin{aligned} \|\Phi u - y\|_{\mathcal{H}} &\geq \|\Phi u - y_0\|_{\mathcal{H}} - \|y - y_0\|_{\mathcal{H}} \\ &\geq t - C\lambda, \end{aligned}$$

so that for $\lambda > 0$ small enough,

$$\inf_{u \in U} \mathcal{E}_\tau(u) \geq r + \frac{1}{2\lambda} (t - C\lambda)^2.$$

Hence for $\tau \rightarrow \tau_0$, we get $\Gamma - \liminf_{\substack{\tau \rightarrow \tau_0 \\ \tau \in \Omega_C}} \mathcal{E}_\tau(\tilde{u}) \geq +\infty = \mathcal{E}_{\tau_0}(\tilde{u})$.

It remains to bound $\Gamma - \limsup_{\substack{\tau \rightarrow \tau_0 \\ \tau \in \Omega_C}} \mathcal{E}_\tau(\tilde{u})$ for $\Phi \tilde{u} = y_0$. Any neighborhood U of \tilde{u} contains \tilde{u} , so that

$$\inf_{u \in U} \mathcal{E}_\tau(u) \leq \mathcal{E}_\tau(\tilde{u}) = R(\tilde{u}) + \frac{1}{2\lambda} \|y_0 - y\|_{\mathcal{H}}^2 \leq R(\tilde{u}) + \frac{C^2\lambda}{2}.$$

As a result,

$$\limsup_{\substack{\tau \rightarrow \tau_0 \\ \tau \in \Omega_C}} \left(\inf_{u \in U} \mathcal{E}_\tau \right) \leq \limsup_{\substack{\tau \rightarrow \tau_0 \\ \tau \in \Omega_C}} \left(R(\tilde{u}) + \frac{C^2\lambda}{2} \right) = R(\tilde{u}).$$

Taking the supremum over U , we get $\Gamma - \limsup_{\substack{\tau \rightarrow \tau_0 \\ \tau \in \Omega_C}} \mathcal{E}_\tau = R(\tilde{u}) = \mathcal{E}_{\tau_0}$. \square

Remark 3.8. *In fact, as noted in [HKPS07, Thm. 3.5], the conclusion holds under the more general assumption $\frac{1}{\lambda} \|y - y_0\|_{\mathcal{H}}^2 \rightarrow 0$, but we shall need the low noise regime Ω_C for the support stability anyway.*

As a consequence of Proposition 3.7, provided some equicoercivity property holds, the solutions to $(\mathcal{P}(\lambda, y))$ (resp. $(\mathcal{D}(\lambda, y))$) converge, up to a subsequence, towards some solutions of $(\mathcal{P}(0, y_0))$ (resp. $(\mathcal{D}(0, y_0))$).

As for the dual problem, in the low noise regime, a particular dual certificate governs the structure of the solutions, which is the cornerstone of the low-noise study of [13, 15, 14].

Proposition 3.8 ([13]). *Let p_λ be the unique solution to $(\mathcal{D}(\lambda, y_0))$. The following alternative holds.*

- *If there is no solution to $(\mathcal{D}(0, y_0))$, then $\lim_{\lambda \rightarrow 0^+} \|p_\lambda\|_{\mathcal{H}} = +\infty$.*
- *If there is a solution to $(\mathcal{D}(0, y_0))$, then $\lim_{\lambda \rightarrow 0^+} p_\lambda = p_0$ (strongly in \mathcal{H}), where p_0 is the solution to $(\mathcal{D}(0, y_0))$ with minimal norm.*

The solution p_0 is of crucial importance when studying the structure of the solutions of $(\mathcal{P}(\lambda, y))$ when the regularization parameter λ is small. With a slight abuse of terminology, we call $\eta_0 \stackrel{\text{def.}}{=} \Phi^* p_0$ the *minimal norm (dual) certificate*⁵.



In general, if $y \neq y_0$, the condition $y \in \Omega_C$ is not sufficient to ensure $p_\lambda \rightarrow p_0$.

⁵When $V = \mathcal{H}$, and Φ is the identity operator, the minimal norm certificate is known as the *minimal section* of $\partial R(u_0)$ in the theory of maximal monotone operators [Br673], and that convergence is well known.

3.5 Conclusion

Together with [Appendix B](#), this chapter explains how standard duality is useful for the identification of faces in the epigraph. As we aim at dealing with spaces of measures and weak-* topologies, we have used the setting of paired spaces. We have discussed the cases of strong duality for our inverse problems, and the effect of varying the parameter $\tau = (\lambda, y)$, in particular the convergence $\lambda \rightarrow 0^+$. Using the source condition from [\[BO04\]](#), it is possible to derive identifiability results.

Let us mention that the theory of inverse problems is rich, and that several results such as the convergence in the Bregman divergence [\[BO04, HKPS07\]](#) are beyond the scope of this thesis.

Chapter 4

Finding the minimal-norm certificate

Contents

4.1	General principle	76
4.1.1	Projecting onto the span of the minimal face	76
4.1.2	The polyhedral case	76
4.1.3	The semi-infinite programming case	77
4.2	The case of ℓ^1-synthesis recovery	79
4.2.1	The tight case and the Fuchs precertificate	79
4.2.2	The non-tight case: finding the extended support	80
4.3	Sparse-spike recovery in the space of measures	80
4.3.1	Non-degenerate certificates	81
4.3.2	The vanishing-derivatives precertificate	82
4.3.3	Connection with interpolation problems	83
4.3.4	Examples	84
4.3.5	How to ensure non-degeneracy?	87
4.4	Total (gradient) variation denoising	88
4.4.1	Calibrable sets	88
4.4.2	Convex sets	93
4.5	Conclusion	96
4.5.1	Summary	96
4.5.2	Discussion with respect to prior works and comments	96

In this chapter, we continue the study of inverse problems initiated in [Chapter 3](#), with a focus on the noiseless problems. We consider

$$\inf_{u \in V} R(u) \quad \text{s.t.} \quad \Phi u = y_0. \quad (\mathcal{P}(0, y_0))$$

and its dual problem

$$\sup_{p \in \mathcal{H}} (\langle p, y_0 \rangle - R^*(\Phi^* p)) \quad (\mathcal{D}(0, y_0))$$

Besides [Assumptions 3.1](#), we assume that strong duality holds and that both problems have solutions (see for instance [Proposition 3.3](#) and [Proposition 3.5](#)).

In [Section 3.4.2](#), we have highlighted a special solution to $(\mathcal{D}(0, y_0))$, the one with minimal-norm, denoted by p_0 . The solution p_0 governs the behavior of the regularized

problems $\mathcal{P}(\lambda, y)$ in the presence of some small noise and small regularization, but its computation of p_0 is in general difficult. In particular, it does not vary continuously with the observation y_0 .

The first three sections of the present chapter deal with strategies to bypass that difficulty by replacing the computation of p_0 with linear projection problems. In the fourth section, we discuss the case of total gradient variation denoising, where we do not know how to extend such an approach. We describe the cases of indicators of calibrable sets and convex sets.

4.1 General principle

Let $u \in V$ be a solution to $(\mathcal{P}(0, y_0))$, and assume that $(\mathcal{D}(0, y_0))$ has a solution. In view of (3.4), we see that

$$p_0 = \operatorname{argmin} \{ \|p\|_{\mathcal{H}} \mid p \in \operatorname{argmax} (\mathcal{D}(0, y_0)) \} = \operatorname{proj}_{(\Phi^*)^{-1}(\partial R(u))}(0), \quad (4.1)$$

so that finding the minimal-norm certificate amounts to projecting 0 on the closed convex set $(\Phi^*)^{-1}(\partial R(u))$ in the Hilbert space \mathcal{H} . That problem is in general nonlinear, and difficult to solve analytically.

4.1.1 Projecting onto the span of the minimal face

A key idea is to replace the above projection with a linear projection problem.

Proposition 4.1. *Let $C \subseteq \mathcal{H}$ be a nonempty closed convex set, and $p_0 = \operatorname{proj}_C(0)$. Let $F_0 \stackrel{\text{def}}{=} \mathcal{F}_C(p_0)$ be the minimal face of p_0 in C . Then,*

$$\operatorname{proj}_C(0) = \operatorname{proj}_{\operatorname{Aff} F_0}(0).$$

Proof. The affine hull of F_0 is equal to $\operatorname{Aff} F_0 = \{ tq + (1-t)p_0 \mid t \in \mathbb{R}, q \in F_0 \}$. By construction of the minimal face (see Section 1.2.1), p_0 is internal to F_0 , so that for $|t|$ small enough, $(tq + (1-t)p_0) \in F_0$.

Since $F_0 \subseteq C$ and p_0 is the minimal-norm element of C , the function $t \mapsto \|tq + (1-t)p_0\|_{\mathcal{H}}^2$ reaches a local minimum at $t = 0$, hence a global minimum by convexity. As a result, p_0 is the minimum norm element of $\operatorname{Aff} F_0$. □

In other words, it is possible to replace $(\Phi^*)^{-1}(\partial R(u))$ with $\operatorname{Aff} F_0$, the affine hull of the minimal face of p_0 in $(\Phi^*)^{-1}(\partial R(u))$, making the projection problem easier. Of course, the main difficulty is now to “guess” beforehand the minimal face F_0 which contains p_0 . That is possible in several cases.

4.1.2 The polyhedral case

Assume for instance that $(\Phi^*)^{-1}(\partial R(u))$ is polyhedral (that is the case, *e.g.*, if $\partial R(u)$ is polyhedral), defined by a finite number of inequalities,

$$\forall i \in I, \quad \langle p, \psi_i \rangle \leq d_i, \quad (4.2)$$

where $\{\psi_i\}_{i \in I} \subseteq \mathcal{H}$, $\{d_i\}_{i \in I} \subseteq \mathbb{R}$.

Lemma 4.1. *Let $p_0 \in (\Phi^*)^{-1}(\partial R(u))$ and $I_0 \stackrel{\text{def.}}{=} \{i \in I \mid \langle p_0, \psi_i \rangle = d_i\}$. Then the minimal face of p_0 in $(\Phi^*)^{-1}(\partial R(u))$ is*

$$F_0 = \left\{ p \in \mathcal{H} \mid \begin{array}{ll} \forall i \in I_0, & \langle p, \psi_i \rangle = d_i, \\ \forall k \in I \setminus I_0, & \langle p, \psi_k \rangle < d_k \end{array} \right\}. \quad (4.3)$$

Moreover, its affine hull is given by

$$\text{Aff } F_0 = \bigcap_{i \in I_0} \{p \in \mathcal{H} \mid \langle p, \psi_i \rangle = d_i\}. \quad (4.4)$$

The proof of [Lemma 4.1](#) is a straightforward simplification of the proof of [Lemma 4.2](#) below, therefore we omit it.

It is thus possible to compute p_0 by projecting 0 onto $\text{Aff } F_0$ (that is, applying to $(d_i)_{i \in I}$ the Moore-Penrose pseudo-inverse of the map $p \mapsto (\langle p, \psi_i \rangle)_{i \in I_0}$ from \mathcal{H} to $\mathbb{R}^{|I_0|}$).

As finding the minimal face F_0 amounts to finding the set I_0 of active inequalities in (4.2), we are led to guess that index set: either by considering the smallest possible set of active constraints in $(\Phi^*)^{-1}(\partial R(u))$ (e.g. by assuming that $\eta_0 = \Phi^* p_0$ is a tight dual certificate), or by adding some extra saturations (corresponding, e.g., to the activation of neighboring gridpoints), see [Section 4.2](#).

4.1.3 The semi-infinite programming case

Another case of interest is when $(\Phi^*)^{-1}(\partial R(u))$ is described by a few continuous families of inequalities

$$\forall z \in Z, \quad \langle p, \psi_1(z) \rangle \leq d_1(z), \dots, \langle p, \psi_n(z) \rangle \leq d_n(z), \quad (4.5)$$

where, for instance, $Z \subseteq \mathbb{R}^k$ is a compact set with nonempty interior, and $\psi_1, \dots, \psi_n: Z \rightarrow \mathcal{H}$ are weakly continuous and weakly \mathcal{C}^2 on $\text{int}(Z)$ ¹, $d_1, \dots, d_n \in (\mathcal{C}(Z) \cap \mathcal{C}^2(\text{int}(Z)))$. For the sake of simplicity, we assume from now on that $n = 1$ (the extension to $n \geq 2$ is not particularly difficult).

For each $p \in \mathcal{H}$, we introduce the function $\gamma_p: Z \rightarrow \mathbb{R}$,

$$\forall z \in Z, \quad \gamma_p(z) \stackrel{\text{def.}}{=} (\langle p, \psi(z) \rangle - d(z)), \quad (4.6)$$

so that $\gamma_p \in (\mathcal{C}(Z) \cap \mathcal{C}^2(\text{int}(Z)))$ and

$$(\Phi^*)^{-1}(\partial R(u)) = \{p \in \mathcal{H} \mid \forall z \in Z, \gamma_p(z) \leq 0\}. \quad (4.7)$$

Contrary to the polyhedral example, we need a non-degeneracy assumption to describe the minimal face of p_0 . We denote by $\gamma'_p(z)$ the derivative of γ_p at $z \in \text{int}(Z)$. We denote by $\gamma''_p(z)$ the Hessian of γ_p at $z \in \text{int}(Z)$, and we write $\gamma''_p(z) \prec 0$ to express that it is negative definite.

Lemma 4.2. *Let $p_0 \in (\Phi^*)^{-1}(\partial R(u))$ and $\mathcal{I}_0 \stackrel{\text{def.}}{=} \{z \in Z \mid \gamma_{p_0}(z) = 0\}$.*

If $\mathcal{I}_0 \subseteq \text{int}(Z)$ and, for all $z \in \mathcal{I}_0$, $\gamma''_{p_0}(z) \prec 0$, then the minimal face of p_0 in $(\Phi^)^{-1}(\partial R(u))$ is*

$$F_0 = \left\{ p \in \mathcal{H} \mid \begin{array}{ll} \forall z \in \mathcal{I}_0, & \gamma_p(z) = 0 \text{ and } \gamma''_p(z) \prec 0, \\ \forall z \in Z \setminus \mathcal{I}_0, & \gamma_p(z) < 0 \end{array} \right\}. \quad (4.8)$$

Moreover, its affine hull is given by

$$\text{Aff } F_0 = \{p \in \mathcal{H} \mid \forall z \in \mathcal{I}_0, \gamma_p(z) = 0 \text{ and } \gamma'_p(z) = 0\}. \quad (4.9)$$

¹That is, for each $p \in \mathcal{H}$, $z \mapsto \langle p, \psi_i(z) \rangle$ is \mathcal{C}^2 on the interior of Z .

Before proving [Lemma 4.2](#), we make the following observation.

Remark 4.1. *If $F \subseteq \mathcal{H}$ is an internal set and $L: \mathcal{H} \rightarrow \mathbb{R}$ is an affine function on \mathcal{H} , then either L is constant on F , or $L(z) < (\sup_F L)$ for every $z \in F$.*

Proof. We denote by F the set in the right-hand side of (4.8). One readily checks that F is convex and $p_0 \in F \subseteq (\Phi^*)^{-1}(\partial R(u))$.

Moreover, F is internal.

➤ Note that the compactness of Z and the assumption that $\gamma''_{p_0}(z) \prec 0$ for all $z \in \mathcal{I}_0$ imply that \mathcal{I}_0 is finite.

Now, if $p, q \in F$, then for all $t \in \mathbb{R}$, $\gamma_{tq+(1-t)p} = \gamma_p + t(\gamma_q - \gamma_p)$ (and similarly for their respective Hessians). Since $\gamma''_p(z) \prec 0$ for all $z \in \mathcal{I}_0$, by continuity of $(t, z) \mapsto \gamma''_{tq+(1-t)p}(z)$, there is some $\alpha > 0$ and some neighborhood \mathcal{N} of \mathcal{I}_0 in Z such that for all $(t, z) \in]-\alpha, \alpha[\times \mathcal{N}$, $\gamma''_{tq+(1-t)p}(z) \prec 0$. In particular $\gamma_{tq+(1-t)p} < 0$ in $\mathcal{N} \setminus \mathcal{I}_0$.

Moreover, by a compactness argument on $\overline{Z \setminus \mathcal{N}}$, for $|t|$ small enough, we also have

$$\max_{z \in \overline{Z \setminus \mathcal{N}}} \gamma_{tq+(1-t)p}(z) < 0.$$

To sum up, there is some $\tilde{\alpha} > 0$ such that for all $t \in]-\tilde{\alpha}, \tilde{\alpha}[$, $\gamma_{tq+(1-t)p} = 0$ on \mathcal{I}_0 and $\gamma_{tq+(1-t)p} < 0$ on $Z \setminus \mathcal{I}_0$. In other words, $(tq + (1-t)p) \in F$, and F is internal.

Additionally, F is the largest internal set which contains p_0 .

➤ Let $\tilde{F} \subseteq (\Phi^*)^{-1}(\partial R(u))$ be an internal set containing p_0 . Note that for each $z \in Z$, the map $p \mapsto \gamma_p(z)$ is affine. By [Remark 4.1](#), either it is identically equal to 0 on \tilde{F} or it is (strictly) negative on \tilde{F} . As a consequence, comparing with the value at p_0 ,

$$\forall p \in \tilde{F}, \quad \begin{cases} \gamma_p(z) = 0 & \text{for all } z \in \mathcal{I}_0, \\ \gamma_p(z) < 0 & \text{for all } z \in Z \setminus \mathcal{I}_0. \end{cases}$$

Now, let $z \in \mathcal{I}_0$ and $h \in \mathbb{R}^k \setminus \{0\}$. By observing that $\gamma''_{p_0}(z)[h, h] < 0$ and by applying [Remark 4.1](#) to $p \mapsto \gamma''_p(z)[h, h]$, we deduce similarly that for all $p \in \tilde{F}$, $\gamma''_p(z)[h, h] < 0$. Hence $\gamma''_p \prec 0$.

As a result, $\tilde{F} \subseteq F$.

Therefore, $F = F_0$.

Now, we denote by G the affine space in the right-hand side of (4.9). It is clear that $F_0 \subseteq G$, hence $\text{Aff } F_0 \subseteq G$. Moreover, using the same compactness argument as above, it is possible to prove that for all $p \in G$, there exists $\alpha > 0$ such that for all $t \in]-\alpha, \alpha[$,

$$\begin{cases} \gamma_{tp+(1-t)p_0}(z) = 0 & \text{for all } z \in \mathcal{I}_0 \\ \gamma_{tp+(1-t)p_0}(z) < 0 & \text{for all } z \in Z \setminus \mathcal{I}_0. \end{cases} \quad (4.10)$$

In other words, F_0 contains the open line segment $\{tp + (1-t)p_0 \mid -\alpha < t < \alpha\}$, hence $\text{Aff } F_0$ contains the whole line it spans. As a result $p \in \text{Aff } F_0$ and $G \subseteq \text{Aff } F_0$. \square

As in the polyhedral case, [Lemma 4.2](#) provides a good candidate to find the minimal-norm dual certificate by means of a pseudo-inverse, see [Section 4.3](#).

4.2 The case of ℓ^1 -synthesis recovery

Here, we consider the sparse recovery setting of [Section 3.2.2](#), where one aims to retrieve spikes on a fixed grid \mathcal{G} , and we apply the general principle of [Section 4.1](#).

The problem $\mathcal{P}^{(\ell^1(\mathcal{G}))}(0, y_0)$ can be reformulated as a standard basis pursuit problem:

$$\min_{a \in \mathbb{R}^{\mathcal{G}}} \|a\|_1 \quad \text{s.t. } \Phi_{\mathcal{G}} a = y_0. \quad (4.11)$$

where $\Phi_{\mathcal{G}} = (\varphi(x))_{x \in \mathcal{G}}$ gathers the impulse responses on the grid, and the vector $a \in \mathbb{R}^{\mathcal{G}}$ encodes the amplitudes of some measure $m = \sum_{x \in \mathcal{G}} a_x \delta_x$.

Fixing $a \in \mathbb{R}^{\mathcal{G}}$ and letting $\mathcal{I} \stackrel{\text{def.}}{=} \{x \in \mathcal{G} \mid a_x \neq 0\}$, the convex set

$$(\Phi^*)^{-1}(\partial R^{\ell^1(\mathcal{G})}(m)) = \left\{ p \in \mathcal{H} \mid \begin{array}{l} \forall x \in \mathcal{I}, \langle p, \varphi(x) \rangle = \text{sign}(a_x) \\ \forall x \in \mathcal{G} \setminus \mathcal{I}, |\langle p, \varphi(x) \rangle| \leq 1 \end{array} \right\} \quad (4.12)$$

is polyhedral.

4.2.1 The tight case and the Fuchs precertificate

We make the ansatz that:

- a is indeed a solution to (4.11) (i.e. m is a solution to $\mathcal{P}^{(\ell^1(\mathcal{G}))}(0, y_0)$). As a result, there is a minimal-norm certificate $\Phi^* p_0$ associated to m , and the sign vector $s_{\mathcal{I}} \stackrel{\text{def.}}{=} (\text{sign}(a_x))_{x \in \mathcal{I}}$ is in $\text{Im } \Phi_{\mathcal{I}}^*$, with $\Phi_{\mathcal{I}} = (\varphi(x))_{x \in \mathcal{I}}$.
- the only active inequalities in (4.12) for p_0 are in \mathcal{I} (i.e. $\Phi^* p_0$ is a *tight* dual certificate).

Under those assumptions, we identify the minimal face and its affine hull using [Lemma 4.1](#). Projecting 0 onto that affine space yields $p_0 = p_F$, the vector introduced by J.-J. Fuchs in [\[Fuc04\]](#), with

$$p_F \stackrel{\text{def.}}{=} (\Phi_{\mathcal{I}}^*)^\dagger s_{\mathcal{I}}. \quad (4.13)$$

The symbol \dagger denotes the Moore-Penrose pseudoinverse².

Remark 4.2. *The above ansatz implies that p_0 has the minimal number of saturations among all solutions of the dual problem. That corresponds to p_0 being in the relative algebraic interior of $(\Phi^*)^{-1}(\partial R^{\ell^1(\mathcal{G})}(m))$.*

Conversely, if we are given a and we do not know in advance that a is a solution, [Equation \(4.13\)](#) provides a good candidate to build a dual “precertificate” as follows.

Proposition 4.2. *Let $a \in \mathbb{R}^{\mathcal{G}}$, $y_0 \stackrel{\text{def.}}{=} \Phi_{\mathcal{G}} a$, $s_{\mathcal{I}} \stackrel{\text{def.}}{=} (\text{sign}(a_x))_{x \in \mathcal{I}}$ and let p_F as in (4.13). The following assertions are equivalent:*

1. the vector a is a solution to (4.11) and $p_0 = p_F$.
2. $s_{\mathcal{I}} \in \text{Im } \Phi_{\mathcal{I}}^*$ and $(\max_{x \in \mathcal{G}} |\langle p_F, \varphi(x) \rangle|) \leq 1$.

The proof of [Proposition 4.2](#) is a straightforward verification. With [Proposition 4.2](#), one has a practical sufficient criterion to ensure that a is a solution to (4.11), and, as a by-product, provides the minimal-norm certificate.

²The Moore-Penrose pseudo-inverse provides the minimum-norm solution to the least-square problem $\min_{p \in \mathcal{H}} \|\Phi_{\mathcal{I}}^* p - s_{\mathcal{I}}\|_2^2$. Such a solution always exists since $\text{Im } \Phi_{\mathcal{I}}^*$ is closed (remember that \mathcal{I} is finite), and it satisfies $\Phi_{\mathcal{I}}^* (\Phi_{\mathcal{I}}^*)^\dagger s_{\mathcal{I}} = s_{\mathcal{I}}$ if and only if $s_{\mathcal{I}} \in \text{Im } \Phi_{\mathcal{I}}^*$. In the case where $\Phi_{\mathcal{I}}$ has full column rank, that range condition holds, and $(\Phi_{\mathcal{I}}^*)^\dagger = \Phi_{\mathcal{I}} (\Phi_{\mathcal{I}}^* \Phi_{\mathcal{I}})^{-1}$.

4.2.2 The non-tight case: finding the extended support

In some cases, there is not any tight dual certificate, or p_0 lies on the relative boundary of $(\Phi^*)^{-1}(\partial R^{\ell^1(\mathcal{G})}(m))$: we have to guess the additional active inequalities. In other words, we have to find the extended support of m ,

$$\text{ext } m \stackrel{\text{def}}{=} \{x \in \mathcal{G} \mid |\langle p_0, \varphi(x) \rangle| = 1\}, \quad (4.14)$$

and the corresponding sign, $s \stackrel{\text{def}}{=} (\langle p_0, \varphi(x) \rangle)_{x \in \text{ext } m}$.

In [15], we have considered the sparse spike recovery on a one-dimensional interval (say, on the torus $X = \mathbb{T}$, to avoid boundary discussions) using a thin regular grid $\mathcal{G} = \{kh \mid 0 \leq k \leq G-1\}$, where $h > 0$ is a stepsize. We have proved that if the unknown signal m satisfies the Non-degenerate Source Condition (see Definition 4.2) and some additional condition holds inducing a natural shift (see (5.59)), it is possible to predict the extended support of m , provided that the grid \mathcal{G} contains the support of m and that the stepsize h is small enough.

More precisely, the extended support is given by the sources of m and one of their immediate neighbors,

$$\text{ext } m = \bigcup_{x \in \mathcal{I}} \{x, x + \varepsilon_x h\} \quad (4.15)$$

for some $\varepsilon \in \{-1, +1\}^{\mathcal{I}}$ which has a closed-form expression, see [15, Th. 2] for more detail. Each saturation is doubled, with the same sign,

$$\forall x \in \mathcal{I}, \quad \langle p_0, \varphi(x + \varepsilon_x h) \rangle = \langle p_0, \varphi(x) \rangle \in \{-1, +1\}. \quad (4.16)$$

As a result, it is possible to compute the minimal-norm certificate in the same way as in (4.13) and Proposition 4.2, by simply replacing \mathcal{I} with $\text{ext } m$.

Note that the Continuous Basis Pursuit proposed by C. Ekanadham *et al.* in [ETS11] is polyhedral too, and that we have carried a similar analysis of the extended support on thin grids in [14].

4.3 Sparse-spike recovery in the space of measures

We consider the framework of Section 3.2.1 with the Basis Pursuit for measures,

$$\min_{m \in \mathcal{M}(X)} |m|(X) \quad \text{s.t. } \Phi m = y_0, \quad (\mathcal{P}^{(\text{TV})}(0, y_0))$$

and its dual problem

$$\sup_{p \in \mathcal{H}} \langle p, y_0 \rangle \quad \text{s.t. } \|\Phi^* p\|_{\infty} \leq 1. \quad (\mathcal{D}^{(\text{TV})}(0, y_0))$$

We assume that $y_0 = \Phi m$ for some measure $m = \sum_{x \in \mathcal{I}} a_x \delta_x$, where $\mathcal{I} \subseteq X$ is a finite set³. The solution set to the dual problem is given by

$$(\Phi^*)^{-1}(\partial R^{(\text{TV})}(m)) = \left\{ p \in \mathcal{H} \mid \begin{array}{l} \forall x \in \mathcal{I}, \langle p, \varphi(x) \rangle = \text{sign}(a_x) \\ \forall x \in X \setminus \mathcal{I}, |\langle p, \varphi(x) \rangle| \leq 1 \end{array} \right\} \quad (4.17)$$

In order to apply the results of Section 4.1.3 on semi-infinite programming, we introduce new assumptions.

³Throughout this dissertation, we may write $m = \sum_{x \in \mathcal{I}} a_x \delta_x$ for some finite set \mathcal{I} , or $m = \sum_{i=1}^s a_i \delta_{x_i}$, with $\mathcal{I} = \{x_1, \dots, x_s\}$. Depending on the context, it may be more convenient to use the former or the latter notation. With a slight abuse of notation, we may switch from one to the other without further notice.

Assumptions 4.1. We require that [Assumptions 3.1](#) hold and that

- $X \subseteq \mathbb{R}^d$ has nonempty interior \mathring{X} , or $X = \mathbb{T}^d$.
- $\varphi \in \mathcal{C}^2(\mathring{X}; \mathcal{H})$. As a consequence, φ is weakly \mathcal{C}^2 in \mathring{X} .

Then, our problems fits⁴ the framework of [Section 4.1.3](#).

We denote by $\varphi''(x)$ the Hessian of φ at $x \in \mathring{X}$, i.e. a bilinear map from $\mathbb{R}^d \times \mathbb{R}^d$ to \mathcal{H} . With a slight abuse of notation we denote by $\langle p, \varphi''(x) \rangle$ the Hessian of $x \mapsto \langle p, \varphi(x) \rangle$ (that is, the bilinear map $(a, b) \mapsto \langle p, \varphi''(x)[a, b] \rangle$ from $\mathbb{R}^d \times \mathbb{R}^d$ to \mathbb{R}). Alternatively, setting $\eta: x \mapsto \langle p, \varphi(x) \rangle$, we denote its Hessian by $\eta''(x) \in \mathcal{S}_d(\mathbb{R})$. We also define the operator $\Gamma_{\mathcal{I}}: \mathbb{R}^{(d+1)|\mathcal{I}|} \rightarrow \mathcal{H}$, by

$$\Gamma_{\mathcal{I}} \stackrel{\text{def.}}{=} (\Phi_{\mathcal{I}} \quad \Phi'_{\mathcal{I}}) \text{ where} \quad (4.18)$$

$$\forall a \in \mathbb{R}^{\mathcal{I}}, \quad \Phi_{\mathcal{I}} a \stackrel{\text{def.}}{=} \sum_{x \in \mathcal{I}} a_x \varphi(x) \quad (4.19)$$

$$\forall b \in (\mathbb{R}^d)^{\mathcal{I}}, \quad \Phi'_{\mathcal{I}} b = \sum_{x \in \mathcal{I}} \varphi'(x)[b_x]. \quad (4.20)$$

Note that under [Assumptions 4.1](#), any function $\eta \in \text{Im } \Phi^*$, i.e. of the form $x \mapsto \langle p, \varphi(x) \rangle$, is in $\mathcal{C}_0(X) \cap \mathcal{C}^2(\mathring{X})$.

4.3.1 Non-degenerate certificates

To describe the minimal face of p_0 in [Section 4.1.3](#), we have assumed that the non-degeneracy of the Hessian of the constraints. In the present setting, this yields the notion of a *non-degenerate certificate*.

Definition 4.1 (Non-degenerate dual certificate). Assume that [Assumptions 4.1](#) hold and let $m = \sum_{x \in \mathcal{I}} a_x \delta_x$ with $\mathcal{I} \subseteq \mathring{X}$ finite and $a \in (\mathbb{R} \setminus \{0\})^{\mathcal{I}}$.

We say that $\eta \in \text{Im } \Phi^*$ is a non-degenerate dual certificate for m if

- i) for all $x \in X \setminus \mathcal{I}$, $|\eta(x)| < 1$,
- ii) for all $x \in \mathcal{I}$, $\eta(x) = \text{sign}(a_x)$,
- iii) for all $x \in \mathcal{I}$, $(\text{sign}(a_x) \eta''(x)) \prec 0$.

Note that the first two assumptions of [Definition 4.1](#) imply that $\eta \in \partial R^{(\text{TV})}(m)$ and that η is a tight subgradient of $R^{(\text{TV})}$ at m .

Since we are particularly interested in the non-degeneracy of the minimal-norm certificate, we refer to that case as the *Non-Degenerate Source Condition*.

Definition 4.2 (Non-Degenerate Source Condition). Assume that [Assumptions 4.1](#) hold and let $m = \sum_{x \in \mathcal{I}} a_x \delta_x$ with $\mathcal{I} \subseteq \mathring{X}$ finite and $a \in (\mathbb{R} \setminus \{0\})^{\mathcal{I}}$.

We say that the Non-Degenerate Source Condition (NDSC) holds for m if

- there is a solution to $(\mathcal{D}^{(\text{TV})}(0, y_0))$, where $y_0 \stackrel{\text{def.}}{=} \Phi m$.
- $\eta_0 \stackrel{\text{def.}}{=} \Phi^* p_0$ is non-degenerate for m , where p_0 is the minimal-norm solution to $(\mathcal{D}^{(\text{TV})}(0, y_0))$.

⁴To be precise, we have assumed that Z is compact whereas here X is only assumed to be locally compact. The arguments [Section 4.1.3](#) can be adapted to the locally compact case with φ weakly decaying at infinity, but we skipped it for the simplicity of exposition.

4.3.2 The vanishing-derivatives precertificate

Now, we can try to compute p_0 using the general principle of [Section 4.1](#). If we make the ansatz that

- m is a solution to $(\mathcal{P}^{(\text{TV})}(0, y_0))$,
- m satisfies the Non-Degenerate Source condition (as a result, the vector

$$\begin{pmatrix} s_{\mathcal{I}} \\ 0 \end{pmatrix} \stackrel{\text{def.}}{=} \begin{pmatrix} (\text{sign}(a_x))_{x \in \mathcal{I}} \\ 0_{d|\mathcal{I}|} \end{pmatrix} \in \mathbb{R}^{(1+d)\mathcal{I}}$$

is in $\text{Im } \Gamma_{\mathcal{I}}^*$,

then we obtain from [Lemma 4.2](#) that p_0 is equal to the projection of 0 onto the affine space of all $p \in \mathcal{H}$ such that, for all $x \in \mathcal{I}$,

$$\begin{cases} \langle p, \varphi(x) \rangle = \text{sign}(a_x), \\ \langle p, \varphi'(x) \rangle = 0. \end{cases} \quad (4.21)$$

As a result, p_V can be computed by a pseudo-inverse,

$$p_V \stackrel{\text{def.}}{=} (\Gamma_{\mathcal{I}}^*)^\dagger \begin{pmatrix} s_{\mathcal{I}} \\ 0 \end{pmatrix}. \quad (4.22)$$

Note that if $\Gamma_{\mathcal{I}}$ has full column rank, then $(\Gamma_{\mathcal{I}}^*)^\dagger = \Gamma_{\mathcal{I}}(\Gamma_{\mathcal{I}}^*\Gamma_{\mathcal{I}})^{-1}$.

We call the corresponding quantity $\eta_V \stackrel{\text{def.}}{=} \Phi^* p_V$ the *vanishing-derivatives precertificate*. The name stems from the property that for all $x \in \mathcal{I}$, $\eta_V(x) = \text{sign}(a_x)$ and $\eta'_V(x) = 0$. Like the Fuchs precertificate in the polyhedral case, it yields a convenient way to compute the minimal-norm certificate using [Equation \(4.22\)](#), in the non-degenerate case.

More precisely, without assuming that the ansatz holds, it is possible to test it a posteriori using the following proposition, whose proof is omitted.

Proposition 4.3. *Let $m = \sum_{x \in \mathcal{I}} a_x \delta_x$ with $\mathcal{I} \subseteq \mathring{X}$ finite, $a \in (\mathbb{R} \setminus \{0\})^{\mathcal{I}}$, $y_0 \stackrel{\text{def.}}{=} \Phi m$, $s_{\mathcal{I}} \stackrel{\text{def.}}{=} (\text{sign}(a_x))_{x \in \mathcal{I}}$ and let p_V as in [\(4.22\)](#). The following assertions are equivalent:*

1. *the measure m is a solution to $(\mathcal{P}^{(\text{TV})}(0, y_0))$, there exists a solution to $(\mathcal{D}^{(\text{TV})}(0, y_0))$, and $p_0 = p_V$.*
2. *$(s_{\mathcal{I}} \ 0)^\top \in \text{Im } \Gamma_{\mathcal{I}}^*$ and $(\max_{x \in X} |\langle p_V, \varphi(x) \rangle|) \leq 1$.*

In particular, the Non-Degenerate Source Condition holds for m if and only if η_V is a non-degenerate dual certificate for m .

Remark 4.3. *As in [Section 4.2.2](#), it is possible to consider extended supports, replacing \mathcal{I} in [\(4.22\)](#) and [Proposition 4.3](#) with*

$$\text{ext } m \stackrel{\text{def.}}{=} \{x \in X \mid |\langle p_0, \varphi(x) \rangle| = 1\}, \quad (4.23)$$

or with a “good candidate” for $\text{ext } m$. However, to the best of our knowledge, in the continuous setting there is no practical situation when one can easily guess the extended support.

4.3.3 Connection with interpolation problems

It is worth noting that the vanishing-derivatives precertificate can be constructed by simply considering the autocorrelation function and its partial derivatives.

Lemma 4.3. *Let $\mathcal{I} \subseteq \mathring{X} \subseteq \mathbb{R}^d$ be finite, $s_{\mathcal{I}} \in \mathbb{R}^{\mathcal{I}}$ such that $(s_{\mathcal{I}} \ 0)^{\top} \in \text{Im } \Gamma_{\mathcal{I}}^*$. Then,*

- *A vector $p \in \mathcal{H}$ is equal to p_V if and only if $p \in \text{Im } \Gamma_{\mathcal{I}}$ and $\Gamma_{\mathcal{I}}^* p = (s_{\mathcal{I}} \ 0)^{\top}$*
- *A function $\eta \in \mathcal{C}_0(X)$ is equal to η_V if and only if there exists $\{\alpha_{x_i}\}_{x_i \in \mathcal{I}} \subseteq \mathbb{R}$, $\{\beta_{x_i}\}_{x_i \in \mathcal{I}} \subseteq \mathbb{R}^d$ such that*

$$\forall x \in X, \quad \eta(x) = \sum_{x_i \in \mathcal{I}} (\alpha_{x_i} K(x, x_i) + \partial_2 K(x, x_i) [\beta_{x_i}]), \quad (4.24)$$

and for all $x_i \in \mathcal{I}$, $\eta(x_i) = s_{x_i}$ and $\eta'(x_i) = 0$.

In (4.24) above, $\partial_2 K(x, x_i)$ denotes the partial derivative with respect to the second variable, so that $\partial_2 K(x, x_i) [\beta_{x_i}] = \langle \varphi(x), \varphi'(x_i) [\beta_{x_i}] \rangle_{\mathcal{H}}$.

Lemma 4.3 is well-known when $\Gamma_{\mathcal{I}}$ has full rank (see [8, 11] and [PP17]), but we provide below a proof for the general case.

Proof. Since $\eta_V = \Phi^* p_V$ and $K(x, x_i) = \langle \varphi(x), \varphi(x_i) \rangle_{\mathcal{H}}$, the second point directly follows from the first one.

By definition, $p_V = (\Gamma_{\mathcal{I}}^*)^{\dagger} (s_{\mathcal{I}} \ 0)^{\top}$. Since $(s_{\mathcal{I}} \ 0)^{\top} \in \text{Im } \Gamma_{\mathcal{I}}^*$, p_V is the minimal-norm element such that $\Gamma_{\mathcal{I}}^* p = (s_{\mathcal{I}} \ 0)^{\top}$. By minimality of the norm, we have $p_V \in (\ker \Gamma_{\mathcal{I}}^*)^{\perp} = \text{Im } \Gamma_{\mathcal{I}}$ (see [Br  11, Cor. 2.18]).

Conversely, if $\Gamma_{\mathcal{I}}^* p = (s_{\mathcal{I}} \ 0)^{\top}$, then p is a solution to

$$\min_{q \in \mathcal{H}} \left\| \Gamma_{\mathcal{I}}^* q - \begin{pmatrix} s_{\mathcal{I}} \\ 0 \end{pmatrix} \right\|_{\mathcal{H}}^2.$$

The fact that $p \in \text{Im } \Gamma_{\mathcal{I}} = (\ker \Gamma_{\mathcal{I}}^*)^{\perp}$ implies that it is the solution with minimal-norm, hence $p = p_V$. □

As a consequence of Lemma 4.3, the problem of finding the minimal-norm precertificate amounts to solving the interpolation problem (4.24), which can be done analytically if the family $\{K(\cdot, x_i), \partial_2 K(\cdot, x_i)\}_{x_i \in \mathcal{I}}$ has some special properties, like polynomials, as we illustrate below.

For now, let us note that taking the vanishing-derivatives precertificate commutes with diffeomorphisms, hence it is sufficient that the family has those special properties “up to a diffeomorphism”.

Proposition 4.4. *Let $h: \mathbb{R}^d \rightarrow \mathbb{R}^d$ be a \mathcal{C}^1 -diffeomorphism, mapping X to $\tilde{X} \stackrel{\text{def.}}{=} h(X)$. Let $\mathcal{I} \subseteq \mathring{X}$ be finite, $\{a_x\}_{x \in \mathcal{I}} \subseteq \mathbb{R} \setminus \{0\}$ and $m \stackrel{\text{def.}}{=} \sum_{x \in \mathcal{I}} a_x \delta_x$. Define its image measure as $\tilde{m} = \sum_{x \in \mathcal{I}} a_x \delta_{h(x)}$, and the image observation operator by $\tilde{\varphi} = \varphi \circ h^{(-1)}$.*

If η_V (resp. $\tilde{\eta}_V$) denotes the vanishing-derivatives precertificate for m (resp. \tilde{m}), then

$$\tilde{\eta}_V = \eta_V \circ h^{(-1)}. \quad (4.25)$$

and $\tilde{\eta}_V$ is a valid dual certificate for \tilde{m} if and only if η_V is a valid dual certificate for m . If, moreover, h is \mathcal{C}^2 , $\tilde{\eta}_V$ is non-degenerate if and only if η_V is non-degenerate.

Proof. We apply [Lemma 4.3](#). To simplify the notation, we write $\tilde{x}_i \stackrel{\text{def.}}{=} h(x_i)$ where $\mathcal{I} \stackrel{\text{def.}}{=} \{x_i\}_{i=1}^{|\mathcal{I}|}$, and we denote by $K(\cdot, \cdot)$ (resp. $\tilde{K}(\cdot, \cdot)$) the autocorrelation of φ (resp. $\tilde{\varphi}$). Note that the support of \tilde{m} , $h(\mathcal{I}) = \{\tilde{x}_1, \dots, \tilde{x}_{|\mathcal{I}|}\}$, is in the interior of \tilde{X} .

Now, we observe that for all $\tilde{x} \in \tilde{X}$, writing $\tilde{x} = h(x)$,

$$\begin{aligned} K(h^{(-1)}(\tilde{x}), x_i) &= \tilde{K}(\tilde{x}, \tilde{x}_i), \\ \partial_2 K(h^{(-1)}(\tilde{x}), x_i) [\beta_{x_i}] &= \partial_2 \tilde{K}(\tilde{x}, \tilde{x}_i) [h'(\beta_{x_i})], \end{aligned}$$

so that $\eta_V \circ h^{(-1)}$ has the form [\(4.24\)](#) corresponding to the autocorrelation $\tilde{K}(\cdot, \cdot)$.

Moreover, since $(\eta_V \circ h^{(-1)})(\tilde{x}_i) = \eta_V(x_i) = \text{sign}(a_{x_i})$ and $(\eta_V \circ h^{(-1)})'(\tilde{x}_i) = (\eta_V)'(x_i) \circ (h'(\tilde{x}_i))^{(-1)} = 0$, the function $\eta_V \circ h^{(-1)}$ satisfies the interpolation condition. As a result, $\eta_V \circ h^{(-1)} = \tilde{\eta}_V$.

The fact that $\tilde{\eta}_V$ is valid (*i.e.* $\|\tilde{\eta}_V\|_\infty \leq 1$) if and only if η_V is valid is immediate. As for the non-degeneracy, we note that for all $v \in \mathbb{R}^d$,

$$\begin{aligned} \tilde{\eta}_V''(\tilde{x}_i)[v, v] &= \eta_V''(x_i)[h'(x_i)v, h'(x_i)v] + \eta_V'(x_i)[h''(x_i)[v, v]] \\ &= \eta_V''(x_i)[h'(x_i)v, h'(x_i)v], \end{aligned}$$

so that $\tilde{\eta}_V$ is non-degenerate if and only if η_V is. □

4.3.4 Examples

The case of a single Dirac mass

The block-structure of $\Gamma_{\mathcal{I}}$ (see [\(4.18\)](#)) may be exploited to compute its pseudo-inverse. Using [\[BB07, Thm. 1\]](#), we note that if $(\text{Im } \Phi_{\mathcal{I}}) \cap (\text{Im } \Phi'_{\mathcal{I}}) = \{0\}$, then

$$\Gamma_{\mathcal{I}}^\dagger = \begin{pmatrix} \left(\Pi_{(\text{Im } \Phi'_{\mathcal{I}})^\perp} \Phi_{\mathcal{I}} \right)^\dagger \\ \left(\Pi_{(\text{Im } \Phi_{\mathcal{I}})^\perp} \Phi'_{\mathcal{I}} \right)^\dagger \end{pmatrix} \quad (4.26)$$

where $\Pi_{(\text{Im } \Phi_{\mathcal{I}})^\perp}$ is the orthogonal projector onto the orthogonal complement to $\text{Im } \Phi_{\mathcal{I}}$ (and similarly for $\Pi_{(\text{Im } \Phi'_{\mathcal{I}})^\perp}$). In the case of a single Dirac mass, $m = \delta_{x_0}$ for some $x_0 \in \mathring{X}$, that is $\mathcal{I} = \{x_0\}$ and $\Gamma_{\mathcal{I}} = (\varphi(x_0) \quad \varphi'(x_0))$, this yields

$$p_V = (\Gamma_{\mathcal{I}}^*)^\dagger \begin{pmatrix} 1 \\ 0 \end{pmatrix} = (\Gamma_{\mathcal{I}}^\dagger)^* \begin{pmatrix} 1 \\ 0 \end{pmatrix} = \frac{\Pi_{(\text{Im } \varphi'(x_0))^\perp} \varphi(x_0)}{\left(\left\| \Pi_{(\text{Im } \varphi'(x_0))^\perp} \varphi(x_0) \right\|_{\mathcal{H}} \right)^2}. \quad (4.27)$$

A particular (yet common) case is when $x \mapsto \|\varphi(x)\|_{\mathcal{H}}^2$ is maximal at x_0 . For instance, in the case of a convolution kernel, the L^2 -norm is constant on X . In that case $\varphi(x_0)$ is already in $(\text{Im } \varphi'(x_0))^\perp$, and the vanishing-derivatives precertificate is

$$\forall x \in X, \quad \eta_V(x) = \langle \varphi(x), p_V \rangle = \frac{\langle \varphi(x), \varphi(x_0) \rangle}{\|\varphi(x_0)\|_{\mathcal{H}}^2}. \quad (4.28)$$

The Cauchy-Schwarz inequality ensures that $|\eta_V(x)| \leq 1$ for all $x \in X$, hence $\eta_V = \eta_0$ (see [Proposition 4.3](#)).

Fourier measurements

Now, we consider the domain $X = \mathbb{T}$, and the ideal low pass filter (3.12), which gathers the Fourier coefficients,

$$\varphi(x) = \left(1, \sqrt{2} \cos(2\pi x), \sqrt{2} \sin(2\pi x), \dots, \sqrt{2} \cos(2f_c \pi x), \sqrt{2} \sin(2f_c \pi x)\right). \quad (4.29)$$

We endow the space of observations $\mathcal{H} = \mathbb{R}^{2f_c+1}$ with the standard Euclidean norm.

In the case of a single Dirac mass, say $m = \delta_{x_0}$, since $\varphi(x)$ has constant norm on X the above discussion yields

$$\eta_V(x) = \frac{\langle \varphi(x), \varphi(x_0) \rangle}{\|\varphi(x_0)\|_{\mathcal{H}}^2} = \frac{1}{2f_c + 1} \left(1 + 2 \sum_{k=1}^{f_c} \cos(2\pi k(x - x_0))\right) = \frac{1}{2f_c + 1} D_{f_c}(x - x_0),$$

where D_{f_c} is the Dirichlet kernel. Since η_V is bounded by 1 in magnitude, we have found the minimal-norm certificate, $\eta_V = \eta_0$.

Alternatively, if m has exactly f_c Dirac masses with the same sign, say $m = \sum_{i=1}^{f_c} \delta_{x_i}$ it is also possible to give an exact expression of the vanishing-derivatives precertificate, as in [PP17]. Since $1 - \eta_V$ is a trigonometric polynomial with f_c double roots, standard results on trigonometric polynomials imply that

$$1 - \eta_V(x) = C \left(\prod_{i=1}^{f_c} \sin^2(\pi(x - x_i)) \right),$$

where $C \in \mathbb{R}$. We may determine the constant C by orthogonality. Indeed, let $p_1 \stackrel{\text{def.}}{=} (1, 0, \dots, 0)^\top$. Since p_1 satisfies (4.21), the minimality of $\|p_V\|_{\mathcal{H}}^2$ yields

$$0 = \langle p_V, p_1 - p_V \rangle.$$

Since Φ^* is an isometry from \mathbb{R}^{2f_c+1} to $L^2(\mathbb{T})$, we have

$$\begin{aligned} 0 &= \int_{\mathbb{T}} \eta_V(t)(1 - \eta_V(t)) dt \\ &= C \int_{\mathbb{T}} \left(\prod_{i=1}^{f_c} \sin^2(\pi(t - x_i)) \right) dt - C^2 \int_{\mathbb{T}} \left(\prod_{i=1}^{f_c} \sin^2(\pi(t - x_i)) \right)^2 dt. \end{aligned}$$

Hence, we deduce

$$\eta_V(x) = 1 - C \left(\prod_{i=1}^{f_c} \sin^2(\pi(x - x_i)) \right), \quad (4.30)$$

$$\text{where } C = \frac{\int_{\mathbb{T}} \left(\prod_{i=1}^{f_c} \sin^2(\pi(t - x_i)) \right) dt}{\int_{\mathbb{T}} \left(\prod_{i=1}^{f_c} \sin^2(\pi(t - x_i)) \right)^2 dt}. \quad (4.31)$$

It is clear that $1 \geq \eta_V$. However, we do not know how to prove that $\eta_V \geq -1$, a property which seems to hold numerically (see Figure 4.1), regardless of the spikes locations.

In the more general case $1 < |\mathcal{I}| < f_c$, it is difficult to provide an explicit formula for η_V , and we are not aware of any such result. Moreover, although there is numerical evidence that it is non-degenerate provided the spikes are sufficiently separated, we are not aware of any theoretical result which supports that observation.

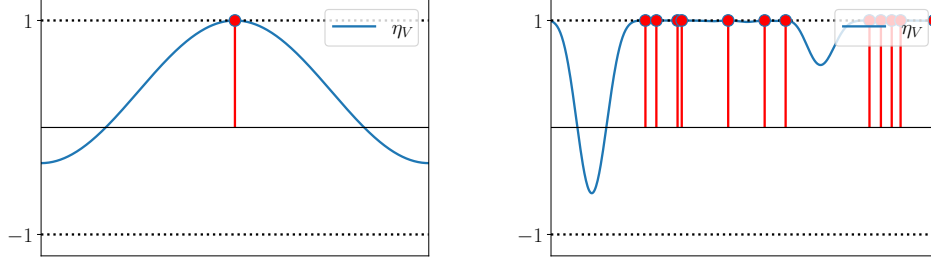


Figure 4.1: The vanishing-derivatives precertificate with the ideal low-pass filter for $m = \delta_0$ (left) and $m = \sum_{i=1}^{12} \delta_{x_i}$ with random locations x_i (right)

Fourier measurements (revisited)

The dual certificate constructed in [CFG14] to derive Theorem 3.1 is *not* the vanishing derivative precertificate corresponding to the above setting, *i.e.* the ideal low-pass filter and the Euclidean metric on $\mathcal{H} = \mathbb{R}^{2f_c+1}$. However, it is worth noting that *this dual certificate becomes the vanishing-derivatives precertificate* (and hence, in some cases, the minimal-norm certificate) *if one endows \mathbb{R}^{2f_c+1} with a specific metric*. Indeed, following [LT20], for $M \in \mathbb{N}$ and $f_c = 2M$, set

$$\|p\|_{\mathcal{H}}^2 \stackrel{\text{def.}}{=} \left\| (p^{(0)}, p^{(1)}, \dots, p^{(2f_c)}) \right\|_{\mathcal{H}}^2 \stackrel{\text{def.}}{=} \alpha_0 |p^{(0)}|^2 + \sum_{k=1}^{f_c} \alpha_k \left(|p^{(2k-1)}|^2 + |p^{(2k)}|^2 \right) \quad (4.32)$$

$$\text{where } \alpha_k \stackrel{\text{def.}}{=} \frac{1}{M^2} \sum_{j=k-M}^M \left(1 - \frac{|j|}{M} \right) \left(1 - \frac{|k-j|}{M} \right) \quad \text{for } k \in \{0, 1, \dots, 2M\}. \quad (4.33)$$

Then, the autocorrelation of φ is given by the Jackson kernel

$$K(x, x') = \langle \varphi(x), \varphi(x') \rangle_{\mathcal{H}} = \left(\frac{\sin(\pi M(x - x'))}{M \sin(\pi(x - x'))} \right)^4, \quad (4.34)$$

which is precisely the kernel used in [CFG14] to construct a dual certificate together with interpolation conditions. From Lemma 4.3, we note that this procedure yields the vanishing-derivatives precertificate η_V and, in essence, the main result of [CFG14] is that η_V is a valid and non-degenerate dual certificate (hence it is equal to η_0).

To summarize, the main point of using the metric (4.32) is that the proof of Theorem 3.1 (in [CFG14]) ensures that the Non-Degenerate Source Condition holds, provided the spikes are sufficiently separated. Relying on that trick, Q. Li and G. Tang have developed in [LT20] a support recovery analysis inspired from [13] with more quantitative bounds.

Convolution operators

The deconvolution problem is a typical application of the BLASSO. We set $X = \mathbb{R}^d$ or \mathbb{T}^d and we consider $\varphi(x) = \varphi(\cdot - x)$, where $\varphi \in L^2(X)$. The autocorrelation kernel is then translation-invariant,

$$K(x, x') = \int_X \varphi(s - x) \varphi(s - x') ds = K(x - x', 0). \quad (4.35)$$

In the case of the Gaussian filter,

$$\varphi(x) = \frac{1}{\sqrt{2\pi}\sigma} e^{-\frac{|x|^2}{2\sigma^2}}, \quad \text{we have } K(x, x') = \frac{1}{\sqrt{4\pi}\sigma} e^{-\frac{|x-x'|^2}{4\sigma^2}}. \quad (4.36)$$

It follows that, given $m = \sum_{x \in \mathcal{I}} a_x \delta_x$, the vanishing derivative certificate is of the form

$$\eta_V(x) = \sum_{x_i \in \mathcal{I}} (c_{x_i} x + d_{x_i}) e^{-\frac{|x-x_i|^2}{4\sigma^2}}. \quad (4.37)$$

Solving the interpolation problem $\eta(x_i) = \text{sign}(a_{x_i})$ and $\eta'(x_i) = 0$ is not straightforward (but it becomes easier when the spikes cluster at one point x_0 see [Section 6.2.2](#)).

Laplace transform

If $X =]0, +\infty]$, $\mathcal{H} = L^2([0, +\infty])$ and the impulse response is the Laplace transform,

$$\varphi(x) = (s \mapsto e^{-xs}) \quad (4.38)$$

then the autocorrelation function is given by

$$K(x, x') = \langle \varphi(x), \varphi(x') \rangle = \int_0^{+\infty} e^{-xs} e^{-x's} ds = \frac{1}{x + x'} \quad (4.39)$$

(see [\[8\]](#)). If we consider a measure $m = \sum_{x_i \in \mathcal{I}} \delta_{x_i}$ (or any masses with the same positive sign), [Lemma 4.3](#) implies that

$$\eta_V(x) = \sum_{x_i \in \mathcal{I}} \left(\frac{\alpha_i}{x + x_i} + \frac{\beta_i}{(x + x_i)^2} \right) = \frac{P(x)}{\prod_{x_i \in \mathcal{I}} (x + x_i)^2}, \quad (4.40)$$

for some coefficients $\alpha_i, \beta_i \in \mathbb{R}$, $i \in \mathcal{I}$ or some polynomial $P \in \mathbb{R}_{2|\mathcal{I}|-1}[X]$. From the conditions $\eta_V(x_i) = 1$, $\eta'_V(x_i) = 0$, we note that P is the only polynomial in $\mathbb{R}_{2|\mathcal{I}|-1}[X]$ which satisfies $P(x_i) = Q(x_i)$, $P'(x_i) = Q'(x_i)$, where $Q(X) \stackrel{\text{def.}}{=} \prod_{x_i \in \mathcal{I}} (X + x_i)^2$. Some inspection of the problem shows that $P(X) = \prod_{x_i \in \mathcal{I}} (X + x_i)^2 - \prod_{x_i \in \mathcal{I}} (X - x_i)^2$, so that

$$\eta_V(x) = 1 - \prod_{x_i \in \mathcal{I}} \left(\frac{x - x_i}{x + x_i} \right)^2. \quad (4.41)$$

That expression clearly shows that η_V is non-degenerate on X .

4.3.5 How to ensure non-degeneracy?

Ensuring that η_V is non-degenerate can sometimes be done on a closed form expression as above, but that is rather exceptional. Alternatively, arguments involving the properties of T-systems can sometimes be used (see [\[dCG12, SRR18\]](#), or [\[11\]](#)), but again, that is rather exceptional (it relies on a special property of the observation operator) and is mostly restricted to the BLASSO with positivity constraints.

In general, one relies on precise (and tedious!) majorization arguments: most proofs of identifiability for the BLASSO consist in building a vanishing derivatives precertificate η_V (for some Hilbertian norm) and exploiting the decaying properties of the kernel $K(\cdot, x_i)$.

In particular Quentin Denoyelle has proved the following result in his PhD thesis.

Theorem 4.1 ([Den18, Th. 2]). *Let $X = \mathbb{R}$, $\varphi \in \mathcal{C}^2(X; \mathcal{H})$ and assume that*

1. *for all $x \in X$ the matrix*

$$D_x \stackrel{\text{def.}}{=} \Gamma_{\{x\}}^* \Gamma_{\{x\}} = \begin{pmatrix} \|\varphi(x)\|_{\mathcal{H}}^2 & \langle \varphi(x), \varphi'(x) \rangle \\ \langle \varphi'(x), \varphi(x) \rangle & \|\varphi'(x)\|_{\mathcal{H}}^2 \end{pmatrix}$$

is invertible with $\|D_x^{-1}\|$ uniformly bounded, and $\|\varphi''(x)\|_{\mathcal{H}}$ is uniformly bounded,

2. *there exists a function $\omega: \mathbb{R}^+ \rightarrow \mathbb{R}^+$ with $\lim_{t \rightarrow +\infty} \omega(t) = 0$ such that, for all $x_1, x_2 \in X$,*

$$\begin{aligned} & |[\langle \varphi(x_1), \varphi(x_2) \rangle] + [\langle \varphi'(x_1), \varphi(x_2) \rangle] + [\langle \varphi'(x_1), \varphi'(x_2) \rangle]| \\ & \quad + [\langle \varphi(x_1), \varphi''(x_2) \rangle]| \leq \omega(|x_1 - x_2|), \end{aligned}$$

3. *There exists $C > 0$, $r > 0$ such that for all $x \in X$, $\eta_{V,x}'' \leq -C$ in $[x - r, x + r]$, where $\eta_{V,x}$ is the vanishing-derivatives precertificate corresponding to $m = \delta_x$,*
4. *for all open neighborhood V of 0, there exists $M > 0$ such that for all $x \in X$,*

$$\forall x' \in X \setminus (x + V), \quad |\eta_{V,x}(x')| \leq 1 - M.$$

Then, for $\mathcal{I} = \{x_1, \dots, x_s\}$ with $\min_{i \neq j} |x_i - x_j|$ large enough, and $m = \sum_{x \in \mathcal{I}} a_x \delta_x$, η_V is non-degenerate.

That result ensures the non-degeneracy of the dual precertificate (hence it is equal to η_0) provided the spikes are sufficiently separated so that they barely interfere with one another. The above results holds for instance with the convolution using a Gaussian filter, or a Cauchy kernel.

Let us mention that many authors have exploited similar ideas (originally in [CFG14]), often in a more quantitative way, but not always on the vanishing derivatives precertificate, see for instance [BDF16]. To the best of our knowledge, the most comprehensive results are given in [PKP20].

4.4 Total (gradient) variation denoising

Now, we turn to the total gradient variation as in Section 3.2.3. The minimal-norm certificate is less understood in that case, and it is not clear how to extend the strategy of Section 3.4.2 to derive good candidates for η_0 . However, in some cases η_0 can be found by direct analysis.

As we did in [6], we focus here on the denoising case, where $V = \mathcal{H} = L^2(\mathbb{R}^2)$ and Φ is the identity operator. Given a function $y_0 = u_0 \in L^2(\mathbb{R}^2)$, the solutions to the dual problem $(\mathcal{D}^{(\text{BV})}(0, y_0))$ (see Section 3.1.3) are exactly given by $\partial R^{(\text{BV})}(u_0)$. In view of Proposition 3.1, η is a solution to $(\mathcal{D}^{(\text{BV})}(0, y_0))$ if and only if the level sets of u_0 (that is, $U_0^{(t)} \stackrel{\text{def.}}{=} \{u_0 \geq t\}$ for $t > 0$, and $U_0^{(t)} \stackrel{\text{def.}}{=} \{u_0 \leq t\}$ for $t < 0$) solve the geometric variational problem (3.29) (resp. (3.30)), that is, $-\eta$ (resp. η) is a variational curvature for u_0 .

4.4.1 Calibrable sets

Calibrable sets were singled out in [BCN02] as the sets which evolve with constant boundary through the total variation flow $\frac{\partial u}{\partial t} \in -\partial R^{(\text{BV})}(u)$, namely:

$$\frac{\partial u}{\partial t} = \text{div} \left(\frac{Du}{|Du|} \right), \quad (4.42)$$

in $[0, \infty] \times \mathbb{R}^2$ subject to initial data $u(\cdot, 0) = u_0 \in L^2(\mathbb{R}^2)$. More precisely, given $u_0 = \mathbb{1}_E$ for $E \subseteq \mathbb{R}^2$, we say that E evolves with constant boundary if $u(x, t) = \lambda(t)\mathbb{1}_E(x)$ is a solution to (4.42), with $\lambda \geq 0$. Such sets are characterized by the fact that $h_E \mathbb{1}_E \in \partial R^{(BV)}(\mathbb{1}_E)$, where $h_E = P(E)/|E|$.

Definition 4.3 (Calibrable sets). *A set of finite perimeter $E \subseteq \mathbb{R}^2$ is said to be calibrable if, writing $v = \mathbb{1}_E$, there exists a vector field $z \in L^\infty(\mathbb{R}^2, \mathbb{R}^2)$ such that $\|z\|_\infty \leq 1$ and*

$$\begin{aligned} \int_{\mathbb{R}^2} (z, Dv) &= \int_{\mathbb{R}^2} |Dv|, \\ -\operatorname{div} z &= h_E v. \end{aligned}$$

In that case, we say that z is a calibration for E .

We refer to [BCN02, AVCM04, ACC05a, BCN05] and the references therein for the main properties of calibrable sets. For our purpose, we are content with their characterization in the plane.

Theorem 4.2 ([AVCM04, Thm. 4.40]). *Let $C \subseteq \mathbb{R}^2$ be a bounded set of finite perimeter. If C is calibrable, then C has a finite number of M -connected components C_1, \dots, C_m and*

1. C_i is convex for any $i \in \{1, \dots, m\}$,
2. ∂C_i is of class $\mathcal{C}^{1,1}$ for any $i \in \{1, \dots, m\}$,
3. the following inequalities hold:

$$\forall i \in \{1, \dots, m\}, \quad \operatorname{ess\,sup}_{p \in \partial C_i} \kappa_{\partial C_i}(p) \leq \frac{P(C_i)}{|C_i|}, \quad (4.43)$$

where $\kappa_{\partial C_i}(p)$ refers to the curvature of C_i (which exists for \mathcal{H}^1 -a.e. $p \in \partial C_i$).

4. $\frac{P(C_i)}{|C_i|} = \frac{P(C_j)}{|C_j|}$ for all $i, j \in \{1, \dots, m\}$.
5. let $I \subseteq \{1, \dots, m\}$ (possibly $I = \emptyset$); for all $E \subseteq \mathbb{R}^2$ with finite perimeter such that

$$\bigcup_{i \in I} C_i \subseteq E \subseteq \bigcup_{j \notin I} (\mathbb{R}^2 \setminus C_j), \quad (4.44)$$

we have

$$P(E) \geq \sum_{i \in I} P(C_i). \quad (4.45)$$

Conversely, if $C \subseteq \mathbb{R}^2$ is a bounded open set which is a union of a finite number C_1, \dots, C_m of connected components satisfying (1 – 5), then C is calibrable.

Remark 4.4. Note that the condition (4.45) implies that the connected components C_i are somehow “well-separated” (e.g. consider the case of two discs). In particular $\overline{C_i} \cap \overline{C_j} = \emptyset$.

Remark 4.5. As a consequence of (4) and the definition of M -connected components, $\frac{P(C)}{|C|} = \frac{P(C_j)}{|C_j|}$ for all $j \in \{1, \dots, m\}$.

The minimal-norm certificate for calibrable sets. Calibrable sets evolve in a self-similar manner through the total variation flow as well as through the Rudin-Osher-Fatemi minimization. Since the behavior of the Rudin-Osher-Fatemi for $\lambda \rightarrow 0^+$ is governed by the minimal-norm certificate (see [Proposition 3.8](#)), we have obtained in [\[6\]](#) the following result using the optimality conditions.

Proposition 4.5 (Minimal norm certificates for calibrable sets [\[6, Prop. 6\]](#)). *Let $C \subseteq \mathbb{R}^2$ be a bounded calibrable set and $y_0 \stackrel{\text{def.}}{=} u_0 \stackrel{\text{def.}}{=} \mathbb{1}_C / P(C)$. Then the minimal-norm certificate is $\eta_0 = p_0 = h_C \mathbb{1}_C$, where $h_C = \frac{P(C)}{|C|}$.*

Is the minimal-norm certificate tight? Once we know the minimal-norm certificate of $u_0 \stackrel{\text{def.}}{=} \mathbb{1}_C / P(C)$, it is natural to wonder if it is a tight certificate. In other words⁵, is $C_{\text{BV}} \cap (\partial R^{(\text{BV})})^{-1}(\eta_0)$ the (linear closure of the) minimal face of u_0 in C_{BV} ?

Since C has m connected components C_1, \dots, C_m (which happen to be simple sets), the results in [Chapter 2](#) imply that the closure of that minimal face is

$$\overline{\mathcal{F}_{C_{\text{BV}}}(u_0)} = \left\{ \sum_{i=1}^m \theta_i \frac{\mathbb{1}_{C_i}}{P(C_i)} \mid \theta_1, \dots, \theta_m \geq 0, \sum_i \theta_i = 1 \right\}, \quad (4.46)$$

and the functions $\frac{\mathbb{1}_{C_i}}{P(C_i)}$, $1 \leq i \leq m$, are the extreme points of that face.

The following new proposition clarifies the link between the above face and the “saturation set” of η_0 , *i.e.* the collection of sets which solve [\(3.29\)](#) for $\eta = \eta_0$.

Proposition 4.6 (Faces exposed by calibrable sets). *Let $C \subseteq \mathbb{R}^2$ be a nonempty calibrable set, with M -connected components $\{C_i\}_{1 \leq i \leq m}$ as in [Theorem 4.2](#), and $y_0 = u_0 = \mathbb{1}_C / P(C)$ so that $\eta_0 = h_C \mathbb{1}_C$ is its minimal-norm certificate.*

Then,

$$\partial R^{(\text{BV})^{-1}}(\eta_0) \cap C_{\text{BV}} = \left\{ \sum_{E \in \mathcal{C}} \theta_E \frac{\mathbb{1}_E}{P(E)} \mid \forall E \in \mathcal{C}, \theta_E \geq 0, \sum_{E \in \mathcal{C}} \theta_E = 1 \right\}, \quad (4.47)$$

where \mathcal{C} is the (finite) collection of all the sets $\overline{\text{conv}}(\bigcup_{i \in I} C_i)$ where $I \subseteq \{1, \dots, m\}$, $I \neq \emptyset$, is such that

$$P\left(\overline{\text{conv}}\left(\bigcup_{i \in I} C_i\right)\right) = \sum_{i \in I} P(C_i). \quad (4.48)$$

In particular, $C_{\text{BV}} \cap \partial R^{(\text{BV})^{-1}}(\eta_0)$ is finite dimensional.

Remark 4.6. *The notation $\overline{\text{conv}}(\bigcup_{i \in I} C_i)$ might call for some explanation, since it depends on the Lebesgue representative. We mean the closed convex hull of the points of density 1 of $(\bigcup_{i \in I} C_i)$. Incidentally, our taking the closed convex hull and not the convex hull is an arbitrary choice, since they both yield the same class of set modulo the Lebesgue measure.*

Remark 4.7. *Condition [\(4.48\)](#) trivially holds if I is a singleton, since each C_i is convex. As a result, the collection \mathcal{C} contains $\{C_1, \dots, C_m\}$ and $\overline{\mathcal{F}_{C_{\text{BV}}}(u_0)} \subseteq (C_{\text{BV}} \cap \partial R^{(\text{BV})^{-1}}(\eta_0))$.*

⁵From the positive homogeneity of $R^{(\text{BV})}$, it is equivalent to asking if $\{(u, R^{(\text{BV})}(u)) \mid u \in L^2(\mathbb{R}^2), \eta_0 \in \partial R^{(\text{BV})}(u)\}$ is equal to the (linear closure of the) minimal face of $(u, R^{(\text{BV})}(u))$ in $\text{epi } R^{(\text{BV})}$, see [Appendix B.3](#).

On the other hand for $|I| \geq 2$, Condition (4.48) expresses that the C_i 's are separated "just enough" for their union to be calibrable, but not more. It is a strong geometric condition, which, when satisfied, adds the corresponding convex hull to the collection \mathcal{C} , see Figure 4.2.

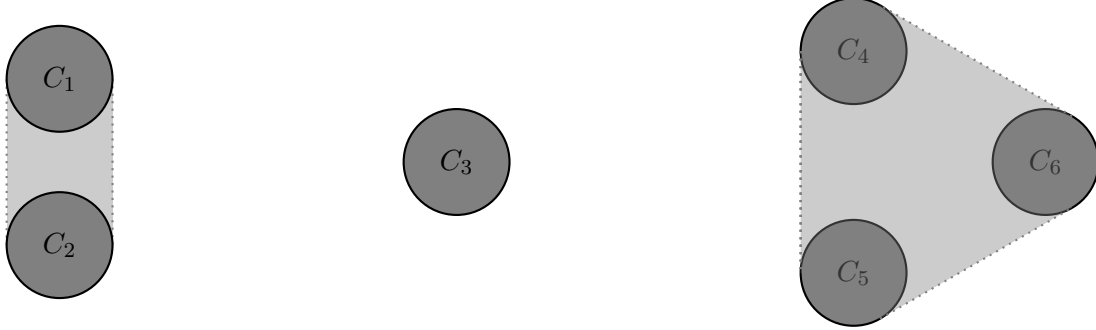


Figure 4.2: A calibrable union of convex calibrable sets (here a union of discs with radius 1). The nontrivial collections such that (4.48) holds are $\{C_1, C_2\}$ (the distance between their centers is π) and $\{C_4, C_5, C_6\}$ (the distance between their centers is $\frac{4}{3}\pi$).

Proof. The convex set

$$\mathfrak{F} \stackrel{\text{def.}}{=} C_{\text{BV}} \cap \partial R^{(\text{BV})^{-1}}(\eta_0) = \underset{u \in C_{\text{BV}}}{\operatorname{argmax}} \langle \eta_0, u \rangle \quad (4.49)$$

is a closed subset of C_{BV} , hence it is compact (where $V = L^2(\mathbb{R}^2)$ is endowed, as usual, with the weak topology). As a result, by the Krein-Milman theorem, \mathfrak{F} is the closed convex hull of its extreme points, and we only need to prove that its extreme points are exactly the functions $\mathbb{1}_E/P(E)$, where $E \in \mathcal{C}$.

From (4.49), we note that \mathfrak{F} is a *face* of C_{BV} , hence its extreme points are exactly the extreme points of C_{BV} that belong to \mathfrak{F} . Using Proposition 2.1, we obtain

$$\operatorname{extr}(\mathfrak{F}) = \left\{ \varepsilon \frac{\mathbb{1}_E}{P(E)} \mid (\varepsilon, E) \in \underset{\substack{0 < |E| < +\infty \\ \varepsilon = \pm 1}}{\operatorname{argmax}} \varepsilon \frac{\int_E \eta_0}{P(E)}, E \text{ simple set} \right\}. \quad (4.50)$$

Since $\eta_0 = h_C \mathbb{1}_C$ and $h_C > 0$, the only maximizers are given for $\varepsilon = 1$, hence $\operatorname{extr}(\mathfrak{F})$ is the collection of simple sets which solve the problem

$$\max_{\substack{E \subset \mathbb{R}^2 \\ 0 < |E| < +\infty}} \frac{|E \cap C|}{P(E)}. \quad (4.51)$$

Note that, C being calibrable, it follows from [AVCM04, Prop. 4.31] that C itself is a solution⁶ to (4.51), hence the value of the problem is $|C|/P(C) = 1/h_C$. Since $P(C)/|C| = P(C_i)/|C_i|$ for all i (see Remark 4.5), we deduce that each C_i is a solution to (4.54). Therefore, the C_i 's are simple sets which are solutions to (4.51). Moreover, if $I \subseteq \{1, \dots, m\}$ satisfies (4.48), then

$$P\left(\overline{\operatorname{conv}}\left(\bigcup_{i \in I} C_i\right)\right) = \sum_{i \in I} P(C_i) = \sum_{i \in I} h_C |C_i| = h_C \left| \overline{\operatorname{conv}}\left(\bigcup_{i \in I} C_i\right) \right|,$$

⁶But C is not a simple set for $m > 1$.

so that $\overline{\text{conv}}(\bigcup_{i \in I} C_i)$ is a maximizer too, and it is a simple set since it is convex. We have thus proved that $\{\mathbb{1}_E/P(E) \mid E \in \mathcal{C}\} \subseteq \text{extr } \mathfrak{F}$.

It remains to prove the converse inclusion. Let $E \subset \mathbb{R}^2$, $0 < |E| < +\infty$, be a simple set which maximizes (4.51). Observe that each C_i is either contained in E or disjoint from E .

➤ Indeed, by submodularity of the perimeter,

$$\begin{aligned} P(E \cup C_i) &\leq P(E) + P(C_i) - P(E \cap C_i) \\ &= h_C(|E \cap C_i| + |C_i|) - P(E \cap C_i) \\ &= h_C(|(E \cup C_i) \cap C_i|) + (h_C|E \cap C_i| - P(E \cap C_i)). \end{aligned}$$

Now, C_i being calibrable, it is Cheeger in itself, *i.e.* C_i is a solution of

$$\min_{F \subseteq C_i} \frac{P(F)}{|F|}$$

(see for instance [AVCM04, Prop. 4.31]). By the uniqueness of the Cheeger set of a convex body (see [Giu78b, KLR06, AC09]), we have $h_C|C_i \cap E| - P(C_i \cap E) < 0$ as soon as $0 < |E \cap C_i| < |C_i|$. As a consequence, if $|E \cap C_i| > 0$, we must have $|E \cap C_i| = |C_i|$, otherwise $|(E \cup C_i) \cap C_i|/P(E \cup C_i) < 1/h_C$, which contradicts the maximality of E .

Now, let $I = \{i \in \{1, \dots, m\} \mid C_i \subseteq E\}$. Necessarily $I \neq \emptyset$ (otherwise $|E \cap C| = 0$, which contradicts the maximality of E). The convex hull of the C_i 's, $i \in I$, is the indecomposable set with the smallest perimeter⁷ which contains $\bigcup_{i \in I} C_i$. In other words, let $G \stackrel{\text{def.}}{=} \overline{\text{conv}}(\bigcup_{i \in I} C_i)$; by [FFDD09, Thm. 1],

$$P(E) \geq P(G) \tag{4.52}$$

with strict inequality if $|E \Delta G| > 0$. As a result,

$$\frac{|E \cap C|}{P(E)} = \frac{\sum_{i \in I} |C_i|}{P(E)} \leq \frac{|G \cap C|}{P(G)} \tag{4.53}$$

with strict inequality if $|E \Delta G| > 0$. Since E is a maximizer of (4.51), we have $E = G = \overline{\text{conv}}(\bigcup_{i \in I} C_i)$, with

$$P\left(\overline{\text{conv}}\left(\bigcup_{i \in I} C_i\right)\right) = h_C \sum_{i \in I} |C_i| = \sum_{i \in I} P(C_i),$$

hence $E \in \mathcal{C}$. □

Remark 4.8. Consider $I, J \subseteq \{1, \dots, m\}$ which satisfy (4.48) and such that $I \cap J = \emptyset$, and let $G_I \stackrel{\text{def.}}{=} \overline{\text{conv}}(\bigcup_{i \in I} C_i)$, $G_J \stackrel{\text{def.}}{=} \overline{\text{conv}}(\bigcup_{j \in J} C_j)$. Then G_I and G_J must be disjoint.

➤ Indeed, by Proposition 2.2, we note that either $G_I \cap G_J = \emptyset$ or $G_I \cap G_J$ is also a maximizer of (4.51). Since G_I and G_J are convex, their intersection is either \emptyset (modulo the Lebesgue measure) or a simple set. As a result $G_I \cap G_J$ is either empty or it belongs to \mathcal{C} . But the latter case is impossible, since we would have $G_I \cap G_J = G_K$ for some $K \subseteq \{1, \dots, m\}$, $K \neq \emptyset$, hence $K \subseteq I \cap J$, a contradiction. As a result $\overline{\text{conv}}(\bigcup_{i \in I} C_i) \cap \overline{\text{conv}}(\bigcup_{j \in J} C_j) = \emptyset$ (up to a Lebesgue-negligible set).

⁷That fact is well known for connected sets with smooth boundary, as a consequence of the Crofton formula involving the Favard length [San04, Eq. (3.17)]. Here we could exploit the regularity of the solutions of (4.51) to reduce to that case, but [FFDD09] provides a direct result which applies to all sets of finite perimeter.

Remark 4.9. *The results presented in this section probably do not extend to the dimension $N > 2$, as they rely on the fact that the closed convex hull of convex sets C_i , $i \in I$, has the least perimeter among the connected sets which contain $\bigcup_{i \in I} C_i$. That property does not hold for $N \geq 3$ (for instance consider two parallel discs: the catenoid which joins them has smaller area than the cylinder which is their convex hull).*

To summarize the results of this section, the minimal-norm dual certificate for calibrable sets $\eta_0 = h_C \mathbf{1}_C$ is tight provided the connected components of C are sufficiently separated. Otherwise, η_0 exposes a face larger than $\overline{\mathcal{F}_{C_{\text{BV}}}}(u_0)$, but that face is still finite-dimensional, and the additional saturations correspond to the convex hull of the connected components that are too close to one another.

4.4.2 Convex sets

It is also possible to derive the minimal-norm certificate for the indicator of smooth convex sets, as we did in [6]. We base our discussion on [BGT87, GM94] which build variational curvatures for C , but in essence that construction is equivalent to the one in [ACC05b] where a vector field governing the evolution of convex sets by the total variation flow (4.42) is built.

Let C be a nonempty open bounded convex subset of \mathbb{R}^2 . We consider the variational problems

$$\min_{E \subseteq C} P(E) + s |C \setminus E|. \quad (\mathcal{Q}_s)$$

for $s > 0$. It is possible to prove (see [GM94, Eq. (2.15)] or [ACC05a, Lemma 4]) that if $s < t$ and if C_s, C_t denote solutions to (\mathcal{Q}_s) and (\mathcal{Q}_t) respectively, then⁸ $C_s \subseteq C_t$. Moreover, $C = \bigcup_{s>0} C_s$, and the solution to (\mathcal{Q}_s) is \emptyset for $0 < s < h_C$, where h_C is the Cheeger constant of C (see [KLR06, Par11]),

$$h_C \stackrel{\text{def.}}{=} \min_{E \subseteq C} \frac{P(E)}{|E|}. \quad (4.54)$$

There is a unique solution to (4.54) (see [ACC05b, KLR06], and [AC09] for $d \geq 2$), called the Cheeger set of C . For $s = h_C$, the solutions to (\mathcal{Q}_s) are exactly \emptyset and the Cheeger set of C , that we denote by C_{h_C} .

Therefore, it makes sense to define the function v_C by

$$v_C(x) \stackrel{\text{def.}}{=} \begin{cases} \inf \{ s > 0 \mid x \in C_s \} & \text{if } x \in C, \\ 0 & \text{otherwise.} \end{cases} \quad (4.55)$$

Remark 4.10. *The function v_C is (minus) the variational curvature proposed by E. Barozzi in [Bar94] and studied in [GM94]. In fact, in [Bar94], v_C is defined symmetrically in the complement of C : in $\mathbb{R}^d \setminus C$, one considers the problem*

$$\min_{E \subseteq (\mathbb{R}^2 \setminus C)} P(E) + s |(\mathbb{R}^2 \setminus C) \setminus E|. \quad (4.56)$$

and for $x \in \mathbb{R}^2 \setminus C$, one sets $v_C(x) \stackrel{\text{def.}}{=} -\inf \{ s > 0 \mid x \in D_s \}$, where D_s is a solution to (4.56). However, taking the complement of E , (4.56) amounts to

$$\min_{\tilde{E} \supseteq C} P(\tilde{E}) + s |\tilde{E} \setminus C|, \quad (4.57)$$

⁸We choose the Lebesgue representatives of points with density 1, hence this inclusion is not ambiguous.

and using the convexity of C (e.g. [FFDD09, Prop. 5]), it is possible to prove that the solution to (4.57) is equal to C for all $s > 0$. In other words, $x \in D_s$ for all $s > 0$ and the construction in [Bar94] yields $v_C(x) = 0$ in $\mathbb{R}^2 \setminus C$, as required in (4.55).

The function v_C turns out to be the minimal-norm certificate we are looking for.

Proposition 4.7. *If $C \subseteq \mathbb{R}^2$ is a nonempty bounded open convex set with $\mathcal{C}^{1,1}$ boundary, then the minimal-norm certificate for $\mathbf{1}_C/P(C)$ is $\eta_0 = v_C$.*

Proof. First, we prove that $v_C \in L^2(\mathbb{R}^2)$. Since $v \in \mathcal{C}^{1,1}$, its curvature is essentially bounded on ∂C ; let $\Lambda = \text{ess sup}_{x \in \partial C} \kappa(x)$ (essential bound with respect to the \mathcal{H}^1 measure). By [ACC05a, Th. 9], for $s > \max(\Lambda, P(C)/|C|)$, the unique solution to (\mathcal{Q}_s) is C . Therefore, $0 \leq v_C \leq \max(\Lambda, P(C)/|C|)$ and since v_C has compact support, $v_C \in L^2(\mathbb{R}^2)$.

Now, we prove that $v_C \in \partial R^{(\text{BV})}(\mathbf{1}_C/P(C))$. In view of Proposition 3.1, it is necessary and sufficient to prove that

$$\forall G \subseteq \mathbb{R}^2, |G| < +\infty, \quad P(G) - \int_G v_C \geq P(C) - \int_C v_C \quad (4.58)$$

(the other condition, for negative level sets, being immediate).

But Equation (4.58) expresses precisely the condition that $-v_C$ should be a variational curvature for C , which is indeed the case as proved in [GM94, Lem. 2.2].

It remains to prove that v_C has minimal-norm in $\partial R^{(\text{BV})}(\mathbf{1}_C/P(C))$. But this follows from the fact that v_C is the variational curvature with minimal $L^2(\mathbb{R}^2)$ norm (see [Bar94, Thm. 3.2]). \square

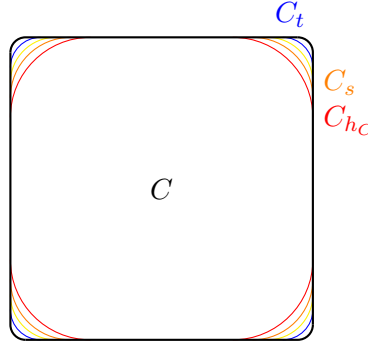


Figure 4.3: The solutions to (\mathcal{Q}_s) for $h_C < s < t$, where C is a square with rounded corners.

Remark 4.11. By [ACC05a, Th. 9], $C_s = C$ if and only if $s > \max(\Lambda, P(C)/|C|)$, where $\Lambda \stackrel{\text{def.}}{=} \text{ess sup}_{x \in \partial C} \kappa(x)$. As a result, there are two cases,

- either $\Lambda \leq P(C)/|C|$ (i.e. C is calibrable hence $h_C = P(C)/|C|$), in which case the solution to (\mathcal{Q}_s) is C for all $s > h_C$,
- or $\Lambda > P(C)/|C|$ (i.e. C is not calibrable, hence $P(C)/|C| > h_C$), in which case, for $h_C < s < \Lambda$ the solution satisfies $\emptyset \subsetneq C_s \subsetneq C$. See Figure 4.3 for the example of a square with rounded corners.

Remark 4.12. Proposition 4.7 holds in dimensions $d \geq 2$, but the case is $d = 2$ is special insofar as it is possible to construct explicitly the solutions C_s . Combining various results

in [AVCM04] and [ACC05a], we proved in [DAG09] that for $s > h_C$, the solution to (Q_s) is given by an opening,

$$C_s = \bigcup_{B(x', 1/s) \subseteq C} B(x', 1/s). \quad (4.59)$$

This draws a connection between the construction in [ACC05b], where foliations with arcs of circle are used to build a vector field (whose divergence eventually is η_0) and the construction in [Bar94].

Is the minimal-norm certificate tight? If C is nonempty, open bounded convex and $\mathcal{C}^{1,1}$, the next proposition shows that several other sets can be “certified” by η_0 .

Proposition 4.8. *Let $C \subseteq \mathbb{R}^2$ be a nonempty bounded open convex set with $\mathcal{C}^{1,1}$ boundary, and let η_0 be its minimal-norm certificate (i.e. $\eta_0 = v_C$). For all $s > h_C$, let C_s be a solution to (Q_s) .*

Then, $\eta_0 \in \partial R^{(\text{BV})}(\mathbb{1}_{C_s}/P(C_s))$.

Proof. For $t < s$, consider the variational problem

$$\min_{E \subseteq C_s} P(E) + t |C_s \setminus E|. \quad (\tilde{Q}_t)$$

Since the solutions to (Q_t) are included in C_s (by the monotonicity property), we note that a set E is a solution to (Q_t) if and only if it is a solution to (\tilde{Q}_t) .

As a result, the variational curvature v_{C_s} defined according to (4.55) (replacing C with C_s) coincides with v_C on C_s . Hence by the variational curvature property (see also [Bar94, Rem. 2.3])

$$P(C_s) - \int_{C_s} v_C = P(C_s) - \int_{C_s} v_{C_s} = 0 \quad (4.60)$$

and by Proposition 3.1, $v_c \in \partial R^{(\text{BV})}(\mathbb{1}_{C_s}/|C_s|)$. \square

As a result, if C is not calibrable, the sets C_s for $h_C < s < \Lambda$ are distinct from C (and \emptyset), and they yield an infinity of sets that are “certified” by η_0 . More precisely, in dimension $d = 2$, we know from [ACC05b] that $\text{int}(C \setminus C_{h_C})$ is foliated by the family $\{\partial C_s \setminus \partial C \mid h_C < s < \Lambda\}$, and that ∂C_s is a union of arcs of circles of radius $1/s$ in $\text{int}(C \setminus C_{h_C})$ (see Figure 4.3). Furthermore, the vector field z_0 which consists in the outer unit normal to C_s on $\partial C_s \setminus \partial C$ satisfies $\text{div } z_0 = v_C$.

Remark 4.13. *A formal integration by parts using the vector field constructed in [ACC05b], suggests that, not only the C_s ’s are certified by η_0 , but so are the convex sets that are obtained by using arcs of circles of different radii in different regions of C (see for instance Figure 4.3: one could choose a yellow arc in the top left-hand corner, a blue one in the top right-hand corner, etc.).*

To summarize, if C is not calibrable, the face exposed by η_0 contains infinitely many indicators of simple sets (hence extreme points). Therefore, it is not finite-dimensional. More complicated examples are studied numerically in Figure 5.2 in Chapter 5.

4.5 Conclusion

4.5.1 Summary

The minimal-norm certificate is the solution to a convex constrained problem. In general, it does not have any closed form expression. However, if one knows beforehand the elementary face it belongs to, it is possible to replace this constrained optimization problem with the orthogonal projection onto an affine space, in other words with the computation of the pseudo-inverse of some linear operator.

That principle can be applied in the case of polyhedral regularization or semi-infinite programming, for instance with the LASSO or the BLASSO respectively. In the case of total variation denoising, it is not clear how to apply that principle. We have discussed the case of indicator function of calibrable sets. In some geometric configurations the minimal-norm dual certificate is not tight, but it exposes a finite-dimensional face.

4.5.2 Discussion with respect to prior works and comments

Minimal sections. The notion of minimal-norm certificate is an extension of the *minimal section* used in the theory of maximal monotone operators (see the monograph [Br  73]). In fact, if J denotes the *atomic norm* [CRPW12] corresponding to $\{\varphi(x) \mid x \in X\}$,

$$J(y) = \|y\|_{\mathcal{A}} = \inf \{t > 0 \mid y \in t\overline{\text{conv}}\{\varphi(x)\}_{x \in X}\} = \inf_{m \in \mathcal{M}(X)} |m|(X) \quad \text{s.t. } \Phi m = y,$$

its subdifferential is exactly the set of solutions to $(\mathcal{D}(0, y))$, see Lemma B.1. The minimal-norm certificate is exactly the minimal section of $\partial J(y)$.

Irrepresentability condition. In the context of sparse inverse problems, the pioneering work of Fuchs [Fuc04] introduces the quantity p_F in a criterion for recovery, also known as irrepresentability condition (IC) in the literature. That criterion was extended by S. Vaiteer *et al.* to ℓ^1 -analysis [VPDF13], polyhedral [VPF13] and partly smooth regularizations [VGFP15, VPF15]. To our knowledge, the interpretation of the Fuchs precertificate a proxy for the minimal-norm dual solution first seems to appear in [13].

It is worth noting that the irrepresentability condition, or more precisely the property that p_0 is equal to $\text{proj}_{\text{Aff } F_0}(0)$ where F_0 is the relative interior of $(\Phi^*)^{-1}(\partial R(u))$ (or even $(\Phi^*)^{-1}(\partial R(u))$ itself), is equivalent to the orthogonality condition which appears in [BGM⁺16], namely $\langle p_0, p - p_0 \rangle = 0$ for all $p \in (\Phi^*)^{-1}(\partial R(u))$. Furthermore, the MINSUB condition, which consists in imposing that property on all $u \in V = \mathbb{R}^N$, has interesting consequences, such as the equivalence of the variational evolution

$$\min_u R(u) + \frac{1}{2t} \|u - f\|_{\mathcal{H}}^2, \tag{4.61}$$

and the gradient flow

$$\partial_t u(t) = -p(t), \quad p(t) \in \partial R(t), \quad u(0) = f, \tag{4.62}$$

provided R is polyhedral (see [BGM⁺16, BBCN21]).

Calibrable sets and Cheeger sets. The role of calibrable sets (including convex Cheeger sets) is central in the study of the total variation flow or the Rudin-Osher-Fatemi (ROF) model: the boundary of such sets does not move, and only the amplitude

of the corresponding indicator function is changed (see [ACC05b, BCN02]). Their characterization is given in [Giu78a, ACC05b, KLR06] in the plane and in [ACC05a] in \mathbb{R}^d . They are also used for image processing applications. In [BB13], the indicator functions of calibrable sets are interpreted as “nonlinear eigenvectors” of $R^{(\text{BV})}$. A nonlinear spectral decomposition based on total variation flow is introduced in [Gil14], inspired by the Fourier transform. It is refined and generalized to positively one-homogeneous functionals in [BGM⁺16] (see also [BBCN21] in the infinite-dimensional setting). The indicator functions of calibrable sets have a spectrum made of a single Dirac mass, they are equivalent to the “pure frequencies” in the Fourier spectrum.

Chapter 5

Support stability

Contents

5.1	Set convergence for supports and level lines	100
5.1.1	Definition	100
5.1.2	Convergence of the support for the BLASSO	101
5.1.3	Convergence of level lines in total gradient variation regularization	104
5.2	Support stability on a continuous domain	108
5.2.1	A counterexample to support stability	108
5.2.2	Non-degenerate certificates for support stability	110
5.3	Support stability for the Lasso problem on discrete grids	112
5.3.1	The existence of a tight dual certificate implies support recovery	112
5.3.2	The LASSO on thin grids	113
5.3.3	Support (in)stability on thin grids	116
5.4	Conclusion	119
5.4.1	Summary	119
5.4.2	Discussion with respect to prior works and comments	119

In this chapter, we focus on providing recovery guarantees for the solutions of the BLASSO ($\mathcal{P}^{(\text{TV})}(\lambda, y)$) or the total (gradient) variation regularized problem ($\mathcal{P}^{(\text{BV})}(\lambda, y)$). The general theory of inverse problems [BO04, HKPS07] provides many interesting results, including weak-* convergence (see [BP13]) or convergence rates in the Bregman divergence. Relying on similar arguments, one may derive bounds formulated in terms of local averages [AdCG15, FG13] or in terms of partial optimal transport [PKP20].

However, we wish to convey here some complementary information on the reconstructed solutions. As its alternative name suggests, the weak-* convergence of measures is *vague*, in the sense that it does not tell us anything about the structure of the measures involved: are they made of diffuse mass which concentrates, Dirac masses which tend to vanish or escape at infinity, or simply Dirac masses whose locations and amplitude converge towards those of the limit measure?

In the case of total variation denoising in imaging, the situation is similar, or worse. It is not difficult in a denoising problem to bound $\|u - f\|_{L^2(\mathbb{R}^2)}$ where u is the solution and f the unknown. But it is well known in image processing that the L^2 error has severe limitations when describing the perceptual difference between two images (see Figure 5.1), and several alternatives have been proposed such as the SSIM, which also have their own limitations. The approach we take here is motivated by a principle in image analysis which stems from the Gestalt theory [Wer23] and the Mathematical

Morphology theory [Ser82]: the shape information should be contained in the level sets of an image, determined in particular by their boundary.

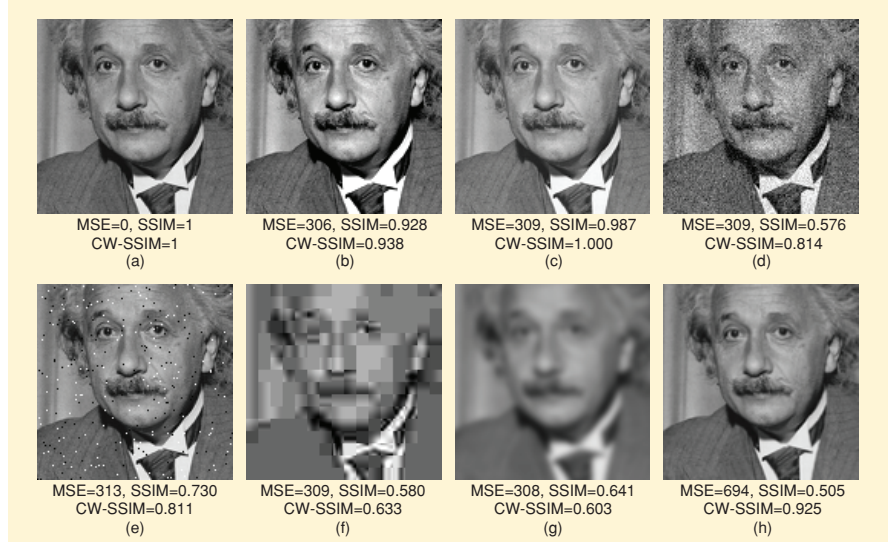


Figure 5.1: Experiments on the mean-square error by Z. Wang and A. Bovik [WB09]. The reference image is (a) and the following ones are obtained by (b) mean contrast stretch, (c) luminance shift, (d) Gaussian noise, (e) Impulsive noise, (f) JPEG compression, (g) blurring, (h) spatial scaling. The perceptual difference between those images is not reflected by the L^2 error (MSE).

As a result, given a solution $u \in L^2(\mathbb{R}^2)$ with finite total variation, we examine its level lines. For $t \geq 0$, we set $U^{(t)} \stackrel{\text{def.}}{=} \{u \geq t\}$, and for $t < 0$, we define $U^{(t)} \stackrel{\text{def.}}{=} \{u \leq t\}$. Our approach consists in examining the behavior of $\partial U^{(t)}$. A closely related notion is the support of the gradient, which turns out to be (see [6, Prop. 4]),

$$\text{supp}(Du) = \overline{\bigcup \{ \partial U^{(t)} \mid t \in \mathbb{R} \setminus \{0\} \}} = \overline{\bigcup \{ \partial^* U^{(t)} \mid t \in \mathbb{R} \setminus \{0\} \}}, \quad (5.1)$$

(where $\partial^* U^{(t)}$ denotes the reduced boundary of $U^{(t)}$, see Appendix A).

From a different perspective, the present chapter echoes Chapter 1: we know that the solutions have a certain representation in terms of extreme points of the level sets of the regularizer, but is that representation stable? What happens when the noise and the regularization parameter change?

Collaboration. The material of the present chapter mostly stems from joint works with Gabriel Peyré, Clarice Poon and Antonin Chambolle, namely [13, 6].

5.1 Set convergence for supports and level lines

5.1.1 Definition

Given a parameter τ in a Hausdorff topological space \mathcal{T} , and a family $(A_\tau)_{\tau \in \mathcal{T}}$ of subsets of X , we define its limit superior and limit inferior for $\tau \rightarrow \tau_0 \in \mathcal{T}$ (also known

as Kuratowski outer and inner limit, see [DM93, RW98]) as

$$\limsup_{\tau \rightarrow \tau_0} A_\tau \stackrel{\text{def.}}{=} \left\{ x \in X \mid \liminf_{\tau \rightarrow \tau_0} d(x, A_\tau) = 0 \right\}, \quad (5.2)$$

$$\liminf_{\tau \rightarrow \tau_0} A_\tau \stackrel{\text{def.}}{=} \left\{ x \in X \mid \limsup_{\tau \rightarrow \tau_0} d(x, A_\tau) = 0 \right\}. \quad (5.3)$$

where $d(x, A_\tau) \stackrel{\text{def.}}{=} \inf \{ d(x, y) \mid y \in A_\tau \}$. Both sets are closed, and if they are equal, we say that the sequence converges towards

$$\lim_{\tau \rightarrow \tau_0} A_\tau \stackrel{\text{def.}}{=} \limsup_{\tau \rightarrow \tau_0} A_\tau = \liminf_{\tau \rightarrow \tau_0} A_\tau. \quad (5.4)$$

If there is some compact set $K \subseteq X$ such that $A \in K$ and $A_\tau \subseteq K$ for all τ large enough, the Painlevé-Kuratowski convergence above is equivalent to the Hausdorff convergence: a closed set A is equal to $\lim_{\tau \rightarrow \tau_0} A_\tau$ if and only if

$$\lim_{\tau \rightarrow \tau_0} \left(\sup_{x \in A \cap A_\tau} |d(x, A) - d(x, A_\tau)| \right) = 0. \quad (5.5)$$

That notion of convergence is useful when studying the support or the level lines of the solutions.

5.1.2 Convergence of the support for the Blasso

In this section, we focus on the example of total variation minimization (see [Section 3.2.1](#)).

$$\begin{aligned} \min_{m \in \mathcal{M}(X)} |m|(X) + \frac{1}{2\lambda} \|\Phi m - y\|_{\mathcal{H}}^2, & \quad (\mathcal{P}^{(\text{TV})}(\lambda, y)) \\ \min_{m \in \mathcal{M}(X)} |m|(X) \quad \text{s.t. } \Phi m = y. & \quad (\mathcal{P}^{(\text{TV})}(0, y)) \end{aligned}$$

The corresponding dual problems are

$$\begin{aligned} \sup_{p \in \mathcal{H}} \left(\langle p, y \rangle - \frac{\lambda}{2} \|p\|_{\mathcal{H}}^2 \right) \quad \text{s.t. } \|\Phi^* p\|_{\infty} \leq 1 & \quad (\mathcal{D}^{(\text{TV})}(\lambda, y)) \\ \sup_{p \in \mathcal{H}} \langle p, y \rangle \quad \text{s.t. } \|\Phi^* p\|_{\infty} \leq 1 & \quad (\mathcal{D}^{(\text{TV})}(0, y)) \end{aligned}$$

For $m \in \mathcal{M}(X)$, we define $m_+, m_- \in \mathcal{M}^+(X)$ by the Hahn-Jordan decomposition $m = m_+ - m_-$. For $\eta \in \mathcal{C}_0(X)$ with $\|\eta\|_{\infty} \leq 1$, we define its (positive and negative) saturation sets as

$$\text{sat}_+ \eta \stackrel{\text{def.}}{=} \{ x \in X \mid \eta(x) = 1 \} \quad \text{and} \quad \text{sat}_- \eta \stackrel{\text{def.}}{=} \{ x \in X \mid \eta(x) = -1 \}. \quad (5.6)$$

With this notation the extremality condition $\eta \in \partial R^{(\text{TV})}(m)$ (see (3.21)) is equivalent to $\text{supp } m_{\pm} \subseteq \text{sat}_{\pm} \eta$.

The following result is an adaptation of [13, Lemma 1] which relies on the extremality conditions.

Proposition 5.1. *Let $(\lambda^*, y^*) \in]0, +\infty[\times \mathcal{H}$ and let p^* be the unique solution to $\mathcal{D}^{(TV)}(\lambda^*, y^*)$, and let $\eta^* \stackrel{\text{def.}}{=} \Phi^* p^*$. For $(\lambda, y) \in]0, +\infty[\times \mathcal{H}$, denote by m any solution to $(\mathcal{P}(\lambda, y))$. Then, there is a neighborhood U of (λ^*, y^*) in $]0, +\infty[\times \mathcal{H}$ and a compact set $K \subseteq X$ such that*

$$(\text{sat}_{\pm} \eta^*) \cup \left(\bigcup_{(\lambda, y) \in U} \text{supp}(m_{\pm}) \right) \subseteq K, \quad (5.7)$$

and

$$\limsup_{(\lambda, y) \rightarrow (y^*, \lambda^*)} (\text{supp}(m_{\pm})) \subseteq (\text{sat}_{\pm} \eta^*). \quad (5.8)$$

If, moreover, the solution m^* to $(\mathcal{P}(\lambda^*, y^*))$ is unique, then

$$\text{supp } m_{\pm}^* \subseteq \liminf_{(\lambda, y) \rightarrow (y^*, \lambda^*)} (\text{supp } m_{\pm}).$$

Proof. We deal with the case of m_+ (the case of m_- being similar). We denote by $p(\lambda, y)$ the unique solution to $(\mathcal{D}(y, \lambda))$.

Inclusion in a compact set. For the first point, if X is compact, we may choose $K = X$ and there is nothing to prove. Hence, we assume that X is only locally compact. We fix $y = y^*$, and we observe that, by [Proposition 3.2](#) and the fact that φ is bounded, the mapping

$$\lambda \mapsto p(\lambda, y^*) \mapsto \Phi^*(p(\lambda, y^*)) = \langle \varphi(\cdot), p(\lambda, y^*) \rangle_{\mathcal{H}} \quad (5.9)$$

is continuous from $]0, +\infty[$ to $(\mathcal{C}_0(X), \|\cdot\|_{\infty})$. As a result, for $\kappa \in]0, \lambda^*[$, the set $\{\eta_{\lambda}\}_{\lambda^* - \kappa \leq \lambda \leq \lambda^* + \kappa}$, where $\eta_{\lambda} \stackrel{\text{def.}}{=} \Phi^* p(\lambda, y^*)$, is compact in $\mathcal{C}_0(X)$. We cover it with a finite number of balls of radius $1/8$ and centers $\eta_{\lambda_1}, \dots, \eta_{\lambda_N}$ with $\lambda_i \in [\lambda^* - \kappa, \lambda^* + \kappa]$ for $1 \leq i \leq N$. Since those functions vanish at infinity, there is a compact set $K \subseteq X$ such that

$$\max_{1 \leq i \leq N} \sup_{x \in X \setminus K} |\eta_{\lambda_i}(x)| \leq \frac{1}{4}.$$

Now, for all $y \in \mathcal{H}$ such that $\|y^* - y\|_{\mathcal{H}} \leq \frac{\lambda^* - \kappa}{8 \max(1, \|\Phi^*\|)}$, all $\lambda \in [\lambda^* - \kappa, \lambda^* + \kappa]$,

$$\begin{aligned} \forall x \in X \setminus K, \quad |(\Phi^* p(\lambda, y))(x)| &\leq |(\Phi^* p(\lambda, y^*))(x)| + \|\Phi^*\| \frac{\|y - y^*\|_{\mathcal{H}}}{\lambda} \\ &\leq |\eta_{\lambda_i}(x)| + \|\eta_{\lambda_i} - \eta_{\lambda}\|_{\infty} + \frac{(\lambda^* - \kappa) \|\Phi^*\|}{8 \lambda \max(1, \|\Phi^*\|)} \\ &\leq \frac{1}{4} + \frac{1}{8} + \frac{1}{8} = \frac{1}{2}, \end{aligned}$$

where $i \in \{1, \dots, N\}$ is such that $\|\eta_{\lambda} - \eta_{\lambda_i}\|_{\infty} \leq \frac{1}{8}$.

As a result $\text{sat}_{\pm}(\Phi^* p(\lambda, y)) \stackrel{\text{def.}}{=} \{x \in X \mid (\Phi^* p(\lambda, y))(x) = \pm 1\} \subseteq K$. Besides, by the optimality conditions [\(3.3\)](#), we have

$$\text{supp}(m_{\pm}) \subseteq \text{sat}_{\pm}(\Phi^* p(\lambda, y))$$

hence its inclusion in K .

Outer limit inclusion. Let $x \in \left(\limsup_{(\lambda, y) \rightarrow (y^*, \lambda^*)} (\text{supp}(m_+)) \right) \subseteq X$. By definition, there exist sequences $(x_n)_{n \in \mathbb{N}}$ in X , $((y_n, \lambda_n))_{n \in \mathbb{N}}$ in $\mathcal{H} \times \mathbb{R}_+^*$ such that

- $\lim_{n \rightarrow \infty} x_n = x$,
- $\lim_{n \rightarrow +\infty} (y_n, \lambda_n) = (y^*, \lambda^*)$,
- $x_n \in \text{supp } m_n$, where $m_n \in \mathcal{M}(X)$ is a solution to $(\mathcal{P}(\lambda_n, y_n))$.

Let p_n be the unique solution to $(\mathcal{D}(\lambda_n, y_n))$. By the optimality conditions (3.3) (see also (3.21)),

$$1 = (\Phi^* p_n)(x_n) = \langle p_n, \varphi(x_n) \rangle. \quad (5.10)$$

By Proposition 3.2, p_n converges (strongly in \mathcal{H}) towards the solution p^* to $(\mathcal{D}(\lambda^*, y^*))$, and by weak continuity of φ , $\varphi(x_n) \rightharpoonup \varphi(x)$. As a result,

$$1 = \lim_{n \rightarrow \infty} \langle p_n, \varphi(x_n) \rangle_{\mathcal{H}} = \langle p^*, \varphi(x) \rangle_{\mathcal{H}} = (\Phi^* p^*)(x), \quad (5.11)$$

hence $x \in \text{sat}_+ \eta^*$.

Inner limit inclusion. Now, we assume that the solution m^* to $(\mathcal{P}(\lambda^*, y^*))$ is unique and we prove the second part of the statement. We note that m weak-* converges towards m^* as $(\lambda, y) \rightarrow (\lambda^*, y^*)$.

➤ By contradiction, if it were not the case, there would exist a neighborhood W of m^* , a sequence of elements (λ_n, y_n) converging to (λ^*, y^*) , and a corresponding sequence of solutions m_n such that $m_n \notin W$ for all $n \in \mathbb{N}$. But it is possible to check that

- the problems $(\mathcal{P}(\lambda_n, y_n))$, for $n \in \mathbb{N}$ are equicoercive, hence the sequence $(m_n)_{n \in \mathbb{N}}$ has a weakly-* convergent subsequence,
- the limit point of each weakly-* converging subsequence is a solution to $(\mathcal{P}(\lambda^*, y^*))$, hence it is equal to m^* ,

(that is in essence the stability result [HKPS07, Th. 3.2], but there it is stated for fixed λ). This contradicts $m_n \notin W$, hence the claimed convergence.

Now, we prove that $\text{supp } m_+^* \subseteq \liminf_{(y, \lambda) \rightarrow (y^*, \lambda^*)} \text{supp}(m_+)$. That is not so trivial since in general, $m \xrightarrow{*} m^*$ does not imply that $(m)_+ \xrightarrow{*} m_+^*$. However, let $x \in \text{supp } m_+^*$ and $r > 0$; a fundamental property of the positive part (see [Bou07a, Sec. III.5 and IV.1]) is that

$$m_+^*(B_X(x, r)) = \sup \left\{ \int_X \psi dm^* \mid \psi \in \mathcal{C}_0(X), 0 \leq \psi \leq 1, \text{supp } \psi \subseteq B_X(x, r) \right\}. \quad (5.12)$$

Choose ψ as above such that $\int_X \psi dm^* \geq \frac{1}{2} m_+^*(B(x, r)) > 0$. By the continuity of the map

$$m \mapsto \int_X \psi dm \quad (5.13)$$

and the fact that $m \xrightarrow{*} m^*$ as $(\lambda, y) \rightarrow (\lambda^*, y^*)$, there is a neighborhood \mathcal{W} of (λ^*, y^*) in $]0, +\infty[\times \mathcal{H}$ such that for all $(\lambda, y) \in \mathcal{W}$,

$$\int_X \psi dm \geq \int_X \psi dm^* - \frac{1}{4} m_+^*(B_X(x, r)) \geq \frac{1}{4} m_+^*(B_X(x, r)) > 0.$$

Hence, $(\text{supp}(m_+^*)) \cap B_X(x, r) \neq \emptyset$. In other words, we have proved that

$$\lim_{(\lambda, y) \rightarrow (y^*, \lambda^*)} d(x, \text{supp}(m_+)) = 0, \quad (5.14)$$

which is the claimed result. \square

Remark 5.1. *Since all the sets are contained in the same compact set K , the outer and inner limit formulations (5.8) and (5.9) are uniform [RW98, Th. 4.10], that is, respectively*

$$\lim_{(\lambda', y') \rightarrow (y, \lambda)} \left(\sup_{x \in \text{supp}(m')_{\pm}} d_X(x, \text{sat}_{\pm}(m)) \right) = 0, \quad (5.15)$$

$$\lim_{(\lambda', y') \rightarrow (y, \lambda)} \left(\sup_{x \in \text{supp}(m)_{\pm}} d_X(x, \text{supp}(m')_{\pm}) \right) = 0. \quad (5.16)$$

As $\text{sat}_+ \eta$ and $\text{sat}_- \eta$ are disjoint, we see that in a sufficiently small neighborhood of (λ, y) , the respective supports of $(m')_+$ and $(m')_-$ are disjoint, each in a neighborhood of $\text{sat}_+ \eta$ or $\text{sat}_- \eta$ respectively.

The above proposition has a counterpart in the low noise regime.

Proposition 5.2 ([13]). *Let $y_0 \in \mathcal{H}$ such that $(\mathcal{D}(0, y_0))$ has solutions, let p_0 be its minimal-norm solution, and let $\eta_0 \stackrel{\text{def.}}{=} \Phi^* p_0$. For $(\lambda, y) \in]0, +\infty[\times \mathcal{H}$, denote by m any solution to $(\mathcal{P}(\lambda, y))$. Then, there are values $\lambda_0 > 0$, $\alpha_0 > 0$ such that*

$$(\text{sat}_{\pm} \eta_0) \cup \left(\bigcup_{\substack{\lambda \in]0, \lambda_0[\\ \|y - y_0\|_{\mathcal{H}} / \lambda \leq \alpha_0}} \text{supp}(m_{\pm}) \right) \subseteq K, \quad (5.17)$$

and

$$\limsup_{\substack{(\lambda, y) \rightarrow (0, y_0) \\ \|y - y_0\|_{\mathcal{H}} / \lambda \rightarrow 0^+}} (\text{supp}^{\pm} m) \subseteq (\text{sat}_{\pm} \eta_0). \quad (5.18)$$

If, moreover, the solution m^* to $(\mathcal{P}(0, y_0))$ is unique, then

$$\text{supp } m_{\pm}^* \subseteq \liminf_{\substack{(\lambda, y) \rightarrow (0, y_0) \\ \|y - y_0\|_{\mathcal{H}} / \lambda \rightarrow 0^+}} (\text{supp}(m_{\pm})). \quad (5.19)$$

The proof follows from Proposition 3.8 and straightforward adaptations of Proposition 5.1, hence we omit it.

5.1.3 Convergence of level lines in total gradient variation regularization

In the case of total variation regularization ($R = R^{(\text{BV})}$, see Section 3.2.3), a similar convergence of the level lines holds, but the proof requires more work. We consider the problems (in dimension $d = 2$):

$$\min_{u \in L^2(\mathbb{R}^2)} \int_{\mathbb{R}^2} |Du| + \frac{1}{2\lambda} \|\Phi u - y\|_{\mathcal{H}}^2, \quad (\mathcal{P}^{(\text{BV})}(\lambda, y))$$

$$\min_{u \in L^2(\mathbb{R}^2)} \int_{\mathbb{R}^2} |Du| \quad \text{s.t. } \Phi u = y. \quad (\mathcal{P}^{(\text{BV})}(0, y))$$

The key property when studying the level lines and the support of the gradient is that for $u \in L^2(\mathbb{R}^2)$ with finite total variation and $\eta \in \partial R^{(\text{BV})}(u)$, see [6, Prop. 4],

$$\begin{aligned} \text{Supp}(Du) &= \overline{\bigcup \{ \partial^* U^{(t)} \mid t \in \mathbb{R} \setminus \{0\} \}} \\ &\subseteq \text{sat}(\eta) \stackrel{\text{def.}}{=} \overline{\bigcup \left\{ \partial^* E \mid |E| < +\infty, P(E) = \pm \int_E \eta \right\}}, \end{aligned} \quad (5.20)$$

where the level sets are $U^{(t)} \stackrel{\text{def.}}{=} \{u \geq t\}$ for $t \geq 0$, $U^{(t)} \stackrel{\text{def.}}{=} \{u \leq t\}$ for $t < 0$, and $\partial^* U^{(t)}$ is their reduced boundary. Note that $\partial^* U^{(t)}$ is dense in the topological boundary for some suitable choice of Lebesgue representative (see [Giu84, Ch. 3 and 4]).

In other words (see Proposition 3.1) the function $(-\eta)$ (resp. η) is a variational curvature for $U^{(t)}$ for $t > 0$ (resp. $t < 0$). The strategy is thus to exploit the geometric variational problems (3.29) and (3.30), and we begin with Lemma 5.1 below which provides uniform bounds for sets which have given variational curvatures. Let $\beta_2 \stackrel{\text{def.}}{=} 2\sqrt{\pi}$ denote the isoperimetric constant, in the sense that $\beta_2 \sqrt{|E|} \leq P(E)$ for all $E \subseteq \mathbb{R}^2$ with finite perimeter and finite measure.

Lemma 5.1 ([6, Lem. 2, 3]). *Let $\mathcal{A} \subseteq L^2(\mathbb{R}^2)$ be nonempty and compact, and let $\tilde{\mathcal{A}} \subseteq (\partial R^{(\text{BV})}(0)) \cap (\mathcal{A} + B_{L^2}(0, \rho))$, where $0 < \rho < \frac{1}{2}\beta_2$. Let*

$$\mathcal{E} \stackrel{\text{def.}}{=} \bigcup_{\substack{\eta \in \tilde{\mathcal{A}}, \\ \varepsilon = \pm 1}} \left\{ E \subseteq \mathbb{R}^2 \mid |E| < +\infty, \varepsilon \int_E \eta = P(E) \right\}. \quad (5.21)$$

Then,

$$0 < \inf_{E \in \mathcal{E}} P(E) \leq \sup_{E \in \mathcal{E}} P(E) < +\infty, \quad (5.22)$$

$$0 < \inf_{E \in \mathcal{E}} |E| \leq \sup_{E \in \mathcal{E}} |E| < +\infty, \quad (5.23)$$

and there exists $N_0 \in \mathbb{N}$ such that every $E \in \mathcal{E}$ has at most N_0 -connected components. Eventually, the family \mathcal{E} is contained in a ball, i.e. there exists $R > 0$ such that

$$\forall E \in \mathcal{E}, E \subseteq B(0, R). \quad (5.24)$$

As in the case of Radon measures, the path $\lambda' \mapsto p(\lambda', y)$ has compact range on sets of the form $I = [\lambda - \kappa, \lambda + \kappa]$ or $I = [0, \lambda_0]$, hence $\mathcal{A} \stackrel{\text{def.}}{=} \{ \Phi^* p(\lambda', y) \mid \lambda' \in I \}$ is compact. This ensures the equiintegrability of order 2 on the dual certificates¹, which is crucial for all these bounds. Moreover, the nonexpansiveness of the proximity operators allows to control the collection $\tilde{\mathcal{A}}$ of certificates $\Phi^* p(\lambda', y')$ for y' in a neighborhood of y .

Not only does this property provide bounds on the level sets $E \in \mathcal{E}$, but it also provides some form of regularity for the solutions to the prescribed curvature problem, as shown in the following lemma. While it stems from [GMT93], in [6, Prop. 7] we have simply emphasized its uniformity over a family of curvatures. It is powerful insofar as it allows us to obtain Hausdorff convergence from the mere L^1 convergence.

¹Following [Bou07a, Sec. IV.5.11], we say that a family $\mathcal{A} \subseteq L^2(\mathbb{R}^2)$ is *equiintegrable of order 2* if

- for all $\varepsilon > 0$, there exists $\delta > 0$ such that for all measurable $E \subseteq \mathbb{R}^2$ with $|E| \leq \delta$, $\sup_{\eta \in \mathcal{A}} \int_E |\eta|^2 \leq \varepsilon$,
- for all $\varepsilon > 0$, there exists a compact set $K \subseteq \mathbb{R}^2$ such that $\sup_{\eta \in \mathcal{A}} \int_{\mathbb{R}^2 \setminus K} |\eta|^2 \leq \varepsilon$.

Lemma 5.2 ([6, Prop. 7], [GMT93, Lem 1.2]). *If the assumptions of Lemma 5.1 hold, then \mathcal{E} is uniformly regular, in the sense that there exists $r_0 > 0$ such that,*

$$\forall E \in \mathcal{E}, \forall x \in \partial E, \forall r \in]0, r_0[, \quad \min \left[\frac{|B(x, r) \cap E|}{|B(x, r)|}, \frac{|B(x, r) \setminus E|}{|B(x, r)|} \right] \geq \frac{1}{16}. \quad (5.25)$$

It is thus possible to prove the main stability result of this section, which is a variant of [6, Thm. 2].

Proposition 5.3. *Let $(\lambda^*, y^*) \in]0, +\infty[\times \mathcal{H}$ and let p^* be the unique solution to $(\mathcal{D}(\lambda, y))$, and let $\eta^* \stackrel{\text{def.}}{=} \Phi^* p^*$. For $(\lambda, y) \in]0, +\infty[\times \mathcal{H}$, denote by u any solution to $(\mathcal{P}(\lambda, y))$. Then, there is a neighborhood W of (λ, y) in $]0, +\infty[\times \mathcal{H}$ and a radius $R > 0$ such that*

$$(\text{sat } \eta^*) \cup \left(\bigcup_{(\lambda, y) \in W} \text{supp}(Du) \right) \subseteq B(0, R), \quad (5.26)$$

and

$$\limsup_{(\lambda, y) \rightarrow (y^*, \lambda^*)} (\text{supp}(Du)) \subseteq (\text{sat } \eta^*). \quad (5.27)$$

If, moreover, the solution u^* to $(\mathcal{P}(\lambda^*, y^*))$ is unique, then

$$\text{supp}(Du^*) \subseteq \liminf_{(\lambda, y) \rightarrow (y^*, \lambda^*)} (\text{supp}(Du)).$$

and there is a sequence $((\lambda_n, y_n))_{n \in \mathbb{N}}$ with $(\lambda_n, y_n) \rightarrow (\lambda, y)$ such that

$$\text{for a.e. } t \in \mathbb{R}, \quad \lim_{n \rightarrow \infty} \left| U^{*(t)} \triangle U_n^{(t)} \right| = 0, \quad \lim_{n \rightarrow \infty} \partial U_n^{(t)} = \partial U^{*(t)}. \quad (5.28)$$

A similar result holds in the low noise regime,

Proposition 5.4 ([6, Thm. 2, extended]). *Let $y_0 \in \mathcal{H}$ such that $(\mathcal{D}(0, y_0))$ has solutions, let p_0 be its minimal-norm solution, and let $\eta_0 \stackrel{\text{def.}}{=} \Phi^* p_0$. For $(\lambda, y) \in]0, +\infty[\times \mathcal{H}$, denote by u any solution to $(\mathcal{P}(\lambda, y))$. Then, there are values $\lambda_0 > 0$, $\alpha_0 > 0$ and a radius $R > 0$ such that*

$$(\text{sat}_{\pm} \eta_0) \cup \left(\bigcup_{\substack{\lambda \in]0, \lambda_0[\\ \|y - y_0\|_{\mathcal{H}} / \lambda \leq \alpha_0}} \text{supp}(Du) \right) \subseteq B(0, R), \quad (5.29)$$

and

$$\limsup_{\substack{(\lambda, y) \rightarrow (0, y_0) \\ \|y - y_0\|_{\mathcal{H}} / \lambda \rightarrow 0^+}} (\text{supp}(Du)) \subseteq (\text{sat } \eta_0). \quad (5.30)$$

If, moreover, the solution u^* to $(\mathcal{P}(0, y_0))$ is unique, then

$$\text{supp}(Du^*) \subseteq \liminf_{\substack{(\lambda, y) \rightarrow (0, y_0) \\ \|y - y_0\|_{\mathcal{H}} / \lambda \rightarrow 0^+}} (\text{supp}(Du)).$$

and there is a sequence $((\lambda_n, y_n))_{n \in \mathbb{N}}$ with $(\lambda_n, y_n) \rightarrow (0, y_0)$ such that $\|y_0 - y_n\|_{\mathcal{H}} / \lambda_n \rightarrow 0^+$ and

$$\text{for a.e. } t \in \mathbb{R}, \quad \lim_{n \rightarrow \infty} \left| U^{*(t)} \triangle U_n^{(t)} \right| = 0, \quad \lim_{n \rightarrow \infty} \partial U_n^{(t)} = \partial U^{*(t)}. \quad (5.31)$$

Figure 5.2 shows the experiments performed in [6, Sec. 10] in a denoising experiment, at low noise and low regularization λ . The convergence of the level lines predicted in Proposition 5.4 eventually appears, but the ratio $\frac{\|y - y^*\|}{\lambda}$ needs to be quite small. In the third row, $\text{sat}(\eta_0)$ is the saturation set of the minimal-norm certificate η_0 (see Chapter 4). In these examples, we see that the saturation set is “thick”, in the sense that it is the union of the boundaries of infinitely many sets. The face exposed by η_0 is therefore infinite-dimensional (see the discussion of toy examples in Section 4.4).

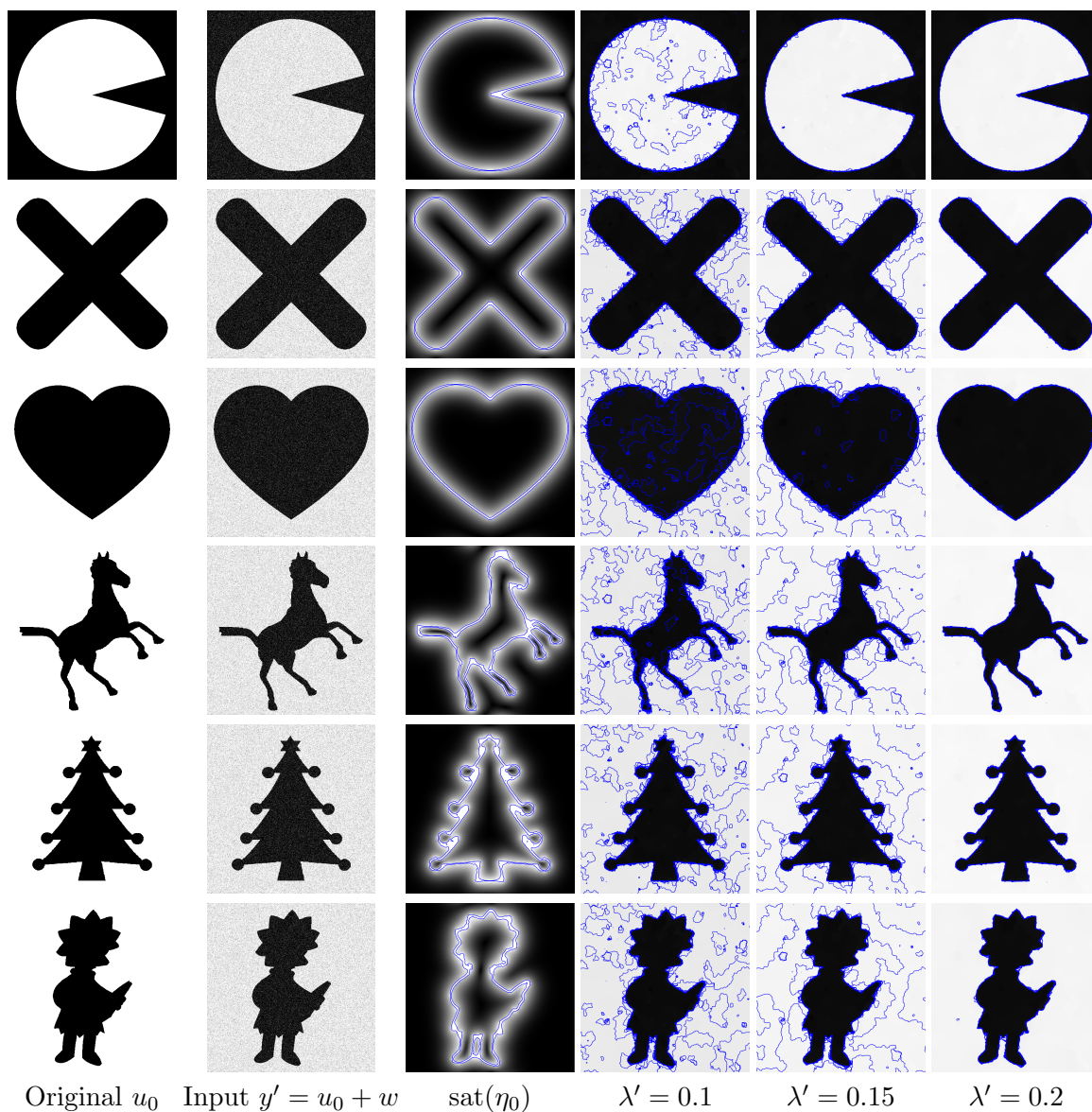


Figure 5.2: Display of the solution u' of a discretization of problem $\mathcal{P}^{(\text{BV})}(\lambda', y')$ in the denoising case (Φ is the identity) for several values of λ' . The blue curves on top u' of indicate the level sets of u' (computed using bilinear interpolation on the grid). The blue curves in the third row indicate an approximation of the boundary of the extended support $\text{sat}(\eta_0)$.

5.2 Support stability on a continuous domain

So far, we have obtained the Hausdorff (or Kuratowski) convergence of the support or the level lines of the solutions. We want to go further and see if the support has the same structure as the original signal. In other words, we want to understand if the representation predicted in [Chapter 1](#) is stable. We focus here on the sparse spikes recovery problem ($(\mathcal{P}^{(\text{TV})}(\lambda, y))$ in [Section 3.2.1](#)). We need to clarify the meaning of support stability (or exact support recovery) in this context. Since the domain X is continuous, one cannot expect to recover exactly the original support of the solution if the parameter $\tau = (\lambda, y)$ is perturbed. But one can hope to recover a measure with the same number of Dirac masses, which converge in locations and amplitudes to those of the original solution.

5.2.1 A counterexample to support stability

We consider in this section the following setting

$$X = \mathbb{T}, \quad \mathcal{H} = \mathbb{R}^3, \quad \varphi(x) = \begin{pmatrix} \cos(2\pi x) \\ \sin(2\pi x) \\ -f(\cos(2\pi x)) \end{pmatrix}, \quad (5.32)$$

where f is a function which satisfies the following assumptions.

Assumptions 5.1. *The function $f: [-1, 1] \rightarrow \mathbb{R}$ is continuous, strictly convex, differentiable, and*

$$f'(1) = 0, \quad f(1) = -1, \quad f(-1) < 0. \quad (5.33)$$

Note that [Assumptions 5.1](#) imply that $f'(c) < 0$ for all $c \in]-1, 1[$ hence f is (strictly) decreasing and $-1 \leq f(c) < 0$ (with equality only at 1).

As a consequence, the set

$$C \stackrel{\text{def.}}{=} \{ \Phi m \mid |m|(X) \leq 1 \} = \text{conv} \{ \pm \varphi(x) \mid x \in \mathbb{T} \} \quad (5.34)$$

has 0 in its interior. [Figure 5.3](#) shows the set C for $f(c) = \frac{1}{8}(c-1)^2 - 1$.

Theorem 5.1. *Let $\lambda \geq 0$, and $t \in \mathbb{T}$. Then, for*

$$y_t = \begin{pmatrix} \cos(2\pi t) \\ 0 \\ -f(\cos(2\pi t)) \end{pmatrix} + \frac{\lambda}{f^*(f'(\cos(2\pi t)))} \begin{pmatrix} f'(\cos(2\pi t)) \\ 0 \\ 1 \end{pmatrix}, \quad (5.35)$$

where f^* denotes the Legendre-Fenchel conjugate of f , the unique solution to $(\mathcal{P}(\lambda, y_t))$ is given by

$$m_t = \begin{cases} \frac{1}{2}(\delta_t + \delta_{-t}) & \text{for } t \notin \{0, \frac{1}{2}\} \pmod{1}, \\ \delta_0 & \text{for } t = 0 \pmod{1}, \\ \delta_{1/2} & \text{for } t = \frac{1}{2} \pmod{1}. \end{cases} \quad (5.36)$$

In particular, the solution for $t = 0$ is a single Dirac mass, but for t arbitrarily close to 0, the solution has two Dirac masses.

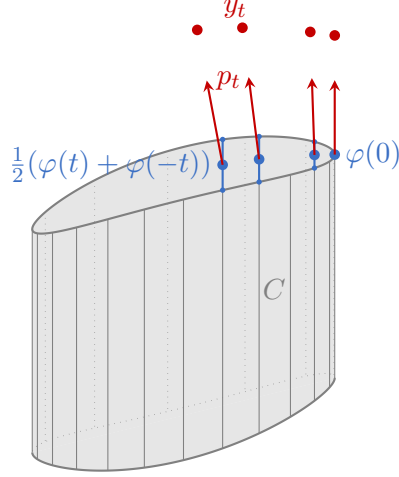


Figure 5.3: The set $C = \text{conv} \{ \pm \varphi(x) \mid x \in \mathbb{T} \}$. The vectors p_t are normal to C at Φm_t , which guarantees the optimality of m_t for $(\mathcal{P}(\lambda, y_t))$.

Proof. Let us consider the following vector

$$p_t \stackrel{\text{def.}}{=} \frac{1}{f^*(f'(\cos(2\pi t)))} \begin{pmatrix} f'(\cos(2\pi t)) \\ 0 \\ 1 \end{pmatrix} \quad (5.37)$$

Setting m_t as in (5.36), we see that $y_t = \Phi m_t + \lambda p_t$. If we prove that $\eta \stackrel{\text{def.}}{=} \Phi^* p_t \in \partial R^{(\text{TV})}(m_t)$, we obtain that $0 \in \lambda \partial R^{(\text{TV})}(m_t) + \Phi^*(\Phi m_t - y_t)$, hence m_t is a solution to $(\mathcal{P}(\lambda, y_t))$.

With the notation of Lemma 5.3 below, we observe that, for all $x \in \mathbb{T}$,

$$\eta(x) \stackrel{\text{def.}}{=} \langle p_t, \varphi(x) \rangle = \frac{1}{f^*(f'(\cos(2\pi t)))} (f'(\cos(2\pi t)) \cos(2\pi x) - f(\cos(2\pi x))) \quad (5.38)$$

$$= g_{\cos(2\pi t)}(\cos(2\pi x)), \quad (5.39)$$

so that by Lemma 5.3 below, $|\langle p_t, \varphi(x) \rangle| < 1$ except for $\cos(2\pi x) = \cos(2\pi t)$, in which case $\langle p_t, \varphi(x) \rangle = 1$. In other words, $\Phi^* p_t \in \partial R^{(\text{TV})}(m_t)$ and m_t is a solution to $(\mathcal{P}(\lambda, y_t))$. Since Φ has full rank on the set of atoms of m_t , the measure m_t is the unique solution to $(\mathcal{P}(\lambda, y_t))$. □

The following lemma is useful to prove that the dual certificate is tight.

Lemma 5.3. Let $f: [-1, 1] \rightarrow \mathbb{R}$ such that Assumptions 5.1 hold, and let $c_0 \in]-1, 1]$.

Then $f^*(f'(c_0)) > 0$ and the function $g_{c_0}: c \mapsto (f'(c_0)c - f(c)) / f^*(f'(c_0))$ satisfies $g_{c_0}(c_0) = 1$, $|g_{c_0}(c)| < 1$ for all $c \in [-1, 1] \setminus \{c_0\}$.

Proof. The first claim follows from $f^*(f'(c_0)) = \sup_{c \in [-1, 1]} (f'(c_0)c - f(c)) \geq -f(0) > 0$.

Moreover, the strictly concave function g_{c_0} satisfies $g'_{c_0}(c_0) = 0$ hence its unique maximizer is c_0 , with $g_{c_0}(c_0) = 1$.

Eventually, we note that for all $c \in [-1, 1]$, $f^*(f'(c_0)) \geq f'(c_0)(-c) - f(-c)$. Hence

$$f'(c_0)c - f(c) \geq -f^*(f'(c_0)) - f(c) - f(-c) > -f^*(f'(c_0)) \quad (5.40)$$

so that $g_{c_0}(c) > -1$. □

The above example shows that the solution for y_0 , which has a single Dirac mass, is approximated for $t \neq 0$ with a solution with two Dirac masses: it suggests that, in general, we cannot expect support stability. A key observation here is that the dual certificate has a vanishing second derivative, $\langle p_0, \varphi''(0) \rangle = 0$. In the next section, we show that preventing such cases enables support stability.

5.2.2 Non-degenerate certificates for support stability

Now, we go back to a more general setting where X and φ satisfy [Assumptions 4.1](#).

We have seen in [Section 4.3.1](#) the notion of non-degenerate certificate and how it allows us to compute a minimal-norm certificate using linearization. We note now that this notion is stable.

Notation: Given pairwise distinct positions $x_1, \dots, x_s \in \mathring{X}$ and nonzero values $a_1, \dots, a_s \in \mathbb{R} \setminus \{0\}$, we write $m_{(a,x)} \stackrel{\text{def.}}{=} \sum_{i=1}^s a_i \delta_{x_i}$.

Lemma 5.4. *Let $x_1^*, \dots, x_s^* \in \mathring{X}$ be pairwise distinct, $a_1, \dots, a_s \in \mathbb{R} \setminus \{0\}$. Assume that $\Phi^* p^*$ is a non-degenerate dual certificate for $m_{(a^*, x^*)} = \sum_{i=1}^s a_i^* \delta_{x_i^*}$.*

Then, there exists $\varepsilon > 0$, a neighborhood P of p^ in \mathcal{H} such that for all $(x_i)_{i=1}^s \in \prod_{i=1}^s B_X(x_i^*, \varepsilon)$, all $p \in P$ such that*

$$\begin{cases} \langle p, \varphi(x_i) \rangle = \text{sign}(a_i^*) \\ \langle p, \varphi'(x_i) \rangle = 0 \end{cases} \quad (5.41)$$

the function $\Phi^ p$ is a non-degenerate dual certificate for $m_{(a,x)} = \sum_{i=1}^s a_i \delta_{x_i}$ for all $a \in (\mathbb{R} \setminus \{0\})^s$ such that $\text{sign}(a) = \text{sign}(a^*)$.*

Proof. Let $K \subseteq \mathring{X}$ be a compact neighborhood of $\{x_1^*, \dots, x_s^*\}$. Since $\varphi \in \mathcal{C}^2(\mathring{X}; \mathcal{H})$, we have $\sup_{x \in K} \|\varphi''(x)\| < +\infty$, and the mapping

$$(\mathcal{H} \times K) \longrightarrow \mathbb{R} \times \mathcal{S}_d(\mathbb{R}) \quad (5.42)$$

$$(p, x) \longmapsto (\langle p, \varphi(x) \rangle, \langle p, \varphi''(x) \rangle), \quad (5.43)$$

is continuous. Hence, there is a neighborhood of $\{x_1^*, \dots, x_s^*\}$ (say, of the form $\bigcup_{i=1}^s B_X(x_i^*, \varepsilon)$, with $\varepsilon > 0$ small enough so that it is contained in K) and a neighborhood P' of p^* in which x and p satisfy $(\text{sign}(a_i^*) \langle p, \varphi(x) \rangle) > 1/2$ and $(\text{sign}(a_i^*) \langle p, \varphi''(x) \rangle) < 0$.

As a result, in each ball $B_X(x_i^*, \varepsilon)$ and for all $p \in P'$, the function $x \mapsto (\text{sign}(a_i^*) \langle p, \varphi(x) \rangle)$ is strictly concave; if p satisfies (5.41), then

$$\forall x \in B_X(x_i^*, \varepsilon), \quad 1/2 < (\text{sign}(a_i^*) \langle p, \varphi(x) \rangle) \leq 1,$$

with equality in the right-hand side only for $x = x_i^*$.

Additionally, since $\Phi^* p^* \in \mathcal{C}_0(X)$, there is a compact set K' such that $|\langle p^*, \varphi(x) \rangle| < 1/2$ for all $x \in X \setminus K'$. Since the set $K'' \stackrel{\text{def.}}{=} K' \setminus \bigcup_{i=1}^s B_X(x_i^*, \varepsilon)$ is compact,

$$\alpha \stackrel{\text{def.}}{=} \inf_{x \in K''} (1 - |\langle p^*, \varphi(x) \rangle|) > 0.$$

Thus, by the continuity of $p \mapsto \Phi^* p$ from \mathcal{H} to $\mathcal{C}_0(X)$ (see (3.11)), there is a neighborhood $P \subseteq P'$ of p^* such that

$$\sup_{x \in X \setminus \bigcup_{i=1}^s B_X(x_i^*, \varepsilon)} |\langle p, \varphi(x) \rangle| < 1.$$

Gathering everything, we see that $\Phi^* p$ is a non-degenerate dual certificate for all $m_{(a,x)}$ such that $\text{sign}(a) = \text{sign}(a^*)$. □

Support stability for $\lambda^* > 0$. The second derivative and the non-degeneracy assumption are crucial to ensure the stability of the structure of the solutions. We begin with the case of $\lambda^* > 0$.

Proposition 5.5. *Let $(\lambda^*, y^*) \in]0, +\infty[\times \mathcal{H}$, with $y^* = \Phi m^*$ for some $m^* = \sum_{i=1}^s a_i^* \delta_{x_i^*}$ with $x_1^*, \dots, x_s^* \in \mathring{X}$ pairwise distinct, $a_1^*, \dots, a_s^* \in \mathbb{R} \setminus \{0\}$. Let p^* be the unique solution to $(\mathcal{D}(\lambda^*, y^*))$, and assume that $\eta^* \stackrel{\text{def.}}{=} \Phi^* p^*$ is non-degenerate and that Φ_{x^*} has full rank. For $(\lambda, y) \in]0, +\infty[\times \mathcal{H}$, denote by m any solution to $(\mathcal{P}(\lambda, y))$.*

Then, for all $\varepsilon > 0$ small enough, there is a neighborhood U of (λ^, y^*) in $]0, +\infty[\times \mathcal{H}$ such that for all $(\lambda, y) \in U$,*

- *m has exactly s spikes, $m = \sum_{i=1}^s a_i \delta_{x_i}$, with $x_i \in B_X(x_i^*, \varepsilon)$ and $|a_i - a_i^*| \leq \varepsilon$ for all $i \in \{1, \dots, s\}$,*
- *p is a non-degenerate dual certificate for m .*
- *m is the unique solution to $(\mathcal{P}(\lambda, y))$.*

Sketch of Proof. By [Proposition 3.6](#), we see that m^* is the unique solution to $(\mathcal{P}(\lambda^*, y^*))$, hence the solutions to $(\mathcal{P}(\lambda, y))$ must converge to m^* as $(\lambda, y) \rightarrow (\lambda^*, y^*)$.

For $\varepsilon > 0$ smaller than the value given in [Lemma 5.4](#), [Proposition 5.1](#) implies that m concentrates its mass in each $B_X(x_i^*, \varepsilon)$ (with the sign of a_i^*). But [Lemma 5.4](#) ensures that the dual certificate $\Phi^* p$ saturates at exactly one point in each $B_X(x_i^*, \varepsilon)$, hence m has the predicted structure.

The fact that m is the unique solution follows from Φ_x having full rank and $\Phi^* p$ being nondegenerate. \square

Once the correct structure for m is obtained, the smoothness of the components a_i, x_i can be obtained using the implicit function theorem. Recalling from [\(5.36\)](#) that the dual solution should be equal to $p_{(\lambda, y)} = \frac{1}{\lambda}(y - \Phi m)$ and should satisfy [\(5.41\)](#), we may introduce the function $\mathcal{E}: (\mathbb{R}^s \times X^s) \times (\mathbb{R} \times \mathcal{H}) \rightarrow \mathbb{R}^{2s}$,

$$\mathcal{E}((a, x), (\lambda, y)) = \begin{pmatrix} \Phi_x^*(\Phi_x a - y) + \lambda s_0 \\ \Phi_x'^*(\Phi_x a - y) \end{pmatrix} = \Gamma_x^*(\Phi_x a - y) + \lambda \begin{pmatrix} s^* \\ 0 \end{pmatrix}. \quad (5.44)$$

By the optimality condition, for each (λ, y) in the neighborhood U , the solution $m_{(a, x)}$ should satisfy $\mathcal{E}((a, x), (\lambda, y)) = 0$.

The Jacobian of \mathcal{E} is given by (see [\[13\]](#) in dimension 1, and [\[PP19\]](#) in dimension d)

$$\frac{\partial \mathcal{E}}{\partial (a, x)} = (\Gamma_x^* \Gamma_x) \begin{pmatrix} \text{Id} & 0 \\ 0 & \text{diag}(a^*) \otimes \text{Id} \end{pmatrix} + \begin{pmatrix} 0 & \text{diag}(\Phi_x'^*(\Phi_x a - y)) \\ 0 & \text{diag}(\Phi_x''^*(\Phi_x a - y)) \end{pmatrix} \quad (5.45)$$

where \otimes denotes the Kronecker product. Observing that it is invertible, one obtains the following result, stated for $\lambda^* > 0$ in [\[PP19\]](#) and similar to the low noise result $\lambda^* = 0$ studied in [\[13\]](#) and below.

Theorem 5.2 ([\[PP19\]](#)). *Let $x_1^*, \dots, x_s^* \in \mathring{X}$ be pairwise distinct, $a_1^*, \dots, a_s^* \in \mathbb{R} \setminus \{0\}$ and assume that $\Phi^* p^*$ is non-degenerate for $m_{(a^*, x^*)}$, where $p^* = \frac{1}{\lambda}(\Phi_{x^*} a^* - y^*)$. Assume moreover that Γ_{x^*} has full rank.*

Then, there is a neighborhood \mathcal{W} of (y^, λ^*) in $\mathcal{H} \times \mathbb{R}$ in which the unique solution to $(\mathcal{P}^{(\text{TV})}(\lambda, y))$ is $m_{(a, x)}$, where (a, x) is the unique solution to $\mathcal{E}((a, x), (\lambda, y)) = 0$.*

Moreover, the mapping $S: (y, \lambda) \mapsto (a, x)$ is \mathcal{C}^1 on \mathcal{W} , with $S(y^, \lambda^*) = (a^*, x^*)$.*

The low noise regime. The case $\lambda^* = 0$ requires a bit more care, because the support stability does not hold in a neighborhood of $(0, y^*)$ but on a low noise regime of the form

$$\Omega_{\lambda_0, \alpha_0} \stackrel{\text{def.}}{=} \{(\lambda, y) \in \mathbb{R} \times \mathcal{H} \mid 0 < \lambda \leq \lambda_0, \|y - y^*\|_{\mathcal{H}} \leq \alpha_0 \lambda\} \quad (5.46)$$

for some $\lambda_0, \alpha_0 > 0$. Still, the line of proof is similar to the case $\lambda^* > 0$, and it is possible to prove the following.

Proposition 5.6 ([13]). *Let $x_1^*, \dots, x_s^* \in \overset{\circ}{X}$ pairwise distinct, $a_1^*, \dots, a_s^* \in \mathbb{R} \setminus \{0\}$ and define $m^* = \sum_{i=1}^s a_i^* \delta_{x_i^*}$ and $y^* = \Phi m^*$. Assume that the non-degenerate source condition (NDSC) holds, i.e. $(\mathcal{D}(0, y^*))$ has solutions, and its minimal-norm solution p_0 yields a non-degenerate dual certificate $\eta_0 \stackrel{\text{def.}}{=} \Phi^* p_0$ for m^* . Assume moreover that Φ_{x^*} has full rank. For $(\lambda, y) \in]0, +\infty[\times \mathcal{H}$, denote by m any solution to $(\mathcal{P}(\lambda, y))$.*

Then, for all $\varepsilon > 0$, there is a low noise regime $\Omega_{\alpha_0, \lambda_0}$ for some $\alpha_0, \lambda_0 > 0$ such that for all $(\lambda, y) \in \Omega_{\alpha_0, \lambda_0}$,

- *m has exactly s spikes, $m = \sum_{i=1}^s a_i \delta_{x_i}$, with $x_i \in B_X(x_i^*, \varepsilon)$ and $|a_i - a_i^*| \leq \varepsilon$ for all $i \in \{1, \dots, s\}$,*
- *p is a non-degenerate dual certificate for m .*
- *m is the unique solution to $(\mathcal{P}(\lambda, y))$.*

Again, the regularity of the positions and amplitudes can be obtained by invoking the implicit function theorem.

Theorem 5.3 ([13]). *Under the assumptions of Proposition 5.6, if Γ_{x^*} has full rank, there is a neighborhood \mathcal{W} of $(y^*, 0)$ in $\mathcal{H} \times \mathbb{R}$, a neighborhood \mathcal{V} of (a^*, x^*) in $\mathbb{R}^s \times X^s$ and a \mathcal{C}^1 -mapping $S: (y, \lambda) \mapsto (a, x)$ from \mathcal{W} to \mathcal{V} such that*

- *for all $(a, x) \in \mathcal{V}$, all (y, λ) in \mathcal{W} , $\mathcal{E}((a, x), (\lambda, y)) = 0$ if and only if $(a, x) = S(y, \lambda)$ (in particular $S(y^*, 0) = (a^*, x^*)$),*
- *there is a low noise regime $\Omega_{\alpha_0, \lambda_0}$ for some $\alpha_0, \lambda_0 > 0$ such that $m_{S(y, \lambda)}$ is the unique solution to $(\mathcal{P}^{(\text{TV})}(\lambda, y))$ for all $(y, \lambda) \in \Omega_{\alpha_0, \lambda_0}$.*

5.3 Support stability for the Lasso problem on discrete grids

5.3.1 The existence of a tight dual certificate implies support recovery

Now, we turn to the LASSO on a finite grid (see Section 3.2.2). As it can be seen as the BLASSO with X replaced with the finite set \mathcal{G} , all the results of Section 5.1 also hold for $(\mathcal{P}^{(\ell^1(\mathcal{G}))}(\lambda, y))$ and $(\mathcal{P}^{(\ell^1(\mathcal{G}))}(0, y))$.

Furthermore, as the set \mathcal{G} is finite, the inclusion holds not only in the limit, but also locally around (λ, y) (see an illustration in Figure 5.4). We thus obtain:

Proposition 5.7. *Let $(\lambda^*, y^*) \in]0, +\infty[\times \mathcal{H}$, let p^* be the unique solution to $(\mathcal{D}(\lambda, y))$, and let $\eta^* \stackrel{\text{def.}}{=} \Phi^* p^*$. For $(\lambda, y) \in]0, +\infty[\times \mathcal{H}$, denote by m any solution to $(\mathcal{P}(\lambda, y))$. Then, there is a neighborhood U of (λ^*, y^*) in $]0, +\infty[\times \mathcal{H}$ such that*

$$\forall (\lambda, y) \in U, (\text{supp}(m_{\pm})) \subseteq (\text{sat}_{\pm} \eta^*). \quad (5.47)$$

If, moreover, the solution m^* to $(\mathcal{P}(\lambda^*, y^*))$ is unique, then U can be chosen so that

$$\forall (\lambda, y) \in U, \text{supp } m_\pm^* \subseteq (\text{supp } m_\pm).$$

In particular, if $\text{sat}_\pm \eta^* = \text{supp}(m_\pm^*)$ (i.e. η^* is tight for m^*)

$$\forall (\lambda, y) \in U, \text{supp } m_\pm^* = (\text{supp } m_\pm).$$

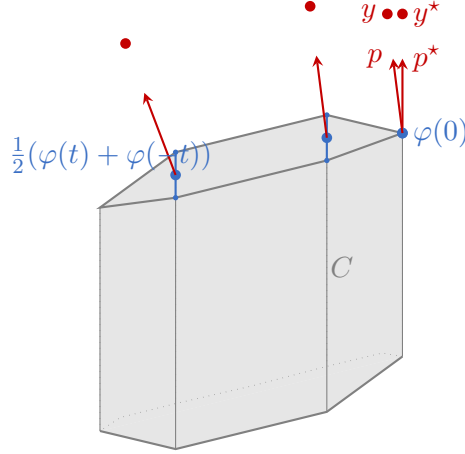


Figure 5.4: For y close enough to y^* , the solution in the discrete problem $(\mathcal{P}^{(\ell^1(\mathcal{G}))}(\lambda, y))$ the same support as for $y = y^*$, contrary to the continuous case (see [Section 5.2.1](#))

Similarly, for low regularization and low noise, we have:

Proposition 5.8 ([Fuc04],[13]). Let $y_0 \in \mathcal{H}$, let p_0 be the minimal-norm solution² to $(\mathcal{D}(0, y_0))$, and let $\eta_0 \stackrel{\text{def.}}{=} \Phi^* p_0$. For $(\lambda, y) \in]0, +\infty[\times \mathcal{H}$, denote by m any solution to $(\mathcal{P}(\lambda, y))$. Then, there are values $\lambda_0 > 0$, $\alpha_0 > 0$ such that

$$\forall (\lambda, y) \in \Omega_{\alpha_0, \lambda_0}, \quad (\text{supp}^\pm m) \subseteq (\text{sat}_\pm \eta_0). \quad (5.48)$$

If, moreover, the solution m^* to $(\mathcal{P}(0, y_0))$ is unique, we may choose λ_0 and α_0 so that

$$\forall (\lambda, y) \in \Omega_{\alpha_0, \lambda_0}, \quad \text{supp } m_\pm^* \subseteq (\text{supp}(m_\pm)). \quad (5.49)$$

In particular, if $\text{sat}_\pm \eta_0 = \text{supp}(m_\pm^*)$ (i.e. η_0 is tight for m^*)

$$\forall (\lambda, y) \in \Omega_{\alpha_0, \lambda_0}, \quad \text{supp } m_\pm^* = (\text{supp}(m_\pm)).$$

Computing explicitly these neighborhoods is possible thanks to the polyhedral nature of the regularization, and it is the key to the low noise analysis in [Fuc04] and homotopy methods like [OPT00]. In the next section, we examine the size of such neighborhoods in the case of thin grids.

5.3.2 The Lasso on thin grids

We begin with the framework of [Section 3.2.1](#) of a locally compact separable metric space. We consider a sequence of grids $(\mathcal{G}_n)_{n \in \mathbb{N}}$ where $\mathcal{G}_n \subseteq X$ and we solve the problems

$$\begin{aligned} \min_{m \in \mathcal{M}(X)} \|m\|_{\ell^1(\mathcal{G}_n)} + \frac{1}{2\lambda} \|\Phi m - y\|_{\mathcal{H}}^2, & \quad (\mathcal{P}^{(\ell^1(\mathcal{G}_n))}(\lambda, y)) \\ \min_{m \in \mathcal{M}(X)} \|m\|_{\ell^1(\mathcal{G}_n)} \quad \text{s.t. } \Phi m = y. & \quad (\mathcal{P}^{(\ell^1(\mathcal{G}_n))}(0, y)) \end{aligned}$$

²As the problem is finite-dimensional, the dual of the LASSO problem always has a solution.

We prove below the Γ -convergence of the discretized problem towards the BLASSO. Together with the equicoercivity of the functionals, that property ensures that any sequence $(m_n)_{n \in \mathbb{N}}$ of minimizers of $(\mathcal{P}^{(\ell^1(\mathcal{G}_n))}(\lambda, y))$ has accumulation points as $n \rightarrow +\infty$, and that those accumulation points are minimizers of $(\mathcal{P}^{(\text{TV})}(\lambda, y))$. Such a Γ -convergence was proved in \mathbb{R}^d in [Hei14] using a slightly different discretization, and in [15] in the one-dimensional torus.

Remark 5.2. *As $\mathcal{M}(X)$, equipped with the weak- $*$ topology, does not satisfy the first axiom of countability (the existence of a countable base of neighborhoods at each point), we work below on a bounded subset, for instance*

$$B \stackrel{\text{def.}}{=} \left\{ m \in \mathcal{M}(X) \mid |m|(X) \leq \frac{1}{2\lambda} \|y\|_{\mathcal{H}}^2 \right\}, \quad (5.50)$$

in which the weak- $*$ topology is metrizable [Br  11, Thm. 3.28]. We may therefore use the sequential definition of Γ -convergence (see [DM93] or Appendix C). Notice that B contains all the minimizers of $(\mathcal{P}^{(\ell^1(\mathcal{G}_n))}(\lambda, y))$ and $(\mathcal{P}^{(\text{TV})}(\lambda, y))$, so that this restriction does not change the solutions of the problems.

Proposition 5.9. *Assume that $\varphi \in \mathcal{C}(X; \mathcal{H})$ (where \mathcal{H} is equipped with the strong topology), and let $(\mathcal{G}_n)_{n \in \mathbb{N}}$ be an increasing family of finite subsets of X , $\mathcal{G}_n \subseteq \mathcal{G}_{n+1} \subseteq X$, such that $\bigcup_{n \in \mathbb{N}} \mathcal{G}_n$ is dense in X . Then, $(\mathcal{P}^{(\ell^1(\mathcal{G}_n))}(\lambda, y))$ Γ -converges towards $(\mathcal{P}^{(\text{TV})}(\lambda, y))$, in the sense that for all $m \in B$,*

- for all sequence $(m_n)_{n \in \mathbb{N}}$ with $\text{supp } m_n \subseteq \mathcal{G}_n$ such that $m_n \xrightarrow{*} m$ (in the weak- $*$ topology), $m_n \in B$, and

$$\left(|m|(X) + \frac{1}{2\lambda} \|\Phi m - y\|_{\mathcal{H}}^2 \right) \leq \liminf_{n \rightarrow \infty} \left(\|m\|_{\ell^1(\mathcal{G}_n)} + \frac{1}{2\lambda} \|\Phi m - y\|_{\mathcal{H}}^2 \right), \quad (5.51)$$

- there exists a sequence $(m_n)_{n \in \mathbb{N}}$ with $\text{supp } m_n \subseteq \mathcal{G}_n$ such that $m_n \xrightarrow{*} m$ (in the weak- $*$ topology), $m_n \in B$, and

$$\left(|m|(X) + \frac{1}{2\lambda} \|\Phi m - y\|_{\mathcal{H}}^2 \right) \geq \limsup_{n \rightarrow \infty} \left(\|m\|_{\ell^1(\mathcal{G}_n)} + \frac{1}{2\lambda} \|\Phi m - y\|_{\mathcal{H}}^2 \right). \quad (5.52)$$



On the other hand, the problems $(\mathcal{P}^{(\ell^1(\mathcal{G}_n))}(0, y))$ generally do not Γ -converge towards Equation $(\mathcal{P}^{(\text{TV})}(0, y))$.

Proof. The “liminf inequality” follows from the lower semi-continuity of the different terms of the energy and is identical to [15]. We focus here on the “limsup inequality” and the construction of a recovery sequence, since we cannot rely on a canonical partition of X .

Let $n \in \mathbb{N}$, and $\mathcal{G}_n = \{g_1, \dots, g_{s_n}\}$, we define for $1 \leq j \leq s_n$ the “Voronoi cells”,

$$V_j^{(n)} \stackrel{\text{def.}}{=} \{x \in X \mid \forall i < j, d_X(x, g_i) > d_X(x, g_j) \text{ and } \forall i > j, d_X(x, g_i) \geq d_X(x, g_j)\}. \quad (5.53)$$

The collection $\{V_j^{(n)}\}_{j=1}^{s_n}$ forms a Borel partition of X . Moreover, for any compact set $K \subseteq X$,

$$\lim_{n \rightarrow \infty} \max_{1 \leq j \leq s_n} \text{diam}(V_j^{(n)} \cap K) = 0. \quad (5.54)$$

➤ Indeed, assume by contradiction that there is $\varepsilon > 0$ and an infinite set of indices n such that there exists $x_1^n, x_2^n \in V_{j(n)}^{(n)} \cap K$ with $d_X(x_1^n, x_2^n) \geq \varepsilon$. We may extract a subsequence along which $x_1^n \rightarrow x_1^*$, $x_2^n \rightarrow x_2^*$ for some $x_1^*, x_2^* \in K$ such that $d_X(x_1^*, x_2^*) \geq \varepsilon$. For n large enough, $x_1^n \in B(x_1^*, \varepsilon/4)$, $x_2^n \in B(x_2^*, \varepsilon/4)$ and by density of $\bigcup_{\ell \in \mathbb{N}} \mathcal{G}_\ell$ there are some grid points $g, g' \in \mathcal{G}_n$ such that $g \in B(x_1^*, \varepsilon/4)$ and $g' \in B(x_2^*, \varepsilon/4)$.

But then, if $g_{j(n)}$ denotes the center of the common Voronoi cell to x_1^n and x_2^n ,

$$\begin{aligned} \max(d_X(x_1^n, g_{j(n)}), d_X(x_2^n, g_{j(n)})) &\geq \frac{1}{2} (d_X(x_1^n, g_{j(n)}) + d_X(x_2^n, g_{j(n)})) \\ &\geq \frac{1}{2} d_X(x_1^n, x_2^n) \\ &\geq \varepsilon/2. \end{aligned}$$

On the other hand

$$\begin{aligned} d_X(x_1^n, g) &\leq d_X(x_1^n, x_1^*) + d_X(x_1^*, g) < \varepsilon/2, \\ d_X(x_2^n, g') &\leq d_X(x_2^n, x_2^*) + d_X(x_2^*, g') < \varepsilon/2, \end{aligned}$$

so x_1^n is strictly closer to g than to $g_{j(n)}$, or x_2^n is strictly closer to g' than to $g_{j(n)}$. That contradicts the fact that both x_1^n and x_2^n belong to the Voronoi cell of center $g_{j(n)}$. As a result (5.54) holds.

Now, let $m \in \mathcal{M}(X)$, and define $m_n \stackrel{\text{def.}}{=} \sum_{i=1}^{s_n} a_j \delta_{g_j}$, where $a_j = m(V_j^{(n)})$. Let $\varepsilon > 0$ and choose a compact set $K \subseteq X$ such that $|m|(X \setminus K) \leq \varepsilon$. Then,

$$\begin{aligned} \|\Phi m - \Phi m_n\|_{\mathcal{H}} &= \left\| \int_X \varphi dm - \int_X \varphi dm_n \right\|_{\mathcal{H}} \\ &\leq \left\| \sum_{n=1}^{s_n} \int_{V_j^{(n)} \cap K} (\varphi(x) - \varphi(g_j)) dm(x) \right\|_{\mathcal{H}} \\ &\quad + \left\| \sum_{n=1}^{s_n} \int_{V_j^{(n)} \setminus K} (\varphi(x) - \varphi(g_j)) dm(x) \right\|_{\mathcal{H}} \\ &\leq \sum_{n=1}^{s_n} \int_{V_j^{(n)} \cap K} \|(\varphi(x) - \varphi(g_j))\|_{\mathcal{H}} d|m|(x) + 2 \|\varphi\|_{\infty} |m|(X \setminus K) \\ &\leq \omega_{\varphi} \left(\max_{1 \leq j \leq s_n} \text{diam}(V_j^{(n)} \cap K) \right) |m|(X) + 2 \|\varphi\|_{\infty} \varepsilon \end{aligned}$$

where ω_{φ} denotes the modulus of continuity of φ on the compact K . As both terms can be made arbitrarily small as $n \rightarrow +\infty$, we deduce that $\Phi m_n \rightarrow \Phi m$ strongly in \mathcal{H} . By similar computations, replacing φ with a test function, one may prove that m_n converges to m in the weak-* topology.

Eventually, we note that $|m_n|(X) \leq |m|(X)$, so that

$$\lim_{n \rightarrow \infty} \left(\lambda |m_n|(X) + \frac{1}{2} \|\Phi m_n - y\|_{\mathcal{H}}^2 \right) = \lambda |m|(X) + \frac{1}{2} \|\Phi m - y\|_{\mathcal{H}}^2. \quad (5.55)$$

□

Therefore, we have the “convergence of the minimizers” towards those of the continuous problem. On the dual side, regarding the problems

$$\begin{aligned} \min_{p \in \mathcal{H}} \left\| \frac{y}{\lambda} - p \right\|_{\mathcal{H}} \quad \text{s.t.} \quad \max_{x \in \mathcal{G}_n} |\langle \varphi(x), p \rangle_{\mathcal{H}}| &\leq 1. & (\mathcal{D}^{\ell^1(\mathcal{G}_n)}(\lambda, y)) \\ \sup_{p \in \mathcal{H}} \langle y, p \rangle \quad \text{s.t.} \quad \max_{x \in \mathcal{G}_n} |\langle \varphi(x), p \rangle_{\mathcal{H}}| &\leq 1. & (\mathcal{D}^{\ell^1(\mathcal{G}_n)}(0, y)) \end{aligned}$$

we also have convergence of the minimizers (under some assumptions for $\lambda = 0$). The proofs given in [13] extend immediately to our setting.

Proposition 5.10 ([13, Prop. 9 and 10]). *Under the assumptions of Proposition 5.9,*

1. *The unique solution $p_{\lambda,n}$ to $(\mathcal{D}^{\ell^1(\mathcal{G}_n)}(\lambda, y))$ converges to the solution $p_{\lambda,\infty}$ of $(\mathcal{D}^{(\text{TV})}(\lambda, y))$.*
2. *If $y = \Phi m$ for some measure m with $\text{supp } m \subseteq \mathcal{G}_n$ for all n large enough, and if m satisfies the source condition, then the minimal-norm solution $p_{0,n}$ to $(\mathcal{D}^{\ell^1(\mathcal{G}_n)}(0, y))$ converges (strongly in \mathcal{H}) towards the minimal-norm solution $p_{0,\infty}$ to $(\mathcal{D}^{(\text{TV})}(0, y))$.*

5.3.3 Support (in)stability on thin grids

Now we focus on a simpler setting, namely the one used in Section 4.2.2. We consider $X = \mathbb{T}$ and a sequence of grids $(\mathcal{G}_n)_{n \in \mathbb{N}}$ such that $\mathcal{G}_n \subseteq \mathcal{G}_{n+1} \subseteq X$ and that the grids are regular

$$\mathcal{G}_n \stackrel{\text{def.}}{=} \{kh_n \pmod{1} \mid 0 \leq k \leq G_n - 1\}, \quad \text{where } h_n \stackrel{\text{def.}}{=} 1/G_n. \quad (5.56)$$

We assume that $y^* = \Phi m^*$, with $m^* = \sum_{x \in \mathcal{I}} a_x^* \delta_x$, with $\mathcal{I} \subseteq \mathcal{G}_n$ for n large enough.

The next theorem states that, at low noise, the LASSO recovers twice the correct number of spikes, with the same signs. This is illustrated by the experiments in Figure 5.5 (see [15] for more detail on the setup): provided $\|y - y^*\|_{\mathcal{H}}/\lambda$ is small enough, each original spike is correctly identified, but one of its immediate neighbor is also activated.

To make this statement precise, given a collection of shifts $\varepsilon \in \{-1, 1\}^{\mathcal{I}}$ (to be fixed below), we define a support $\mathcal{J} \subseteq \mathcal{G}_n$ and a sign $s \in \{-1, 1\}^{\mathcal{J}}$ by

$$\mathcal{J} \stackrel{\text{def.}}{=} \mathcal{I} \cup \{x + \varepsilon_x h_n \mid x \in \mathcal{I}\} \quad (5.57)$$

$$\forall x \in \mathcal{I}, \quad s_x \stackrel{\text{def.}}{=} \text{sign}(a_x^*), \quad s_{x+\varepsilon_x h_n} \stackrel{\text{def.}}{=} s_x. \quad (5.58)$$

Theorem 5.4. *Assume that m^* satisfies the Non-Degenerate Source Condition and that $\Gamma_{\mathcal{I}}$ has full rank. Assume moreover that the components of the vector*

$$\rho \stackrel{\text{def.}}{=} (\Phi'_{\mathcal{I}} \Pi \Phi'_{\mathcal{I}})^{-1} \Phi'_{\mathcal{I}} \Phi_{\mathcal{I}}^* \text{sign}(a_{\mathcal{I}}), \quad (5.59)$$

are all nonzero, where Π is the orthogonal projector onto $(\text{Im } \Phi_{\mathcal{I}})^{\perp}$. Define $\varepsilon_x \stackrel{\text{def.}}{=} \text{sign}(a_x) \text{sign}(\rho_x)$ for all $x \in \mathcal{I}$, and \mathcal{J} and s by (5.57) and (5.58).

Then, there exists constants $\alpha_0 > 0$, $\lambda_0 > 0$, such that for all (λ, y) such that $\|y - y^\|_{\mathcal{H}} \leq \alpha_0$ and $0 < \lambda < \lambda_0 h_n$,*

- *The solution to $(\mathcal{P}^{\ell^1(\mathcal{G}_n)}(\lambda, y))$ is unique, with the form $m = \sum_{x \in \mathcal{J}} a_x \delta_x$ where $\text{sign}(a_x) = s_x$,*
- *The vector a is given by*

$$a_{\mathcal{J}} = a_{\mathcal{J}}^* + \Phi_{\mathcal{J}}^{\dagger}(y - y^*) - \lambda(\Phi_{\mathcal{J}}^* \Phi_{\mathcal{J}})^{-1} s. \quad (5.60)$$

Sketch of proof. The main idea of the proof is to construct the solution of the dual problem $(\mathcal{D}^{\ell^1(\mathcal{G}_n)}(\lambda, y))$ which is a projection problem. As in Chapter 4, the key is to guess the correct face the solution belongs to, so as to linearize the problem. Since we expect that at low noise, $p(\lambda, y)$ lies on the same elementary face as $p_{0,n}$ we replace the projection onto

$$D_n \stackrel{\text{def.}}{=} \left\{ p \in \mathcal{H} \mid \max_{x \in \mathcal{G}_n} |\langle \varphi(x), p \rangle_{\mathcal{H}}| \leq 1 \right\}, \quad (5.61)$$

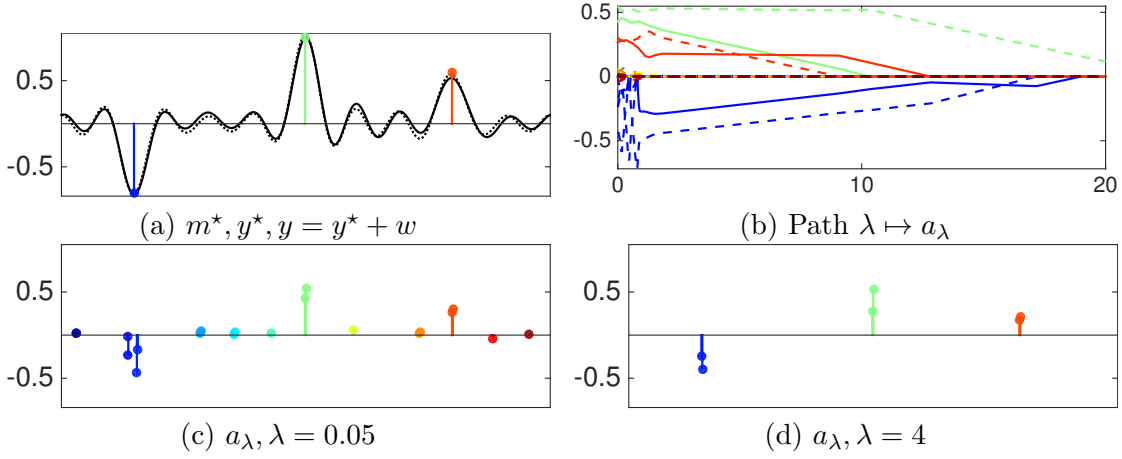


Figure 5.5: Sparse spikes deconvolution results obtained by computing the solution a_λ of $(\mathcal{P}^{(\ell^1(\mathcal{G}_n))}(\lambda, y))$. The color reflects the positions of the spikes on the 1-D grid. (a) shows the input measure m^* and the observation $y = y^* + w$. (b) shows how the solution a_λ (vertical axis) evolves with λ (horizontal axis). Each curve shows the evolution of $\lambda \mapsto (a_\lambda)_i$ for indexes $i \in \{1, \dots, G-1\}$. The color encodes the value of i . Plain curves correspond to correct spikes locations i associated to the input measure m^* . Dashed curves correspond to incorrect spikes (not present in the input measure m_0). (c,d) show the results a_λ obtained for two different values of λ .

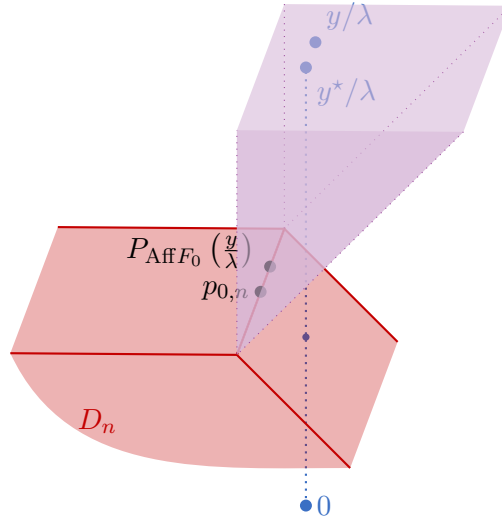


Figure 5.6: Illustration of the proof of Theorem 5.4. The solution set to the dual problem $\mathcal{D}^{\ell^1(\mathcal{G}_n)}(0, y^*)$ is the horizontal face, but the solution with minimal-norm $p_{0,n}$ lies on the smaller face (edge) F_0 . For λ and $\|y - y^*\|_{\mathcal{H}}/\lambda$ small enough, the projection of y/λ onto D_n is $P_{\text{Aff } F_0}(y/\lambda)$.

with the projection onto

$$\text{Aff } F_0 = \{ p \in \mathcal{H} \mid \forall x \in \mathcal{J}, \langle p, \varphi(x) \rangle = s_x \}. \quad (5.62)$$

where $s_x = \text{sign}(a_x)$ for $x \in \mathcal{I}$ and $s_{x'} = \text{sign}(a_x)$ for $x' = x + \varepsilon_x h_n$, $x \in \mathcal{I}$ (each spike is doubled, with the same sign, see [Section 4.2.2](#)). Indeed, it is possible to prove that for n large enough, the saturation set of $p_{0,n}$ is exactly \mathcal{J} , with sign s (see [\[15, Appendix D.2\]](#)).

Then, we write

$$\frac{y}{\lambda} = P_{\text{Aff } F_0} \left(\frac{y}{\lambda} \right) + \left(\frac{y}{\lambda} - P_{\text{Aff } F_0} \left(\frac{y}{\lambda} \right) \right), \quad (5.63)$$

and we check that $P_{\text{Aff } F_0} \left(\frac{y}{\lambda} \right) \in D_n$ and that $\left(\frac{y}{\lambda} - P_{\text{Aff } F_0} \left(\frac{y}{\lambda} \right) \right)$ is in the normal cone $\mathcal{N}_{D_n} \left(P_{\text{Aff } F_0} \left(\frac{y}{\lambda} \right) \right)$ so as to conclude that we have found the solution to $(\mathcal{D}^{\ell^1(\mathcal{G}_n)}(\lambda, y))$.

For the first point, we note that the projection onto an affine space yields

$$P_{\text{Aff } F_0} \left(\frac{y}{\lambda} \right) = (I - \Phi_{\mathcal{J}}^* \Phi_{\mathcal{J}}^*) \left(\frac{y}{\lambda} \right) + \Phi_{\mathcal{J}}^* s_{\mathcal{J}} \quad (5.64)$$

$$= P_{\text{Ker } \Phi_{\mathcal{J}}^*} \left(\frac{w}{\lambda} \right) + p_{0,n} \quad (5.65)$$

since $y \stackrel{\text{def.}}{=} y^* + w = (\Phi_{\mathcal{I}} a_{\mathcal{I}}^* + w) \in (w + \text{Im } \Phi_{\mathcal{J}})$ and $\Phi_{\mathcal{J}}^* s_{\mathcal{J}} = p_{0,n}$. Then, one may check that, since $p_{0,n} \rightarrow p_{0,\infty}$, for n large enough

$$\forall x \in \mathcal{G}_n \setminus \mathcal{J}, \left| \left\langle P_{\text{Ker } \Phi_{\mathcal{J}}^*} \left(\frac{w}{\lambda} \right) + p_{0,n}, \varphi(x) \right\rangle \right| < 1 \quad (5.66)$$

provided $\|w\|_{\mathcal{H}} / \lambda \leq C_1$, for some constant $C_1 > 0$ independent of n . On the other hand, by construction,

$$\forall x \in \mathcal{J}, \left\langle P_{\text{Ker } \Phi_{\mathcal{J}}^*} \left(\frac{w}{\lambda} \right) + p_{0,n}, \varphi(x) \right\rangle = s_x, \quad (5.67)$$

so that $P_{\text{Aff } F_0} \left(\frac{y}{\lambda} \right) \in D_n$.

For the second point, using [\(5.65\)](#) we get

$$\left(\frac{y}{\lambda} - P_{\text{Aff } F_0} \left(\frac{y}{\lambda} \right) \right) = (\Phi_{\mathcal{J}}^* \Phi_{\mathcal{J}}^*) \left(\frac{y}{\lambda} \right) - p_{0,n}. \quad (5.68)$$

Since $(\Phi_{\mathcal{J}}^* \Phi_{\mathcal{J}}^*)$ is the orthogonal projector onto $\text{Im } \Phi_{\mathcal{I}}$, we may write $(\Phi_{\mathcal{J}}^* \Phi_{\mathcal{J}}^*) w = \sum_{x \in \mathcal{J}} w_x \varphi(x)$. Moreover, since $p_{0,n}$ minimizes the square-norm over the constraint set

$$\{ p \in \mathcal{H} \mid \forall x \in \mathcal{I}, \langle p, s_x \varphi(x) \rangle = 1, \langle p, s_x \varphi(x + \varepsilon_x h_n) \rangle \leq 1 \}, \quad (5.69)$$

we deduce that

$$p_{0,n} = \sum_{x \in \mathcal{J}} p_x \varphi(x), \quad \text{with } s_x p_x \leq 0 \text{ for } x \in \mathcal{J} \setminus \mathcal{I}. \quad (5.70)$$

In fact, it is possible to prove that since ρ has all nonzero components, $s_x p_x < 0$ for $x \in \mathcal{J} \setminus \mathcal{I}$ and n large enough, with

$$\min_{x \in \mathcal{J} \setminus \mathcal{I}} |p_x| \geq \frac{1}{2h_n} \min_{x \in \mathcal{I}} |\rho_x|. \quad (5.71)$$

As a result,

$$\left(\frac{y}{\lambda} - P_{\text{Aff } F_0} \left(\frac{y}{\lambda} \right) \right) = \frac{1}{\lambda} \sum_{x \in \mathcal{I}} (a_x^* + w_x - \lambda p_x) \varphi(x) + \frac{1}{\lambda} \sum_{x \in \mathcal{J} \setminus \mathcal{I}} (w_x - \lambda p_x) \varphi(x) \quad (5.72)$$

with $(w_x - \lambda p_x)s_x > 0$ for $x \in \mathcal{J} \setminus \mathcal{I}$ provided that

$$\left(\max_{x \in \mathcal{I}} |w_x| \right) < \left(\min_{x \in \mathcal{J} \setminus \mathcal{I}} |p_x| \right) \quad (5.73)$$

and $(a_x + w_x - \lambda p_x)s_x > 0$ provided

$$\min_{x \in \mathcal{I}} |a_x| > \left(\max_{x \in \mathcal{I}} |w_x| \right) + \lambda \left(\max_{x \in \mathcal{I}} |p_x| \right). \quad (5.74)$$

It is possible to prove (see [15, Sec. 3.5]) that $\max_{x \in \mathcal{I}} |w_x| \leq \frac{C_2}{h_n} \|w\|_{\mathcal{H}}$ and $\max_{x \in \mathcal{I}} |p_x| \leq \frac{C_3}{h_n}$ for some constants $C_2, C_3 > 0$ independent of n .

To summarize, we have proved that

$$\frac{y}{\lambda} \in P_{\text{Aff } F_0} \left(\frac{y}{\lambda} \right) + \text{cone} \{ s_x \varphi(x) \mid x \in \mathcal{J} \} \quad (5.75)$$

and since the convex cone, $\text{cone} \{ s_x \varphi(x) \mid x \in \mathcal{J} \}$, is precisely the normal cone $\mathcal{N}_{D_n} (P_{\text{Aff } F_0} (\frac{y}{\lambda}))$ (the constraints are qualified since they are affine), we deduce that $P_{\text{Aff } F_0} (\frac{y}{\lambda})$ is precisely the solution to $(\mathcal{D}^{\ell^1(\mathcal{G}_n)}(\lambda, y))$.

Eventually, we read the solution m in (5.72) as

$$m = \sum_{x \in \mathcal{I}} (a_x^* + w_x - \lambda p_x) \delta_x + \sum_{x \in \mathcal{J} \setminus \mathcal{I}} (w_x - \lambda p_x) \delta_x \quad (5.76)$$

and we check that it satisfies the optimality condition. \square

5.4 Conclusion

5.4.1 Summary

In this chapter, we have studied the stability of the structure of the solutions of variational problems. A first property which holds without any special assumption is the convergence of the support or the level lines.

To obtain a real stability of the support, one needs to make additional assumptions: in the case of the BLASSO, the non-degeneracy of the second derivatives is a sufficient (and, apparently, almost necessary) condition to ensure that each original spike is approximated by exactly one spike.

In the case of the (discrete) LASSO, the situation seems easier since having simply a *tight* dual certificates provides the desired support stability. However, as we see, in deterministic problems stemming from the physical world, such as the deconvolution problem, that tightness of the minimal-norm certificate is rarely achieved. Spurious spikes tend to appear, as we have pointed out on a one-dimensional framework.

5.4.2 Discussion with respect to prior works and comments

Discrete versus continuous support stability Compared to the case of the BLASSO (Section 5.2.2), we see that support stability is somewhat easier to obtain in the discrete case (Section 5.3.1): it is sufficient to have a *tight* dual certificate (*i.e.* $|\eta(x)| < 1$ for $x \notin \text{supp } m^*$), there is no need to consider second derivatives. However, as we have seen in Section 5.3.3, that kind of stability result is a bit deceptive: it is a byproduct of the polyhedral nature of the problem (see Figure 5.4). When the grid \mathcal{G} gets thin, the corresponding neighborhoods or low noise regimes become very small. The dictionary

$\{\varphi(x)\}_{x \in \mathcal{G}}$ becomes so coherent that the support stability domains vanish. When slightly changing the parameters, the solutions move from one face to another.

Tracking those faces beyond the first one is tedious. On the contrary, the continuous point of view the BLASSO with a support which varies smoothly, provides fixed non-trivial neighborhoods and low noise regimes, even with a highly coherent dictionary.

(In?)Stability on thin grids Let us mention the study in [Hei14] of the case of a single unknown Dirac mass. The author proves that if the spike is not too far from a gridpoint, the LASSO recovers one single Dirac mass, located at that grid point. If the spike is in the middle region between two gridpoints, the LASSO reconstructs two spikes at those gridpoints, as if it were interpolating the positions of the grid points. On the contrary, our analysis (which relies on assumptions that require at least two unknown Dirac masses!) shows that in more complex situations, *even if the unknown signal lies on the grid and there is little noise and regularization*, spurious spikes appear. That phenomenon is due to the interactions between the unknown Dirac masses. It is difficult to quantify it, but we think that this behavior is rather the rule than the exception.

While such an instability of the support might seem disappointing, one should keep in mind that only the neighbors are activated, which makes the situation not so bad for source localization. On the contrary, taking that behavior into account can lead to the justification of a sparsification procedure which takes a cluster of spikes and interpolates their locations to form a single Dirac mass (see [Hei14, KHB21] and [FW19]), with surprisingly good performance!

Sparsity, partly smooth functions and sparse measures reconstruction. There is a large body of literature in the field of sparse recovery that deals with support stability guarantees ([Fuc04, Tro06, CR13, VPDF13]. Interestingly, such results were unified (at least in the finite-dimensional setting) in [VPF18] using the notion of *partly smooth functions* introduced in [Lew02]. The regularizer R is a smooth function when restricted to some submanifolds which encode the structure of the signal (the so-called *models*), and in the orthogonal directions, it has “kinks” which provide stability to those models in an optimization problem. In the case of the BLASSO and the reconstruction of sparse measures, it is natural to wonder if the results presented in this section fit into that framework. Adapting the notion of partly smooth function to the infinite dimensional setting is far from being trivial and remains an open problem, to the best of our knowledge. However, there is a way to reduce the BLASSO to the finite dimensional setting, if $\mathcal{H} = \mathbb{R}^M$, by considering the minimization problem

$$\min_{z \in \mathbb{R}^M} \lambda \|z\|_{\mathcal{A}} + \frac{1}{2} \|y - z\|_{\mathcal{H}}^2$$

where $\|z\|_{\mathcal{A}}$ denotes the *atomic norm* of z , *i.e.*

$$\|z\|_{\mathcal{A}} = \inf \{ t > 0 \mid z \in t \overline{\text{conv}} \{ \varphi(x) \}_{x \in X} \} = \inf_{m \in \mathcal{M}(X)} |m|(X) \quad \text{s.t. } \Phi m = z.$$

The solutions of the dual problem $(\mathcal{D}(0, y))$ are exactly the subgradients to $\|\cdot\|_{\mathcal{A}}$ at y (see Lemma B.1). It seems that the support stability results of Section 5.2.2 can be obtained directly provided that the atomic norm is partly smooth with respect to the manifolds,

$$\mathcal{M}_{\varepsilon} \stackrel{\text{def.}}{=} \left\{ \sum_i^M a_i \varphi(x_i) \mid \text{sign}(a_i) = \varepsilon_i, x_i \in \mathring{X} \text{ pairwise distinct} \right\}.$$

where $\varepsilon \in \{-1, 1\}^s$, $s \in \mathbb{N}$. Alas, checking that the atomic norm is partly smooth locally around a point y is as difficult as proving the results of [Section 5.2.2](#) directly.

Duality and mirror-stratifiability. Our proofs in [\[13\]](#) extensively use the connections between the dual and the primal problems, in particular the fact that the saturation set (which somehow encodes the “codimension” of the family of dual certificates) are in duality with the support (which encodes the dimension of the family of solutions). That kind of proof technique was later generalized by J. Fadili *et al.* to “mirror-stratifiable functions” in [\[FMP18\]](#) which have similar properties.

Support stability for total variation denoising While our work and the works of G. Mercier *et al.* [\[IMS17, IM20b\]](#) establish the convergence of the level lines in total (gradient) variation regularization, the question of support stability (*i.e.*, the solutions having the same number of level sets, with similar topology) remains a challenging problem. It requires the extension of the considerations on second derivatives to sets of finite perimeter.

Low noise regimes In the case of low regularization parameters λ for regularizing $(\mathcal{P}(0, y^*))$, one should note that there are two kind of results: on the one hand, the results of [Section 5.1](#) ensure the convergence of the support (or level lines), but they require to have both λ and the ratio noise/regularization $\|y - y^*\|_{\mathcal{H}}/\lambda$ arbitrarily small. On the other hand the results like [Theorem 5.3](#) are nonasymptotic: they state the existence of low noise regimes, in which $\|y - y^*\|_{\mathcal{H}}/\lambda$ can be fixed, and in which the structure of the support is preserved and the support converges. The main difference is that the later exploits the second derivatives of the dual certificates, which allow to exploit the “kinks” (more precisely, the partly smooth nature) of the set

$$C \stackrel{\text{def.}}{=} \{ \Phi m \mid |m|(X) \leq 1 \} = \overline{\text{conv}} \{ \pm \varphi(x) \mid x \in X \}.$$

Such results are much stronger. For the total (gradient) variation however, it is not clear how to generalize such properties.

Chapter 6

Below the “Rayleigh limit”

Contents

6.1	Close opposite spikes are not recoverable	124
6.1.1	The separation requirement is fundamental	124
6.1.2	The case of the ideal low-pass filter	125
6.2	Clustering spikes and the $(2s - 1)$-vanishing derivatives pre-certificate	126
6.2.1	An approximate factorization	127
6.2.2	The $(2s - 1)$ -vanishing dual precertificate	128
6.2.3	Support recovery for clustered spikes	131
6.3	Extended totally positive kernels	132
6.3.1	A characterization of the Non-degenerate Source Condition (NDSC)	132
6.3.2	Extended-totally positive kernels and non-degeneracy	134
6.4	Conclusion and comments	137
6.4.1	Summary	137
6.4.2	Comments	137

A striking feature of the identifiability theorem by E. Candès and C. Fernandez-Granda for the BASIS PURSUIT FOR MEASURES (see [Theorem 3.1](#) or [\[CFG14\]](#)) is the requirement of a *minimum separation distance*. This is a significant difference from similar identifiability results, in compressed sensing theory, concerning the BASIS PURSUIT for finite dimensional signals, which only involve the sparsity of the unknown. The use of a continuous domain makes it possible to have arbitrarily close opposite spikes which almost “cancel out” when the observation operator Φ (typically, a convolution kernel) is applied.

As we explain in [Section 6.1](#), the BASIS PURSUIT FOR MEASURES and the BLASSO are not able to recover such signals. That is a strong limitation compared to, *e.g.*, Prony’s method [\[dP95\]](#), MUSIC [\[Sch86\]](#) or ESPRIT [\[Kai90\]](#), which, on the other hand, rely on strong structural properties of the observation operator. The separation assumption of [Theorem 3.1](#) is in some sense *necessary* when dealing with signed measures. But in the case of a positive signal, *arbitrarily close spikes can be recovered*, under some non-degeneracy assumption ([Definition 6.1](#)). The main result of this chapter is [Theorem 6.1](#), which ensures that, provided the noise and the regularization parameter are small enough, the BLASSO is able to estimate the unknown measure with exact support recovery (that is, it provides a measure with the same number of spikes, which converge in amplitude and position to those of the unknown as the noise tends to zero). As the required non-degeneracy assumption relies on the computation of a “precertificate”,

which might not be available in closed-form expression, we discuss in [Section 6.3](#) a way to ensure that property a priori, using the properties of *extended totally positive kernels*. That alternative approach only works for some specific kernels (*e.g.* Laplace, Gauss), but it can deal with arbitrary sampling patterns, for which the dual precertificate is in general not known.

Collaboration. The content of [Section 6.2.2](#) follows from the collaboration with Gabriel Peyré and our student Quentin Denoyelle, in particular [\[8\]](#).

6.1 Close opposite spikes are not recoverable

In this section, we assume that $\dim(\mathcal{H}) < +\infty$. Since $\text{dom } R^{(\text{TV})} = \mathcal{M}(X) = V$, [Corollary 3.1](#) ensures that strong duality holds and that a dual solution exists. In particular, if $m_0 = m_{(a,x)} = \sum_{i=1}^s a_i \delta_{x_i}$ is a solution to $(\mathcal{P}(0, y_0))$, where $y_0 = \Phi m_0$, there must exist a dual certificate $\eta = \Phi^* p$ for some $p \in \mathcal{H}$, such that

$$\|\eta\|_\infty \leq 1 \quad \text{and} \quad \forall i \in \{1, \dots, s\}, \quad \eta(x_i) = \text{sign}(a_i). \quad (6.1)$$

In the case where X is a compact convex subset of \mathbb{R}^d and $\varphi \in \mathcal{C}^1(X; \mathcal{H})$, a straightforward application of the mean value theorem yields (if $\text{sign}(a_i) = -\text{sign}(a_j)$)

$$2 = |\eta(x_i) - \eta(x_j)| \leq \|\nabla \eta\|_\infty |x_i - x_j| \leq C |x_i - x_j|, \quad (6.2)$$

where $C > 0$ is the operator norm of the linear map $\eta \mapsto (\nabla \eta)$ from $(\text{Im } \Phi, \|\cdot\|_\infty)$ to $(\mathcal{C}(X; \mathcal{H}), \|\cdot\|_\infty)$, which is continuous since $\dim \text{Im } \Phi < +\infty$. As a result, *if m_0 is identifiable, any two opposite spikes must lie at distance at least $2/C$.*

The above argument can be extended to different cases, *e.g.* where X is \mathbb{R}^d , the torus \mathbb{T}^d , or more generally a Riemannian manifold. In some special cases (*e.g.* polynomial measurements on a compact set, Fourier measurements on the torus), the constant C is known, provided by the famous *Bernstein inequality* (see [\[Tan15\]](#) for various examples using the atomic norm; for Fourier measurements a sharper constant has been provided in [\[13\]](#) using Turán’s theorem).

However, the above argument can be refined in different directions, and we propose below two variants.

6.1.1 The separation requirement is fundamental

First, we note that the differential structure is not an essential requirement. In the following proposition, given $m \in \mathcal{M}(X)$, $m = m_+ - m_-$ denotes its Hahn-Jordan decomposition.

Proposition 6.1. *Let X be a locally compact separable metric space and assume that [Assumptions 3.1](#) hold, with $\dim \mathcal{H} < +\infty$. Then, there exists a constant $C > 0$ such that for all $y \in \mathcal{H}$ and all solution m to $(\mathcal{P}^{(\text{TV})}(0, y))$ (or $(\mathcal{P}^{(\text{TV})}(\lambda, y))$),*

$$\forall (x_+, x_-) \in (\text{supp } m_+) \times (\text{supp } m_-), \quad d_X(x, x') \geq C > 0. \quad (6.3)$$

Proof. The ball $\mathcal{B} \stackrel{\text{def.}}{=} \{\eta \in \text{Im } \Phi^* \mid \|\eta\|_\infty \leq 1\}$ is bounded and closed in the finite dimensional space $\text{Im } \Phi^*$. As a result, it must be compact in $(\mathcal{C}_0(X), \|\cdot\|_\infty)$, hence uniformly equicontinuous.

➤ If X is compact, the uniform equicontinuity of \mathcal{B} follows from the standard Arzelà-Ascoli theorem. Otherwise (*i.e.* X is only locally compact), let $\varepsilon > 0$. There exists a finite family $\{\eta_i\}_{i \in I} \subseteq \mathcal{B}$ such that for all $\eta \in \mathcal{B}$, $\min_{i \in I} \|\eta - \eta_i\|_\infty \leq \varepsilon/3$.

By definition of $\mathcal{C}_0(X)$, there exists a compact set $K_1 \subseteq X$ such that

$$\forall i \in I, \quad \sup_{x \in X \setminus K_1} |\eta_i(x)| \leq \varepsilon/6. \quad (6.4)$$

Since X is locally compact, there exists a compact set $K_2 \subseteq X$ such that $K_1 \subseteq \text{int}(K_2)$ (see *e.g.* [Bou07c, I. p.65 Prop. 10]). We set $\alpha = \min_{x \in K_1} d_X(x, X \setminus K_2)$. As each η_i is uniformly continuous on the compact set K_2 , there exists $\alpha' > 0$ such that for all $x, x' \in K_2$ such that $d_X(x, x') \leq \alpha'$, $|\eta_i(x) - \eta_i(x')| \leq \varepsilon/3$.

Setting $\alpha'' \stackrel{\text{def.}}{=} \min(\alpha, \alpha') > 0$, we see that for all $x, x' \in X$ such that $d_X(x, x') \leq \alpha''$ and all $\eta \in \mathcal{B}$, $|\eta(x') - \eta(x)| \leq \varepsilon$. Hence, the family is uniformly equicontinuous.

Let ω be the modulus of equicontinuity of \mathcal{B} , *i.e.*

$$\forall t \geq 0, \quad \omega(t) \stackrel{\text{def.}}{=} \sup \left\{ |\eta(x) - \eta(x')| \mid \eta \in \mathcal{B}, d_X(x, x') \leq t \right\}.$$

Note that $\omega: \mathbb{R}_+ \rightarrow \mathbb{R}_+$ is nondecreasing and continuous at 0 with $\omega(0) = 0$.

As explained above, since $\dim \mathcal{H} < +\infty$, the primal problem is stable, hence there exists a solution η_* to the dual problem, and for all solution m of the primal problem, all $x_+ \in \text{supp } m_+$ (resp. $x_- \in \text{supp } m_-$), $\eta_*(x_\pm) = \pm 1$.

Then $\omega(d_X(x_+, x_-)) \geq |\eta_*(x_+) - \eta_*(x_-)| = 2$, hence

$$d_X(x_+, x_-) \geq C \stackrel{\text{def.}}{=} \inf \{ t \geq 0 \mid \omega(t) \geq 2 \} > 0.$$

□

6.1.2 The case of the ideal low-pass filter

Alternatively, in the particular case of the ideal low-pass filter on the torus, it is possible to provide a sharper constant than the one provided by the Bernstein inequality [13] and to describe the solutions when the input measure does not meet that separation condition [12]. Let us consider an initial measure¹ $m_0 = \delta_{h/2} - \delta_{-h/2}$, $h > 0$, and an observation given by the ideal low-pass filter (see Equation (3.12)). In that case, the constant C involved in (6.2) is provided by the Bernstein inequality, $C = 2\pi f_c$, yielding a necessary separation distance $d_X(x_+, x_-) \geq \frac{1}{\pi f_c}$ in [Tan15]. However, that bound is not sharp, and a better constant, proposed in [13], is the separation $d_X(x_+, x_-) \geq \frac{1}{2f_c}$.

Furthermore, in [Con20], Laurent Condat observed numerically that for $h < 1/(2f_c)$, the solution to $(\mathcal{P}(0, y_0))$ is a Dirac comb, *i.e.* a sum of equispaced Dirac masses. As a consequence, the solution is given by

$$m = \sum_{j=-f_c}^{f_c-1} a_j \delta_{t_j}, \quad \text{where} \quad t_j \stackrel{\text{def.}}{=} \frac{1}{4f_c} + \frac{j}{2f_c}, \quad \text{and} \quad (6.5)$$

$$a_j = (-1)^j \frac{\cos(\pi h f_c)}{2f_c} \left(\cotan\left(\pi\left(\frac{1}{4f_c} + \frac{j}{2f_c} - h/2\right)\right) - \cotan\left(\pi\left(\frac{1}{4f_c} + \frac{j}{2f_c} + h/2\right)\right) \right). \quad (6.6)$$

hence it differs from m_0 . We have proved the above observation in [12] by solving the dual problem $(\mathcal{D}(0, y_0))$.

¹The domain is $X = \mathbb{T}$, but with a slight abuse of notation, we write $h/2$ instead of $h/2 \pmod{1}$.

Proposition 6.2 ([12]). *Let $y = \Phi m_0$ with $m_0 = \delta_{h/2} - \delta_{-h/2}$ and $0 < h \leq 1/(2f_c)$. Then,*

1. *The unique solution to $(\mathcal{D}(0, y_0))$ is $p = (0, \dots, 0, 1)$, corresponding to the function $\eta : t \mapsto \sin(2\pi f_c t)$.*
2. *The unique solution to $(\mathcal{P}(0, y_0))$ is given by (6.5) for $0 < h < 1/(2f_c)$, and m_0 for $h = 1/(2f_c)$.*

Our proof relies on typical T-systems arguments such as the counting of the roots of a trigonometric polynomial (see [12]).

As a consequence of Proposition 6.2, the number of Dirac masses predicted by the Representer Theorem (Theorem 1.1) is *almost optimal*: $2f_c$ masses actually appear for $2f_c + 1$ observations, see Section 1.4.3 for a discussion.

For $h > 1/(2f_c)$ it seems that the measure $m_0 = \delta_{h/2} - \delta_{-h/2}$ is always identifiable (as observed by computing numerically the vanishing derivative precertificate η_V), but we do not have any proof of that. On the other hand, the case of two spikes is not fully representative of the difficulty of reconstructing signed spikes, and it was proved in [DCD18] that the optimal separation distance in Theorem 3.1 should be at least $1/f_c - \gamma/f_c^2$, for $\gamma > 0$ arbitrarily small, provided f_c is large enough. To this end, they construct non identifiable measures with a number of spikes which increases with f_c .

6.2 Clustering spikes and the $(2s - 1)$ -vanishing derivatives precertificate

If the spikes have the same sign, things are radically different. The BLASSO does not require any separation condition, and we show in the rest of this chapter that in some cases, reconstruction guarantees can be provided.

We work in the one-dimensional setting $X = \mathbb{R}$ (or a subinterval which contains 0 in its interior, or $X = \mathbb{T}$). We consider s points which cluster around $x_0 = 0 \in \overset{\circ}{X}$. More precisely, let $x_1^*, \dots, x_s^* \in X$ be pairwise distinct points, and let $a_1^*, \dots, a_s^* > 0$ be some amplitudes. We define the measure $m_t^* \stackrel{\text{def.}}{=} \sum_{i=1}^s a_i^* \delta_{tx_i^*}$ and we consider the limit $t \rightarrow 0^+$.

We introduce the compact set

$$\mathcal{B} \stackrel{\text{def.}}{=} \{ (x_1, \dots, x_s) \in X^s \mid \forall i, |x_i - x_i^*| \leq \Delta/4 \} \quad \text{where} \quad \Delta \stackrel{\text{def.}}{=} \min_{i \neq j} |x_i^* - x_j^*|. \quad (6.7)$$

The constant Δ is the minimum separation distance between the x_i^* 's. In this setting it is fixed, but our main focus is on (tx_1^*, \dots, tx_s^*) , whose minimum separation distance is $t\Delta$. By $\mathcal{I} = (x_1, \dots, x_s)$, we denote any element of \mathcal{B} .

We assume that we observe $y_t \in \mathcal{H}$, some noisy version of $y_t^* \stackrel{\text{def.}}{=} \Phi m_t^*$, and we want to recover m_t^* using the BLASSO,

$$\min_{m \in \mathcal{M}(X)} |m|(X) + \frac{1}{2} \|\Phi m - y_t\|_{\mathcal{H}}. \quad (\mathcal{P}(\lambda, y_t))$$

Remark 6.1. *We only consider one cluster point ($x_0 = 0$) for the sake of simplicity, but as explained in Quentin Denoyelle's PhD thesis [Den18], the analysis extends to several clusters of spikes without major difficulty.*

6.2.1 An approximate factorization

The whole procedure for the study of $(\mathcal{P}(\lambda, y_t))$ as $t \rightarrow 0^+$ is a bit similar to finding the osculating plane of a curve (see [Kre91, Sec. 11]): it relies on a Taylor expansion and on suitable matrix operations. Therefore we need some regularity, a bit more than we did in [Assumptions 4.1](#).

Assumptions 6.1. *We require that [Assumptions 3.1](#) hold and that*

- $X \subseteq \mathbb{R}$, with $0 \in \mathring{X}$.
- $\varphi \in \mathcal{C}^{2s}(\mathring{X}; \mathcal{H})$. As a consequence, φ is weakly \mathcal{C}^{2s} in \mathring{X} .

Remark 6.2. *The second item of [Assumptions 6.1](#) typically holds in the case of a convolution, $\varphi(x) = \tilde{\varphi}(\cdot - x)$, where $\tilde{\varphi}$ is smooth with all its derivatives in $\mathcal{H} \stackrel{\text{def.}}{=} L^2(\mathbb{R})$, e.g. if $\tilde{\varphi}$ is the Gaussian filter.*

➤ Assume that $\tilde{\varphi} \in \mathcal{C}^1(\mathbb{R})$ and $\tilde{\varphi}, \tilde{\varphi}' \in L^2(\mathbb{R})$. Then for all $z, h \in \mathbb{R}$, with $h \neq 0$,

$$\frac{1}{h} [\tilde{\varphi}(z - (x + h)) - \tilde{\varphi}(z - x)] - \tilde{\varphi}'(z - x) = \int_0^1 (\tilde{\varphi}'(z - x - vh) - \tilde{\varphi}'(z - x)) dv. \quad (6.8)$$

Taking the square and integrating over $z \in \mathbb{R}$, we use the Jensen inequality to deduce

$$\left\| \frac{1}{h} [\tilde{\varphi}(\cdot - (x + h)) - \tilde{\varphi}(\cdot - x)] - \tilde{\varphi}'(\cdot - x) \right\|_{L^2(\mathbb{R})}^2 \leq \int_0^1 \|\tilde{\varphi}'(\cdot - x - vh) - \tilde{\varphi}'(\cdot - x)\|_{L^2(\mathbb{R})}^2 dv. \quad (6.9)$$

By the continuity of the translation in $L^2(\mathbb{R})$, the right-hand side vanishes as $h \rightarrow 0$. Hence $\varphi \in \mathcal{C}^1(\mathbb{R}; \mathcal{H})$ with $\varphi'(x) = \tilde{\varphi}'(\cdot - x)$. The general conclusion follows by induction.

Throughout this section, we suppose that [Assumptions 6.1](#) hold.

We consider the operator $\Psi: \mathbb{R}^{2s} \rightarrow \mathcal{H}$, defined by

$$\forall b \in \mathbb{R}^{2s}, \quad \Psi b \stackrel{\text{def.}}{=} \sum_{k=0}^{2s-1} b_k \varphi^{(k)}(0). \quad (6.10)$$

where $\varphi^{(k)}(0)$ is the k -th derivative of φ at 0. We also consider the operator (that we have already encountered in [Section 4.3](#)),

$$\forall c, d \in \mathbb{R}^s, \quad \Gamma_{t\mathcal{I}} \begin{pmatrix} c \\ d \end{pmatrix} \stackrel{\text{def.}}{=} \sum_{i=0}^s (c_i \varphi(tx_i) + d_i \varphi'(tx_i)). \quad (6.11)$$

The Taylor expansion of φ around 0 yields

$$\begin{aligned} \varphi(tx_i) &= \varphi(0) + \varphi'(0)(tx_i) + \cdots + \varphi^{2s-1}(0) \frac{(tx_i)^{2s-1}}{(2s-1)!} \\ &\quad + (tx_i)^{2s} \int_0^1 \frac{(1-v)^{2s-1}}{(2s-1)!} \varphi^{(2s)}(vtx_i) dv, \end{aligned}$$

and similarly

$$\begin{aligned} \varphi'(tx_i) &= \varphi'(0) + \varphi''(0)(tx_i) + \cdots + \varphi^{2s-1}(0) \frac{(tx_i)^{2s-2}}{(2s-2)!} \\ &\quad + (tx_i)^{2s-1} \int_0^1 \frac{(1-v)^{2s-2}}{(2s-2)!} \varphi^{(2s)}(vtx_i) dv. \end{aligned}$$

As a result, we obtain the following factorization,

Lemma 6.1 ([8, Lem.1, Prop. 7]). *The following factorization holds²*

$$\Gamma_{t\mathcal{I}} = \Psi_{t\mathcal{I}} H_{t\mathcal{I}}, \quad \text{where} \quad \Psi_{t\mathcal{I}} = \Psi + O(t), \quad (6.13)$$

$$\text{and } H_{t\mathcal{I}} \stackrel{\text{def.}}{=} \begin{pmatrix} 1 & \dots & 1 & 0 & \dots & 0 \\ tx_1 & \dots & tx_s & 1 & \dots & 1 \\ \vdots & & \vdots & \vdots & & \vdots \\ \frac{(tx_1)^{2s-1}}{(2s-1)!} & \dots & \frac{(tx_1)^{2s-1}}{(2s-1)!} & \frac{(tx_1)^{2s-2}}{(2s-2)!} & \dots & \frac{(tx_1)^{2s-2}}{(2s-2)!} \end{pmatrix}. \quad (6.14)$$

Lemma 6.1 is obtained by carefully controlling the remainder and exploiting the structure of $H_{t\mathcal{I}}$. The matrix $(H_{t\mathcal{I}})^*$ is the matrix of the evaluation of a polynomial of degree $2s - 1$ and its first derivative at the points tx_i , $1 \leq i \leq s$. As a result, it is invertible, and $(H_{t\mathcal{I}})^{*, -1}$ is the matrix of Hermite interpolation. The matrix $H_{t\mathcal{I}}$ has a useful factorization

$$H_{t\mathcal{I}} = \text{diag}(1, t, \dots, t^{2s-1}) H_{\mathcal{I}} \text{diag}\left(1, \dots, 1, \frac{1}{t}, \dots, \frac{1}{t}\right) \quad (6.15)$$

which is crucial for the control of all the quantities that are involved in the problem, as $t \rightarrow 0^+$.

6.2.2 The $(2s - 1)$ -vanishing dual precertificate

As we have discussed in Section 4.3.2, in favorable cases, the minimal-norm certificate η_0 (which governs the support recovery at low noise), is equal to the vanishing-derivatives precertificate η_V , a quantity which can be computed more easily, using a pseudo inverse. More precisely, the vanishing-derivatives precertificate for a measure $m = \sum_{x \in \mathcal{I}} b_x \delta_x$ is defined as $\eta_V \stackrel{\text{def.}}{=} \Phi^* p_V$, where $p_V \stackrel{\text{def.}}{=} \Gamma_{\mathcal{I}}^{*\dagger} (\text{sign}(b), 0_s)^\top$. It is equal to the minimal norm certificate η_0 if and only if $\text{sign}(b) \in \text{Im } \Gamma_{\mathcal{I}}^*$ and $\|\eta_V\|_\infty \leq 1$. In the case where $\Gamma_{\mathcal{I}}$ has full column rank, $\Gamma_{\mathcal{I}}^{*\dagger} = \Gamma_{\mathcal{I}} (\Gamma_{\mathcal{I}}^* \Gamma_{\mathcal{I}})^{-1}$.

The following proposition describes the limit of such precertificates for non-negative measures supported on $t\mathcal{I}$, $t \rightarrow 0^+$. We introduce³

$$p_{W, 2s-1} \stackrel{\text{def.}}{=} \Psi^{*\dagger} \begin{pmatrix} 1 \\ 0_{2s-1} \end{pmatrix} \quad (6.16)$$

$$= \text{argmin} \left\{ \|p\|_{\mathcal{H}} \mid (\Phi^* p)(0) = 1, (\Phi^* p)'(0) = 0, \dots, (\Phi^* p)^{(2s-1)}(0) = 0 \right\} \quad (6.17)$$

provided $(1, 0_{2s-1})^\top \in \text{Im } \Psi^*$. The function $\eta_{W, 2s-1} \stackrel{\text{def.}}{=} \Phi^* p_{W, 2s-1}$ is called the $(2s - 1)$ -vanishing-derivatives precertificate. It is a function of the form

$$\eta_{W, 2s-1} = \sum_{k=0}^{2s-1} \gamma_k (\partial_2)^k K(\cdot, 0) \quad \text{where} \quad \{\gamma_k\}_{0 \leq k \leq 2s-1} \subseteq \mathbb{R}, \quad (6.18)$$

and if $(1, 0_{2s-1})^\top \in \text{Im } \Psi^*$ it is characterized by

$$\eta_{W, 2s-1}(0) = 1, \quad \eta'_{W, 2s-1}(0) = \dots = \eta^{(2s-1)}_{W, 2s-1}(0) = 0. \quad (6.19)$$

Using Lemma 6.1, it is possible to prove the following result.

²The notation $f(\mathcal{I}, t) = O(t)$ used here is uniform, in the sense that

$$\limsup_{t \rightarrow 0^+} \left(\sup_{\mathcal{I} \in \mathcal{B}} \left| \frac{f(\mathcal{I}, t)}{t} \right| \right) < +\infty. \quad (6.12)$$

³By 0_{2s-1} , we denote the entry 0 repeated $2s - 1$ times (and similarly below, 1_s is used to denote the entry 1 repeated s times).

Proposition 6.3 ([8, Prop. 4]). *If Ψ has full column rank, then for $t > 0$ small enough, $\Gamma_{t\mathcal{I}}$ has full column rank for all $\mathcal{I} \in \mathcal{B}$, hence $p_{V,t\mathcal{I}} = \Gamma_{t\mathcal{I}}(\Gamma_{t\mathcal{I}}^* \Gamma_{t\mathcal{I}})^{-1}(1_s, 0_s)^\top$.*

Moreover, the following convergences hold uniformly for $\mathcal{I} \in \mathcal{B}$

$$\lim_{t \rightarrow 0^+} p_{V,t\mathcal{I}} = p_{W,2s-1} \quad \text{strongly in } \mathcal{H}, \quad (6.20)$$

$$\lim_{t \rightarrow 0^+} \eta_{V,t\mathcal{I}} = \eta_{W,2s-1} \quad \text{uniformly on } X, \quad (6.21)$$

$$\lim_{t \rightarrow 0^+} \eta_{V,t\mathcal{I}}^{(k)} = \eta_{W,2s-1}^{(k)} \quad \text{uniformly on compact subsets of } \overset{\circ}{X}, \quad 1 \leq k \leq 2s. \quad (6.22)$$

Figure 6.1 illustrates the convergence of $\eta_{V,t\mathcal{I}}$ as $t \rightarrow 0^+$, for $s = 2$. Figure 6.2 shows $\eta_{W,2s-1}$ for different values of s : the larger the value of s , the flatter the function in a neighborhood of 0.

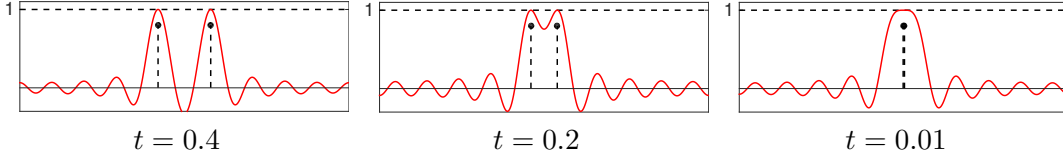


Figure 6.1: $\eta_{V,t\mathcal{I}}$ for several values of t , showing the convergence toward $\eta_{W,2s-1}$. The operator Φ is an ideal low-pass filter with a cutoff frequency $f_c = 10$.

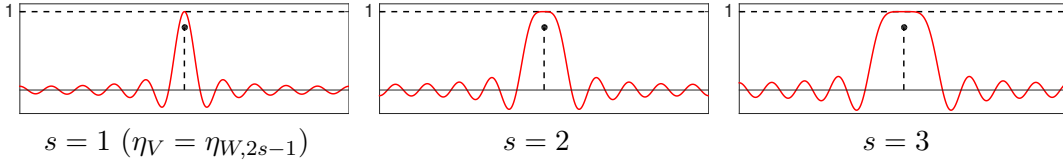


Figure 6.2: $\eta_{W,2s-1}$ for several values of s . The operator Φ is an ideal low-pass filter with cutoff frequency $f_c = 10$.

Just like the minimal-norm certificate governs the dual solutions at low noise, the $(2s-1)$ dual certificate $\eta_{W,2s-1}$ governs the behavior of $\eta_{V,t\mathcal{I}}$ for t small.

Definition 6.1 ($(2s-1)$ -non-degeneracy). *We say that $\eta_{W,2s-1}$ is $(2s-1)$ -non-degenerate if $\eta_{W,2s-1}^{(2s)}(0) < 0$ and $|\eta_{W,2s-1}(x)| < 1$ for all $x \in X \setminus \{0\}$.*

Proposition 6.4 (Consequence of [8, Thm. 1]). *Suppose that $\eta_{W,2s-1}$ is $(2s-1)$ -non-degenerate. Then, there exist $t_0 > 0$ such that for all $t \in]0, t_0[$, all $\mathcal{I} \in \mathcal{B}$, $\eta_{V,t\mathcal{I}}$ is non-degenerate, i.e.*

$$\forall x \in X \setminus \{tx_1, \dots, tx_s\}, \quad |\eta_{V,t\mathcal{I}}(x)| < 1, \quad (6.23)$$

$$\forall i \in \{1, \dots, s\}, \quad \eta''(tx_i) < 0. \quad (6.24)$$

In other words, the $(2s-1)$ -non-degeneracy of $\eta_{W,2s-1}$ ensures the Non-Degenerate Source Condition (NDSC) for all non-negative measures $m = \sum_{i=1}^s a_i \delta_{tx_i}$ provided $t > 0$ is small enough. Therefore we may apply Theorem 5.3 to deduce that there is a low noise regime in which the BLASSO recovers exactly the correct number of spikes, with amplitudes and locations which converge to the correct one as $(\lambda, y_t - y_t^*) \rightarrow (0, 0)$.

However, it does not tell us anything about the scaling of the low noise regime (e.g. the size of the neighborhoods in the implicit function theorem) or the amplification of errors as $t \rightarrow 0^+$: it might very well shrink (resp. blow up) very rapidly. For that reason, we state Theorem 6.1 below, which takes into account the scaling of every quantity

involved in the BLASSO and describes precisely the scaling of the low noise regime and the errors.

Before that, let us examine a few examples of computations of $\eta_{W,2s-1}$.

Fourier measurements. We consider the ideal low pass filter (3.12), which gathers the Fourier coefficients,

$$\varphi(x) = \left(1, \sqrt{2} \cos(2\pi x), \sqrt{2} \sin(2\pi x), \dots, \sqrt{2} \cos(2f_c \pi x), \sqrt{2} \sin(2f_c \pi x)\right). \quad (6.25)$$

The expression of the vanishing-derivatives precertificate for a f_c -sparse non-negative measure is given in (4.30). Substituting the locations with (tx_1, \dots, tx_{f_c}) and letting $t \rightarrow 0^+$ we recover the result of [PP17]:

$$\eta_{W,2s-1}(x) = 1 - \left(\frac{\int_{\mathbb{T}} \sin^{2f_c}(\pi u) du}{\int_{\mathbb{T}} \sin^{4f_c}(\pi(u)) du} \right) \sin^{2f_c}(x) = 1 - \frac{((2f_c)!)^2}{(4f_c)!} \sin^{2f_c}(x) \quad (6.26)$$

using the value of Wallis integrals. We see that $\eta_{W,2s-1}$ is $(2s-1)$ -non-degenerate.

Laplace transform. If $X =]0, +\infty[$, $\mathcal{H} = L^2([0, +\infty])$ and the impulse response is the Laplace transform,

$$\varphi(x) = (s \mapsto e^{-xs}) \quad (6.27)$$

we have seen in (4.41) the expression of η_V . Substituting (x_1, \dots, x_s) with $(x_0 + t(x_1 - x_0), \dots, x_0 + t(x_s - x_0))$ and letting $t \rightarrow 0^+$, we get

$$\eta_{W,2s-1}(x) = 1 - \left(\frac{x - x_0}{x + x_0} \right)^{2s}. \quad (6.28)$$

and we see that $\eta_{W,2s-1}$ is $(2s-1)$ -non-degenerate.

Gaussian convolution. Now, we consider, the case of the Gaussian filter, with $\mathcal{H} = L^2(\mathbb{R})$,

$$\varphi(x) = \frac{1}{\sqrt{2\pi}\sigma} e^{-\frac{(x-x')^2}{2\sigma^2}}, \quad \text{so that } K(x, x') = \frac{1}{\sqrt{4\pi}\sigma} e^{-\frac{(x-x')^2}{4\sigma^2}}. \quad (6.29)$$

In the following we set $\sigma = 1$ for simplicity. For spikes which cluster at $x_0 = 0$, it is clear from (6.18) that $\eta_{W,2s-1}$ is of the form $\eta_{W,2s-1}(x) = P(x)e^{-\frac{x^2}{4}}$, where P is a polynomial of degree at most $2s-1$, i.e. $P \in \mathbb{R}_{2s-1}[X]$. Next, we may use the following lemma from Quentin Denoyelle’s PhD thesis, which relies on the general Leibniz formula.

Lemma 6.2 ([Den18, Lem. 6]). *Let $g: X \rightarrow \mathbb{R}$, $\eta: X \rightarrow \mathbb{R}$ be two smooth functions. If η satisfies*

$$\eta(x_0) = 1, \quad \eta'(x_0) = \dots = \eta^{(2s-1)}(x_0) = 0, \quad (6.30)$$

then $P = \eta \times g$ satisfies

$$P(x_0) = g(x_0), \quad P'(x_0) = g'(x_0), \dots, P^{(2s-1)}(x_0) = g^{(2s-1)}(x_0). \quad (6.31)$$

In particular, if $P \in \mathbb{R}_{2s-1}[X]$, then P is the Taylor expansion of g at x_0 of order $2s-1$, and $\eta^{(2s)}(x_0) = -g^{(2s)}(x_0)/g(x_0)$ provided $g(x_0) \neq 0$.

We deduce that P is the Taylor expansion of $\left(x \mapsto e^{\frac{x^2}{4}}\right)$, so that

$$\eta_{W,2s-1}(x) = e^{-\frac{x^2}{4}} \sum_{k=0}^{s-1} \frac{x^{2k}}{2^{2k} k!}. \quad (6.32)$$

That precertificate is $(2s-1)$ -non-degenerate.

More generally, given an observation operator Φ , computing the $(2s-1)$ -vanishing-derivatives precertificate is an entertaining mathematical puzzle, but we are only aware of a few cases where it is possible. Those few cases can be translated to different acquisition settings by a change of variable (as in [Proposition 4.4](#) for η_V).

Proposition 6.5 ([\[Den18\]](#)). *Let $X, \tilde{X} \subseteq \mathbb{R}$ be two open intervals, and $h: \tilde{X} \rightarrow X$ be a smooth diffeomorphism. Let $x_0 \in X$, $\tilde{x}_0 = h^{-1}(x_0)$, and let $\eta: X \rightarrow \mathbb{R}$ be a smooth function. Then η satisfies*

$$\eta(x_0) = 1, \quad \eta'(x_0) = \dots = \eta^{(2s-1)}(x_0) = 0, \quad (6.33)$$

if and only if $\nu \stackrel{\text{def.}}{=} \eta \circ h$ satisfies

$$\nu(x_0) = 1, \quad \nu'(x_0) = \dots = \nu^{(2s-1)}(x_0) = 0. \quad (6.34)$$

Moreover, $\nu^{(2s)}(\tilde{x}_0) = \eta^{(2s)}(x_0)(h'(\tilde{x}_0))^{2s}$.

See for instance the case the L^2 -normalized Laplace transform in Quentin Denoyelle's PhD thesis [\[Den18, Prop. 14\]](#). However, for more involved acquisition frameworks, especially when the transform is sampled, it is more difficult. See [Section 6.3](#) for a way to prove the non-degeneracy a priori in some cases.

6.2.3 Support recovery for clustered spikes

The main result of this section is the following theorem, which guarantees exact support recovery for clustered spikes with positive sign.

Theorem 6.1 ([\[8, Thm. 2\]](#)). *Suppose that Ψ has full column rank and that $\eta_{W,2s-1}$ is $(2s-1)$ -non-degenerate. Assume moreover that $\varphi \in \mathcal{C}^{2s+1}(\overset{\circ}{X}; \mathcal{H})$.*

Then, there exist positive constants $t_0, \alpha_0, \lambda_0, C > 0$ (which only depend on $\varphi, (a_i^)_{1 \leq i \leq s}$ and $(x_i^*)_{1 \leq i \leq s}$), such that for $0 < t < t_0$, $\|y_t - y_t^*\|_{\mathcal{H}} \leq \alpha_0 \lambda$, $0 < \lambda \leq \lambda_0 t^{2s-1}$,*

- *The solution to $(\mathcal{P}(\lambda, y_t))$ is unique,*
- *That solution has exactly s spikes, $m_t = \sum_{i=1}^s a_i \delta_{x_i}$, where (a, x) coincides with a \mathcal{C}^{2s} function of $(\lambda, y_t - y_t^*)$ in a neighborhood of $(0, 0) \in \mathbb{R} \times \mathcal{H}$.*
- *The following inequality holds,*

$$\max_{1 \leq i \leq s} |(a_i, x_i) - (a_i^*, x_i^*)| \leq C \left(\frac{\lambda + \|y_t - y_t^*\|_{\mathcal{H}}}{t^{2s-1}} \right). \quad (6.35)$$

As a result, under the $(2s-1)$ -non-degeneracy assumption, the BLASSO successfully estimates the unknown measure, and the amplification of errors is of order t^{2s-1} , where t represents the minimum separation distance between the spikes.

6.3 Extended totally positive kernels

In the previous section, we have seen that the BLASSO is able to resolve clustered spikes, provided the $(2s - 1)$ -vanishing derivatives dual precertificate $\eta_{W,2s-1}$ is $(2s - 1)$ -non-degenerate. That can be checked on specific cases if one knows a closed form expression for $\eta_{W,2s-1}$, or observed numerically.

In this section we provide a sufficient criterion, to ensure a priori the non-degeneracy of using ideas of the theory of T-systems (also known as Tchebycheff systems) and totally positive kernels (see [KS66, Kar68, KN77] for reference on these topics). The properties of T-systems were used in [dCG12, SRR18] to ensure identifiability of non-negative sparse measures using the BASIS PURSUIT FOR MEASURES, but the specificity of our approach is that we work with the autocorrelation kernel and we handle its derivatives, so as to ensure the non-degeneracy (or $(2s - 1)$ -non-degeneracy) of vanishing-derivatives dual precertificates.

6.3.1 A characterization of the Non-degenerate Source Condition (NDSC)

We discuss here a determinantal formulation of the non-degeneracy of dual certificates. We assume that $X \subseteq \mathbb{R}$ is an interval.

The vanishing derivatives precertificate. For now, we consider a measure $m_0 = \sum_{i=1}^s a_i \delta_{x_i}$ with pairwise distinct locations x_i and amplitudes a_i of arbitrary sign $s_{\mathcal{I}} \stackrel{\text{def.}}{=} (\text{sign}(a_i))_{1 \leq i \leq s}$. Recalling the expression of the corresponding vanishing-derivatives precertificate (4.24)

$$\forall x \in X, \quad \eta_V(x) = \sum_{i=1}^s (\alpha_i K(x, x_i) + \beta_i \partial_2 K(x, x_i)), \quad (6.36)$$

we define

$$(v_1, v_2, \dots, v_{2s-1}, v_{2s}) \stackrel{\text{def.}}{=} (K(\cdot, x_1), \partial_2 K(\cdot, x_1), \dots, K(\cdot, x_s), \partial_2 K(\cdot, x_s)), \quad (6.37)$$

$$\text{so that } \eta_V = \sum_{n=1}^{2s} \gamma_n v_n, \text{ with } \gamma_n \in \mathbb{R}, 1 \leq n \leq 2s. \quad (6.38)$$

If $(s_{\mathcal{I}} \ 0)^\top \in \text{Im } \Gamma_{\mathcal{I}}^*$, by construction η_V is the only such function satisfying $\eta_V(x_i) = \text{sign}(a_i)$ and $\eta'_V(x_i) = 0$ for all $i \in \{1, \dots, s\}$ (see Lemma 4.3). Let $I^+ = \{i \in \{1, \dots, s\} \mid a_i > 0\}$. We introduce the determinant

$$\forall x \in X \setminus \{x_i\}_{i \in I^+}, \quad D_V^+(x) \stackrel{\text{def.}}{=} \frac{2}{\prod_{i \in I^+} (x - x_i)^2} \begin{vmatrix} 1 & v_1(x) & \cdots & v_{2s}(x) \\ \text{sign}(a_1) & v_1(x_1) & \cdots & v_{2s}(x_1) \\ 0 & v'_1(x_1) & \cdots & v'_{2s}(x_1) \\ \vdots & \vdots & & \vdots \\ \text{sign}(a_s) & v_1(x_s) & \cdots & v_{2s}(x_s) \\ 0 & v'_1(x_s) & \cdots & v'_{2s}(x_s) \end{vmatrix}, \quad (6.39)$$

Subtracting the $n + 1$ -th column with weight γ_n , for all n , to the first one, we see that

$$D_V^+(x) = \left(\frac{2}{\prod_{i \in I^+} (x - x_i)^2} \right) (1 - \eta_V(x)) \det(\Gamma_{\mathcal{I}}^* \Gamma_{\mathcal{I}}), \quad (6.40)$$

$$\text{with } \det(\Gamma_{\mathcal{I}}^* \Gamma_{\mathcal{I}}) = \begin{vmatrix} v_1(x_1) & \cdots & v_{2s}(x_1) \\ v'_1(x_1) & \cdots & v'_{2s}(x_1) \\ \vdots & & \vdots \\ v_1(x_s) & \cdots & v_{2s}(x_s) \\ v'_1(x_s) & \cdots & v'_{2s}(x_s) \end{vmatrix}. \quad (6.41)$$

As a result, D_V^+ can be extended by continuity to X , with

$$\forall j \in I^+, \quad D_V^+(x_j) = \left(\frac{-2}{\prod_{i \in I^+ \setminus \{j\}} (x_j - x_i)^2} \right) \eta_V''(x_j) \det(\Gamma_{\mathcal{I}}^* \Gamma_{\mathcal{I}}). \quad (6.42)$$

Similarly, introducing $I^- = \{i \in \{1, \dots, s\} \mid a_i < 0\}$, and

$$\forall x \in X \setminus \{x_i\}_{i \in I^-}, \quad D_V^-(x) \stackrel{\text{def.}}{=} \frac{2}{\prod_{i \in I^-} (x - x_i)^2} \begin{vmatrix} -1 & v_1(x) & \cdots & v_{2s}(x) \\ \text{sign}(a_1) & v_1(x_1) & \cdots & v_{2s}(x_1) \\ 0 & v'_1(x_1) & \cdots & v'_{2s}(x_1) \\ \vdots & \vdots & & \vdots \\ \text{sign}(a_s) & v_1(x_s) & \cdots & v_{2s}(x_s) \\ 0 & v'_1(x_s) & \cdots & v'_{2s}(x_s) \end{vmatrix} \quad (6.43)$$

$$\text{we have } D_V^-(x) = \left(\frac{2}{\prod_{i \in I^-} (x - x_i)^2} \right) (-1 - \eta_V(x)) \det(\Gamma_{\mathcal{I}}^* \Gamma_{\mathcal{I}}). \quad (6.44)$$

As a result, D_V^+ and D_V^- contain all the information relevant for the Non-Degenerate Source Condition (see [Proposition 4.3](#) and [Definition 4.2](#)).

Proposition 6.6 ([11, Thm. 3.2 and Sec. 3.4]). *If $\Gamma_{\mathcal{I}}$ has full rank (i.e. $\det(\Gamma_{\mathcal{I}}^* \Gamma_{\mathcal{I}}) > 0$), then*

- $(s_{\mathcal{I}} \ 0)^\top \in \text{Im } \Gamma_{\mathcal{I}}^*$, so that η_V solves the interpolation problem $\eta_V(x_i) = \text{sign}(a_i)$, $\eta_V'(x_i) = 0$,
- the Non-Degenerate Source Condition holds for the measure $m_0 = \sum_{i=1}^s a_i \delta_{x_i}$ if and only if

$$\forall x \in X, \quad D_V^+(x) > 0 \quad \text{and} \quad D_V^-(x) < 0. \quad (6.45)$$

The $(2s - 1)$ -vanishing-derivatives precertificate. It is possible to do the same with the $(2s - 1)$ -vanishing derivatives precertificate defined in [Section 6.2.2](#). In view of the Laplace model below, we assume that the spikes cluster at some point x_0 instead of 0 as before. Introduce

$$(w_1, w_2, \dots, w_{2s-1}, w_{2s}) \stackrel{\text{def.}}{=} (K(\cdot, x_0), \partial_2 K(\cdot, x_0), \dots, K(\cdot, x_0), \partial_2 K(\cdot, x_0)), \quad (6.46)$$

$$\text{so that } \eta_{W, 2s-1} = \sum_{n=1}^{2s} \rho_n w_n, \quad \rho_n \in \mathbb{R}, \quad (6.47)$$

$$\text{with } \eta_{W, 2s-1}(x_0) = 1, \quad \eta'_{W, 2s-1}(x_0) = \dots = \eta_{W, 2s-1}^{(2s-1)}(x_0) = 0. \quad (6.48)$$

Then, setting

$$\forall x \in X \setminus \{x_0\}, \quad D_W^\pm(x) \stackrel{\text{def.}}{=} \frac{(2s)!}{(x - x_0)^{2s}} \begin{vmatrix} \pm 1 & w_1(x) & \cdots & w_{2s}(x) \\ 1 & w_1(x_1) & \cdots & w_{2s}(x_1) \\ 0 & w'_1(x_1) & \cdots & w'_{2s}(x_1) \\ \vdots & \vdots & & \vdots \\ 0 & w_1^{(2s-1)}(x_s) & \cdots & w_{2s}^{(2s-1)}(x_s) \end{vmatrix}. \quad (6.49)$$

$$\text{we have } D_W^\pm(x) = \frac{(2s)!}{(x - x_0)^{2s}} (\pm 1 - \eta_{W,2s-1}(x)) \det(\Psi^* \Psi), \quad (6.50)$$

$$\text{with } D_W^\pm(x_0) = \mp \eta_{W,2s-1}^{(2s)}(x_0) \det(\Psi^* \Psi). \quad (6.51)$$

We deduce similarly:

Proposition 6.7 ([11, Thm. 3.2, extended]). *If Ψ has full rank (i.e. $\det(\Psi^* \Psi) > 0$), then*

- $(1, 0_{2s-1})^\top \in \text{Im } \Psi^*$, so that $\eta_{W,2s-1}$ solves the interpolation problem $\eta_{W,2s-1}(x_0) = 1$, $\eta_{W,2s-1}^{(k)}(x_0) = 0$ for $1 \leq k \leq 2s-1$,
- the precertificate $\eta_{W,2s-1}$ is $(2s-1)$ -non-degenerate if and only if

$$\forall x \in X, \quad D_W^+(x) > 0 \quad \text{and} \quad D_W^-(x) < 0. \quad (6.52)$$

6.3.2 Extended-totally positive kernels and non-degeneracy

The main point of proposing determinantal formulations of non-degeneracy is that they are strongly connected to the theory of extended T-systems and extended totally positive kernels. A family of functions (u_0, \dots, u_n) is an extended T-system if any non-trivial combination of the u_i 's has at most n roots, counting multiplicities. The canonical example is the family of monomials $(1, X, \dots, X^n)$. Extended totally positive (ETP) kernels $\psi(x, s)$ have a similar property, but the index n is replaced with a continuous variable s . We refer to [KS66, Kar68] for more detail on these topics. The key is that it is possible to encode the T-system property using determinants similar to D_V^\pm and D_W^\pm .

In this section we focus on non-negative measures only, so that we may even add a non-negativity constraint to the BLASSO,

$$\min_{m \in \mathcal{M}^+(X)} m(X) + \frac{1}{2} \|\Phi m - y\|_{\mathcal{H}}^2, \quad (\mathcal{P}^+(\lambda, y))$$

which changes the constraint $\|\eta\|_\infty \leq 1$, in the dual problem, to $\eta \leq 1$, where $\eta = \Phi^* p$. For that problem, the non-degeneracy of η_V is equivalent to $1 - \eta_V$ being nonnegative and having exactly $2s$ roots, counting multiplicities, which is equivalent to $D_V^+ > 0$.

Letting $v_0 = 1$, we see that if (v_0, \dots, v_{2s-1}) is an extended T-system⁴, then $D_V^+ > 0$, and the Non-Degenerate Source Condition holds⁵.

Examples of extended T-systems include

- the monomials $(1, x, \dots, x^n)$ on \mathbb{R} .
- the functions $(x^{\alpha_0}, \dots, x^{\alpha_n})$ with $\alpha_0 < \dots < \alpha_n$, on $]0, +\infty[$.

⁴More precisely, if we only count roots, D_V does not vanish. But the definition in [KS66] also assumes positivity, so that the examples given below satisfy $D_V > 0$.

⁵Provided that $\det(\Gamma_{\mathcal{I}}^* \Gamma_{\mathcal{I}}) > 0$, which can be ensured by assuming that (v_1, \dots, v_{2s-1}) is a T-system too.

- the Cauchy system $\left(\frac{1}{\alpha_k + x}\right)_{0 \leq k \leq n}$ for $\alpha_0 < \dots < \alpha_n$, on $]0, +\infty[$,
- the Gauss system $\left(e^{-(x-\alpha_k)^2}\right)_{0 \leq k \leq n}$ for $\alpha_0 < \dots < \alpha_n$, on \mathbb{R} ,

and there is a composition formula [KS66, Sec. 3, ex. 8], which relies on an integral version of the Cauchy-Binet formula, and which allows us to build new T-systems from a T-system and an ETP kernel. We omit the detail, but this integral formulation of the Cauchy-Binet is the key ingredient that we have used in [11] (see also [SRR18]) so as to derive the non-degeneracy results described below.

From now on, we consider an impulse response of the form

$$\varphi(x): z \mapsto \psi(x, z) \quad (6.53)$$

for some kernel $\psi: X \times Z \rightarrow \mathbb{R}$, where $Z \subseteq \mathbb{R}$ is an interval. We endow Z with a (non-negative) measure P_Z , and we choose \mathcal{H} as $L^2(Z, P)$. The typical cases that we consider are

- the Gaussian kernel $\psi(x, z) = e^{-(x-z)^2}$. For $P_Z = \mathcal{L}$ (the Lebesgue measure on \mathbb{R}),

$$\Phi m = \int_X e^{-(x-\cdot)^2} dm(x) \quad (6.54)$$

is the convolution with a Gaussian kernel, observed on \mathbb{R} , with $\mathcal{H} = L^2(\mathbb{R})$.

- the Gaussian kernel with $P_Z = \sum_{k=1}^M c_k \delta_{z_k}$. In other words, we observe the convolution of m with a Gaussian kernel, sampled on a finite set $\{z_k\}_{1 \leq k \leq M}$,

$$\Phi m = \left(\int_X e^{-(x-z_k)^2} dm(x) \right)_{1 \leq k \leq M} \quad (6.55)$$

The norm on \mathcal{H} is determined by $\|p\|_{\mathcal{H}}^2 = \sum_{k=1}^s c_k |p_k|^2$.

- the Laplace kernel $\psi(x, z) = e^{-xz}$, where $X = [d, +\infty[$ $d > 0$, $Z =]0, +\infty[$.

$$\Phi m = \int_0^{+\infty} e^{-x \cdot} dm(x). \quad (6.56)$$

and P_Z is the Lebesgue measure on $]0, +\infty[$.

- the Laplace kernel with $P_Z = \sum_{k=1}^M c_k \delta_{z_k}$, and $\{z_k\}_{1 \leq k \leq M} \subseteq]0, +\infty[$, that is,

$$\Phi m = \left(\int_0^{+\infty} e^{-xz_k} dm(x) \right)_{1 \leq k \leq M}. \quad (6.57)$$

Without sampling, both the Gaussian filter and the Laplace transform are injective, so we already have identifiability of the unknown original measure in a noiseless setting. Still it is interesting to consider those cases for the study of their stability to noise. A discrete measure P_Z may model the sampling of such transforms, since in real applications we only have access to a finite number of measurements. It also encodes the weights of the L^2 -norm in \mathcal{H} , which reflects how we trust each sensor z (depending on the physical setup or the noise model).

Being ubiquitous in signal and image processing, the Gaussian filter (sampled or not) is a particularly important example. The Laplace transform appears in the Multi-Angle Total Internal Reflection Fluorescence (MA-TIRF) microscopy problem that we study in Section 7.2.3. Therefore, we focus on these two modalities.

Proposition 6.8 (Laplace measurements [11, Cor. 4.1]). *Let $s \in \mathbb{N}^*$, $X = [d, +\infty)$ with $d \geq 0$, $Z \subseteq (0, +\infty)$ and P_Z be a positive measure such that $\int_Z (1 + |z|)^{4s} e^{-2cz} dP_Z(z) < +\infty$.*

If $\psi(x, z) = e^{-xz}$ and $\text{card}(\text{supp}(P_Z)) \geq 2s$, the following holds.

- *If $m_0 = \sum_{i=1}^s a_i \delta_{x_i}$, with $\{x_i\}_{i=1}^s \subseteq \overset{\circ}{X}$ pairwise distinct and $a_i > 0$ for all i , then m_0 satisfies the non-degenerate source condition.*
- *If $x_0 \in \overset{\circ}{X}$, then the precertificate $\eta_{W, 2s-1}$ for the point x_0 is $(2s-1)$ -non-degenerate.*

The first conclusion of Proposition 6.8 ensures that any positive measure m_0 having s spikes can be recovered exactly *regardless of the minimum distance*, with support stability, provided we have at least $2s$ measurements. The second conclusion ensures that, if the spikes cluster around x_0 , Theorem 6.1 may be applied, providing the stability regions of order t^{2s-1} where t is proportional to the minimum distance between the spikes. In fact, a more general result holds ([11, Prop. 3.3]), but we prefer to focus on the case of Laplace observations, which is the only concrete application that we know.

The case of the Gaussian filter is not as simple. We first state the result without sampling, which ensures the support stability of the reconstruction.

Proposition 6.9 (Fully sampled Gaussian convolution [11, Prop. 4.2]). *Let P_Z be the Lebesgue measure on $X = \mathbb{R}$, and $\psi(x, z) \stackrel{\text{def.}}{=} e^{-(x-z)^2}$. Then*

- *If $m_0 = \sum_{i=1}^s a_i \delta_{x_i}$, with $\{x_i\}_{i=1}^s \subseteq \mathbb{R}$ pairwise distinct and $a_i > 0$ for all i , then m_0 satisfies the Non-Degenerate Source Condition.*
- *If $x_0 \in \mathbb{R}$, then the precertificate $\eta_{W, 2s-1}$ for the point x_0 is $(2s-1)$ -non-degenerate.*

The proof relies on [SRR18, Lem. 2.7] which provides a T-system property for a specific family of functions involving the Gaussian kernel and its derivative.

The result extends to sequences of measures $(P_{Z,n})_{n \in \mathbb{N}}$ which approximate the Lebesgue measure in the following sense:

$$\lim_{n \rightarrow +\infty} \max_{0 \leq k, \ell \leq 2s} \sup_{x \in X} \left| \int_{\mathbb{R}} x^k z^\ell e^{-(x-z)^2 - (x_i-z)^2} dP_{Z,n}(z) - \int_{\mathbb{R}} x^k z^\ell e^{-(x-z)^2 - (x_i-z)^2} dz \right| = 0. \quad (6.58)$$

Proposition 6.10 (Sufficiently dense sampling [11, Prop. 4.4]). *Let $X \subseteq \mathbb{R}$, $\psi(x, z) = e^{-(x-z)^2}$, and let $(P_{Z,n})_{n \in \mathbb{N}}$ be a sequence of positive measures with finite total mass such that (6.58) holds.*

Then,

- *If $m_0 = \sum_{i=1}^s a_i \delta_{x_i}$, with $\{x_i\}_{i=1}^s \subseteq \overset{\circ}{X}$ pairwise distinct and $a_i > 0$ for all i , then m_0 satisfies the non-degenerate source condition for n large enough.*
- *If $x_0 \in \overset{\circ}{X}$, then the precertificate $\eta_{W, 2s-1}$ for the point x_0 is $(2s-1)$ -non-degenerate for n large enough.*

Several extensions are discussed in [11], notably the L^1 renormalization of the Laplace or Gaussian kernels, and sampling sets which are contained in a small interval.

6.4 Conclusion and comments

6.4.1 Summary

There is a fundamental limitation to the BLASSO, which is its inability to resolve Dirac masses with opposite signs when their locations are too close to one another. Below that separation distance the solution can be very different from the unknown, as illustrated in [Proposition 6.2](#) in the case of Fourier measurements.

However, if the spikes have the same sign, provided a non-degeneracy assumption holds, the BLASSO is able to recover them, with an “exact support recovery”, at least when the noise and the regularization parameter scale as t^{2s-1} , where t is the minimal distance between the spikes. That non-degeneracy assumption can be checked numerically (but one may face numerical errors), or may be checked analytically provided one has access to the $(2s - 1)$ -vanishing derivatives precertificate. That is typically possible for several classical forward operators such as the Gaussian convolution or the Laplace transform, but it is difficult to check in general, especially if a sampling operation is involved.

Alternatively, relying on the properties of extend T-systems, it is possible to ensure the non-degeneracy a priori, for arbitrary sampling patterns (with at least twice as many measurements as the number of spikes), when working operators such as the Gaussian convolution or the Laplace transform.

6.4.2 Comments

Minimal separation distance. The necessity of a minimal separation, at least in the case of Fourier measurements, has been observed since [\[CFG14\]](#), which takes it as a fundamental assumption for an identifiability theorem. Relying on such hypotheses, several authors have proposed identifiability results, see [\[TBSR13, BDF16, PKP20\]](#)

Higher dimension. Dealing with clustering spikes in dimension $d \geq 2$ is considerably more difficult than in dimension $d = 1$. That problem was investigated by G. Peyré and C. Poon in [\[PP17\]](#). One reason of that difficulty is that Hermite interpolation (used for the construction of η_V and then $\eta_{W,2s-1}$) is not as straightforward as in dimension $d = 1$ (e.g. when relating the minimal degree with the number of points involved, see for instance [\[dBR90\]](#)). Moreover, the limit of the dual certificates η_V when the spikes cluster depends on the geometric configuration of the x_i 's. If they are aligned, the interpolation problem solved by $\eta_{W,2s-1}$ will differ from if the points are not aligned. See [\[PP17\]](#) for more detail.

Normalizing the kernels. In [\[SRR18\]](#) (which was the inspiration for [\[11\]](#)), an exact reconstruction property for the sampled Gaussian convolution operator was provided: there is exact reconstruction, regardless of the separation of the spikes, provided $\text{card}(\text{supp}(P_Z)) \geq 2s + 1$. It differs from our result [Proposition 6.10](#) which requires the measure to approximate the Lebesgue measure.

There is a subtle difference between the considered settings. In [\[SRR18\]](#), they use a *weighted total variation* (with a weight which depends on the location of the spike). That is equivalent to using the standard total variation but renormalizing the atoms in the L^1 sense, i.e. taking

$$\psi(x, z) = \frac{e^{-(x-z)^2}}{\int_Z e^{-(x-z)^2} dP_Z(z)}. \quad (6.59)$$

In that case, minimizing the total mass is useless, since Φm already contains the information on $m(X)$,

$$\int_Z (\Phi m)(z) dP_Z(z) = \int_Z \int_X \psi(x, z) dm(x) dP_Z(z) = \int_X 1 dm, \quad (6.60)$$

so that all the admissible measures m have the same mass. So, in favorable cases, there is an alternative:

- either use a variational approach as discussed in this chapter, with an unnormalized kernel $\psi(x, z) = e^{-(x-z)^2}$, in which case one needs $2s$ measurements,
- or use normalized atoms as in (6.59), in which case the problem is more a feasibility problem (at least in the noiseless formulation), and one needs one more measurement, that is $2s + 1$ measurements.

See [11] for a more detailed discussion.

Chapter 7

Exploiting the structure of the solutions

Contents

7.1	The Frank-Wolfe algorithm	140
7.1.1	Description of the algorithm	140
7.1.2	Convergence results	141
7.1.3	Discussion	142
7.2	The Sliding Frank-Wolfe in the space of measures	142
7.2.1	Description of the algorithm	143
7.2.2	Illustration of the finite-time convergence	146
7.2.3	Application to fluorescence microscopy	147
7.3	The Fourier-Frank-Wolfe algorithm in the space of Moment matrices	154
7.3.1	Spectral approximation	154
7.3.2	Atomic norm reformulation	155
7.3.3	The Fourier-Frank-Wolfe Algorithm	158
7.3.4	Extracting the support from the moment matrices	160
7.3.5	Numerical examples	161
7.4	Conclusion	162
7.4.1	Summary	162
7.4.2	Comments	164

So far, we have studied the structure of the solutions to variational problems and its stability. It is now time to exploit to take advantage of that structure in numerical methods.

The Frank-Wolfe algorithm [FW56], also called the Conditional Gradient Method (CGM) [LP66], plays a key role in this chapter. Initially introduced for quadratic programming, it has recently gained a lot of popularity in inverse problems and machine learning (see the reviews [Jag13, BRZ21]). Its main advantage with respect to most first order optimization scheme (such as gradient descent or proximal splitting descent) is that it does not rely on any underlying Hilbertian structure, and only makes use of directional derivatives. It is thus particularly adapted to optimize, *e.g.* over the space of Radon measures, as was proposed in [BP13] (see also [BSR17]).

Collaboration. This chapter follows from [9, 5] and the PhD theses of Quentin Denoyelle and Paul Catala, co-supervised with Gabriel Peyré.

7.1 The Frank-Wolfe algorithm

We begin with the setting of [Chapter 3](#), that is, we consider V and Υ , two linear spaces endowed with a duality pairing which is separating. Unless otherwise stated, we fix some compatible topologies (see [Appendix B.1.1](#)), for instance the weak topologies $\sigma(V, \Upsilon)$ and $\sigma(\Upsilon, V)$. Let $F: V \rightarrow \mathbb{R}$ be a convex, proper, lower semi-continuous function. Our goal is to solve

$$\min_{u \in C} F(u), \quad (7.1)$$

where $C \subseteq V$ is nonempty convex.

Assumptions 7.1. *The key assumptions that we make in the current section are the following:*

1. C is compact or sequentially compact, i.e. every sequence in C has a convergent subsequence.
2. F is Gateaux-differentiable at every $x \in C$, i.e. for all $x \in C$, $d \in V$,

$$\lim_{\substack{t \rightarrow 0 \\ t \neq 0}} \frac{F(u + td) - F(u)}{t} \quad (7.2)$$

exists, depends linearly on d , and can be represented by some (necessarily unique) element in Υ that we denote by $F'(u)$.

7.1.1 Description of the algorithm

The Frank-Wolfe (FW) algorithm consists in minimizing a linearization of F at each step. This results in [Algorithm 1](#). Note that under the above compactness assumption, a solution to (7.1) exists; moreover, for every $u \in C$, the functional $s \mapsto \langle F'(u), s \rangle$ has a minimizer on C , hence [Line 3](#) is well defined.

Algorithm 1 Frank-Wolfe Algorithm

```

1: Initialize  $u^{[0]} \leftarrow 0$ .
2: for  $k = 0, 1, \dots$  do
3:   Minimize:  $s^{[k]} \ni \operatorname{argmin}_{s \in C} F(u^{[k]}) + \langle F'(u^{[k]}), (s - u^{[k]}) \rangle$ .
4:   if  $\langle F'(u^{[k]}), (s^{[k]} - u^{[k]}) \rangle = 0$  then
5:      $u^{[k]}$  is a solution of (7.1). Stop.
6:   else
7:     Update:  $u^{[k+1]} \in \operatorname{argmin}_{u \in [u^{[k]}, s^{[k]}]} F(u)$ .
8:   end if
9: end for
```

The stopping criterion. The criterion in [Line 4](#) (see for instance [\[DR70, Ch. 3, Sec.1.2\]](#)) is satisfied if and only if

$$\forall s \in C, \quad \left\langle F'(u^{[k]}), s - u^{[k]} \right\rangle \geq 0. \quad (7.3)$$

That is equivalent to $-F'(u^{[k]})$ being in the normal cone to C at $u^{[k]}$ (see [Appendix B.2](#)), which is a well-known characterization of optimality in convex constrained problems (see [\[ET76, Prop. II.2.1\]](#)). It is equivalent to $u^{[k]}$ being a solution.

Update rules. We have only represented an exact line search on Line 7 of Algorithm 1. Several update rules which are typical with the Frank-Wolfe algorithm are given below.

$$u^{[k+1]} \in \operatorname{argmin}_{u \in [u^{[k]}, s^{[k]}]} F(u) \quad (\text{exact line search}) \quad (7.4)$$

$$u^{[k+1]} \leftarrow (1 - \gamma^{[k]})u^{[k]} + \gamma^{[k]}s^{[k]} \quad \text{where } \gamma^{[k]} \stackrel{\text{def.}}{=} \frac{2}{k+2} \quad (\text{open loop rule}) \quad (7.5)$$

$$u^{[k+1]} \in \operatorname{argmin}_{u \in \operatorname{conv}\{s^{[0]}, \dots, s^{[k]}\}} F(u) \quad (\text{fully corrective variant}) \quad (7.6)$$

$$u^{[k+1]} \in \left\{ u \in C \mid F(u) \leq \min_{[u^{[k]}, s^{[k]}]} F \right\} \quad (\text{better than line-search}) \quad (7.7)$$

The last update rule is quite flexible: any choice of point in C is possible provided it is better than the exact line search. As we see in Proposition 7.1, it benefits from the same convergence guarantees as (7.4) or (7.5). It is a key to the non-convex refinements that we discuss in Section 7.2 and Section 7.3.

7.1.2 Convergence results

Several convergence results are known, depending on the assumptions on F or on C . In the infinite-dimensional setting, most results [DR70, DH78] are stated in Banach spaces, often with a Lipschitz assumption on F' . However, as highlighted in [Jag13], the common Lipschitz assumption on F' can be bypassed with an assumption on the *curvature*,

$$\kappa_F \stackrel{\text{def.}}{=} \sup \left\{ \frac{2}{\gamma^2} (F(u + \gamma(s - u)) - F(u) - \langle F'(u), \gamma(s - u) \rangle) \mid 0 < \gamma < 1, u, s \in C \right\}. \quad (7.8)$$

As a result, the convergence in energy results hold in our general setting.

Proposition 7.1. *Let $C \subseteq V$ be nonempty convex and $F: V \rightarrow \mathbb{R}$, proper, convex, lower semi-continuous such that Assumptions 7.1 hold, and assume that the update rule is chosen among Eqs. (7.4) to (7.7). Then Algorithm 1 produces a sequence of iterates such that*

1. For every $k \in \mathbb{N}$, $u^{[k]} \in C$,
2. If $\kappa_F < +\infty$ (see (7.8)), then

$$\left(F(u^{[k]}) - \min_C F \right) \leq \frac{2\kappa_F}{k+2}, \quad (7.9)$$

and every cluster point of $(u^{[k]})_{k \in \mathbb{N}}$ is a minimizer of F over C .

Proof. The first point follows directly from the update rules. The second point is the convergence rate derived in [Jag13, Th. 1]. Since it essentially relies on the values of the function and the definition of the curvature, the proof extends to our setting without change. Eventually, if the sequence $(u^{[k]})_{k \in \mathbb{N}}$ has cluster points (for instance if C is sequentially compact), the lower semi-continuity of F together with (7.9) imply that they are minimizers of F . \square

7.1.3 Discussion

Extreme points. If C is compact, then at Line 3, there is some minimizer s which is an *extreme point* of C . That is particularly interesting, since in several cases, finding an extreme point which minimizes a linear form can be done efficiently. For example,

- if C is a ℓ^p ball on \mathbb{R}^n ($1 < p < +\infty$), it can be done using a simple rescaling.
- if C is the set of bistochastic matrices (of size $n \times n$), it can be done using the Hungarian algorithm (in $O(n^3)$ operations).
- if C is a level set of a matrix Schatten norm, it can be done by computing a Singular Value Decomposition (SVD)...

We refer to [Jag13, BRZ21] for more detail. As a consequence, each iterate $u^{[k]}$ is sparse, in the sense that it is a convex combination of at most k extreme points of C . That property is useful for storing efficiently the variable. Even more interesting, it allows to tackle infinite-dimensional problems, provided one knows how to encode the extreme points. In Section 7.2, we discuss the resolution of optimization problems in $\mathcal{M}(X)$.

In some exceptional cases (such as the total variation unit ball), writing $u^{[k]}$ as the convex combination of extreme points directly provides its minimal face.

The case of Banach spaces. In the literature [DR70, DH78], V is usually chosen as a Banach space, see also the extension to unconstrained problems in Hilbert spaces known as generalized conditional gradient [BLM09]. Another interesting choice, which covers optimization in the space of Radon measures and in separable reflexive Banach spaces, is to choose V as the topological dual of a separable Banach space Υ . Then, as soon as C is bounded (in norm) and closed, the Banach-Alaoglu theorem ensures that C is compact in the weak-* topology, (and since that topology is metrizable on C , compactness is equivalent to sequential compactness).

Whether V is a dual or simply a Banach space, one may bound the curvature provided F' is Lipschitz (see [Jag13, Lem. 7]),

$$\kappa_F \leq \text{Lip}(F') (\text{diam}(C))^2. \quad (7.10)$$

Approximate linear minimization. In Line 3, the minimization may not be exact, for instance if it is performed by an iterative process. A variant taking errors into account is given in [Jag13], ensuring the convergence rate

$$\left(F(u^{[k]}) - \min_C F \right) \leq \frac{2\kappa_F}{k+2} (1 + \delta), \quad (7.11)$$

provided $s^{[k]}$ approximately minimizes the linear form, *i.e.*

$$\left\langle F'(u^{[k]}), (s^{[k]} - u^{[k]}) \right\rangle \leq \min_{s \in C} \left\langle F'(u^{[k]}), (s - u^{[k]}) \right\rangle + \frac{\delta\kappa_F}{k+2} \quad (7.12)$$

for some $\delta > 0$ independent from k .

7.2 The Sliding Frank-Wolfe in the space of measures

The goal of this section is to numerically solve the BLASSO (see Section 3.2.1),

$$\min_{m \in \mathcal{M}(X)} |m|(X) + \frac{1}{2\lambda} \|\Phi m - y\|_{\mathcal{H}}^2. \quad (\mathcal{P}^{(\text{TV})}(\lambda, y))$$

That is not a constrained problem in the sense of (7.1), hence the Frank-Wolfe algorithm is not directly applicable. In [BP13], the generalized conditional gradient algorithm introduced in [BLM09] is extended to $(\mathcal{P}^{(\text{TV})}(\lambda, y))$, using a direct study. In [9], following an idea in [HJN15], we have related the latter algorithm to the standard Frank-Wolfe algorithm applied to the truncated epigraph of the total variation $R^{(\text{TV})}: m \mapsto |m|(X)$.

7.2.1 Description of the algorithm

The idea is to reformulate $(\mathcal{P}^{(\text{TV})}(\lambda, y))$ as

$$\min_{(m,t) \in C} t + \frac{1}{2\lambda} \|\Phi m - y\|_{\mathcal{H}}^2, \quad (7.13)$$

$$\text{where } C \stackrel{\text{def.}}{=} \left\{ (m, t) \in \mathcal{M}(X) \times \mathbb{R} \mid |m|(X) \leq t \leq \frac{1}{2\lambda} \|y\|_{\mathcal{H}}^2 \right\}. \quad (7.14)$$

The connection between both problems is that $m \in \mathcal{M}(X)$ is a solution to $(\mathcal{P}^{(\text{TV})}(\lambda, y))$ if and only if (m, t) is a solution to (7.13) for some $t \in \mathbb{R}$, in which case $t = |m|(X)$.

Introducing the function $F: (\mathcal{M}(X) \times \mathbb{R}) \rightarrow \mathbb{R}$, $(m, t) \mapsto t + \frac{1}{2\lambda} \|\Phi m - y\|_{\mathcal{H}}^2$, we note that we are back to the setting of Section 7.1. The function F is Gateaux-differentiable with

$$F'(m, t) = \left(\frac{1}{\lambda} \Phi^*(\Phi m - y), 1 \right) \quad (7.15)$$

and its curvature satisfies

$$\kappa_F \leq \frac{1}{\lambda^3} \left(\sup_X \|\varphi\|_{\mathcal{H}} \right)^2 \|y\|_{\mathcal{H}}^4. \quad (7.16)$$

The (sequential) compactness follows from the Banach-Alaoglu theorem (see the discussion on dual spaces in Section 7.1.3).

Extreme points and linear minimization. Setting $M \stackrel{\text{def.}}{=} \frac{\|y\|_{\mathcal{H}}^2}{2\lambda}$, one may observe that the extreme points of C are

$$\text{ext}(C) = \{(0, 0)\} \cup \{M(\pm\delta_x, 1) \mid x \in X\}. \quad (7.17)$$

As a result, Line 3 is equivalent to picking $s^{[k]}$ as the best competitor among $(0, 0)$ and any point in

$$\text{argmin}_{(x, \varepsilon) \in X \times \pm 1} \frac{1}{\lambda} \left\langle \Phi^*(\Phi m^{[k]} - y), \varepsilon \delta_x \right\rangle + 1 = \text{argmin}_{(x, \varepsilon) \in X \times \pm 1} \left(1 - \varepsilon \eta^{[k]}(x) \right), \quad (7.18)$$

where $\eta^{[k]} \stackrel{\text{def.}}{=} \frac{1}{\lambda} \Phi^*(y - \Phi m^{[k]})$. In dimension $d = 1, 2$ or 3 , one may find ε and x simply by evaluating $\eta^{[k]}$ on a grid in X , possibly refining the estimation using a gradient descent or a Newton method (see Remark 7.2 below).

Stopping criterion. As explained in Section 7.1, the stopping criterion corresponds to $(-F'(m^{[k]}, t^{[k]}))$ being in the normal cone to C at $(m^{[k]}, t^{[k]})$. Since its second component is -1 , the point $(m^{[k]}, t^{[k]})$ must lie on the relative boundary of the epigraph $\text{epi } R^{(\text{TV})}$

Algorithm 2 Sliding Frank-Wolfe (SFW) Algorithm

- 1: Initialize with $m^{[0]} = 0$ and $n = 0$.
- 2: **for** $k = 0, 1, \dots$ **do**
- 3: $m^{[k]} = \sum_{i=1}^{N^{[k]}} a_i^{[k]} \delta_{x_i^{[k]}}$, $a_i^{[k]} \in \mathbb{R}$, $x_i^{[k]}$ pairwise distinct, find $x_*^{[k]} \in X$ s.t.:

$$x_*^{[k]} \in \operatorname{argmax}_{x \in X} |\eta^{[k]}(x)| \quad \text{where} \quad \eta^{[k]} \stackrel{\text{def.}}{=} \frac{1}{\lambda} \Phi^*(y - \Phi m^{[k]}),$$

- 4: **if** $|\eta^{[k]}(x_*^{[k]})| \leq 1$ **then**
- 5: $m^{[k]}$ is a solution of $(\mathcal{P}^{(\text{TV})}(\lambda, y))$. Stop.
- 6: **else**
- 7: Obtain $m^{[k+1/2]} = \sum_{i=1}^{N^{[k]}} a_i^{[k+1/2]} \delta_{x_i^{[k]}} + a_{N^{[k]}+1}^{[k+1/2]} \delta_{x_*^{[k]}}$, s.t.:

$$a^{[k+1/2]} \in \operatorname{argmin}_{a \in \mathbb{R}^{N^{[k]}+1}} \frac{1}{2} \|\Phi_{x^{[k+1/2]}} a - y\|_{\mathcal{H}}^2 + \lambda \|a\|_1$$

where $x^{[k+1/2]} = (x_1^{[k]}, \dots, x_{N^{[k]}}^{[k]}, x_*^{[k]})$

- 8: Find a critical point $m^{[k+1]} = \sum_{i=1}^{N^{[k]}+1} a_i^{[k+1]} \delta_{x_i^{[k+1]}}$ by minimizing locally

$$(a, x) \in \mathbb{R}^{N^{[k]}+1} \times X^{N^{[k]}+1} \mapsto \frac{1}{2} \|\Phi_x a - y\|_{\mathcal{H}}^2 + \lambda \|a\|_1,$$

by initializing with $(a^{[k+1/2]}, x^{[k+1/2]})$.

- 9: Eventually remove zero amplitudes Dirac masses from $m^{[k+1]}$.
- 10: **end if**
- 11: **end for**

(rather than on the top face corresponding to the truncation). In other words, we must have $t^{[k]} = |m^{[k]}|(X)$.

First, we assume that $|m^{[k]}|(X) < M$. From the relationship between subdifferentials and the normals to their epigraphs¹ (see [Appendix B.3](#)), we deduce that $\eta^{[k]} \stackrel{\text{def.}}{=} \frac{1}{\lambda} \Phi^*(y - \Phi m^{[k]})$ is a subgradient to $R^{(\text{TV})}$ at $m^{[k]}$.

Now, we deal with the case $|m^{[k]}|(X) = M$. The stopping criterion ensures that $(m^{[k]}, t^{[k]})$ is a minimizer, hence

$$F(0, 0) \geq F(m^{[k]}, t^{[k]}) \geq M = F(0, 0). \quad (7.19)$$

As a result $(0, 0)$ is a minimizer too, and the strict convexity of $p \mapsto \|p - y\|_{\mathcal{H}}^2$ implies that $\Phi 0 = \Phi m^{[k]}$, so that $|m^{[k]}|(X) = |0|(X) = 0$. As a result $m^{[k]} = 0$ and this corresponds to the trivial case where $y = 0$ and C is reduced to a point. Necessarily $\eta^{[k]} = 0$.

To summarize, in both cases, at convergence, *the Frank-Wolfe algorithm computes a dual certificate $\eta^{[k]}$ for $m^{[k]}$.*

Non-convex refinement. Taking advantage of the fact that, in the update rule, one may choose any point which is better than the linesearch (see [Section 7.1](#)), the authors of [\[BP13\]](#) have proposed to refine the estimation of the locations $\{x\}_{x \in \mathcal{I}}$ by using a local descent (using, *e.g.*, a gradient descent or BFGS algorithm). That idea is crucial: it

¹Since C and $\operatorname{epi} R^{(\text{TV})}$ coincide in a neighborhood of $(m^{[k]}, t^{[k]})$, they have the same normal cone at that point.

takes advantage of the continuous nature of the problem, as opposed to imposing a fixed grid (see Section 5.3) and solving the LASSO with a proximal method. As advocated in [BSR17], the non-convex refinement step improves the estimation of the support, hence speeds up convergence. Moreover, its memory footprint is bounded: at the k -th iteration, the recovery of the amplitudes is a LASSO in dimension $N^{[k]} + 1 \leq k + 1$; in fact, if the number of measurements M is finite, using the representer theorem, one may bound the dimension by $\min(k + 1, M)$.

In [9], we have proposed a slight modification of [BP13, BSR17] which consists in performing the non-convex descent on the locations and amplitudes simultaneously. The resulting algorithm, called *Sliding Frank-Wolfe* is summarized in Algorithm 2. Though the prescribed change might seem minor, it allows finite time termination of the algorithm, as the next theorem shows.

Theorem 7.1 ([9, Thm. 3]). *Suppose that Assumptions 4.1 hold, and let $y \in \mathcal{H}$. Assume that there is a unique solution m^* to $(\mathcal{P}^{(\text{TV})}(\lambda, y))$, and that $m^* = m_{a, \mathcal{I}} = \sum_{x \in \mathcal{I}} a_x \delta_x$ with \mathcal{I} finite (and $a_x \neq 0$). If the dual certificate $\eta_\lambda \stackrel{\text{def.}}{=} \frac{1}{\lambda} \Phi^*(y - \Phi m^*)$ is nondegenerate, i.e.*

$$\forall x \in X \setminus \mathcal{I}, \quad |\eta_\lambda(x)| < 1 \quad \text{and} \quad \forall x \in \mathcal{I}, \quad (\text{sign}(a_x) \eta''(x)) \prec 0, \quad (7.20)$$

then Algorithm 2 recovers m^ after a finite number of steps (i.e. there exists $k \in \mathbb{N}$ such that $m^{[k]} = m^*$).*

One way to ensure the non-degeneracy of η_λ a priori is to work in a low-noise regime, assuming that $y = \Phi m_0 + w$ where m_0 satisfies the Non-Degenerate Source condition (see Section 5.2.2). For several standard acquisition settings, that property can be ensured if the unknown spikes are well separated, see [PKP20]. In practice, the algorithm stops after s iterations, where $s = |\mathcal{I}|$ is the number of spikes of m_0 . Alternatively, the non-degeneracy of η_λ can be ensured using a T-system argument (see Section 6.3).

Remark 7.1. *It is possible to extend the proposed algorithm to the BLASSO with positivity constraints, see [9].*

Remark 7.2 (Implementation details). *The SFW algorithm relies on three different solvers for respectively step 3, step 7 and step 8. Quentin Denoyelle's implementation² for [9], corresponds to the following choices.*

- A Newton method, initialized by a grid search, is used to find the maximum of $|\eta^{[k]}|$ over the compact domain X in step 3. The size of the grid depends on the operator Φ . For example, when Φ is the convolution by the Dirichlet kernel with cutoff frequency f_c , we choose a number of points proportional to f_c .
- The LASSO problem at Line 7 is solved using the fast iterative shrinkage thresholding algorithm (FISTA) [BT09].
- To solve the non-convex optimization problem at Line 8, we deploy a bounded BFGS. It allows to enforce the positions x_i to be in the domain X and to preserve the sign of the amplitudes a_i in the case of a BLASSO with positivity constraints.

²<https://github.com/qdenoyelle/sfw4blasso>

7.2.2 Illustration of the finite-time convergence

Now, we illustrate the behavior of the algorithm and we show that it converges in exactly N iterations in practice (when the noise level and the regularization parameter are appropriate, *i.e.* $\max(\lambda, \|w\|_{\mathcal{H}}/\lambda)$ is small enough).

We consider $X = [0, 1]$ and a convolution operator with a sampled Gaussian kernel for Φ

$$\Phi : m \in \mathcal{M}(X) \mapsto \int_{[0,1]} \varphi dm \in \mathbb{R}^K \quad \text{where} \quad \varphi(x) = \left(\frac{1}{\sqrt{2\pi\sigma^2}} e^{-\frac{(\frac{i-1}{K-1}-x)^2}{2\sigma^2}} \right)_{1 \leq i \leq K}.$$

We set $\sigma = 0.05$ and $K = 100$. The initial measure used is $m_0 = 1.3\delta_{0.3} + 0.8\delta_{0.37} + 1.4\delta_{0.7}$ and the noise is small ($y = \Phi m_0 + w$, with $w = 10^{-4}w_0$ where $w_0 = \text{randn}(K)$).

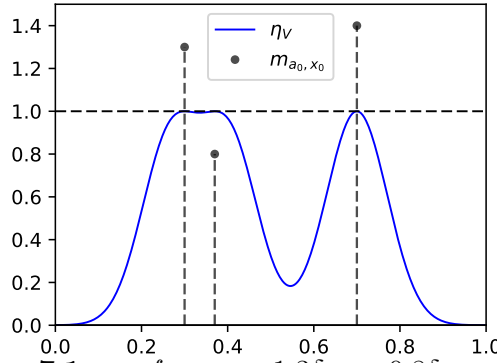


Figure 7.1: η_V for $m_0 = 1.3\delta_{0.3} + 0.8\delta_{0.37} + 1.4\delta_{0.7}$.

Figure 7.1 shows η_V for this configuration. One can see that it is nondegenerate. Hence, in a low noise regime, with the appropriate choice of λ , there is a unique measure solution of BLASSO which is composed of the same number of spikes as m_0 , and the corresponding η_λ is non-degenerate. By Theorem 7.1, the Sliding Frank-Wolfe (SFW) algorithm recovers it in a finite number of iterations.

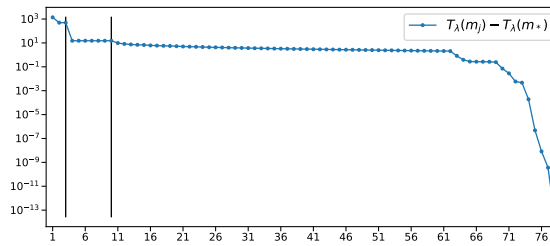


Figure 7.2: Values of the objective function throughout the SFW algorithm (cumulative iterations of the BFGS). The vertical black lines separate the main outer iterations of the algorithm.

The decrease of the objective function throughout the algorithm iterations (cumulative iterations of BFGS) is presented in Figure 7.2. As indicated by the two vertical black lines, which show the intermediate iterations, the algorithm converges in exactly 3 iterations. One can observe an important decrease of the objective function each time a spike is added. Also, it is noteworthy that BFGS converges with very few iterations when $k = 0$ and $k = 1$ (first two spikes added) and that the main computational load for the non-convex step occurs for $k = 2$ (more iterations of BFGS).

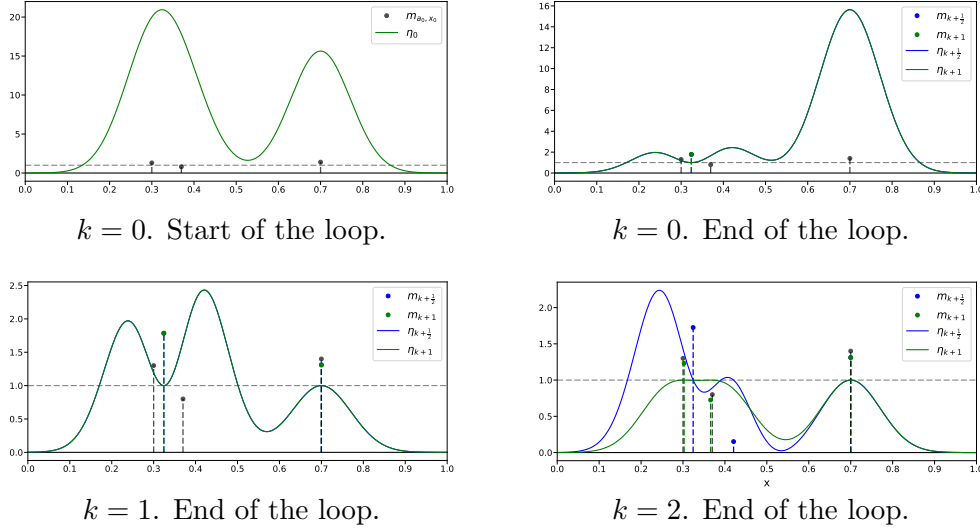


Figure 7.3: Main steps of the SFW algorithm.

Figure 7.3 shows $m^{[k]}$ and $\eta^{[k]}$ at different times of the algorithm. More precisely, for $k \in \{0, 1, 2\}$, we display the initial measure m_0 , the recovered measure, and the associated η . Moreover, we present them after the LASSO step (*i.e.* $m^{[k+1/2]}$ and $\eta^{[k+1/2]}$) as well as after the BFGS step (*i.e.* $m^{[k+1]}$ and $\eta^{[k+1]}$).

One remarks, as expected, that for all i , $\eta^{[k+1/2]}(x_i) = 1$, $\eta^{[k+1]}(x_i) = 1$ and $\eta^{[k+1]'}(x_i) = 0$. In the first two main iterations, the spikes are almost not moved by the BFGS. However, at the last iteration, the displacement of the positions and amplitudes of the spikes is crucial to obtain $\eta^{[k+1]} \in \partial R^{(\text{TV})}(m^{[k+1]})$, and thus recover the solution of BLASSO in three steps.

7.2.3 Application to fluorescence microscopy

In this section we illustrate the performance of the SFW algorithm in fluorescence microscopy, using the experiments of [9]. We refer to Quentin Denoyelle's PhD thesis [Den18] for more comprehensive benchmarks. The reader may also consult [7], where we have used the Sliding Frank-Wolfe in a series of static images for the tracking of mesoscale convective systems (big clouds in tropical areas), see Figure 7.4.

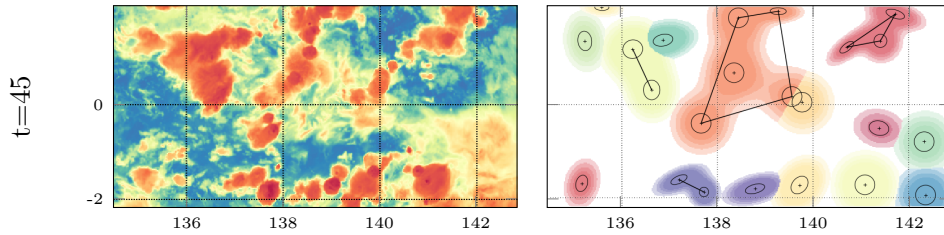


Figure 7.4: Tracking of mesoscale convective systems in satellite images in [7].

The field of fluorescence microscopy has experienced an important revolution during the past two decades with the emergence of super-resolution techniques. These modalities, such as structured illumination microscopy (SIM) [Gus00], stimulated emission depletion (STED) [HW94], or single molecule localization microscopy (SMLM) (which includes photoactivated localization microscopy (PALM) [BPS⁺06, HPGM07] and stochastic optical reconstruction microscopy (STORM) [RBZ06]) bypass the diffraction limit so as to reach unprecedented nanoscale resolution. The main principle behind

these methods relies on a combined use of optics and numerical processing, which is commonly called computational imaging. The resolution improvement is thus directly related to the performance of the reconstruction algorithms employed to process the acquired data.

SMLM techniques use photoactivable fluorescent probes to sequentially image a subset of activated molecules. Then, dedicated algorithms are deployed to precisely extract the position of these molecules. While the difficulty of the localization problem increases with the density of activated molecules per acquisitions, low density activations drastically reduce the temporal resolution of the system which makes the method limited for live imaging. Hence, current trends in SMLM concern the development of efficient algorithms dealing with high density data for which classical point-spread function (PSF) fitting or centroid localization methods [HLF⁺10] fail. In particular, off-the-grid sparse regularized methods have shown their efficiency for high density settings [HSMC17, BSR17]. For a complete review and comparisons of existing methods, we refer the reader to the two recent SMLM challenges [SKP⁺15, SPB⁺18].

Initially introduced for two-dimensional imaging, SMLM has been extended to 3D thanks to Point Spread Function (PSF) engineering. The principle relies on the design of PSFs which vary in the axial direction (*i.e.* z) in order to encode an information about the depth of molecules. Conventional PSF models include astigmatism [HWBZ08] and double-helix [RPPATSB⁺09]. An alternative to PSF engineering is to record simultaneously multiple focal planes, as in the biplane modality [JJGL⁺08]. It is noteworthy that these two approaches can also be combined as in [HSG⁺15] where the authors use both an astigmatism PSF and multi-focal acquisitions.

In this section, we study the performance of the SFW algorithm on both astigmatism and double-helix modalities with various number of focal planes (typically from 1 to 4). We compare these two modalities to an alternative approach where depth information is extracted from multi-angle total internal reflection fluorescence (MA-TIRF) microscopy acquisitions. That approach consists in illuminating the scene with different angles so as to deduce the depth from the attenuation of the response, and it is quite new and promising in microscopy imaging (see [BGM⁺14, SRG⁺19] for recovery methods on a grid). In [9], we designed numerical simulations as a proof of concept to explore the potential of off-the-grid methods with the MA-TIRF technique. One of the main interest in combining SMLM with MA-TIRF is that classical PSFs, which are better localized laterally than astigmatism or double-helix, can be used. This would reduce the difficulty of lateral molecule localization for high density settings while recovering the depth through the MA-TIRF acquisitions.

Let us describe the corresponding impulse responses. In the following, $X \stackrel{\text{def.}}{=} [0, b_1] \times [0, b_2] \times [0, b_3]$ is a subset of \mathbb{R}^3 , and we write $x = (x_1, x_2, x_3) \in X$. We consider a camera containing $N_1 \times N_2$ pixels and we denote the center of the i th pixel by $(c_{i,1}, c_{i,2})$. An additional parameter, K , is related to depth estimation and encodes the number of focal planes in astigmatism and double helix, or the number of angles in MA-TIRF. We take into account the integration over camera pixels

$$\Omega_i \stackrel{\text{def.}}{=} (c_{i,1}, c_{i,2}) + \left[-\frac{b_1}{2N_1}, \frac{b_1}{2N_1} \right] \times \left[-\frac{b_2}{2N_2}, \frac{b_2}{2N_2} \right] \subset \Omega \stackrel{\text{def.}}{=} [0, b_1] \times [0, b_2].$$

Astigmatism model. This modality provides depth information using an astigmatism deformation of the PSF with respect to the axial direction z . It is customary to model the latter with a Gaussian function whose variances σ_1 and σ_2 vary with z according to

[HSMC17, KVU13]

$$\sigma_1(z) \stackrel{\text{def.}}{=} \sigma_0 \sqrt{1 + \left(\frac{\alpha z - \beta}{d} \right)^2} \quad \text{and} \quad \sigma_2(z) \stackrel{\text{def.}}{=} \sigma_1(-z). \quad (7.21)$$

The constants involved in (7.21) can be calibrated from real data [HWBZ08, KVU13]. Then, integrating this Gaussian model over camera pixels, we have for all $i \in \{1, \dots, N_1 N_2\}$ and $k \in \{1, \dots, K\}$

$$[\varphi(x)]_{i,k} \stackrel{\text{def.}}{=} \frac{1}{2\pi\sigma_1(x_3 - z_k)\sigma_2(x_3 - z_k)} \int_{\Omega_i} e^{-\left(\frac{(x_1 - s_1)^2}{2\sigma_1^2(x_3 - z_k)} + \frac{(x_2 - s_2)^2}{2\sigma_2^2(x_3 - z_k)} \right)} ds_1 ds_2,$$

where $(z_k)_{k=1}^K$ are the positions of the considered focal planes.

Double-helix model. Here, depth information is obtained by using a PSF formed out of two lobes which coil around each other along z to form a double-helix shape. In this paper, we model these lobes by two Gaussian functions with fixed variances $\sigma_1 = \sigma_2$, and with a center whose lateral position (r_1, r_2) (respectively, $(-r_1, -r_2)$) varies with z according to

$$r_1(z) \stackrel{\text{def.}}{=} \frac{\omega}{2} \cos(\theta(z)) \quad \text{and} \quad r_2(z) \stackrel{\text{def.}}{=} -\frac{\omega}{2} \sin(\theta(z)) \quad \text{where} \quad \theta(z) = \theta_{\text{speed}} z. \quad (7.22)$$

Parameters $\omega > 0$ and $\theta_{\text{speed}} > 0$ correspond to the distance between the two Gaussian and the rotation speed of the double-helix (rad/nm), respectively. Then, integrating this model over camera pixels, we have for all $i \in \{1, \dots, N_1 N_2\}$ and $k \in \{1, \dots, K\}$

$$[\varphi(x)]_{i,k} \stackrel{\text{def.}}{=} \frac{1}{2\pi\sigma_1\sigma_2} \sum_{u \in \{-1, 1\}} \int_{\Omega_i} e^{-\left(\frac{(x_1 + ur_1(x_3 - z_k) - s_1)^2}{2\sigma_1^2} + \frac{(x_2 + ur_2(x_3 - z_k) - s_2)^2}{2\sigma_2^2} \right)} ds_1 ds_2,$$

where $(z_k)_{k=1}^K$ are the positions of the considered focal planes.

MA-TIRF model. With this modality, each activated set of molecules is imaged using $K \in \mathbb{N}$ TIRF illuminations with incident angles $(\alpha_k)_{k=1}^K$. We only give a brief account of the acquisition process, and we refer to [SSR⁺16, SRG⁺19] for the detail of the setup. Let $n_i > 0$ and $n_t > 0$ be the refractive indices of the incident (*i.e.* glass coverslip) and the transmitted (*i.e.* sample) medium, respectively. A TIRF excitation is obtained when the incident angle α is greater than the critical angle $\alpha_c = \arcsin(n_t/n_i)$ for which we have total internal reflection of the light within the incident medium. This phenomenon produces an evanescent wave which decays in the transmitted medium as $\exp(-sx_3)$, where $s = (4\pi n_i)/\lambda_\ell (\sin^2(\alpha) - \sin^2(\alpha_c))$ is the penetration depth and λ_ℓ is the wavelength of the incident laser beam [Axe81, Axe08]. Because the decay of this evanescent excitation vary with the incident angle, the depth of biological structures can be recovered with a nanometric precision from multi-angle acquisitions [BGM⁺14, DSDVJ16, ZZL⁺18]. Combining this principle with SMLM techniques lead to a forward model Φ defined, for all $i \in \{1, \dots, N_1 N_2\}$ and $k \in \{1, \dots, K\}$, by

$$[\varphi(x)]_{i,k} \stackrel{\text{def.}}{=} \frac{\xi(x_3)e^{-s_k x_3}}{2\pi\sigma_1\sigma_2} \int_{\Omega_i} e^{-\left(\frac{(x_1 - s_1)^2}{2\sigma_1^2} + \frac{(x_2 - s_2)^2}{2\sigma_2^2} \right)} ds_1 ds_2, \quad (7.23)$$

where $\xi(z) = \left(\sum_{k=1}^K e^{-2s_k z} \right)^{-1/2}$ is a normalization factor. This model comes from the combination of a lateral convolution with the axial TIRF excitation. Here the PSF of the

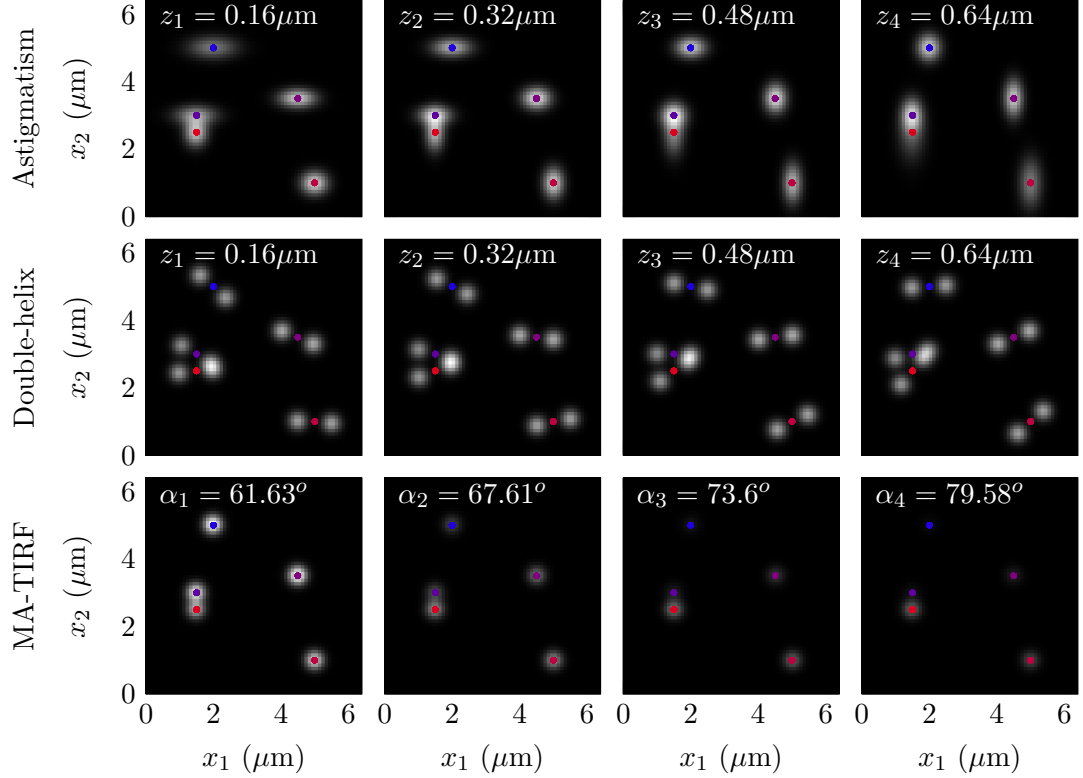


Figure 7.5: Noiseless acquisitions y_0 for the measure m_0 displayed with colored balls and $K = 4$. The color of the molecules represent their depths: 0 (red) – $0.8\mu\text{m}$ (blue).

system is assumed to be a Gaussian with variances $\sigma_1 = \sigma_2$, and to be constant along x_3 (because only a thin layer of few hundred nanometers is excited by the evanescent wave). The values $(s_k)_{k=1}^K$ correspond to the penetration depths associated to the incident angles $(\alpha_k)_{k=1}^K$.

An example of the corresponding three acquisitions is displayed on [Figure 7.5](#).

Numerical results. We simulate an acquisition experiment by designing filaments which are piecewise linear curves. We draw random points on those curves and we shift them by a vector which is drawn uniformly at random in a ball of radius 10 nm.

The $N_{\text{tot}} \in \mathbb{N}^*$ molecules of the simulated structure are divided into $n \in \mathbb{N}^*$ sparse set of $N \in \mathbb{N}^*$ molecules using a random permutation (*i.e.* $N_{\text{tot}} = n \times N$). This models the sequential stochastic activation of fluorophores used in SMLM. For each of the n subsets of molecules, we define a Radon measure composed of a sum of Dirac masses—located at the position of the molecules—with positive amplitudes

$$m_0 = \sum_{i=1}^N a_i \delta_{x_i} \quad \text{where} \quad a_i > 0 \quad \text{and} \quad x_i \in X.$$

The amplitudes are randomly generated within $[1, 1.5]$. An example of a set of activated molecules is shown in [Figure 7.6](#) (black crosses). Then, the data is obtained by applying the forward model on each subset and adding noise.

For the reconstruction, we solve the BLASSO for each subset of activated fluorophores, using a value λ that maximizes the Jaccard index on a training set (see [\[9\]](#) for more detail).

[Figure 7.7](#) shows the detection rate using standard metrics [\[SPB⁺18, SKP⁺15\]](#). Given a recovered frame and a tolerance radius $r > 0$, we pair estimated molecules and ground

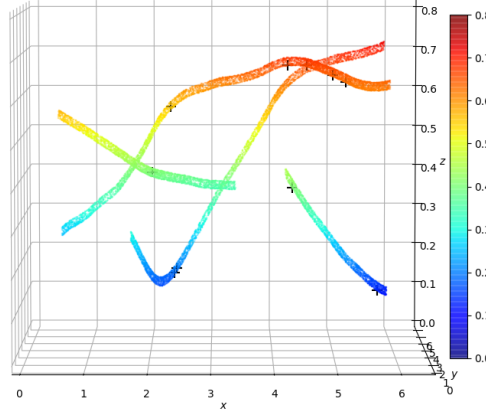


Figure 7.6: *Microtubules structure used for the simulations. The diameter of the filaments is 20 nm. The color encodes the depth of molecules within the range 0–0.8 μm . Black crosses represent a subset of activated molecules (i.e. a measure m_0).*

truth (GT) molecules when the distance between them is lower than r . Paired estimated molecules are then referred as true positive (TP) while unpaired ones as false positive (FP). Finally, the unpaired GT molecules are identified as false negative (FN). These quantities being determined for each frame, we can compute the Jaccard index (Jac), the Recall (Rec) and the Precision (Pre) metrics,

$$\text{Jac} = \frac{\#TP}{\#TP + \#FP + \#FN} \quad \text{Rec} = \frac{\#TP}{\#TP + \#FN} \quad \text{Pre} = \frac{\#TP}{\#TP + \#FP}. \quad (7.24)$$

The visual reconstructions are displayed in [Figure 7.8](#) and [Figure 7.9](#), showing respectively the effect of the number N of simultaneously activate molecules and the number K of focal planes or illumination angles. These results suggest that moving from $K = 1$ focal plane to $K = 2$ focal planes greatly improve the performance of the detection (while going further only provides marginal improvements), which corroborates the results of [\[HSG⁺15\]](#). To the best of our knowledge, current commercial microscopes which include the Astigmatism or Double-Helix modalities only implement 1 focal plane.

While the benchmark tends to show the superiority of the Double-Helix acquisition model with $K \geq 2$ focal planes, other criteria must be taken into account, such as the manufacturing cost or the difficulty of the calibration process. It appears that when taking those into accounts, the MA-TIRF procedure is an interesting alternative.

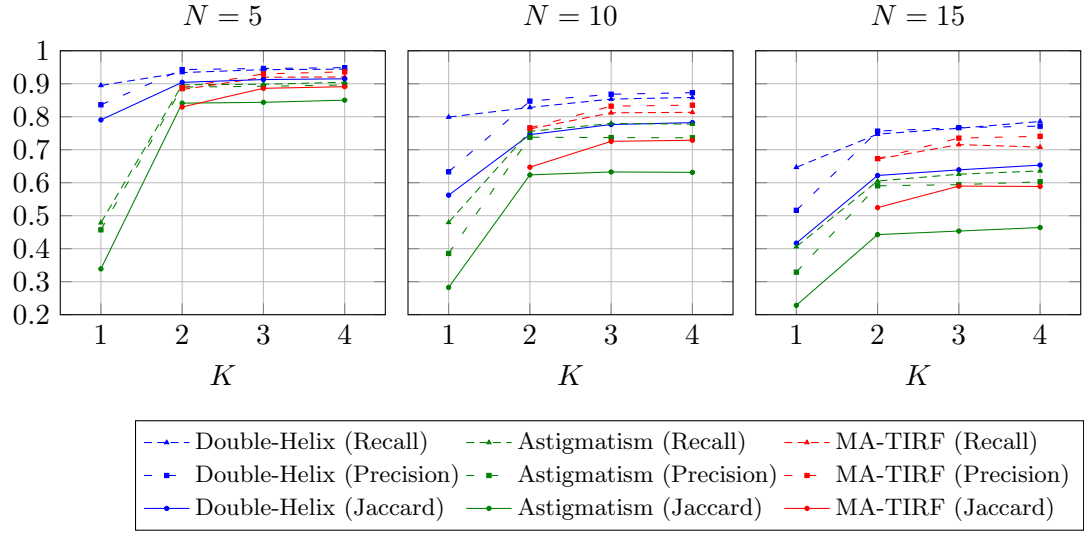


Figure 7.7: Evolution of Jaccard, Recall and Precision metrics with respect to K , for a radius of detection $r = 0.02$ (20nm).

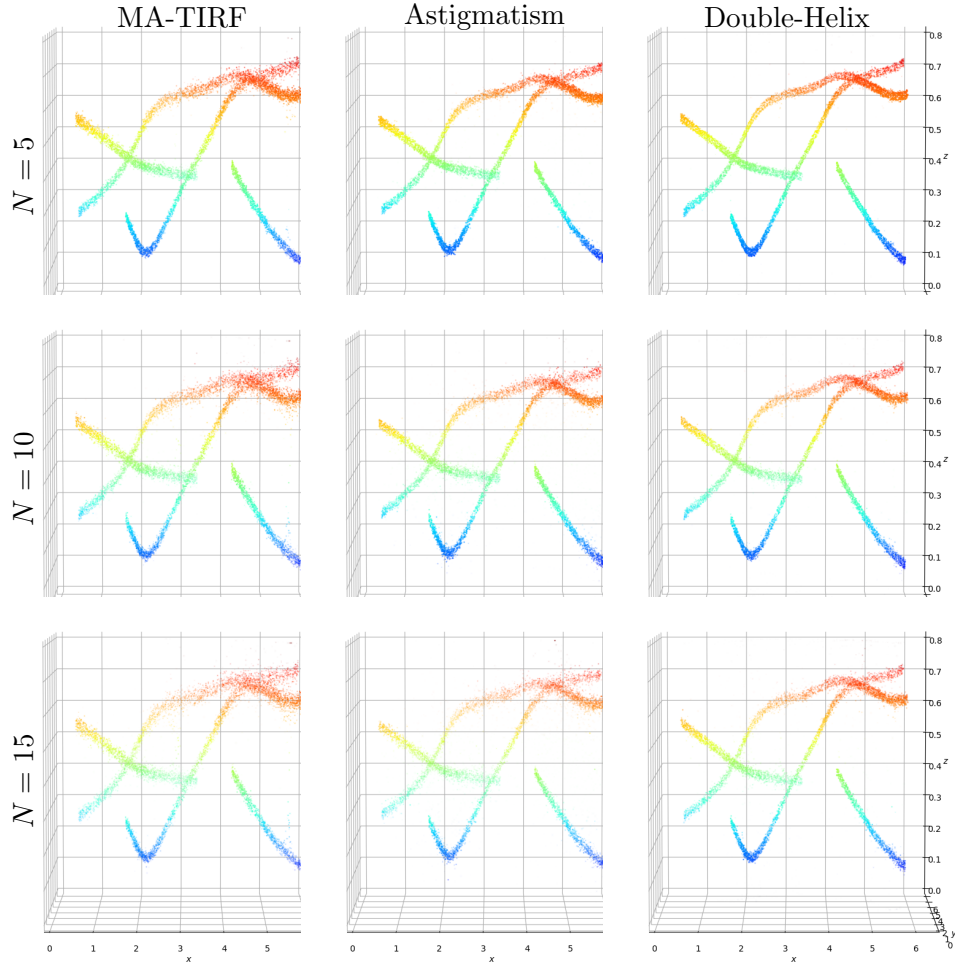


Figure 7.8: Recovered structures for $K = 4$.

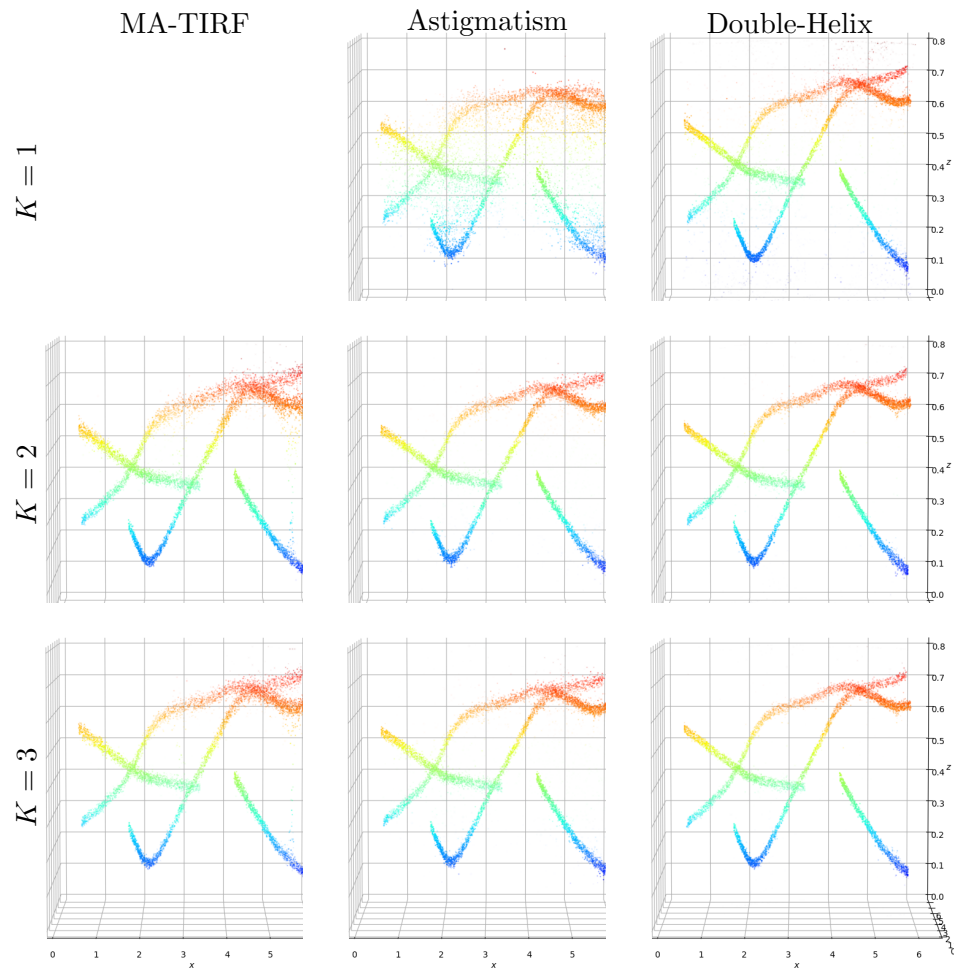


Figure 7.9: *Recovered structures for $N = 10$.*

7.3 The Fourier-Frank-Wolfe algorithm in the space of Moment matrices

Now, we discuss an alternative method to solve the BLASSO. A way to handle measures numerically is to work with their moments. We assume in this section that $X = \mathbb{T}^d$, so that we may characterize a measure $m \in \mathcal{M}(X)$ by its trigonometric moments (*i.e.* its Fourier coefficients),

$$\forall k \in \mathbb{Z}^d, \quad c_k(m) \stackrel{\text{def.}}{=} \int_{\mathbb{T}^d} e^{-2i\pi \langle k, x \rangle} dm(x). \quad (7.25)$$

7.3.1 Spectral approximation

In order to write our problem in terms of the trigonometric moments, we assume that $\Phi: \mathcal{M}(\mathbb{T}^d) \rightarrow \mathcal{H}$ only depends on the first Fourier coefficients of m , $(c_k(m))_{k \in \llbracket -f_c, f_c \rrbracket^d}$, for some $f_c \in \mathbb{N}$. That is not so restrictive, since we may approximate any Φ with smooth impulse response with such an operator. For $\varphi: \mathbb{T}^d \rightarrow \mathcal{H}$ smooth enough, we define

$$\Phi_c(m) \stackrel{\text{def.}}{=} \int_{\mathbb{T}^d} \varphi_c(x) dm(x) \quad \text{where} \quad (7.26)$$

$$\varphi_c(x) \stackrel{\text{def.}}{=} \sum_{k \in \llbracket -f_c, f_c \rrbracket^d} c_k(\varphi) e^{2i\pi \langle k, x \rangle} \quad \text{and} \quad c_k(\varphi) \stackrel{\text{def.}}{=} \int_{\mathbb{T}^d} \varphi(x) e^{-2i\pi \langle k, x \rangle} dx. \quad (7.27)$$

Proposition 7.2 ([5]). *Let $y \in \mathcal{H}$, $\varphi \in \mathcal{C}^j(\mathbb{T}^d; \mathcal{H})$ with $j \geq \lfloor \frac{d}{2} \rfloor + 1$, and define Φ_c by (7.26). For all $f_c \in \mathbb{N}$, Let m_{f_c} denote any minimizer of the energy $\mathcal{E}_{f_c}(m) \stackrel{\text{def.}}{=} \lambda |m|(\mathbb{T}^d) + \frac{1}{2} \|\Phi_c m - y\|_{\mathcal{H}}^2$. Then, the sequence $(m_{f_c})_{f_c \in \mathbb{N}}$ has accumulation points in the weak-* topology and each of them is a minimizer of $\mathcal{E}(m) \stackrel{\text{def.}}{=} \lambda |m|(\mathbb{T}^d) + \frac{1}{2} \|\Phi m - y\|_{\mathcal{H}}^2$.*

Denoting by $\mathcal{F}_c: \mathcal{M}(\mathbb{T}^d) \rightarrow \mathbb{C}^{\llbracket -f_c, f_c \rrbracket^d}$ the operator which maps m to $(c_k(m))_{k \in \llbracket -f_c, f_c \rrbracket^d}$, we have the factorization $\Phi_c = H_\varphi \mathcal{F}_c$, where $H_\varphi: \mathbb{C}^{(2f_c+1)^d} \rightarrow \mathcal{H}$. If \mathcal{H} has finite dimension, H_φ is a matrix with entries $(c_{-k}(\varphi_j))_{1 \leq j \leq \dim \mathcal{H}, k \in \llbracket -f_c, f_c \rrbracket^d}$.

Convolution. If Φ is a convolution operator ((3.14)), then H_φ is a diagonal matrix

$$H_\varphi = \text{diag} (c_k(\tilde{\varphi}))_{k \in \llbracket -f_c, f_c \rrbracket^d}. \quad (7.28)$$

where $\tilde{\varphi}$ is the impulse response of the filter.

For instance, if $\tilde{\varphi}$ is the Dirichlet kernel with cutoff frequency f_c , then $c_k(\tilde{\varphi}) = 1$ if $\|k\|_\infty \leq f_c$, and 0 otherwise. In that case, $\varphi = \varphi_c$.

Alternatively, if $\tilde{\varphi}$ is the 1-periodization of some (sufficiently decaying) function $f: \mathbb{R}^d \rightarrow \mathbb{R}$, *i.e.* $\tilde{\varphi}(x) = \sum_{j \in \mathbb{Z}^d} f(x + j)$, the Poisson summation formula yields $\tilde{\varphi}(x) = \sum_{k \in \mathbb{Z}^d} \hat{f}(k) e^{2i\pi \langle k, x \rangle}$, where \hat{f} is the Fourier transform of f . The function φ_c is simply the corresponding truncated sum for $k \in \llbracket -f_c, f_c \rrbracket^d$.

$$H_\varphi = \text{diag} (\hat{f}(k))_{k \in \llbracket -f_c, f_c \rrbracket^d}. \quad (7.29)$$

An illustration of such approximated impulse responses is given in Figure 7.10 in the case of the periodized Gaussian kernel.

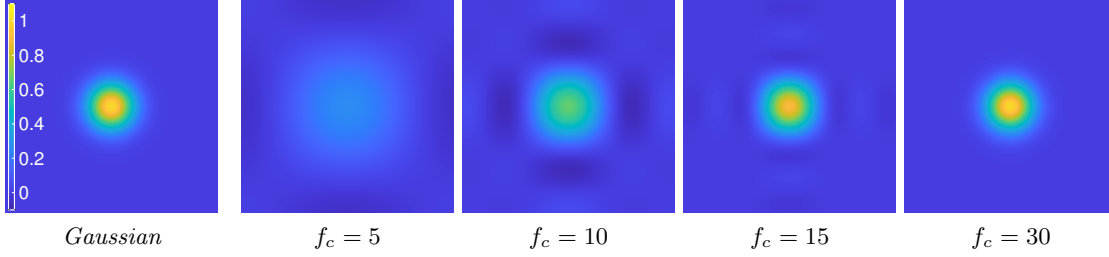


Figure 7.10: Evolution of $\Phi_c \delta_{x_0}$, $x_0 \in \mathbb{T}^2$, for different values of f_c , in the Gaussian case. Left image is a true (periodized) Gaussian convolution kernel.

Sampled convolution. In practical cases, one often only has access to convolution measurements over some sampling grid \mathcal{G} . In fluorescence microscopy for instance [Gro13], the observations are accurately described as subsampled Gaussian measurements. In that case, given some convolution kernel $\tilde{\varphi} \in L^2(\mathbb{T}^d)$ (typically a Gaussian), φ may be defined as

$$\varphi(x) = (\tilde{\varphi}(t - x))_{t \in \mathcal{G}} \quad (7.30)$$

which leads to

$$H_\varphi = \left(c_k(\tilde{\varphi}) e^{2i\pi \langle k, t \rangle} \right)_{t \in \mathcal{G}, k \in \llbracket -f_c, f_c \rrbracket^d}.$$

Spatially varying filter. A typical example where filters are expected to be non-stationary is in astrophysical imaging, see for instance [Ala00, SHM⁺02, GCM13]. These variations are for instance very important for the observation of the early universe, due to the impact of the lensing effect, see e.g. [CHK⁺13, NS17]. While it is sometimes possible to account for these variations by deforming the observation, this is often non-trivial. In such general cases, φ may be defined as

$$\varphi(x) = (\tilde{\varphi}(t, x))_{t \in \mathcal{G}}, \quad (7.31)$$

and the lines of H_φ consist in the Fourier coefficients of $x \mapsto \tilde{\varphi}(t, x)$ at frequencies taken in $\llbracket -f_c, f_c \rrbracket^d$.

Although the quality of the approximation proposed in this section depends on the chosen cutoff frequency f_c , and hence on the size of the approximation matrix H_φ , this matrix does not need to be fully stored in many situations, see Section 7.3.3.

7.3.2 Atomic norm reformulation

Introduction

From now on, we fix $f_c \in \mathbb{N}$ and, possibly applying the above approximation procedure, we assume the spectral factorization $\Phi = H_\varphi \mathcal{F}_c$. The problem $(\mathcal{P}^{(\text{TV})}(\lambda, y))$ can be reformulated as

$$\min_{z \in \mathbb{C}^{(2f_c+1)^d}} \frac{1}{2} \|y - H_\varphi z\|_{\mathcal{H}}^2 + \lambda \left(\min_{m \in \mathcal{M}(\mathbb{T}^d)} |m|(\mathbb{T}^d) \quad \text{s.t. } c_k(m) = z_k \quad \forall k \in \llbracket -f_c, f_c \rrbracket^d \right). \quad (7.32)$$

Given a vector $z \in \mathbb{C}^{(2f_c+1)^d}$ of Fourier coefficients, we focus in this section on the second term, namely the atomic norm [TBSR13] of z ,

$$\|z\|_{\mathcal{A}} \stackrel{\text{def.}}{=} \min \left\{ |m|(\mathbb{T}^d) \mid m \in \mathcal{M}(\mathbb{T}^d), \forall k \in \llbracket -f_c, f_c \rrbracket^d, c_k(m) = z_k \right\}. \quad (\mathcal{Q}_0(z))$$

To solve $(\mathcal{Q}_0(z))$ using only trigonometric moments, we extend the following result of G. Tang *et al.*.

Proposition 7.3 ([TBSR13]). *If $d = 1$, then*

$$\|z\|_{\mathcal{A}} = \min_{\substack{u \in \mathbb{C}^{2f_c+1}, \\ \tau \in \mathbb{R}}} \frac{1}{2} \left(\frac{1}{2f_c+1} \text{Tr}(\text{Toep}(u)) + \tau \right) \quad \text{s.t.} \quad \begin{bmatrix} \text{Toep}(u) & z \\ z^* & \tau \end{bmatrix} \succeq 0. \quad (7.33)$$

where $\text{Toep}(u)$ is the Hermitian Toeplitz matrix with first row u .

The cornerstone of the proof [Proposition 7.3](#) is the Carathéodory-Toeplitz theorem [[Car07](#), [Toe11](#)]: any positive semi-definite Toeplitz matrix T , of size $(2f_c+1) \times (2f_c+1)$, has a Vandermonde decomposition³,

$$T = \sum_{j=1}^r b_j v(x_j)(v(x_j))^* \quad \text{where} \quad v(x_j) \stackrel{\text{def.}}{=} \begin{pmatrix} e^{2i\pi f_c x_j} \\ e^{2i\pi(f_c-1)x_j} \\ \vdots \\ e^{-2i\pi(f_c)x_j} \end{pmatrix} \quad (7.34)$$

for some $b_j \geq 0$, $x_j \in \mathbb{T}$ (for all $1 \leq j \leq r$), and $r = \text{rank}(T)$. As a result, in [Proposition 7.3](#), $\text{Toep}(u)$ is the moment matrix (see below) of the measure $\sum_{j=1}^r b_j \delta_{x_j}$, and it is then possible to prove that there is a measure $m = \sum_{j=1}^r a_j \delta_{x_j}$ with $z = \mathcal{F}_c m$ and $b_j = |a_j|$. That measure is a solution to $(\mathcal{Q}_0(z))$.

The problem of computing the atomic norm is thus reduced to a semi-definite program, which can be solved *e.g.* using interior point methods. But when tackling higher dimensions $d \geq 2$, two problems arise.

1. The Carathéodory-Toeplitz theorem does not hold anymore: some "Toeplitz" positive semi-definite matrices do not have a Vandermonde decomposition.
2. Even if a formulation like (7.33) were true, it would involve matrices of size $(2f_c+1)^d \times (2f_c+1)^d$, which becomes quickly intractable using current interior point methods.

In the rest of this section we show how to extend [Proposition 7.3](#) and how to design an algorithm which is able to solve such large scale semi-definite programs.

Moment matrices

For $d, \ell \in \mathbb{N}^*$, and $m \in \mathcal{M}(\mathbb{T}^d)$, we define the moment matrix of m as the matrix $\mathbb{M}_\ell(m)$ indexed⁴ by $\llbracket -\ell, \ell \rrbracket^d$ such that

$$\forall i, j \in \llbracket -\ell, \ell \rrbracket^d, (\mathbb{M}_\ell(m))_{i,j} \stackrel{\text{def.}}{=} c_{i-j}(m) = \int_{\mathbb{T}^d} e^{-2i\pi \langle (i-j), x \rangle} dm(x). \quad (7.35)$$

The fundamental properties of moment matrices are the following:

- The matrix $\mathbb{M}_\ell(m)$ is *generalized Toeplitz* (also called Toeplitz-block Toeplitz, or multi-level Toeplitz), in the sense that for every multi-indices $i, j \in \llbracket -\ell, \ell \rrbracket^d$ and $k \in \mathbb{Z}^d$ such that $(i+k), (j+k) \in \llbracket -\ell, \ell \rrbracket^d$,

$$(\mathbb{M}_\ell(m))_{i+k, j+k} = (\mathbb{M}_\ell(m))_{i,j}. \quad (7.36)$$

³If $r < N$, that decomposition is unique.

⁴For now, we need not choose an order on the index set, but to fix ideas we can assume that the indices are in the colexicographic order.

- If the measure m is s -sparse, $m = \sum_{k=1}^s a_k \delta_{x_k}$, then $\text{rank}(\mathbb{M}_\ell(m)) \leq s$, since

$$\mathbb{M}_\ell(m) = \left(\int_{\mathbb{T}^d} e^{-2i\pi \langle (i-j), x \rangle} dm(x) \right)_{i,j} = \sum_{k=1}^s a_k v_\ell(x_k) (v_\ell(x_k))^* \quad (7.37)$$

$$\text{where } v_\ell(x) \stackrel{\text{def}}{=} (e^{-2i\pi \langle j, x \rangle})_{j \in \llbracket -\ell, \ell \rrbracket^d}. \quad (7.38)$$

- If the measure m is nonnegative, then $\mathbb{M}_\ell(m)$ is positive semi-definite, since

$$\forall q \in \mathbb{C}^{(2\ell+1)^d}, \quad q^* (\mathbb{M}_\ell(m)) q = \int_{\mathbb{T}^d} \overline{\left(\sum_i q_i e^{2i\pi \langle i, x \rangle} \right)} \left(\sum_j q_j e^{2i\pi \langle j, x \rangle} \right) dm(x) \quad (7.39)$$

$$= \int_{\mathbb{T}^d} \left| \sum_j q_j e^{2i\pi \langle j, x \rangle} \right|^2 dm(x) \geq 0. \quad (7.40)$$

Moreover, $q \in \ker \mathbb{M}_\ell(m)$ if and only if $(\text{supp } m) \subseteq \left\{ x \in \mathbb{T}^d \mid \sum_j q_j e^{2i\pi \langle j, x \rangle} = 0 \right\}$.

However, it is not true (contrary to the case $d = 1$) that every (generalized) Toeplitz Hermitian positive semi-definite matrix is the moment matrix of a nonnegative measure. Such a question was investigated in the pioneering work of R. Curto and L. Fialkow [CF96] (see also [CF00, Lau05, LM09]) who have highlighted the importance of the flatness property.

Definition 7.1 (Flatness). *Let $\ell \geq 1$, let R be a matrix indexed by $\llbracket -\ell, \ell \rrbracket^d$, and assume that R is Hermitian, positive semi-definite, and generalized Toeplitz. We say that R is flat if its submatrix \tilde{R} corresponding to the indices in $\llbracket -(\ell-1), \ell-1 \rrbracket^d$ satisfies $\text{rank } R = \text{rank } \tilde{R}$.*

The flatness property is sufficient to ensure that R is a moment matrix. As our setting is not exactly the same as in [CF96] (the degrees of our polynomials are evaluated in the ℓ^∞ -norm instead of the ℓ^1 -norm), we have adapted the results of [CF96] using [LM09].

Proposition 7.4 ([5], adapted from [CF96]). *Let R be a Hermitian, p.s.d., generalized Toeplitz matrix. If R is flat, then there exists a unique non-negative measure m such that $R = \mathbb{M}_\ell(m)$, and that measure is $(\text{rank } R)$ -sparse.*

In fact, a sufficient condition for existence (without uniqueness) is that R admits a flat extension, i.e. a matrix indexed by $\llbracket -(\ell+1), \ell+1 \rrbracket^d$ which extends R and which is flat. But it is difficult to check that property in practice, and checking that R itself is flat is one practical way to ensure that such a flat extension exists.

A hierarchy of Semi-Definite Programs

Following the principle of the hierarchies introduced by J.-B. Lasserre [Las01], we introduce a family of problems on p.s.d. generalized Toeplitz matrices, with the hope that some solution is a moment matrix, so that the energy coincides with the problem on measures ($\mathcal{Q}_0(z)$). We denote by \mathcal{H}_ℓ^+ the set of Hermitian, positive semi-definite matrices indexed by $\llbracket -\ell, \ell \rrbracket^d$, and by \mathcal{T}_ℓ the set of generalized Toeplitz matrices.

Given $\ell \geq f_c$ we introduce the following problems.

$$\min_{\substack{R \in \mathcal{H}_\ell^+, \\ \tilde{z} \in \mathbb{C}^{(2\ell+1)^d}, \tau \in \mathbb{R}}} \frac{1}{2} \left(\frac{1}{(2\ell+1)^d} \text{Tr}(R) + \tau \right) \quad \text{s.t.} \quad \begin{cases} (a) & \begin{bmatrix} R & \tilde{z} \\ \tilde{z}^* & \tau \end{bmatrix} \succeq 0 \\ (b) & \tilde{z}_k = z_k, \quad \forall k \in \Omega_c \\ (c) & R \in \mathcal{T}_\ell \end{cases} \cdot (\mathcal{Q}_0^{(\ell)}(z))$$

The following result ensures that those problems approximate $(\mathcal{Q}_0(z))$ better and better.

Proposition 7.5 ([5, Prop. 2]). *Let $z \in \mathbb{C}^{(2f_c+1)^d}$. For any $\ell \geq f_c$,*

$$\min(\mathcal{Q}_0^{(\ell)}(z)) \leq \min(\mathcal{Q}_0^{(\ell+1)}(z)) \leq \min(\mathcal{Q}_0(z)). \quad (7.41)$$

Moreover, $\lim_{\ell \rightarrow +\infty} \min(\mathcal{Q}_0^{(\ell)}(z)) = \min(\mathcal{Q}_0(z))$.

It may happen that the equality holds not only in the limit but also for finite ℓ . In that case, the connection between $(\mathcal{Q}_0^{(\ell)}(z))$ and $(\mathcal{Q}_0(z))$ is clarified by the following Proposition.

Proposition 7.6 ([5, Prop. 3]). *Let $\ell \geq f_c$. Then, $\min(\mathcal{Q}_0^{(\ell)}(z)) = \min(\mathcal{Q}_0(z))$ if and only if there exist (R, z, τ) solution to $(\mathcal{Q}_0^{(\ell)}(z))$ and m solution to $(\mathcal{Q}_0(z))$ such that*

$$\tau = |m|(\mathbb{T}^d) \quad \text{and} \quad R_{i,j} = \int_{\mathbb{T}^d} e^{-2i\pi\langle i-j, x \rangle} d|m|(x) \quad (7.42)$$

for all $i, j \in \llbracket -\ell, \ell \rrbracket^d$. In particular, if m is a discrete measure with cardinal s , then $\text{rank } R \leq s$.

In fact, as shown in Paul Catala's PhD thesis, the connection between R, \tilde{z} and m hold as soon as R is a moment matrix.

Proposition 7.7 ([Cat20, Prop. 8]). *Let $\mathcal{R} = \begin{pmatrix} R & \tilde{z} \\ \tilde{z}^* & \tau \end{pmatrix}$ be a solution to $(\mathcal{Q}_0^{(\ell)}(z))$. If R is the moment matrix of a sparse measure $\tilde{m} = \sum_{j=1}^s b_j \delta_{x_j}$ ($\tilde{m} \geq 0$), then \tilde{z} is the vector of Fourier coefficients of some measure m solution to $(\mathcal{Q}_0(z))$ with $|m| = \tilde{m}$. Moreover, $\min(\mathcal{Q}_0^{(\ell)}(z)) = \min(\mathcal{Q}_0(z))$.*

7.3.3 The Fourier-Frank-Wolfe Algorithm

Although we have focused on the constrained problem $(\mathcal{Q}_0(z))$, let us note that the above discussion allows to reformulate (7.32) as

$$\min_{\substack{R \in \mathcal{H}_\ell^+, \\ \tilde{z} \in \mathbb{C}^\ell, \\ \tau \in \mathbb{R}}} \frac{1}{2} \left(\frac{\text{Tr}(R)}{(2\ell+1)^d} + \tau \right) + \frac{1}{2\lambda} \|y - H_\varphi z\|_{\mathcal{H}}^2 \quad \text{s.t.} \quad \begin{cases} (a) & \begin{bmatrix} R & \tilde{z} \\ \tilde{z}^* & \tau \end{bmatrix} \succeq 0 \\ (b) & z_k = \tilde{z}_k \quad \forall k \in \llbracket -f_c, f_c \rrbracket^d \\ (c) & R \in \mathcal{T}_\ell \end{cases} \quad (\mathcal{Q}_\lambda^{(\ell)}(y))$$

The same convergence properties for the hierarchies of relaxations hold.

Our goal is to use Algorithm 1 (or a variant) to solve $(\mathcal{Q}_\lambda^{(\ell)}(y))$. However, the constraint set is the intersection of the positive semi-definite cone and the vector space of generalized Toeplitz matrices. It is not clear how to minimize linear forms on such a convex set. Therefore, we relax the Toeplitz constraint and we consider the following problem.

$$\min_{\tau, z, R} \frac{1}{2} \left(\frac{1}{(2\ell+1)^d} \text{Tr}(R) + \tau \right) + \frac{1}{2\lambda} \|y - H_\varphi z\|_{\mathcal{H}}^2 + \frac{1}{2\rho} \|R - P_{\mathcal{T}_\ell}(R)\|^2 \quad (\mathcal{Q}_{\lambda, \rho}^{(\ell)}(y))$$

$$\text{s.t.} \quad \begin{cases} \begin{bmatrix} R & \tilde{z} \\ \tilde{z}^* & \tau \end{bmatrix} \succeq 0 \\ \tilde{z}_k = z_k, \quad \forall k \in \llbracket -f_c, f_c \rrbracket^d \end{cases}$$

where $P_{\mathcal{T}_\ell}$ is the projector on the set \mathcal{T}_ℓ and the parameter ρ controls the penalization of the Toeplitz constraint. Such a penalization produces good approximation of the solutions of $(\mathcal{Q}_\lambda^{(\ell)}(y))$ (see the theoretical and numerical study in [5]).

To work on a compact domain, we truncate it using a constraint set of the form

$$K \stackrel{\text{def.}}{=} \left\{ \mathcal{R} = \begin{pmatrix} R & \tilde{z} \\ \tilde{z}^* & \tau \end{pmatrix} \mid \mathcal{R} \succeq 0, \frac{1}{(2\ell+1)^d} \text{Tr}(R) + \tau \leq \frac{1}{2\lambda} \|y\|_{\mathcal{H}}^2 \right\}. \quad (7.43)$$

Up to rescalings, minimizing a linear form on K , say $\mathcal{R} \mapsto \text{Tr}(\mathcal{R}M)$ for some matrix M , can be done by applying the *power iterations method*.

In our setting, let

$$f(\mathcal{R}) \stackrel{\text{def.}}{=} C_0 \left(\frac{1}{2} \left(\frac{\text{Tr}(R)}{(2f_c+1)^d} + \tau \right) + \frac{1}{2\lambda} \|y - \mathcal{A}z\|_{\mathcal{H}}^2 + \frac{1}{2\rho} \|R - P_{\mathcal{T}_\ell}(R)\|^2 \right), \quad (7.44)$$

where $C_0 \stackrel{\text{def.}}{=} 2\lambda / \|y\|_{\mathcal{H}}^2$. The matrix M that we have to iterate is

$$\nabla f(\mathcal{R}) = C_0 \begin{bmatrix} \frac{1}{2(2f_c+1)^d} I + \frac{1}{\rho} (R - P_{\mathcal{T}_\ell}(R)) & \frac{1}{2\lambda} H_\varphi^* (H_\varphi z - y) \\ \frac{1}{2\lambda} (H_\varphi^* (H_\varphi z - y))^* & \frac{1}{2} \end{bmatrix}, \quad (7.45)$$

Although the matrix \mathcal{R} is very large, several key observations make this approach tractable:

Memory-efficient storage. If the algorithm starts from $\mathcal{R}^{(0)} = 0$, at the k -th iteration the iterate $\mathcal{R}^{(k)}$ has rank at most k , since at each iteration the Frank-Wolfe procedure adds one eigenvector of $\nabla f(\mathcal{R}^{(k)})$ (up to some rescalings, see [Algorithm 3](#)). Therefore, we write our iterate as $\mathcal{R}^{(k)} = \mathcal{U}^{(k)} \mathcal{U}^{(k)*}$, where $\mathcal{U}^{(k)} \in \mathbb{C}^{((2f_c+1)^d+1) \times k}$. We only store the matrix $\mathcal{U}^{(k)}$, and at each iteration we add a column to it.

Fast Fourier Transform (FFT) computations. When applying the matrix $M = \nabla f(\mathcal{R}^{(k)})$ to a vector $\begin{pmatrix} w_1 \\ \omega \end{pmatrix}$, the computation of $\frac{1}{2(2f_c+1)^d} I + \frac{1}{\rho} R$ $w_1 = (\frac{1}{2(2f_c+1)^d} w_1 + \frac{1}{\rho} \mathcal{U}^{(k)} (\mathcal{U}^{(k)*} w_1))$ involves only the products of small matrices. But the computation of $P_{\mathcal{T}_\ell}(R)$ can be quite involved. It turns out that computing this projection and applying the corresponding Toeplitz operator amount to a discrete convolution with zero-padding of well chosen vectors (see [5, Prop. 5 and 6]). As a result, it can be computed using the Fast Fourier Transform (FFT), which requires only $O(N \log N)$ operations, where $N = (2\ell+1)^d + 1$.

Diagonal matrices. It remains to compute $H_\varphi^* H_\varphi z$. That is not necessarily very difficult. As noted above, in the convolution case H_φ is diagonal. In the case of sub-sampled convolution observations on a regular grid \mathcal{G} of dimension $L_1 \times \dots \times L_d$, if $2f_c < \min(L_1, \dots, L_d)$, the columns of H_φ are orthogonal, and therefore the matrix $H_\varphi^* H_\varphi$ is diagonal. If $2f_c \geq \min(L_1, \dots, L_d)$, $H_\varphi^* H_\varphi$ is not diagonal, but only a few of its diagonals are non-zeros. Therefore, in these two cases, the computation and the storage of $H_\varphi^* H_\varphi z$ are not very expensive.

However, for general non-translation-invariant operators (such as spatially varying filtering case), the matrix $H_\varphi^* H_\varphi$ is of size $(2f_c+1)^d \times (2f_c+1)^d$ (since H_φ is of size $|\mathcal{G}| \times (2f_c+1)^d$) and needs to be fully stored.

As in the case of the Sliding Frank-Wolfe, a key to a fast convergence of the algorithm is to add a *non-convex corrective step*. The non-convex step that we add after each Frank-Wolfe update consists, in a gradient (or BFGS) descent on $F : \mathcal{U} \mapsto f(\mathcal{U}\mathcal{U}^*)$. The idea

is to continuously move the iterate \mathcal{U} in the manifold of fixed rank matrices to improve the value of the functional. This is similar to the celebrated Burer-Monteiro non-convex method for low-rank minimization, which has proven to be very efficient in practice [BVB16].

The full algorithm is summarized in Algorithm 3. In Line 3, the matrix J_ℓ is simply a diagonal matrix, of the form,

$$J_\ell \stackrel{\text{def.}}{=} \begin{pmatrix} \frac{1}{(2\ell+1)^d} I_{(2\ell+1)^d} & 0 \\ 0 & 1 \end{pmatrix} \quad (7.46)$$

and the argmin is computed using the power iterations, which can be done efficiently as explained above. In Line 7, the optimal coefficients α and β can be computed explicitly (see [5, Prop. 7]). In Line 8, a local descent is performed using the BFGS algorithm, which can be done efficiently too, using the same tricks. In particular, both the objective and its gradient can be evaluated using $H_\varphi^* H_\varphi$ (and not H_φ), for instance $\|y - H_\varphi z\|_{\mathcal{H}}^2 = \|y\|_{\mathcal{H}}^2 - 2\Re \langle H_\varphi^* y, z \rangle + \langle H_\varphi^* H_\varphi z, z \rangle$, and the vector $H_\varphi^* y$ can be pre-computed. In the case of convolutions or subsampled convolutions on a regular grid, that is particularly interesting since $H_\varphi^* H_\varphi$ is diagonal. The computational costs of evaluating the gradients in Line 3 and Line 8 are gathered in Table 7.1 in the different cases (assuming regular grids).

Algorithm 3 Fourier-Frank-Wolfe Algorithm

1: Initialize with $\mathcal{U}_0 = [0 \dots 0]^\top$, $D_0 = 2f(0)$.

2: **for** $r = 0, 1, \dots$ **do**

3: Linear minimization:

$$v_r = D_0 J_\ell^{-\frac{1}{2}} \left(\arg \min_{\|v\| \leq 1} v^\top \cdot \left(J_\ell^{-\frac{1}{2}} \nabla f(\mathcal{U}_r \mathcal{U}_r^*) J_\ell^{-\frac{1}{2}} \right) \cdot v \right) J_\ell^{-\frac{1}{2}}$$

4: **if** $\langle \mathcal{U}_r \mathcal{U}_r^* - v_r v_r^*, \nabla f(v_r v_r^*) \rangle \leq \varepsilon f(x_0)$ **then**

5: (R, \tilde{z}, τ) such that $\mathcal{U}_r = \begin{pmatrix} R & \tilde{z} \\ \tilde{z}^* & \tau \end{pmatrix}$ is an (approximate) solution of $(\mathcal{Q}_0^{(\ell)}(z))$.

Stop.

6: **else**

7: Obtain

$$\hat{\mathcal{U}}_{r+1} = \left[\sqrt{\alpha_r} \mathcal{U}_r, \sqrt{\beta_r} v_r \right], \text{ where}$$

$$\alpha_r, \beta_r = \arg \min_{\alpha \geq 0, \beta \geq 0, \alpha + \beta \leq 1} f(\alpha \mathcal{U}_r \mathcal{U}_r^* + \beta v_r v_r^*)$$

8: Corrective step (local minimization)

$$\mathcal{U}_{r+1} = \text{bfgs} \left\{ \mathcal{U} \mapsto f(\mathcal{U} \mathcal{U}^*) \mid \mathcal{U} \in \mathbb{C}^{((2\ell+1)^d+1) \times (r+1)}, \text{ starting from } \hat{\mathcal{U}}_{r+1} \right\}$$

9: **end if**

10: **end for**

7.3.4 Extracting the support from the moment matrices

Once the moment matrix R has been found, it remains to extract the support and find the corresponding measure, which is not trivial. We only briefly sketch some directions,

Table 7.1: *Computational costs.*

Filter Φ	$f'(\mathcal{U})$ w	$F'(\mathcal{U})$
convolution	$O(r\ell^d \log \ell)$	$O(r^2\ell^d + r\ell^d \log \ell)$
subsampled convolution (with regular grid)	$O(r\ell^d \log \ell)$	$O(r^2\ell^d + r\ell^d \log \ell)$
spatially varying filtering	$O(r\ell^d \log \ell + f_c^{2d})$	$O(r^2\ell^d + r\ell^d \log \ell + f_c^{2d})$

since it would lead us too far in the description of notions of algebraic geometry, but that is roughly an extension to the multidimensional setting of Prony’s method [dP95]. We refer to Paul Catala’s PhD thesis [Cat20] for more detail.

Assuming that R is flat (hence it provides the moments of a uniquely determined measure), the Stetter-Möller method [MS95] consists in building the so-called multiplication matrices corresponding to the moment matrix R (see [Las10, Ch.4], [HKM17, JLM19]), which can be done using the singular value decomposition (SVD) or a Gram-Schmidt decomposition of R .

Roughly speaking, one builds a matrix N_j ($1 \leq j \leq d$) which represents the operation of multiplying a (class of) trigonometric polynomial (in a well chosen quotient space which depends on $\ker R$) with a monomial $e^{2i\langle e_j, x \rangle}$,

$$N_j: P \longmapsto \left(x \mapsto e^{2i\langle e_j, x \rangle} P(x) \right),$$

where e_j is j -th vector of the canonical basis of \mathbb{R}^d . The N_j ’s are co-diagonalizable and their common eigenvalues are $e^{2i\langle e_j, x_i \rangle}$ ($1 \leq i \leq s$) if the underlying measure is $\sum_{i=1}^s b_i \delta_{x_i}$. In practice, the joint diagonalization of the N_j ’s allows us to recover the different components $(e^{2i\langle e_j, x_i \rangle})_{1 \leq j \leq d}$ for each x_i in the support. That joint diagonalization is usually done by diagonalizing a random linear combination of the N_j ’s. We refer to [JLM19] for a comparison of this method with several variants.

In his PhD thesis [Cat20], Paul Catala has shown that, when trying to estimate measures which have a continuous support (e.g. curves, or sets with nonempty interior), the above joint diagonalization procedure may fail in finding the correct support. He has proposed a joint diagonalization algorithm which addresses that issue with a variational approach. The proposed method works much better than the previous method for non sparse measures. The interested reader may consult [Cat20, Sec. 1.6.3].

7.3.5 Numerical examples

We discuss here numerical results provided by Paul Catala’s implementation of the Fourier-Frank-Wolfe algorithm⁵. A first reconstruction example using different forward operators is shown in Figure 7.11 (on synthetic data). We have also tested our method on images from the Single-Molecule Localization Microscopy (SMLM) challenge [EPF13], see Section 7.2.3 for the principle of SMLM. An example of frame is shown in Figure 7.12. The full reconstruction Figure 7.13, left image, is obtained by super-resolving 12000 such images with randomly activated molecules.

We display the performance (in terms of the Jaccard index, see Equation (7.24)), versus the number of BFGS iterations in Figure 7.13. Indeed, as the non-convex

⁵<https://github.com/Paulcat/Super-Resolution-SDP>

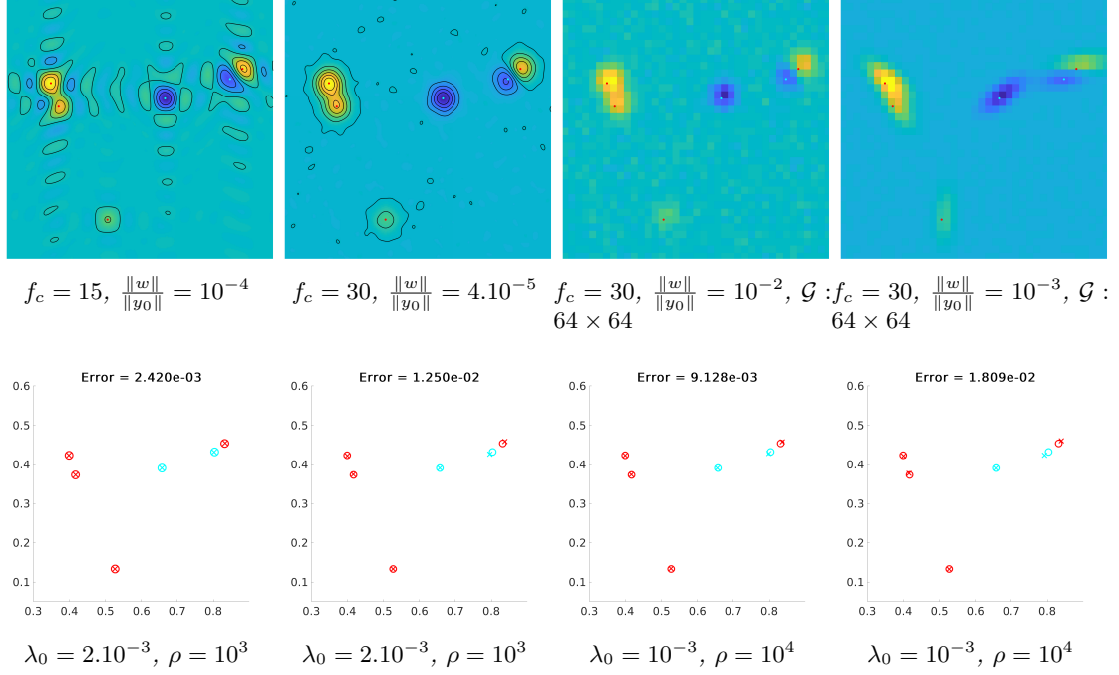


Figure 7.11: From left to right: Measurements $y = \Phi m_0 + w$ (we plot $\mathcal{F}_c^* y$ in the first two figures) in the case of Dirichlet convolution, Gaussian convolution, Subsampled Gaussian convolution, and (Subsampled) Gaussian foveation. The support of m_0 is represented by red (positive spikes) and blue (negative spikes) dots. On the bottom line, the indicated errors are defined as $\|x_0 - x_r\| / \|x_0\|$, x_0 and x_r being respectively the ground-truth and the reconstructed supports.

corrective step is the most costly step, one may wish to bound the number of BFGS iterations.

Empirically, it seems that a finite convergence as in the Sliding-Frank-Wolfe algorithm occurs, at least when the spikes of the unknown measure are sufficiently separated.

Eventually, let us mention that the Fourier Frank-Wolfe method can be adapted to other problems than the BLASSO. In Paul Catala's PhD thesis, the algorithm is extended to Optimal Transport problems, see for instance Figure 7.14 for an example of transport between two continuous measures. Numerically, that is quite challenging, as a transport plan between two measures 2-dimensional domains is a measure defined on a 4-dimensional domain. As a result, the relaxation is only taken to the order $\ell = 10$.

7.4 Conclusion

7.4.1 Summary

The use of extreme points in inverse problems is not only relevant theoretically, but also numerically. The Frank-Wolfe (or conditional gradient) algorithm is an optimization method which is suitable beyond the framework of Hilbert spaces, one may typically apply it in Banach spaces or locally convex vector spaces; for our concern we have used in the space of Radon measures. It turns out that the linear minimization step can be solved by choosing an extreme point of the constraint set (or level set of the regularizer). When the set of extreme points has a smooth structure, one may take advantage of that, using an additional property of Frank-Wolfe: one may choose the next iterate as any feasible point which has lower energy than the exact line search. It results in algorithms which interwind linear minimizations and local (non-convex) descents which optimize

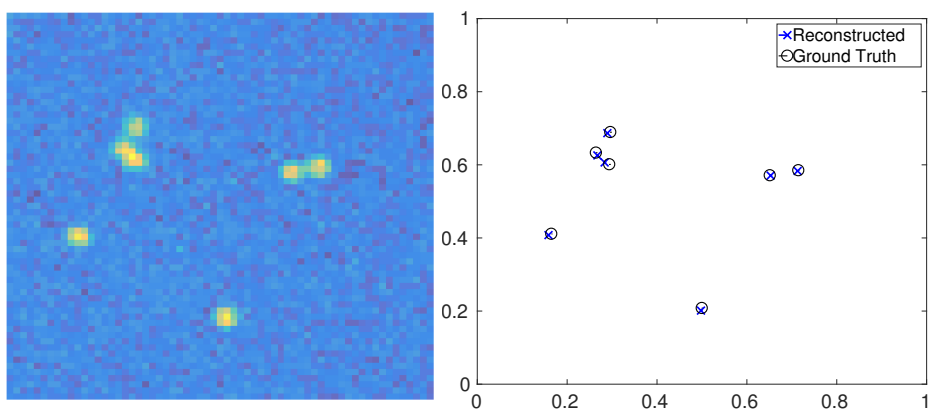


Figure 7.12: Example of reconstruction on data from the smlm challenge. Relative error is $\|x_{rec} - x_0\| / \|x_0\| = 1.57 \times 10^{-2}$

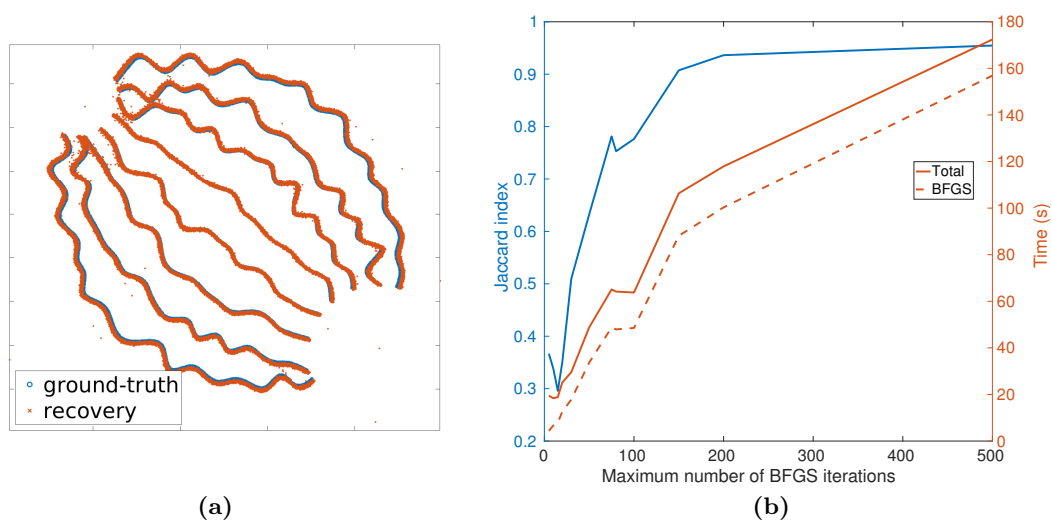


Figure 7.13: Left: Recovery from a full dataset of SMLM challenge. This result is obtained by combining the super-resolved output of 12000 individual frames similar to Figure 7.12. Right: Performance versus maximum number of BFGS iterations

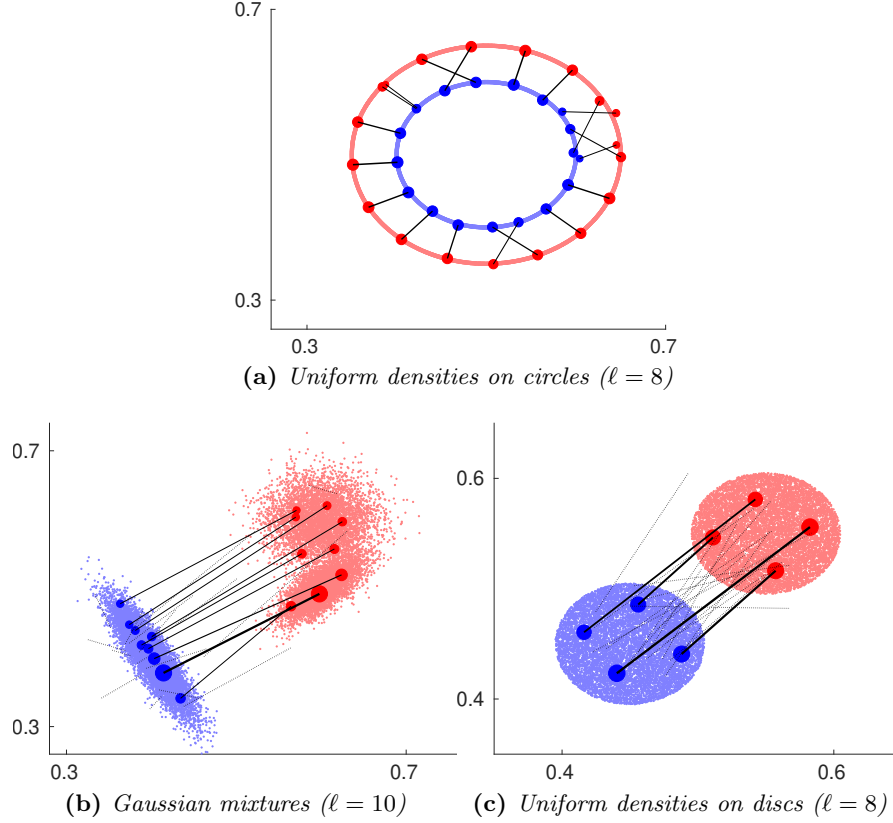


Figure 7.14: Examples of transport between “continuous” measures recovery using the FFW algorithm.

over all the selected extreme points, as suggested in [BP13, BSR17]. We have applied that powerful principle to the case of Radon measures and moment matrices, corresponding respectively to the Sliding Frank-Wolfe and the Fourier Frank-Wolfe algorithms. One major advantage of the non-convex refinement is that it allows for convergence after a finite number of outer iterations, under some non-degeneracy property.

7.4.2 Comments

Sliding Frank-Wolfe versus FISTA on a grid. A standard approach for solving super-resolution problems is to define a grid on the domain X and to solve the corresponding LASSO problem, for instance using FISTA [BT09]. As we have seen in Chapter 5 this induces moderate discretization artifacts. Still, proximal methods are well understood and are quite efficient, and it is not obvious that an “infinite-dimensional” method like the SFW could be a viable alternative. In his PhD thesis [Den18], Quentin Denoyelle has made an extensive comparison of both approaches, using the sampled Laplace forward operator. It turns out that SFW outperforms FISTA both in terms of quality of estimation (even if the output of FISTA is postprocessed with a clustering step) and in computation time. That illustrates the power of “gridless” methods: the elementary steps such as the update rule are done on small vectors, yielding small problems, and the continuous nature of the observation operator is exploited by the sliding step.

Update rules in the Sliding Frank-Wolfe. In Line 3 of Algorithm 2, we only add one element of the set of maximizers of $|\eta^{[k]}|$ to the current support, as follows straightforwardly from the standard Frank-Wolfe algorithm. Still, other strategies may

be employed. Motivated by a connection with exchange methods in semi-infinite programming (see also [ET19]), the authors of [FdGW21] have advocated for the addition of every local maximizer of $\eta^{[k]}$, which seems to be more efficient.

Semi-definite programs and hierarchies for the Blasso. It should be noted that semi-definite programs for the resolution of the BLASSO and variants have been used since [CFG14, CFG13]. However, the problem they use is a reformulation of the dual problem $(\mathcal{D}^{(\text{TV})}(0, y))$ (resp. $(\mathcal{D}^{(\text{TV})}(\lambda, y))$) which aims at finding a dual polynomial. It turns out that the p.s.d. matrices involved do not have low rank, in fact the dimension of their kernel is typically the number of saturations points of the polynomial (in general, the number of recovered Dirac masses), which is generally small. Therefore, it is difficult to encode such matrices. On the contrary, the moment approach that we have used (inspired from [TBSR13]) takes advantage of the low rank of moment matrices and makes it possible to solve 2D (and even 4D when recovering transport plans in optimal transport) problems. Let us mention that hierarchies for the BLASSO in the real polynomial setting were developed in [DCGHL17]. In [YXS16], the authors develop a trigonometric moment approach similar but complementary to ours (relying on a Vandermonde decomposition, which hold only in specific cases, instead of hierarchies).

Conic Particle Gradient Descent. An alternative to the Sliding Frank-Wolfe or the Semi-definite programs for the resolution of the BLASSO is the Conic Particle Gradient Descent proposed in [CB18, Chi21]. The idea is to initialize the algorithm with many Dirac masses, and then to let them evolve according to a gradient flow for a specific metric. The main result is that, if the initialization point is sufficiently close to the uniform measure on X , the algorithm converges towards a solution of the problem. Key properties of the Conic Particle Gradient Descent are its easiness of implementation and the low computational cost of each iteration.

For a detailed comparison of semi-definite programs, Sliding Frank-Wolfe, and the Conic Particle Gradient Descent on Single Molecule Localization Microscopy (SMLM) data, see the review [LBFA21].

Finite convergence of hierarchies In dimension $d = 2$, the hierarchy of relaxations introduced in Section 7.3.2 should be tight at some finite order $\ell \geq f_c$, as a consequence of a result of Scheiderer [Sch06] which states that a positive trigonometric polynomial admits a sum-of-squares representation. However, the corresponding order is unknown. In our experiments, we have always observed convergence at $\ell = f_c$.

A recent result [YXS16] (see also [AC16]) states that every Hermitian p.s.d. generalized Toeplitz matrix with rank $r \leq f_c$ has a Vandermonde decomposition. Since our variational problem $(\mathcal{Q}_0^{(\ell)}(z))$ involves the trace, which tends to promote low-rank solutions, that could explain why we have always observed this convergence at $\ell = f_c$.

Chapter 8

Conclusion and perspectives

The classical Carathéodory theorem and the decomposition of a convex set into its elementary faces are simple principles which have far-reaching consequences in linear inverse problems.

When the number of measurements is finite (as is the case in practical applications), it is possible to decompose some solutions of variational problems as convex combinations of the extreme points of the level sets of the regularizer ([Chapter 1](#)). The family of “decomposable” solutions is rich enough to describe the whole solution set, insofar as it includes all the extreme points and the extreme rays of the solution set.

The “atoms” of that decomposition provide a lot of information on the structures promoted by the regularizer R . But sometimes the knowledge of the extreme points of the level sets of R is not enough. One needs to understand how they are organized into finite-dimensional faces to describe finely the structure of the solutions. In that respect, the case of the total (gradient) variation is particularly interesting ([Chapter 2](#)).

When it comes to studying the stability of such decompositions, one needs to assume more regularity. The theory of duality exposed in [Chapter 3](#) is helpful for that: the solutions to the dual problem give access to a “dual certificate”, *i.e.* a subgradient of R , which exposes a face of the epigraph of R which contains the solutions of the primal problem. Therefore it gives access to a face (perhaps not the minimal one) which contains them.

When both the noise and the regularization are small, the dual solutions concentrate around the minimal-norm solution to the (noiseless) dual problem, which gives access to the *minimal-norm certificate*. Understanding that certificate is the key to understanding the behavior of the reconstruction at low noise. We have described in [Chapter 4](#) a linearization procedure which gives access to it if one is able to guess its minimal face in the feasible set of the dual problem.

The stability of the decomposition is then studied in [Chapter 5](#) in the cases of the LASSO, BLASSO, and total variation denoising. In all cases, it is possible to obtain the Hausdorff convergence of the support when the noise and the regularization parameter vary. In the polyhedral case, the support is thus locally constant, provided the dual certificate is tight. However, if the problem comes from the discretization of a continuous one, the tightness of the dual certificate almost never holds, and discretization artifacts appear. For the BLASSO, the support identification is not granted: even with a tight dual certificate, the cardinal of the support may vary. It is the examination of the *second derivatives* of the dual certificate which allow to ensure identification of the support. In that case, the solutions have the same structure and the locations and amplitudes vary smoothly.

A limitation of the BLASSO is the impossibility to recover measures with spikes with

opposite signs that are too close. However, if all the spikes have the same sign, it is possible, under some assumptions, to recover the unknown measure and the condition on the noise is studied in [Chapter 6](#).

On the numerical side, the Frank-Wolfe algorithm produces iterates that have the same structure as our “decomposable” solutions: they are a convex combination of a few extreme points of the level sets of the regularizer. The Sliding Frank-Wolfe and Fourier Frank-Wolfe described in [Chapter 7](#) take advantage of that property together with the possibility of improving the iterates using a non-convex update which consists in moving the selected extreme points. Such a non-convex update allows for finite-time termination of the global algorithm in non-degenerate cases. It results in very efficient algorithms which solve the BLASSO in a competitive way compared to the state of the art. Their applicability to practical problems has been demonstrated on Single-Molecule Localization Microscopy datasets, which are particularly suited to the BLASSO.

While investigating all the above-mentioned topics, I was struck by the power of the continuous approach (BLASSO) compared to the discrete one (LASSO). For instance, the study of support stability in discrete problems is possible on the last solution path (which corresponds to some face of the regularizer), but it becomes tedious beyond that last path (which is all the shorter as the grid is thin). That study is considerably simplified in the continuous problem by the use of differential calculus: the faces vary continuously and it is then easy to track them as the parameters (noise, regularization level) vary. The grid, which is introduced as a computational tool rather than an object relevant to the physical problem, somehow obscures the problem. In terms of numerical computations, thin grids also tend to induce a heavy computational load and numerical instabilities. On the contrary, algorithms which work in the continuous setting have a low memory footprint, and exploit the differential structure of the problem.

The surprising thing is that, after all, it is possible to study and numerically solve problems in the space of Radon measures, which is infinite-dimensional - and rather complicated. The cornerstone is the representer theorem and the Frank-Wolfe algorithm, which rely on Carathéodory’s theorem and the decomposition of convex sets into their elementary faces. As they only manipulate the atoms induced by the total variation of measures (Dirac masses), which are easy to work with, they open the door to analysis and computations. It is therefore natural to ask if it can be extended beyond that case.

Is it possible to go beyond the recovery of pointwise sources and recover more complex objects (like curves, or shapes)?

That is certainly a challenging question, since the corresponding atoms would be more difficult to handle than the simple Dirac masses. However, capturing the essence of a continuous problem and removing the artifacts induced by the discretization grids (anisotropy, blur) is a promising avenue.

Recently, a step towards the recovery of curves in a continuous setting has been made with the series of papers [[BCFR20](#), [BF20](#), [BCF20](#), [BCFR21](#)] which relate the extreme points of the optimal transport squared distance (through the Benamou-Brenier formula) and measures supported on curves. An algorithm has been proposed, but it is computationally demanding, as the space of curves (even though they are sampled in time) is large. Providing a fast algorithm is crucial for practical applications. Understanding the performance of the model is also interesting (stability, identifiability).

As for the total (gradient) variation, we have already gathered some information in this thesis, with the structure of the faces and the Hausdorff convergence of the support. Designing an algorithm which exploits the faces of the total variation unit ball is quite challenging, and several approaches are possible. Moreover, it is natural to wonder if an equivalent condition of the “non-degeneracy” of the dual certificates of the BLASSO

(namely, the fact that the Hessian is definite) exists for the total gradient variation. In particular, is it possible to ensure that the reconstructed solution has the same number of simple sets as the reference solution?

Together with my students Romain Petit (PhD, co-supervised with Yohann De Castro) and Robert Tovey (postdoc), we are currently investigating those two problems that I find fascinating.

Beyond, the understanding of more modern regularizers such as the total generalized variation (TGV) seems to be an even more challenging horizon [\[TW21\]](#).

Appendix A

Reminder on the properties of BV functions

This appendix summarizes a few basic notions on functions with bounded variation and sets of finite perimeter. We refer the reader to [AFP00, Mag12] for more detail on this topic.

Definition A.1. Let $\Omega \subseteq \mathbb{R}^d$ be an open set, and $u: \Omega \rightarrow \mathbb{R}$ a locally integrable function. We define the variation of u as

$$V(u, \Omega) \stackrel{\text{def.}}{=} \sup \left\{ \int_{\mathbb{R}^d} u \operatorname{div}(\varphi) \mid \varphi \in \mathcal{C}_c^1(\mathbb{R}^d; \mathbb{R}^d), \sup_{x \in \mathbb{R}^d} |\varphi(x)|_2 \leq 1 \right\}. \quad (\text{A.1})$$

By the Radon-Riesz representation theorem, $V(u, \Omega) < +\infty$ if and only if the distributional derivative Du is a bounded (vector) Radon measure, in which case $V(u, \Omega)$ is the (vector) total variation of the measure Du . In any case, we commonly write $|Du|(\Omega)$ for $V(u, \Omega)$.

Given a Lebesgue measurable set $A \subseteq \Omega$, we say that A has finite perimeter (in Ω) if $V(\mathbb{1}_A, \Omega) < +\infty$, and we define its perimeter as $P(A, \Omega) \stackrel{\text{def.}}{=} V(\mathbb{1}_A, \Omega)$. If $\Omega = \mathbb{R}^d$, we simply denote it by $P(A)$. Note that A has finite perimeter if and only if so has A^c , and $P(A) = P(A^c)$.

If A has smooth boundary, then $P(A, \Omega)$ is simply the $(d-1)$ -surface of its boundary $(\partial A) \cap \Omega$. In the general case, $P(A, \Omega)$ is the $(d-1)$ -dimensional Hausdorff measure of its *reduced boundary* $\partial^* A$, $P(A, \Omega) = \mathcal{H}^{d-1}((\partial^* A) \cap \Omega)$, where

$$\partial^* A \stackrel{\text{def.}}{=} \left\{ x \in \operatorname{Supp}(D\mathbb{1}_A) \mid \lim_{r \rightarrow 0^+} \frac{-D\mathbb{1}_A(B(x, r))}{|D\mathbb{1}_A(B(x, r))|} \text{ exists and has unit norm} \right\}. \quad (\text{A.2})$$

For $x \in \partial^* A$, the measure theoretic outer unit normal $\nu_A(x)$ is defined as the limit in (A.2).

An important property of the perimeter is its *submodularity*, namely

$$P(A \cup B) + P(A \cap B) \leq P(A) + P(B). \quad (\text{A.3})$$

The variation of a function is related to the perimeter of its level sets through the *coarea formula*.

Theorem A.1 (Coarea formula, [AFP00, Thm. 3.40]). For any open set $\Omega \subseteq \mathbb{R}^d$, and all locally integrable function $u: \Omega \rightarrow \mathbb{R}$, the variation of

$$V(u, \Omega) = \int_{-\infty}^{+\infty} P(\{x \in \Omega \mid u(x) > t\}, \Omega) dt.$$

In particular, if $V(u, \mathbb{R}^d) < +\infty$ the set $\{u > t\}$ has finite perimeter for a.e. $t \in \mathbb{R}$ and

$$|Du|(B) = \int_{-\infty}^{+\infty} |D\mathbf{1}_{\{u>t\}}|(B)dt, \quad (\text{A.4})$$

for any Borel set $B \subseteq \Omega$.

We have used the notation $\{u > t\} \stackrel{\text{def.}}{=} \{x \in \Omega \mid u(x) > t\}$ (and similarly for $<$, \geq , and \leq).

Since the set of $t \in \mathbb{R}$ such that $L^d(\mathbb{R}^d)(\{x \in \Omega \mid u(x) = t\}) > 0$ is at most countable, we may replace the sets $\{x \in \Omega \mid u(x) > t\}$ with $\{x \in \Omega \mid u(x) \geq t\}$, or even with $\{x \in \Omega \mid u(x) < t\}$ or $\{x \in \Omega \mid u(x) \leq t\}$ using that $P(A) = P(A^c)$.

Appendix B

Duality and subdifferentials

The subdifferential of a convex function as well as the duality between variational problems involve the notion of *dual space*. The reader might be surprised that, in our analysis, we regard spaces such as the space $\mathcal{M}(X)$ of bounded Radon measures as the *primal space* where the *primal problem* should be solved, while we see the space $\mathcal{C}_0(X)$ of continuous functions (vanishing at infinity) as its *dual space*. Indeed, $\mathcal{C}_0(X)$ is a non-reflexive Banach space, and while $\mathcal{M}(X)$ is its (topological) dual, the dual of $\mathcal{M}(X)$ is strictly larger than $\mathcal{C}_0(X)$!

The present chapter explains that, instead of considering each set as a Banach space together with its topological dual, using a duality pairing together with suitable topologies makes the situation perfectly symmetric: spaces like $\mathcal{M}(X)$ and $\mathcal{C}_0(X)$ are dual to each other. After describing that duality pairing, we explain how the subdifferential of a convex function R yields information on the faces $\mathcal{F}_{\text{epi } R}(u, R(u))$ of its epigraph.

B.1 Duality pairing

B.1.1 Definition

Following [Roc89], we consider a *duality pairing* between two real linear spaces V and Υ , *i.e.* a bilinear form $\langle \cdot, \cdot \rangle$ on $V \times \Upsilon$. We say that the duality pairing is *separating in V* if for all $u \in V \setminus \{0\}$, there exists $\eta \in \Upsilon$ such that $\langle u, \eta \rangle \neq 0$. In that case, the mapping $u \mapsto \langle u, \cdot \rangle$ from V to the (algebraic) dual of Υ is injective. The definition of “ V separates the points of Υ ” is symmetric. If both separation properties hold, we say the pairing is separating.

B.1.2 Choice of a topology

A locally convex topology τ_V on V (resp. τ_Υ on Υ) is said to be *compatible* with the pairing if every linear form $\langle \cdot, \eta \rangle$ for $\eta \in \Upsilon$ (resp. $\langle u, \cdot \rangle$ for $u \in V$) is continuous for τ_V (resp. τ_Υ), and if every continuous linear form on V (resp. Υ) has that form.

The weak topology $\sigma(V, \Upsilon)$ induced by Υ on V is always compatible with the pairing [Bou07b, Prop. II.6.3], and it is the weakest of all such topologies. We note that the pairing is separating in V if and only if $\sigma(V, \Upsilon)$ is Hausdorff [Bou07b, Prop II.6.2]. Symmetrically, the pairing is separating in Υ if and only if $\sigma(\Upsilon, V)$ is Hausdorff.

Other choices of compatible topologies are possible, and that choice can become crucial to ensure strong duality between variational problems (see Corollary B.1 below). For instance, the strongest locally convex topology which is compatible with the pairing is known as the Mackey topology [Roc89]. Nevertheless, the Hahn-Banach theorem implies that the closed convex sets (hence the lower semi-continuous convex functions)

only depend on the choice of the linear spaces V and Υ , and not on the particular choice of compatible topology. In the following, when we say that $(V, \Upsilon, \langle \cdot, \cdot \rangle)$ is a *duality pairing* between V and Υ , we always endow V and Υ with compatible topologies which we need not specify, as far as we deal with closed convex sets or lower semi-continuous convex functions.

Example B.1. Let $X \subseteq \mathbb{R}^d$ be an open set and $V \stackrel{\text{def.}}{=} L^p(X)$, $\Upsilon \stackrel{\text{def.}}{=} L^q(X)$ for $1 < p < +\infty$, $1/p + 1/q = 1$. Define

$$\forall (f, g) \in V \times \Upsilon, \quad \langle f, g \rangle \stackrel{\text{def.}}{=} \int_X f(x)g(x)dx. \quad (\text{B.1})$$

On V (resp. Υ), both the strong $L^p(X)$ topology and the weak $L^p(X)$ topology (resp. strong $L^q(X)$ and weak $L^q(X)$ topologies) are compatible with the pairing.

More generally, if V , endowed with some norm, is a Banach space and $\Upsilon = V'$ is its topological dual, then both the strong (induced by the norm) and the weak topologies on V are compatible with the pairing. However, if V is not reflexive, the strong topology of V' (induced by the dual norm) is not compatible with the pairing, since some continuous linear forms on V' are not represented by V . Such is the case of [Example B.1](#) when $p = 1$ and $q = +\infty$ (see [\[Roc89, Sec. 3\]](#)), as well as continuous functions and Radon measures.

Example B.2. Let X be a locally compact separable metric space, and set $V \stackrel{\text{def.}}{=} \mathcal{M}(X)$, $\Upsilon \stackrel{\text{def.}}{=} \mathcal{C}_0(X)$ with

$$\forall (m, \eta) \in V \times \Upsilon, \quad \langle m, \eta \rangle \stackrel{\text{def.}}{=} \int_X \eta(x)dm(x). \quad (\text{B.2})$$

On Υ , both the strong topology induced by $\|\cdot\|_\infty$ and the corresponding weak topology are compatible with the pairing. However, on V , the (strong) topology induced by the total variation norm $\|m\|_{\mathcal{M}} = |m|(X)$ is *not* compatible with the pairing. The dual of the Banach space $\mathcal{M}(X)$ is rather complicated (see [\[Kap57, Kap59, Kap61\]](#)) and strictly contains $\mathcal{C}_0(X)$. On the other hand, the weak-* topology $\sigma(\mathcal{M}(X), \mathcal{C}_0(X))$, *i.e.* the topology induced on $\mathcal{M}(X)$ by $\mathcal{C}_0(X)$ is compatible with the pairing.

B.1.3 Legendre-Fenchel conjugation

The duality pairing allows us to define the Legendre-Fenchel conjugate of a function on V or Υ . Given $f : V \rightarrow \overline{\mathbb{R}}$ (resp. $g : \Upsilon \rightarrow \overline{\mathbb{R}}$) we set $f^* : \Upsilon \rightarrow \overline{\mathbb{R}}$ (resp. $g^* : V \rightarrow \overline{\mathbb{R}}$) as

$$\forall \eta \in \Upsilon, \quad f^*(\eta) \stackrel{\text{def.}}{=} \sup_{u \in V} (\langle u, \eta \rangle - f(u)), \quad \forall u \in V, \quad g^*(u) \stackrel{\text{def.}}{=} \sup_{\eta \in \Upsilon} (\langle u, \eta \rangle - g(\eta)). \quad (\text{B.3})$$

The biconjugate of f is defined as $f^{**} \stackrel{\text{def.}}{=} (f^*)^*$ (and similarly for g). It is equal to f provided f is convex, proper, and lower semi-continuous. We refer to [\[ET76\]](#) for the properties of the Legendre-Fenchel conjugate.

B.2 Normals and subdifferentials

In this section, we discuss the notion of normal cone and relate it the subdifferential of a convex function.

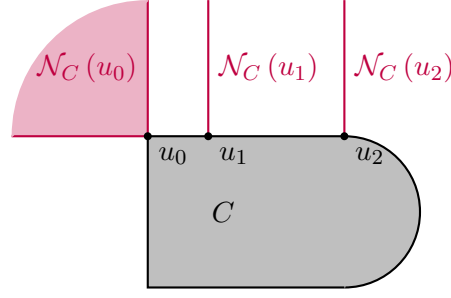


Figure B.1: The point u_2 is an extreme point of C , but it is not exposed. The normal cone at u_2 is the same as the normal cone at u_1 , but they lie on different elementary faces.

B.2.1 Normal cones and exposed faces

We consider a duality pairing $(V, \Upsilon, \langle \cdot, \cdot \rangle)$. Let $C \subseteq V$ be a convex set and $u \in C$. The normal cone to C at u is

$$\mathcal{N}_C(u) \stackrel{\text{def.}}{=} \{ \eta \in \Upsilon \mid \forall u' \in C, \langle u' - u, \eta \rangle \leq 0 \}. \quad (\text{B.4})$$

In other words, $\eta \in \mathcal{N}_C(u)$ if and only if $u \in \mathcal{N}_C^{-1}(\eta)$, where

$$\mathcal{N}_C^{-1}(\eta) \stackrel{\text{def.}}{=} \operatorname{argmax}_{u' \in C} \langle u', \eta \rangle. \quad (\text{B.5})$$

Given $\eta \in \Upsilon$, the set $\{ u' \in C \mid \eta \in \mathcal{N}_C(u') \} = \mathcal{N}_C^{-1}(\eta)$ is therefore a face of C . All the subsets of C of that form are called the *exposed faces* of C . In an elementary face, the normal cone is constant: for all $u' \in \mathcal{F}_C(u)$, $\mathcal{N}_C(u) = \mathcal{N}_C(u')$.

➤ Indeed, let $\eta \in \mathcal{N}_C(u)$. Since $\mathcal{N}_C^{-1}(\eta)$ is a face of C containing u , it must contain $\mathcal{F}_C(u)$, see [Section 1.2.1](#). Hence, $\eta \in \mathcal{N}_C(u)$ implies $\eta \in \mathcal{N}_C(u')$ for all $u' \in \mathcal{F}_C(u)$, so that $\mathcal{N}_C(u) \subseteq \mathcal{N}_C(u')$. Swapping the roles of u and u' (since $\mathcal{F}_C(u) = \mathcal{F}_C(u')$) we obtain the equality.

However, the normal cones do not characterize the elementary faces. In other words, $\mathcal{N}_C(u) = \mathcal{N}_C(u')$ does not imply $\mathcal{F}_C(u) = \mathcal{F}_C(u')$, see [Figure B.1](#).

It is possible to prove that $\{ u' \in C \mid \mathcal{N}_C(u') = \mathcal{N}_C(u) \}$ is a face of C , hence it is a *union of elementary faces* of C (including $\mathcal{F}_C(u)$). Often, one cannot have access to the full cone $\mathcal{N}_C(u)$, but one can simply find one element in $\mathcal{N}_C(u)$. The normals which provide the maximal amount of information are those in the relative algebraic interior of $\mathcal{N}_C(u)$ (provided it is nonempty).

Proposition B.1. *Let $C \subseteq V$ be a convex set, $u \in C$ and $\eta \in \operatorname{rcore}(\mathcal{N}_C(u))$. Then, for all $\eta' \in \mathcal{N}_C(u)$,*

$$\mathcal{F}_C(u) \subseteq \{ u' \in C \mid \mathcal{N}_C(u') = \mathcal{N}_C(u) \} \subseteq \mathcal{N}_C^{-1}(\eta) \subseteq \mathcal{N}_C^{-1}(\eta'). \quad (\text{B.6})$$

Proof. The first inclusion has already been discussed, and the second one is straightforward since $\mathcal{N}_C(u') = \mathcal{N}_C(u)$ implies $\eta \in \mathcal{N}_C(u')$. We prove the third one.

Since $\eta \in \operatorname{rcore}(\mathcal{N}_C(u))$, there exists $\varepsilon > 0$ such that $(\eta - \varepsilon(\eta' - \eta)) \in \mathcal{N}_C(u)$. In particular, for any $u' \in \mathcal{N}_C^{-1}(\eta)$,

$$\langle u - u', \eta - \varepsilon(\eta' - \eta) \rangle \geq 0. \quad (\text{B.7})$$

Since $u, u' \in \mathcal{N}_C^{-1}(\eta) = \operatorname{argmax}_C \langle \cdot, \eta \rangle$, we have $\langle u - u', \eta \rangle = 0$, hence, by (B.7), $\varepsilon \langle u' - u, \eta' \rangle \geq 0$. Thus, for all $u'' \in C$,

$$\langle u' - u'', \eta' \rangle = \underbrace{\langle u' - u, \eta' \rangle}_{\geq 0} + \underbrace{\langle u - u'', \eta' \rangle}_{\geq 0} \geq 0 \quad (\text{B.8})$$

(the second term is nonnegative since $\eta' \in \mathcal{N}_C(u)$). \square

Let us note that each inclusion in (B.6) might be strict, as illustrated in Fig. B.1.

Remark B.1. *As the first inclusion in (B.6) might be strict, let us stress again that relying on the normal cone to locate x is not as sharp as identifying its minimal face. Nevertheless, normal vectors appear naturally when writing optimality conditions, and they are a powerful tool to study the stability of representations.*

Remark B.2. *In infinite dimension, the existence of η (i.e. $\operatorname{rcore}(\mathcal{N}_C(u)) \neq \emptyset$) is not guaranteed. Moreover, there exist nonempty closed convex sets whose normal cone is everywhere reduced to $\{0\}$ [Bou07b, Sec. II.3]. Such sets must have empty interior.*

B.3 Subdifferentials

Observe that the pairing $(V, \Upsilon, \langle \cdot, \cdot \rangle)$ can be “lifted” into a pairing $(V \times \mathbb{R}, \Upsilon \times \mathbb{R}, \langle \cdot, \cdot \rangle')$ on the epigraphical space, with

$$\langle (u, t), (\eta, \beta) \rangle' \stackrel{\text{def.}}{=} \langle u, \eta \rangle + t\beta. \quad (\text{B.9})$$

Let $R : V \rightarrow \mathbb{R} \cup \{+\infty\}$ be a convex function. Given $u \in V$, $\eta \in \Upsilon$, we say that η is a subgradient to R at u , i.e. $\eta \in \partial R(u)$, if

$$\forall v \in V, \quad R(v) \geq R(u) + \langle \eta, v - u \rangle. \quad (\text{B.10})$$

The subdifferential $\partial R(u)$ is related to the epigraph of R (see [HUL93, Prop. VI.1.3.1]): $\eta \in \partial R(u)$ if and only if the vector $(\eta, -1)$ is in the normal cone to $\operatorname{epi} R$ at $u, R(u)$. Moreover, one may check that

$$\mathcal{N}_{\operatorname{epi} R}(u, R(u)) = \{ \gamma(\eta, -1) \mid \gamma > 0, \eta \in \partial R(u) \} \cup (\mathcal{N}_{\operatorname{dom} R}(u) \times \{0\}). \quad (\text{B.11})$$

As a result, studying the subdifferential $\partial R(u)$ gives access to a normal of $\operatorname{epi} R$ at $u, R(u)$, hence to a superset of $\mathcal{F}_{\operatorname{epi} R}(u, R(u))$.

According to Proposition B.1, the normals which provide the sharpest bound on $\mathcal{F}_C(u)$ are those in $\operatorname{rcore}(\mathcal{N}_{\operatorname{epi} R}(u, R(u)))$. As the next result shows, that is equivalent to $\eta \in \operatorname{rcore}(\partial R(u))$.

Proposition B.2. *Assume that $\partial R(u) \neq \emptyset$, and let $(\alpha, \beta) \in \Upsilon \times \mathbb{R}$. The following assertions are equivalent.*

1. $(\alpha, \beta) \in \operatorname{rcore}(\mathcal{N}_{\operatorname{epi} R}(u, R(u)))$,
2. $(\alpha, \beta) = \gamma(\eta, -1)$ with $\gamma > 0$ and $\eta \in \operatorname{rcore}(\partial R(u))$.

Proof. For brevity, write $K \stackrel{\text{def.}}{=} \mathcal{N}_{\operatorname{epi} R}(u, R(u))$ and consider the cone $K_0 \stackrel{\text{def.}}{=} \{ \gamma(\eta, -1) \mid \gamma > 0, \eta \in \partial R(u) \}$. We note that $K_0 \subseteq K$ and

$$\forall (\alpha, \beta) \in K_0, \forall (\alpha', \beta') \in K, \quad [(\alpha, \beta), (\alpha', \beta')] \subseteq K_0.$$

In particular, K is the linear closure of K_0 , and thus $\text{rcore}(K) = \text{rcore}(K_0)$.

As a result, $(\alpha, \beta) \in \text{rcore}(K)$ if and only if $(\alpha, \beta) \in K_0$ and for all $(\alpha', \beta') \in K_0$, $(\alpha'', \beta'') \stackrel{\text{def.}}{=} (\alpha, \beta) - \varepsilon((\alpha', \beta') - (\alpha, \beta)) \in K_0$ for all $\varepsilon > 0$ small enough.

Let $\eta \stackrel{\text{def.}}{=} -\alpha/\beta$ (resp. $\eta' \stackrel{\text{def.}}{=} -\alpha'/\beta'$). We note that for $\varepsilon > 0$ small enough,

$$(\alpha'', \beta'') = \gamma'' \left((\eta, -1) - \frac{(-\beta')\varepsilon}{\gamma''} ((\eta', -1) - (\eta, -1)) \right)$$

where $\gamma'' \stackrel{\text{def.}}{=} -(\beta - \varepsilon(\beta' - \beta)) > 0$.

As a result, $(\alpha'', \beta'') \in K_0$ if and only if $\left((\eta, -1) - \frac{(-\beta)\varepsilon}{\gamma''} ((\eta', -1) - (\eta, -1)) \right) \in \partial R(u)$.

Hence, if $\eta \in \text{rcore}(\partial R(u))$, then $(\alpha, \beta) \in \text{rcore}(K_0)$, and conversely. \square

In the favorable case where $\eta \in R(u)$ is such that $\mathcal{N}_{\text{epi } R}^{-1}((\eta, -1)) = \overline{\mathcal{F}_{\text{epi } R}(u, R(u))}$, we say that η is a *tight dual certificate*.

B.4 Dual problems

This section is a reminder about the perturbative approach to convex duality. Standard references on the topic include [ET76, Roc89]. Our goal here is to emphasize the symmetry between the primal and dual problems, even though we work with “non-reflexive spaces”. Let $(V, \Upsilon, \langle \cdot, \cdot \rangle)$ and $(\Pi, P, \langle \cdot, \cdot \rangle)$ denote two duality pairings¹.

B.4.1 Perturbed problems.

We assume that we are given a convex function $F : V \times \Pi \rightarrow \mathbb{R} \cup \{+\infty\}$ and we consider the family of problems

$$\begin{aligned} \inf_{u \in V} F(u, \rho), & \quad (\mathcal{P}_\rho) \\ \sup_{p \in P} (-F^*(\eta, p)). & \quad (\mathcal{D}_\eta) \end{aligned}$$

Each problem (\mathcal{P}_ρ) , $\rho \neq 0$, is regarded as a perturbed problem, while our main goal is to solve the *primal problem* $((\mathcal{P}_0))$. Symmetrically, each (\mathcal{D}_η) is a perturbed version of the *dual problem* $((\mathcal{D}_0))$, and the Legendre-Fenchel inequality implies the weak duality inequality $\inf(\mathcal{P}_0) \geq \sup(\mathcal{D}_0)$. The equality case (strong duality) is obtained when (\mathcal{P}_0) (resp. (\mathcal{D}_0)) is called *normal*.

Proposition B.3 ([ET76, Prop. III.2.1]). *Assume that F is convex, proper, lower semi-continuous (l.s.c.). Then, the following properties are equivalent.*

1. $\inf(\mathcal{P}_0) = \sup(\mathcal{D}_0)$ and that number is finite,
2. The function $\varphi : P \rightarrow \overline{\mathbb{R}}$, $\varphi(\rho) \stackrel{\text{def.}}{=} \inf_{u \in V} F(u, \rho)$, is l.s.c. at 0, with $\varphi(0)$ finite,
3. The function $\gamma : \Upsilon \rightarrow \overline{\mathbb{R}}$, $\gamma(\eta) \stackrel{\text{def.}}{=} \sup_{p \in P} (-F^*(\eta, p))$, is l.s.c. at 0, with $\gamma(0)$ finite.

Proving that (\mathcal{P}_0) or (\mathcal{D}_0) is normal is not easy in general, and one usually proves a sufficient property, namely that (\mathcal{P}_0) (or (\mathcal{D}_0)) is *stable*: the function φ (or γ) is finite and subdifferentiable at 0.

Additionally, the subdifferential of φ is related to the solution set of the dual problem (a symmetrical statement holds for γ and (\mathcal{P}_0) if F is convex, l.s.c., proper).

¹We use the same notation $\langle \cdot, \cdot \rangle$ for the pairings since the risk of ambiguity is minor.

Lemma B.1 ([ET76, Lem. III.2.4]). *Let F be a proper convex function. Then, the solution set to (\mathcal{D}_0) is equal to $\partial\varphi^{**}(0)$. In particular, if $\varphi^{**}(0) = \varphi(0)$, the solution set to (\mathcal{D}_0) is equal to $\partial\varphi(0)$.*

Remark B.3. *So far, in this convex framework, the duality theory exposed above only depends on the linear spaces V, Υ, Π, P , but not on the chosen compatible topologies, as they all have the same closed convex sets and l.s.c. functions. The key point is that, in order to prove the stability of the (primal or dual) problem, one usually invokes a continuity argument, proving that φ (or γ) is finite at 0 and upper-bounded in a neighborhood of 0 (see [Corollary B.1](#)). The continuity of convex functions does depend on the choice of topology, and for that purpose, it is convenient to choose one with neighborhoods which are “as small as possible”.*

B.4.2 Duality in our inverse problem.

Now, we specialize our discussion to the family of perturbed problems

$$F(u, \rho) \stackrel{\text{def.}}{=} R(u) + f(\Phi u - y - \rho), \quad (\text{B.12})$$

where R and f are convex, proper, l.s.c., $y \in \Pi$ is a fixed parameter (the observation) and $\Phi : V \rightarrow \Pi$ is linear.

In the spirit of [Remark B.3](#), we do not assume that Φ is continuous for the chosen compatible topologies τ_V and τ_Π . We assume instead that Φ is continuous from $\sigma(V, \Upsilon)$ to $\sigma(\Pi, P)$, which ensures that F is l.s.c. for any choice of compatible topology.

➤ Since f is convex and lower semi-continuous (for the chosen topology τ_Π hence also for $\sigma(\Pi, \Upsilon)$), the mapping $(u, \rho) \mapsto f(\Phi u - y - \rho)$ is l.s.c. for the product topology generated by $\sigma(V, \Upsilon) \times \sigma(\Pi, P)$. Since the closed convex sets for that topology are the same as those for the product topology generated by $\tau_V \times \tau_\Pi$, we obtain the lower semi-continuity of $(u, \rho) \mapsto f(\Phi u - y - \rho)$ (hence of F) for the chosen topologies.

Additionally, we assume that the duality pairing $(V, \Upsilon, \langle \cdot, \cdot \rangle)$ is separating in Υ (so that $\Phi^* : P \rightarrow \Upsilon$ is well defined and continuous from $\sigma(P, \Pi)$ to $\sigma(\Upsilon, V)$, see [\[Bou07b, Prop. II.6.5\]](#)) and that $(\Pi, P, \langle \cdot, \cdot \rangle)$ is separating in Π (so that Φ^{**} is well-defined and equal to Φ).

Since $F^*(\eta, p) = R^*(\eta + \Phi^*p) + f^*(-p) - \langle y, p \rangle$, the dual problem is

$$\sup_{p \in P} (-R^*(\Phi^*p) - f^*(-p) + \langle y, p \rangle).$$

Adapting [\[ET76, Th. II.4.2\]](#) to make it symmetric yields

Corollary B.1. *Let $R : V \rightarrow \mathbb{R} \cup \{+\infty\}$ and $f : \Pi \rightarrow \mathbb{R} \cup \{+\infty\}$ be convex, proper, lower semi-continuous functions and $\Phi : V \rightarrow \Pi$ be linear, continuous from $\sigma(V, \Upsilon)$ to $\sigma(\Pi, P)$. Assume that the duality pairings are separating as described above.*

Then, the strong duality holds (i.e. $\inf(\mathcal{P}_0) = \sup(\mathcal{D}_0)$) provided one of the following two properties holds.

1. *$\inf(\mathcal{P}_0)$ is finite, there exists $u_0 \in V$ such that $R(u_0) < +\infty$, $f(\Phi u_0 - y) < +\infty$ and f is continuous at $\Phi u_0 - y$ for some compatible topology τ_Π ,*
2. *$\sup(\mathcal{D}_0)$ is finite, there exists $p_0 \in P$ such that $R^*(\Phi^*p_0) < +\infty$, $f^*(-p_0) < +\infty$, and R^* is continuous at Φ^*p_0 for some compatible topology τ_Υ .*

Moreover, in the first (resp. second) case, the problem (\mathcal{P}_0) (resp. (\mathcal{D}_0)) is stable.

Under strong duality, studying the dual problem (\mathcal{D}_0) is instructive since its solutions (if they exist) are related to those the primal problem (if they exist). Any pair $(u, p) \in V \times P$ such that u is a solution (\mathcal{P}_0) and p is a solution to (\mathcal{D}_0) satisfies

$$\Phi^* p \in \partial R(u) \quad \text{and} \quad -p \in \partial f(\Phi u - y). \quad (\text{B.13})$$

Conversely, for any pair $(u, p) \in V \times P$, if (B.13) holds, then u is a solution to (\mathcal{P}_0) and p is a solution to (\mathcal{D}_0) .

Remark B.4. *Not only do the relations (B.13) yield a convenient means to check that some given u is a solution to (\mathcal{P}_0) , but, if u is unknown, they also provide a subgradient of R at u , hence an a priori estimate of $\mathcal{F}_{\text{epi } R}(u, R(u))$.*

B.4.3 Uniqueness in the dual problem for almost every data

Problems of the form (B.12) exhibit a surprising uniqueness property when the data y varies. Observing that the value function φ defined in Appendix B.4.1 actually depends on the data y , we denote it by φ_y and we observe that

$$\varphi_y(\rho) = \varphi_0(\rho + y). \quad (\text{B.14})$$

In particular, φ_y is (Gateaux)-differentiable at 0 if and only if φ_0 is (Gateaux)-differentiable at y . Since, by Lemma B.1, the uniqueness of the solution to (\mathcal{D}_0) is related to the differentiability of φ_y at 0, standard results on the continuity and differentiability of convex functions yield the following two propositions.

Proposition B.4 (Generic uniqueness, finite-dimensional case). *Assume that $\Pi = P$ is finite-dimensional, and let $R : V \rightarrow \mathbb{R} \cup \{+\infty\}$ and $f : \Pi \rightarrow \mathbb{R} \cup \{+\infty\}$ be convex, proper, l.s.c. functions, and let $\Phi : V \rightarrow \Pi$ be linear continuous for $\sigma(V, \Upsilon)$. Assume that the duality pairings are separating as described in Appendix B.4.2.*

If φ_0 is finite on an open subset $\omega \subseteq \Pi$, then

- *strong duality holds for every $y \in \omega$,*
- *there is a unique solution to (\mathcal{D}_0) for (Lebesgue) almost every $y \in \omega$.*

We omit the proof since the above proposition directly follows from the continuity and differentiability almost everywhere of convex functions in the interior of their domain. A similar result holds in the infinite-dimensional case, where a generic set is understood as a dense G_δ set.

Proposition B.5 (Generic uniqueness, infinite-dimensional case). *Assume that for some compatible topologies τ_Υ and τ_Π , Υ is a Banach space and Π is a separable Banach space. Let $R : V \rightarrow \mathbb{R} \cup \{+\infty\}$ and $f : \Pi \rightarrow \mathbb{R} \cup \{+\infty\}$ be convex, proper, l.s.c. functions, and let $\Phi : V \rightarrow \Pi$ be linear continuous from $\sigma(V, \Upsilon)$ to $\sigma(\Pi, P)$. Assume that the duality pairings are separating as described in Appendix B.4.2.*

If φ_0 is finite on a convex open subset $\omega \subseteq \Pi$, then

- *strong duality holds for every $y \in \omega$,*
- *the set of data points $y \in \omega$ for which there is a unique solution to (\mathcal{D}_0) is a dense G_δ subset of ω .*

Proof. Since Π and Υ are both Banach spaces, that F is convex l.s.c. and proper, and $0 \in \text{int}(\text{dom } \varphi_y) = \text{core}(\text{dom } \varphi_y)$, we deduce from [Roc89, Thm. 18.c)] that φ_y is bounded above in a neighborhood of 0, hence continuous at 0 (hence strong duality holds).

As a result, the function φ_0 is convex continuous on the convex open set $\omega \subseteq \Pi$ and Π is a separable Banach space. By a theorem of Mazur [Phe93, Thm. 1.20], the set of points for which φ_0 is Gateaux-differentiable is a dense G_δ subset of ω . The uniqueness result follows from the link between the differentiability of $\varphi_y = \varphi_0(\cdot + y)$ at 0 and the solutions of the dual problem (see Lemma B.1). \square

More generally, convex continuous functions are generically Gateaux-differentiable provided that the ambient space is weak Asplund (see [Phe93]), which includes the case of Banach spaces whose topological dual is separable. We should not need any generalization of Proposition B.5 to that setting.

Appendix C

Reminder on Γ -convergence

The notion of Γ -convergence was introduced by E. De Giorgi to describe the convergence of energies and of their minimizers. We only provide elementary notions here and we refer to [DM93, Bra02] for more detail.

Let V be a topological vector space, \mathcal{T} a metric space, and a family of functionals $\{\mathcal{E}_\tau\}_{\tau \in \mathcal{T}}$, with $\mathcal{E}_\tau: V \rightarrow \overline{\mathbb{R}}$. For $\tilde{u} \in V$, we denote by $\mathcal{V}(\tilde{u})$ the collection of all neighborhoods of \tilde{u} .

Definition C.1. Let $\tau_0 \in \mathcal{T}$. The Γ -lower limit (resp. Γ -upper limit) of \mathcal{E}_τ for $\tau \rightarrow \tau_0$ is defined as

$$\Gamma - \liminf_{\tau \rightarrow \tau_0} \mathcal{E}_\tau(\tilde{u}) \stackrel{\text{def.}}{=} \sup_{U \in \mathcal{V}(\tilde{u})} \liminf_{\tau \rightarrow \tau_0} \inf_{u \in U} \mathcal{E}_\tau(u), \quad (\text{C.1})$$

$$\text{resp. } \Gamma - \limsup_{\tau \rightarrow \tau_0} \mathcal{E}_\tau(\tilde{u}) \stackrel{\text{def.}}{=} \sup_{U \in \mathcal{V}(\tilde{u})} \limsup_{\tau \rightarrow \tau_0} \inf_{u \in U} \mathcal{E}_\tau(u). \quad (\text{C.2})$$

If both quantities are equal for all $\tilde{u} \in V$, we say that \mathcal{E}_τ Γ -converges, and we refer to the corresponding function as the Γ -limit of \mathcal{E}_τ , denoted by $\Gamma - \lim_{\tau \rightarrow \tau_0} \mathcal{E}_\tau$.

If V satisfies the first axiom of countability (the existence of a countable base of neighborhoods at each point), then it is possible to use sequences in the characterization of Γ -convergence.

Proposition C.1 ([DM93, Prop. 8.1]). Assume that V satisfies the first axiom of countability, and let $\tau_0 \in \mathcal{T}$. Then \mathcal{E}_τ Γ -converges towards some function \mathcal{E} if and only if

- for every $\tilde{u} \in V$ and every sequence $(\tau^{(n)})_{n \in \mathbb{N}}$ converging to τ_0 in \mathcal{T} and every sequence $(u_n)_{n \in \mathbb{N}}$ converging to \tilde{u} in V ,

$$\mathcal{E}(\tilde{u}) \leq \liminf_{n \rightarrow +\infty} \mathcal{E}_{\tau^{(n)}}(u_n) \quad (\text{C.3})$$

- for every $\tilde{u} \in V$ and every sequence $(\tau^{(n)})_{n \in \mathbb{N}}$ converging to τ_0 in \mathcal{T} , there exists a sequence $(u_n)_{n \in \mathbb{N}}$ converging to \tilde{u} in V such that

$$\mathcal{E}(\tilde{u}) \geq \limsup_{n \rightarrow +\infty} \mathcal{E}_{\tau^{(n)}}(u_n). \quad (\text{C.4})$$

The interest of the notion of Γ -convergence lies in the convergence of the minimizers.

Proposition C.2 ([DM93, Cor. 7.20]). Let $\tau_0 \in \mathcal{T}$, and assume that \mathcal{E}_τ Γ -converges towards \mathcal{E} for $\tau \rightarrow \tau_0$. Let $(\tau^{(n)})_{n \in \mathbb{N}}$ be a sequence converging to τ_0 , and let $(u_n)_{n \in \mathbb{N}}$ be a sequence of minimizers of $\mathcal{E}_{\tau^{(n)}}$, $n \in \mathbb{N}$.

If $u \in V$ is a cluster point of $(u_n)_{n \in \mathbb{N}}$, then u is a minimizer of \mathcal{E} .

In particular, if the family $\{\mathcal{E}_\tau\}_{\tau \in \mathcal{T}}$ is (sequentially) equicoercive, *i.e.* for every $t \in \mathbb{R}$ there exists a (sequentially) compact set $K_t \subseteq V$ such that

$$\forall \tau \in \mathcal{T}, \quad \{\mathcal{E}_\tau \leq t\} \subseteq K_t, \quad (\text{C.5})$$

the existence of the cluster points in [Proposition C.1](#) is guaranteed.

Index

- ($2s - 1$)-non-degenerate dual precertificate, [129](#)
- ($2s - 1$)-vanishing precertificate, [128](#)
- Calibrable set, [88](#)
- Compatible topology, [173](#)
- Core, [24](#)
- Dual pair, [173](#)
- Duality pairing, [60](#), [61](#), [173](#)
- Epigraph, [143](#)
- equiintegrability, [105](#)
- Extreme point, [142](#)
- Face, elementary, [25](#)
- Flat extension, [157](#)
- Fuchs precertificate, [79](#)
- Generic uniqueness, [68](#), [179](#)
- Hole, [46](#)
- Indecomposable set, [41](#)
- Internal point, [24](#)
- Internal set, [25](#)
- \liminf , \limsup of a sequence of sets, [100](#)
- Linearly bounded set, [26](#)
- Linearly closed set, [26](#)
- M-connected set, [41](#)
- Minimal norm certificate, [72](#)
- Moore-Penrose pseudoinverse, [79](#)
- Non-degenerate dual certificate, [81](#)
- Non-degenerate Source condition, [81](#)
- Normal cone, [175](#)
- Paired spaces, [61](#)
- Positive Semi-definite Cone, [33](#)
- Positively homogeneous function, [61](#)
- Separating duality, [173](#)
- Simple set, [41](#)
- Sparse measure $m_{(a,x)}$, [110](#)
- T-system, [134](#)
- Tight dual certificate, [177](#)
- Total variation, of a function, [39](#)
- Vanishing-derivatives precertificate η_V , [82](#)

Bibliography

- [AABFC05] Jean-François Aujol, Gilles Aubert, Laure Blanc-Féraud, and Antonin Chambolle. Image Decomposition into a Bounded Variation Component and an Oscillating Component. *Journal of Mathematical Imaging and Vision*, 22(1):71–88, January 2005.
- [AC09] François Alter and Vicente Caselles. Uniqueness of the Cheeger set of a convex body. *Nonlinear Analysis: Theory, Methods & Applications*, 70(1):32–44, 2009.
- [AC16] Fredrik Andersson and Marcus Carlsson. On the Structure of Positive Semi-Definite Finite Rank General Domain Hankel and Toeplitz Operators in Several Variables. *Complex Analysis and Operator Theory*, 11(4), 2016. Number: 4 Publisher: Springer Science + Business Media.
- [ACC05a] François Alter, Vicente Caselles, and Antonin Chambolle. A characterization of convex calibrable sets in \mathbb{R}^N . *Math. Ann.*, 7:29–53, 2005.
- [ACC05b] François Alter, Vicente Caselles, and Antonin Chambolle. Evolution of characteristic functions of convex sets in the plane by the minimizing total variation flow. *Interfaces and free boundaries*, 7(1):29, 2005.
- [ACMM01] Luigi Ambrosio, Vicent Caselles, Simon Masnou, and Jean-Michel Morel. Connected components of sets of finite perimeter and applications to image processing. *Journal of the European Mathematical Society*, 3(1):39–92, 2001.
- [AdCG15] Jean-Marc Azaïs, Yohann de Castro, and Fabrice Gamboa. Spike detection from inaccurate samplings. *Applied and Computational Harmonic Analysis*, 38(2):177–195, March 2015.
- [AFP00] Luigi Ambrosio, Nicola Fusco, and Diego Pallara. *Functions of bounded variation and free discontinuity problems*. Oxford mathematical monographs. Clarendon Press, Oxford ; New York, 2000.
- [Ala00] C. Alard. Image subtraction using a space-varying kernel. *Astronomy and Astrophysics Supplement*, 144:363–370, 2000.
- [AVCM04] Fuensanta Andreu-Vaillo, Vicente Caselles, and José M. Mazon. *Parabolic Quasilinear Equations Minimizing Linear Growth Functionals*. Progress in Mathematics. Springer Verlag NY, 2004.
- [Axe81] Daniel Axelrod. Cell-substrate contacts illuminated by total internal reflection fluorescence. *The Journal of cell biology*, 89(1):141–145, 1981.

- [Axe08] Daniel Axelrod. Total internal reflection fluorescence microscopy. *Methods in cell biology*, 89:169–221, 02 2008.
- [Bac11] Francis R. Bach. Shaping Level Sets with Submodular Functions. In J. Shawe-Taylor, R. S. Zemel, P. L. Bartlett, F. Pereira, and K. Q. Weinberger, editors, *Advances in Neural Information Processing Systems 24*, pages 10–18. Curran Associates, Inc., 2011.
- [Bac13] Francis Bach. Learning with Submodular Functions: A Convex Optimization Perspective. *Foundations and Trends® in Machine Learning*, 6(2-3):145–373, 2013.
- [Bar94] Elisabetta Barozzi. The curvature of a set with finite area. *Atti della Accademia Nazionale dei Lincei. Classe di Scienze Fisiche, Matematiche e Naturali. Serie IX. Rendiconti Lincei. Matematica e Applicazioni*, 5(2):149–159, 1994. Publisher: European Mathematical Society (EMS) Publishing House, Zurich.
- [Bar95] Alexander. I. Barvinok. Problems of distance geometry and convex properties of quadratic maps. *Discrete & Computational Geometry*, 13(2):189–202, March 1995.
- [BB00] Jean-David Benamou and Yann Brenier. A computational fluid mechanics solution to the Monge-Kantorovich mass transfer problem. *Numerische Mathematik*, 84(3):375–393, January 2000.
- [BB07] Jerzy K. Baksalary and Oskar Maria Baksalary. Particular formulae for the Moore–Penrose inverse of a columnwise partitioned matrix. *Linear Algebra and its Applications*, 421(1):16–23, February 2007.
- [BB13] Martin Benning and Martin Burger. Ground states and singular vectors of convex variational regularization methods. *Methods and Applications of Analysis*, 20(4):295–334, 2013.
- [BBCN21] Leon Bungert, Martin Burger, Antonin Chambolle, and Matteo Novaga. Nonlinear spectral decompositions by gradient flows of one-homogeneous functionals. *Analysis & PDE*, 14(3):823–860, May 2021. Publisher: Mathematical Sciences Publishers.
- [BC01] Coloma Ballester and Vicent Caselles. The M-components of level sets of continuous functions in WBV. *Publicacions matemàtiques*, pages 477–527, 2001.
- [BC19] Kristian Bredies and Marcello Carioni. Sparsity of solutions for variational inverse problems with finite-dimensional data. *Calculus of Variations and Partial Differential Equations*, 59, 12 2019.
- [BCC07] Giuseppe Buttazzo, Guillaume Carlier, and Myriam Comte. On the selection of maximal cheeger sets. *Differential Integral Equations*, 20(9):991–1004, 2007.
- [BCF20] Kristian Bredies, Marcello Carioni, and Silvio Fanzon. A superposition principle for the inhomogeneous continuity equation with Hellinger-Kantorovich-regular coefficients. *arXiv:2007.06964 [math]*, July 2020. arXiv: 2007.06964.

- [BCFR20] Kristian Bredies, Marcello Carioni, Silvio Fanzon, and Francisco Romero. A generalized conditional gradient method for dynamic inverse problems with optimal transport regularization. *arXiv:2012.11706 [cs, math]*, December 2020. arXiv: 2012.11706.
- [BCFR21] Kristian Bredies, Marcello Carioni, Silvio Fanzon, and Francisco Romero. On the extremal points of the ball of the Benamou–Brenier energy. *Bulletin of the London Mathematical Society*, 53(5):1436–1452, 2021. eprint: <https://onlinelibrary.wiley.com/doi/pdf/10.1112/blms.12509>.
- [BCM03] Coloma Ballester, Vicent Caselles, and P. Monasse. The tree of shapes of an image. *ESAIM: Control, Optimisation and Calculus of Variations*, 9:1–18, January 2003.
- [BCN02] Giovanni Bellettini, Vicente Caselles, and Matteo Novaga. The total variation flow in \mathbb{R}^N . *J. Differential Equations*, 184(2):475–525, 2002.
- [BCN05] Giovanni Bellettini, Vicente Caselles, and Matteo Novaga. Explicit solutions of the eigenvalue problem $\operatorname{div} \left(\frac{d}{u} |du| \right) = u$ in \mathbb{R}^2 . *SIAM Journal on Mathematical Analysis*, 36(4):1095–1129, 2005.
- [BDF16] Tamir Bendory, Shai Dekel, and Arie Feuer. Robust recovery of stream of pulses using convex optimization. *Journal of Mathematical Analysis and Applications*, 442(2):511–536, 2016.
- [Beu38] Arne Beurling. Sur les intégrales de Fourier absolument convergentes et leur application à une transformation fonctionnelle. In *Ninth Scandinavian Mathematical Congress*, pages 345–366, 1938.
- [BF20] Kristian Bredies and Silvio Fanzon. An optimal transport approach for solving dynamic inverse problems in spaces of measures. *ESAIM: Mathematical Modelling and Numerical Analysis*, 54(6):2351–2382, November 2020. arXiv: 1901.10162.
- [BGM⁺14] Jérôme Boulanger, Charles Gueudry, Daniel Münch, Bertrand Cinquin, Perrine Paul-Gilloteaux, Sabine Bardin, Christophe Guérin, Fabrice Senger, Laurent Blanchoin, and Jean Salamero. Fast high-resolution 3d total internal reflection fluorescence microscopy by incidence angle scanning and azimuthal averaging. *Proceedings of the National Academy of Sciences*, 111(48):17164–17169, 2014.
- [BGM⁺16] Martin Burger, Guy Gilboa, Michael Moeller, Lina Eckardt, and Daniel Cremers. Spectral Decompositions Using One-Homogeneous Functionals. *SIAM Journal on Imaging Sciences*, 9(3):1374–1408, January 2016. Publisher: Society for Industrial and Applied Mathematics.
- [BGT87] Elisabetta Barozzi, Eduardo Gonzalez, and Italo Tamanini. The mean curvature of a set of finite perimeter. *AMS*, 99:313–316, 1987.
- [BH16] Kristian Bredies and Martin Holler. A pointwise characterization of the subdifferential of the total variation functional, 2016.

- [BLM09] Kristian Bredies, Dirk A. Lorenz, and Peter Maass. A generalized conditional gradient method and its connection to an iterative shrinkage method. *Computational Optimization and Applications*, 42(2):173–193, March 2009.
- [BO04] Martin Burger and Stanley Osher. Convergence rates of convex variational regularization. *Inverse Problems*, 20(5):1411–1421, October 2004.
- [Bou07a] Nicolas Bourbaki. *Eléments de mathématique / N. Bourbaki. Ch. 1/4: Intégration*. Springer, Berlin Heidelberg New York, réimpr. inchangée de l’éd. originale de paris, 1965 edition, 2007.
- [Bou07b] Nicolas Bourbaki. *Espaces vectoriels topologiques: Chapitres 1à 5*. Springer-Verlag, Berlin Heidelberg, 2007.
- [Bou07c] Nicolas Bourbaki. *Topologie générale: Chapitres 1 à 4*. Bourbaki, Nicolas. Springer Berlin Heidelberg, 2007.
- [BP13] Kristian Bredies and Hanna Katriina Pikkarainen. Inverse problems in spaces of measures. *ESAIM: Control, Optimisation and Calculus of Variations*, 19(1):190–218, January 2013.
- [BPS⁺06] Eric Betzig, George H. Patterson, Rachid Sougrat, O. Wolf Lindwasser, Scott Olenych, Juan S. Bonifacino, Michael W. Davidson, Jennifer Lippincott-Schwartz, and Harald F. Hess. Imaging intracellular fluorescent proteins at nanometer resolution. *Science*, 313(5793):1642–1645, 2006.
- [Bra02] Andrea Braides. *Gamma-convergence for beginners*. Number 22 in Oxford lecture series in mathematics and its applications. Oxford University Press, New York, 2002.
- [Bré73] Haïm Brézis. *Opérateurs maximaux monotones et semi-groupes de contractions dans les espaces de Hilbert*. ISSN. Elsevier Science, 1973.
- [Bré11] Haïm Brézis. *Functional Analysis, Sobolev Spaces and Partial Differential Equations*. Springer New York, New York, NY, 2011.
- [BRZ21] Immanuel M. Bomze, Francesco Rinaldi, and Damiano Zeffiro. Frank–Wolfe and friends: a journey into projection-free first-order optimization methods. *4OR*, 19(3):313–345, September 2021.
- [BSR17] Nicholas Boyd, Geoffrey Schiebinger, and Benjamin Recht. The alternating descent conditional gradient method for sparse inverse problems. *SIAM J. Optim.*, 27(2):616–639, 2017.
- [BT09] Amir Beck and Marc Teboulle. A fast iterative shrinkage-thresholding algorithm for linear inverse problems. *SIAM J. Imaging Sci.*, 2(1):183–202, 2009.
- [BV19] Kristian Bredies and David Vicente. A perfect reconstruction property for PDE-constrained total-variation minimization with application in Quantitative Susceptibility Mapping. *ESAIM: Control, Optimisation and Calculus of Variations*, 25:83, 2019. Publisher: EDP Sciences.

- [BVB16] Nicolas Boumal, Vladislav Voroninski, and Afonso S. Bandeira. The non-convex burer-monteiro approach works on smooth semidefinite programs. *Advances in Neural Information Processing Systems*, pages 2765–2773, 2016.
- [Car07] Constantin Carathéodory. Über den Variabilitätsbereich der Koeffizienten von Potenzreihen, die gegebene Werte nicht annehmen. *Mathematische Annalen*, 64(1):95–115, March 1907.
- [Cat20] Paul Catala. *Positive Semidefinite Relaxations for Imaging Science*. Theses, Ecole Normale Supérieure, October 2020.
- [CB18] Lénaïc Chizat and Francis Bach. On the Global Convergence of Gradient Descent for Over-parameterized Models using Optimal Transport. In S. Bengio, H. Wallach, H. Larochelle, K. Grauman, N. Cesa-Bianchi, and R. Garnett, editors, *Advances in Neural Information Processing Systems*, volume 31. Curran Associates, Inc., 2018.
- [CDS99] Scott S. Chen, David L. Donoho, and Michael A. Saunders. Atomic decomposition by basis pursuit. *SIAM journal on scientific computing*, 20(1):33–61, 1999.
- [CF96] Raúl E. Curto and Lawrence A. Fialkow. Solution of the truncated complex moment problem for flat data. *Memoirs of the AMS*, 568, 1996.
- [CF00] Raúl E. Curto and Lawrence A. Fialkow. The truncated complex k-moment problem. *Transactions of the AMS*, 352(6):2825–2855, 2000.
- [CFG13] Emmanuel J. Candès and Carlos Fernandez-Granda. Super-Resolution from Noisy Data. *Journal of Fourier Analysis and Applications*, 19(6):1229–1254, December 2013.
- [CFG14] Emmanuel J Candès and Carlos Fernandez-Granda. Towards a mathematical theory of super-resolution. *Communications on Pure and Applied Mathematics*, 67(6):906–956, 2014.
- [CGN15] Antonin Chambolle, Michaël Goldman, and Matteo Novaga. Fine properties of the subdifferential for a class of one-homogeneous functionals. *Adv. Calc. Var.*, 8(1):31–42, 2015.
- [Chi21] Lénaïc Chizat. Sparse optimization on measures with over-parameterized gradient descent. *Mathematical Programming*, March 2021.
- [CHK⁺13] Mark Cropper, Henk Hoekstra, Thomas D. Kitching, Richard Massey, Jerome Amiaux, Lance Miller, Yannick Mellier, Jason Rhodes, Barnaby Rowe, Sandrine Pires, Curtis J. Saxton, and Roberto Scaramella. Defining a weak lensing experiment in space. *Monthly Notices on the Royal Astronomical Society*, 431(4):3103–3126, 2013.
- [CK94] Guy Chavent and Karl Kunisch. Convergence of Tikhonov regularization for constrained ill-posed inverse problems. *Inverse Problems*, 10(1):63–76, February 1994. Publisher: IOP Publishing.

- [CL97] Antonin Chambolle and Pierre-Louis Lions. Image recovery via total variation minimization and related problems. *Numerische Mathematik*, 76(2):167–188, apr 1997.
- [Con20] Laurent Condat. Atomic Norm Minimization for Decomposition into Complex Exponentials and Optimal Transport in Fourier Domain. *Journal of Approximation Theory*, 258:105456, October 2020.
- [CP11] Antonin Chambolle and Thomas Pock. A First-Order Primal-Dual Algorithm for Convex Problems with Applications to Imaging. *Journal of Mathematical Imaging and Vision*, 40(1):120–145, May 2011.
- [CR09] Emmanuel J Candès and Benjamin Recht. Exact matrix completion via convex optimization. *Foundations of Computational mathematics*, 9(6):717, 2009.
- [CR13] Emmanuel Candès and Benjamin Recht. Simple bounds for recovering low-complexity models. *Mathematical Programming*, 141(1-2):577–589, October 2013.
- [CRPW12] Venkat Chandrasekaran, Benjamin Recht, Pablo A Parrilo, and Alan S Willsky. The convex geometry of linear inverse problems. *Foundations of Computational mathematics*, 12(6):805–849, 2012.
- [DAG09] Vincent Duval, Jean-François Aujol, and Yann Gousseau. The TVL1 model: A geometric point of view. *Multiscale Modeling & Simulation*, 8(1):154–189, 2009.
- [Dat05] Jon Dattorro. *Convex Optimization & Euclidean Distance Geometry*. Meboo Publishing, 2005.
- [DBFZ⁺06] Nicolas Dey, Laure Blanc-Feraud, Christophe Zimmer, Pascal Roux, Zvi Kam, Jean-Christophe Olivo-Marin, and Josiane Zerubia. Richardson–Lucy algorithm with total variation regularization for 3D confocal microscope deconvolution. *Microscopy Research and Technique*, 69(4):260–266, April 2006.
- [dBR90] Carl de Boor and Amos Ron. On multivariate polynomial interpolation. *Constructive Approximation*, 6:287–302, September 1990.
- [DCD18] Maxime Ferreira Da Costa and Wei Dai. A Tight Converse to the Spectral Resolution Limit via Convex Programming. In *2018 IEEE International Symposium on Information Theory (ISIT)*, pages 901–905, June 2018. ISSN: 2157-8117.
- [dCG12] Yohann de Castro and Fabrice Gamboa. Exact reconstruction using Beurling minimal extrapolation. *Journal of Mathematical Analysis and Applications*, 395(1):336–354, November 2012.
- [DCGHL17] Yohann De Castro, Fabrice Gamboa, Didier Henrion, and Jean-Bernard Lasserre. Exact Solutions to Super Resolution on Semi-Algebraic Domains in Higher Dimensions. *IEEE Transactions on Information Theory*, 63(1):621–630, January 2017.

- [Den18] Quentin Denoyelle. *Theoretical and Numerical Analysis of Super-Resolution Without Grid*. PhD thesis, SDOSE, Université Paris-Dauphine, 2018. Thèse de doctorat dirigée par Peyré, Gabriel Sciences Paris Sciences et Lettres (ComUE) 2018.
- [DH78] Joseph C. Dunn and Stephanie L. Harshbarger. Conditional gradient algorithms with open loop step size rules. *Journal of Mathematical Analysis and Applications*, 62(2):432–444, February 1978.
- [DK00] Françoise Dibos and Georges Koepfler. Global Total Variation Minimization. *SIAM Journal on Numerical Analysis*, 37(2):646–664, 2000.
- [DM93] Gianni Dal Maso. *An Introduction to Γ -convergence*. Number v. 8 in Progress in nonlinear differential equations and their applications. Birkhäuser, Boston, MA, 1993.
- [DM95] Georg Dolzmann and Stefan Müller. Microstructures with finite surface energy: the two-well problem. *Archive for Rational Mechanics and Analysis*, 132(2):101–141, June 1995.
- [DMR00] Sylvain Durand, François Malgouyres, and Bernard Rougé. Image deblurring, spectrum interpolation and application to satellite imaging. *ESAIM: Control, Optimisation and Calculus of Variations*, 5:445–475, 2000. Publisher: EDP Sciences.
- [Don06] David L Donoho. Compressed sensing. *IEEE Transactions on Information Theory*, 52(4):1289–1306, 2006.
- [dP95] Gaspard de Prony. Essai expérimental et analytique: sur les lois de la dilatabilité de fluides élastique et sur celles de la force expansive de la vapeur de l’alcool, à différentes températures. *Journal de l’Ecole Polytechnique*, 1(22):24?–76, 1795.
- [DR70] Vladimir Fedorovich Demyanov and Aleksandr Moiseevich Rubinov. *Approximate methods in optimization problems*, volume 32. Elsevier Publishing Company, 1970.
- [DSDVJ16] Marcelina Cardoso Dos Santos, Régis Déturche, Cyrille Vézé, and Rodolphe Jaffiol. Topography of cells revealed by variable-angle total internal reflection fluorescence microscopy. *Biophysical journal*, 111(6):1316–1327, 2016.
- [DT05] David L Donoho and Jared Tanner. Sparse nonnegative solution of underdetermined linear equations by linear programming. *Proceedings of the National Academy of Sciences of the United States of America*, 102(27):9446–9451, 2005.
- [Dub62] Lester E. Dubins. On extreme points of convex sets. *Journal of Mathematical Analysis and Applications*, 5(2):237–244, October 1962.
- [EHBN00] Heinz W. Engl, Martin Hanke-Bourgeois, and Andreas Neubauer. *Regularization of inverse problems*. Number 375 in Mathematics and its applications <Dordrecht>. Kluwer Acad. Publ, Dordrecht, 2000.
- [EPF13] EPFL Biomedical Imaging Group. Benchmarking of single-molecule localization microscopy software. <http://bigwww.epfl.ch/palm/>, 2013.

- [ET76] Ivar Ekeland and Roger Témam. *Convex Analysis and Variational Problems*. Number vol. 1 in Classics in Applied Mathematics. Society for Industrial and Applied Mathematics, 1976.
- [ET19] Armin Eftekhari and Andrew Thompson. Sparse Inverse Problems over Measures: Equivalence of the Conditional Gradient and Exchange Methods. *SIAM Journal on Optimization*, 29(2):1329–1349, January 2019. Publisher: Society for Industrial and Applied Mathematics.
- [ETS11] Chaitanya Ekanadham, Daniel Tranchina, and Eero P. Simoncelli. Recovery of sparse translation-invariant signals with continuous basis pursuit. *Signal Processing, IEEE Transactions on*, 59(10):4735–4744, 2011.
- [FdGW21] Axel Flinth, Frédéric de Gournay, and Pierre Weiss. On the linear convergence rates of exchange and continuous methods for total variation minimization. *Mathematical Programming*, 190(1-2):221–257, November 2021.
- [FFDD09] Alessandro Ferriero, Nicola Fusco, ,Departamento de Matemáticas, Universidad Autónoma de Madrid, Campus de Cantoblanco,28049 Madrid, and ,Dipartimento di Matematica e Applicazioni “R. Caccioppoli”, Università di Napoli “Federico II”, 80126 Napoli. A note on the convex hull of sets of finite perimeter in the plane. *Discrete & Continuous Dynamical Systems - B*, 11(1):103–108, 2009.
- [FG13] Carlos Fernandez-Granda. Support detection in super-resolution. In *Proceedings of the 10th International Conference on Sampling Theory and Applications (SampTA)*, pages 145–148, 2013.
- [FG16] Carlos Fernandez-Granda. Super-resolution of point sources via convex programming. *Information and Inference: A Journal of the IMA*, 5(3):251–303, 2016.
- [FJ75] Stephen D. Fisher and Joseph W. Jerome. Spline solutions to L1 extremal problems in one and several variables. *Journal of Approximation Theory*, 13(1):73–83, 1975.
- [Fle57] Wendell H. Fleming. Functions with generalized gradient and generalized surfaces. *Annali di Matematica Pura ed Applicata*, 44(1):93–103, 1957.
- [FMP18] Jalal Fadili, Jérôme Malick, and Gabriel Peyré. Sensitivity Analysis for Mirror-Stratifiable Convex Functions. *SIAM J. Optim.*, 28(4):2975–3000, January 2018.
- [FR60] Wendell H. Fleming and Raymond Rishel. An integral formula for total gradient variation. *Archiv der Mathematik*, 11(1):218–222, December 1960.
- [FR13] Simon Foucart and Holger Rauhut. *A Mathematical Introduction to Compressive Sensing*. Springer New York, 2013.
- [Fuc04] Jean-Jacques Fuchs. On sparse representations in arbitrary redundant bases. *IEEE Transactions on Information Theory*, 50(6):1341–1344, June 2004. Conference Name: IEEE Transactions on Information Theory.

- [Fuj05] Satoru Fujishige. *Submodular functions and optimization*. Number 58 in Annals of discrete mathematics. Elsevier, Boston, 2nd ed edition, 2005.
- [FW56] Marguerite Frank and Philip Wolfe. An algorithm for quadratic programming. *Naval Res. Logist. Quart.*, 3:95–110, 1956.
- [FW19] Axel Flinth and Pierre Weiss. Exact solutions of infinite dimensional total-variation regularized problems. *Information and Inference: A Journal of the IMA*, 8(3):407–443, September 2019.
- [GCM13] M. Gentile, F. Courbin, and G. Meylan. Interpolating point spread function anisotropy. *Astronomy and Astrophysics*, 549:A1, 2013.
- [GFU18] Harshit Gupta, Julien Fageot, and Michael Unser. Continuous-Domain Solutions of Linear Inverse Problems With Tikhonov Versus Generalized TV Regularization. *IEEE Transactions on Signal Processing*, 66(17):4670–4684, September 2018. Conference Name: IEEE Transactions on Signal Processing.
- [Gil14] Guy Gilboa. A Total Variation Spectral Framework for Scale and Texture Analysis. *SIAM Journal on Imaging Sciences*, 7(4):1937–1961, January 2014. Publisher: Society for Industrial and Applied Mathematics.
- [Giu78a] Enrico Giusti. On the equation of surfaces of prescribed mean curvature. *Invent. Math.*, 46(2):111–137, 1978.
- [Giu78b] Enrico Giusti. On the Equation of Surfaces of Prescribed Mean Curvature. Existence and Uniqueness without Boundary Conditions. *Inventiones mathematicae*, 46:111–138, 1978.
- [Giu84] Enrico Giusti. *Minimal surfaces and functions of bounded variation*. Number 80 in Monographs in mathematics. Birkhäuser, Boston Basel, 1984.
- [GM94] E. H. A. Gonzalez and U. Massari. Variational mean curvatures. *Rend. Sem. Mat. Univ. Pol. Torino*, 52:1–28, 1994.
- [GMT93] E. HA Gonzales, U. Massari, and I. Tamanini. Boundaries of prescribed mean curvature. *Atti della Accademia Nazionale dei Lincei. Classe di Scienze Fisiche, Matematiche e Naturali. Rendiconti Lincei. Matematica e Applicazioni*, 4(3):197–206, 1993.
- [Gro13] Biomedical Imaging Group. Benchmarking of single-molecule localization microscopy software. <http://bigwww.epfl.ch/palm/>, 2013.
- [Gus00] M. G. L. Gustafsson. Surpassing the lateral resolution limit by a factor of two using structured illumination microscopy. *Journal of Microscopy*, 198(2):82–87, 2000.
- [Had07] Ali Haddad. Texture Separation \$BV-G\$ and \$BV-L^1\$ Models. *Multiscale Modeling & Simulation*, 6(1):273–286, January 2007. Publisher: Society for Industrial and Applied Mathematics.

- [Hei14] Pia Heins. *Reconstruction using Local Sparsity*. PhD thesis, Westfälische Wilhelms-Universität Münster, 2014.
- [HJN15] Zaid Harchaoui, Anatoli Juditsky, and Arkadi Nemirovski. Conditional gradient algorithms for norm-regularized smooth convex optimization. *Mathematical Programming*, 152(1-2):75–112, 2015.
- [HKM17] J. Harmouch, H. Khalil, and B. Mourrain. Structured low rank decomposition of multivariate Hankel matrices. *Linear Algebra and its Applications*, 542:162 – 185, 2017.
- [HKPS07] Bernd Hofmann, Barbara Kaltenbacher, Christiane Pöschl, and Otmar Scherzer. A convergence rates result for Tikhonov regularization in Banach spaces with non-smooth operators. *Inverse Problems*, 23(3):987–1010, June 2007.
- [HLF⁺10] Ricardo Henriques, Mickael Lelek, Eugenio F Fornasiero, Flavia Valtorta, Christophe Zimmer, and Musa M Mhlanga. Quickpalm: 3d real-time photoactivation nanoscopy image processing in imagej. *Nature methods*, 7(5):339, 2010.
- [HM07] Ali Haddad and Yves Meyer. An improvement of Rudin–Osher–Fatemi model. *Applied and Computational Harmonic Analysis*, 22(3):319–334, May 2007.
- [HPKGM07] Samuel Hess, Thanu P K Girirajan, and Michael Mason. Ultra-high resolution imaging by fluorescence photoactivation localization microscopy. *Biophysical journal*, 91:4258–72, 01 2007.
- [HSG⁺15] Jiaqing Huang, Mingzhai Sun, Kristyn Gumpfer, Yuejie Chi, and Jianjie Ma. 3d multifocus astigmatism and compressed sensing (3d macs) based superresolution reconstruction. *Biomed. Opt. Express*, 6(3):902–917, Mar 2015.
- [HSMC17] Jiaqing Huang, Mingzhai Sun, Jianjie Ma, and Yuejie Chi. Super-resolution image reconstruction for high-density three-dimensional single-molecule microscopy. *IEEE Transactions on Computational Imaging*, 3(4):763–773, 2017.
- [HUL93] Jean-Baptiste Hiriart-Urruty and Claude Lemaréchal. *Convex Analysis and Minimization Algorithms I*, volume 305 of *Grundlehren der mathematischen Wissenschaften*. Springer Berlin Heidelberg, Berlin, Heidelberg, 1993.
- [HW94] Stefan W. Hell and Jan Wichmann. Breaking the diffraction resolution limit by stimulated emission: stimulated-emission-depletion fluorescence microscopy. *Opt. Lett.*, 19(11):780–782, Jun 1994.
- [HWBZ08] Bo Huang, Wenqin Wang, Mark Bates, and Xiaowei Zhuang. Three-dimensional super-resolution imaging by stochastic optical reconstruction microscopy. *Science*, 2008.
- [IM20a] José A. Iglesias and Gwenael Mercier. Convergence of level sets in tv denoising through variational curvatures in unbounded domains, 2020.

- [IM20b] Iglesias, José A. and Mercier, Gwenael. Influence of dimension on the convergence of level-sets in total variation regularization*. *ESAIM: COCV*, 26:52, 2020.
- [IMS17] José Iglesias, Gwenael Mercier, and Otmar Scherzer. A note on convergence of solutions of total variation regularized linear inverse problems. *Inverse Problems*, 34, 11 2017.
- [IW21] José A. Iglesias and Daniel Walter. Extremal points of total generalized variation balls in 1D: characterization and applications. *arXiv:2112.06846 [math]*, December 2021. arXiv: 2112.06846.
- [Jag13] Martin Jaggi. Revisiting frank-wolfe: Projection-free sparse convex optimization. In *ICML (1)*, pages 427–435, 2013.
- [JJGL⁺08] Manuel Juette, Travis J Gould, Mark Lessard, Michael Mlodzianoski, Bhupendra S Nagpure, Brian Thomas Bennett, Samuel Hess, and Joerg Bewersdorf. Three-dimensional sub-100 nm resolution fluorescence microscopy of thick samples. *Nature methods*, 5:527–9, 07 2008.
- [JLM19] Cédric Josz, Jean Bernard Lasserre, and Bernard Mourrain. Sparse polynomial interpolation: sparse recovery, super-resolution, or Prony? *Advances in Computational Mathematics*, 45(3):1401–1437, June 2019.
- [Kai90] Thomas Kailath. ESPRIT—estimation of signal parameters via rotational invariance techniques. *Optical Engineering*, 29(4):296, 1990.
- [Kap57] Samuel Kaplan. On The Second Dual of the Space of Continuous Functions. *Transactions of the American Mathematical Society*, 86(1):70–90, 1957. Publisher: American Mathematical Society.
- [Kap59] Samuel Kaplan. The Second Dual of the Space of Continuous Functions, II. *Transactions of the American Mathematical Society*, 93(2):329–350, 1959. Publisher: American Mathematical Society.
- [Kap61] Samuel Kaplan. The Second Dual of the Space of Continuous Functions, III. *Transactions of the American Mathematical Society*, 101(1):34–51, 1961. Publisher: American Mathematical Society.
- [Kar68] Samuel Karlin. *Total Positivity*. Number vol. 1 in Total Positivity. Stanford University Press, 1968.
- [Ker16] Michel Kern. *Méthodes numériques pour les problèmes inverses*. Collection mathématiques et statistiques. ISTE editions, London, 2016.
- [KHB21] Alexandra Koulouri, Pia Heins, and Martin Burger. Adaptive superresolution in deconvolution of sparse peaks. *IEEE Trans. Signal Process.*, 69:165–178, 2021.
- [Kle57] Victor Klee. Extremal structure of convex sets. *Archiv der Mathematik*, 8(3):234–240, Aug 1957.
- [Kle63] Victor Klee. On a theorem of Dubins. *Journal of Mathematical Analysis and Applications*, 7(3):425–427, December 1963.

- [KLR06] Bertrand Kawohl and Thomas Lachand-Robert. Characterization of Cheeger sets for convex subsets of the plane. *Pacific J. Math.*, 225(1):103–118, 2006.
- [KN77] M. G. Krein and Adolf Abramovich Nudelman. *The Markov moment problem and extremal problems: ideas and problems of P. L. Chebyshev and A. A. Markov and their further development*. Number v. 50 in Translations of mathematical monographs. American Mathematical Society, Providence, R.I., 1977.
- [KOX06] Stefan Kindermann, Stanley Osher, and Jinjun Xu. Denoising by BV-duality. *Journal of Scientific Computing*, 28(2-3):411–444, 2006.
- [Kre38] M.G. Kreĭn. The L-problem in an abstract normed linear space. In I. Ahiezer and M.G. Kreĭn, editors, *Some questions in the theory of moments*, chapter 4. Gos. Naučno-Tehn. Izdat. Ukraine, 1938. English Transl. Amer. Math. Soc., Providence, R.I., 1962. MR 29 # 5073.
- [Kre91] Erwin Kreyszig. *Differential geometry*. Dover Publications, New York, 1991.
- [KS66] S. Karlin and W.J. Studden. *Tchebycheff systems: with applications in analysis and statistics*. Pure and applied mathematics. Interscience Publishers, 1966.
- [KVU13] Hagai Kirshner, Cédric Vonesch, and Michael Unser. Can localization microscopy benefit from approximation theory? In *2013 IEEE 10th International Symposium on Biomedical Imaging (ISBI)*, pages 588–591. IEEE, 2013.
- [LAG09] Bin Luo, Jean-François Aujol, and Yann Gousseau. Local Scale Measure from the Topographic Map and Application to Remote Sensing Images. *Multiscale Modeling & Simulation*, 8(1):1–29, January 2009.
- [Lan02] Serge Lang. *Algebra*. Number 211 in Graduate texts in mathematics. Springer, New York, rev. 3rd ed edition, 2002.
- [Las01] Jean-Bernard Lasserre. Global optimization with polynomials and the problem of moments. *SIAM Journal on Optimization*, 11(3):796–817, 2001.
- [Las10] Jean-Bernard Lasserre. *Moments, positive polynomials and their applications*. Imperial College Press Optimization Series. Imperial College Press, London, 2010.
- [Lau05] Monique Laurent. Revisiting two theorems of curto and fialkow on moment matrices. *Proceedings of the American Mathematical Society*, 133(10):2965–2976, 2005.
- [LBFA21] Bastien Laville, Laure Blanc-Féraud, and Gilles Aubert. Off-The-Grid Variational Sparse Spike Recovery: Methods and Algorithms. *Journal of Imaging*, 7(12):266, December 2021.
- [Lew02] Adrian S. Lewis. Active Sets, Nonsmoothness, and Sensitivity. *SIAM J. Optim.*, 13(3):702–725, January 2002.

- [LM09] Monique Laurent and Bernard Mourrain. A generalized flat extension theorem for moment matrices. *Archiv der Mathematik*, 93(1):87–98, 2009.
- [LP66] Evgenii Solomonovich Levitin and Boris Teodorovich Polyak. Constrained minimization methods. *Zhurnal Vychislitel'noi Matematiki i Matematicheskoi Fiziki*, 6(5):787–823, 1966.
- [LT20] Qiuwei Li and Gongguo Tang. Approximate support recovery of atomic line spectral estimation: A tale of resolution and precision. *Applied and Computational Harmonic Analysis*, 48(3):891–948, 2020.
- [Mag12] Francesco Maggi. *Sets of Finite Perimeter and Geometric Variational Problems: An Introduction to Geometric Measure Theory*. Cambridge Studies in Advanced Mathematics. Cambridge University Press, Cambridge, 2012.
- [Mey01] Yves Meyer. *Oscillating Patterns in Image Processing and Nonlinear Evolution Equations: The Fifteenth Dean Jacqueline B. Lewis Memorial Lectures*. American Mathematical Society, Boston, MA, USA, 2001.
- [MG00] Pascal Monasse and Frédéric Guichard. Scale-Space from a Level Lines Tree. *J. Vis. Comun. Image Represent.*, 11(2):224–236, June 2000.
- [MLB99] Saunders Mac Lane and Garrett Birkhoff. *Algebra*. AMS Chelsea Publishing, 1999. Third Edition.
- [Mon99] P. Monasse. Contrast invariant registration of images. In *1999 IEEE International Conference on Acoustics, Speech, and Signal Processing. Proceedings. ICASSP99 (Cat. No.99CH36258)*, volume 6, pages 3221–3224 vol.6, March 1999.
- [Mor84] V. A. Morozov. *Methods for Solving Incorrectly Posed Problems*. Springer New York, New York, NY, 1984.
- [MS95] H.M. Möller and H.J. Stetter. Multivariate polynomial equations with multiple zeros solved by matrix eigenproblems. *Numerische Mathematik*, 70:311–329, 1995.
- [NS17] F. Ngolé and J.-L. Starck. Point spread function field learning based on optimal transport distances. *SIAM Journal on Imaging Sciences*, 10(3):1549–1578, 2017.
- [OPT00] MR Osborne, B Presnell, and BA Turlach. A new approach to variable selection in least squares problems. *IMA Journal of Numerical Analysis*, 20(3):389–403, July 2000.
- [Par11] Enea Parini. An introduction to the Cheeger problem. *Surveys in Mathematics and its Applications*, 6:9–21, 2011.
- [Phe93] Robert R. Phelps. *Convex Functions, Monotone Operators and Differentiability*. Lecture Notes in Mathematics. Springer Berlin Heidelberg, 1993.

- [PKP20] Clarice Poon, Nicolas Keriven, and Gabriel Peyré. The geometry of off-the-grid compressed sensing. *arXiv:1802.08464 [cs, math]*, February 2020. arXiv: 1802.08464.
- [PP17] Clarice Poon and Gabriel Peyré. Multi-dimensional Sparse Super-resolution. *arXiv:1709.03157 [math]*, September 2017. arXiv: 1709.03157.
- [PP19] Clarice Poon and Gabriel Peyré. Degrees of freedom for off-the-grid sparse estimation. *arXiv:1911.03577 [cs, math, stat]*, November 2019. arXiv: 1911.03577.
- [RBZ06] Michael J Rust, Mark Bates, and Xiaowei Zhuang. Sub-diffraction-limit imaging by stochastic optical reconstruction microscopy (storm). *Nature methods*, 3(10):793–796, 2006.
- [Roc89] Ralph Tyrrell Rockafellar. *Conjugate duality and optimization*. Number 16 in Regional conference series in applied mathematics. Soc. for Industrial and Applied Mathematics, Philadelphia, Pa, 2. print edition, 1989. OCLC: 258450647.
- [Roc97] Ralph Tyrrell Rockafellar. *Convex analysis*. Princeton landmarks in mathematics and physics. Princeton Univ. Press, Princeton, NJ, 1997. OCLC: 247646720.
- [ROF92] Leonid I Rudin, Stanley Osher, and Emad Fatemi. Nonlinear total variation based noise removal algorithms. *Physica D: nonlinear phenomena*, 60(1-4):259–268, 1992.
- [RPPATSB⁺09] Sri Rama Prasanna Pavani, Michael A Thompson, Julie S Biteen, Samuel Lord, Na Liu, Robert Twieg, Rafael Piastun, and William Moerner. Three-dimensional, single-molecule fluorescence imaging beyond the diffraction limit by using a double-helix point spread function. *Proceedings of the National Academy of Sciences of the United States of America*, 106:2995–9, 03 2009.
- [RW98] Ralph Tyrrell Rockafellar and Roger J.-B. Wets. *Variational Analysis*. Grundlehren der mathematischen Wissenschaften. Springer-Verlag, Berlin Heidelberg, 1998.
- [San04] Luis A. Santaló. *Integral geometry and geometric probability*. Cambridge mathematical library. Cambridge University Press, Cambridge, UK ; New York, 2nd ed edition, 2004. OCLC: ocm52055341.
- [SC82] Jean Paul Serra and Noel A. C Cressie. *Image analysis and mathematical morphology*. London ; New York : Academic Press, 1982.
- [Sch66] Laurent Schwartz. *Théorie des Distributions*. Hermann, 1966.
- [Sch86] R. Schmidt. Multiple emitter location and signal parameter estimation. *IEEE Transactions on Antennas and Propagation*, 34(3):276–280, mar 1986.
- [Sch06] Claus Scheiderer. Sums of squares on real algebraic surfaces. *manuscripta mathematica*, 119(4):395–410, April 2006.

- [Ser82] Jean Serra. *Image analysis and mathematical morphology*. Academic Press, London, 1982.
- [SHM⁺02] S.M. Steinbrig, E. Faber, S. Hinkley, B.A. Macintosh, D. Gavel, E.L. Gates, J.C. Christou, M. Le Louarn, L.M. Raschke, S.A. Severson, F. Rigaut, D. Crampton, Lloyd J.P., and J.R. Graham. Characterizing the adaptive optics off-axis point-spread function - i: A semi-empirical method for use in natural-guide-star observations. *Publications of the Astronomical Society of the Pacific*, 114(801):1267–1280, 2002.
- [SKHK12] Thomas Schuster, Barbara Kaltenbacher, Bernd Hofmann, and Kamil S. Kazimierski. *Regularization Methods in Banach Spaces*. Walter de Gruyter, July 2012.
- [SKP⁺15] Daniel Sage, Hagai Kirshner, Thomas Pengo, Nico Stuurman, Junhong Min, Suliana Manley, and Michael Unser. Quantitative evaluation of software packages for single-molecule localization microscopy. *Nature methods*, 12, 06 2015.
- [SPB⁺18] Daniel Sage, Thanh-An Pham, Hazen Babcock, Tomas Lukes, Thomas Pengo, Ramraj Velmurugan, Alex Herbert, Anurag Agarwal, Silvia Colabrese, Ann Wheeler, Anna Archetti, Bernd Rieger, Raimund Ober, Guy M. Hagen, Jean-Baptiste Sibarita, Jonas Ries, Ricardo Henriques, Michael Unser, and Seamus Holden. Super-resolution fight club: A broad assessment of 2d & 3d single-molecule localization microscopy software. *bioRxiv*, 2018.
- [SRG⁺19] Emmanuel Soubies, Agata Radwanska, Dominique Grall, Laure Blanc-Féraud, Ellen Van Obberghen-Schilling, and Sébastien Schaub. Nanometric axial resolution of fibronectin assembly units achieved with an efficient reconstruction approach for multi-angle-tirf microscopy. *Scientific Reports*, 9(1):1926, 2019.
- [SRR18] Geoffrey Schiebinger, Elina Robeva, and Benjamin Recht. Superresolution without separation. *Information and Inference: A Journal of the IMA*, 7(1):1–30, March 2018.
- [SS02] Bernhard Scholkopf and Alexander J Smola. *Learning with kernels* .: MIT Press,, 2002.
- [SSR⁺16] Emmanuel Soubies, Sébastien Schaub, Agata Radwanska, Ellen Van Obberghen-Schilling, Laure Blanc-Féraud, and Gilles Aubert. A framework for multi-angle tirf microscope calibration. In *Biomedical Imaging (ISBI), 2016 IEEE 13th International Symposium on*, pages 668–671. IEEE, 2016.
- [Tan15] Gongguo Tang. Resolution limits for atomic decompositions via markov-bernstein type inequalities. In *2015 International Conference on Sampling Theory and Applications (SampTA)*, pages 548–552, 2015.
- [TBSR13] Gongguo Tang, Badri Narayan Bhaskar, Parikshit Shah, and Benjamin Recht. Compressed sensing off the grid. *IEEE Transactions on Information Theory*, 59(11):7465–7490, 2013.

- [Tib96] Robert Tibshirani. Regression shrinkage and selection via the Lasso. *Journal of the Royal Statistical Society. Series B. Methodological*, 58(1):267–288, 1996.
- [Tik43] Andreï N. Tikhonov. On the stability of inverse problems. *Dokl. Akad. Nauk SSSR*, 39:195–198, 1943.
- [Tik63] Andreï N. Tikhonov. On the solution of ill-posed problems and the method of regularization. *Dokl. Akad. Nauk SSSR*, 151(3):501–504, 1963.
- [Toe11] Otto Toeplitz. über die Fouriersche Entwicklung positiver Funktionen. *Rend. Circ. Mat. Palermo*, 32:191–192, 1911.
- [Tro06] Joel A. Tropp. Just relax: Convex programming methods for identifying sparse signals in noise. *IEEE Transactions on Information Theory*, 52(3):1030–1051, 2006.
- [UFW17] Michael Unser, Julien Fageot, and John Paul Ward. Splines are universal solutions of linear inverse problems with generalized tv regularization. *SIAM Review*, 59(4):769–793, 2017.
- [Uns19] Michael Unser. A Representer Theorem for Deep Neural Networks. *J. Mach. Learn. Res.*, 20(110):1–30, 2019.
- [Uns21] Michael Unser. A Unifying Representer Theorem for Inverse Problems and Machine Learning. *Foundations of Computational Mathematics*, 21(4):941–960, August 2021.
- [VGFP15] Samuel Vaiter, Mohammad Golbabaee, Jalal Fadili, and Gabriel Peyré. Model selection with low complexity priors. *Information and Inference*, page iav005, April 2015.
- [VPDF13] Samuel Vaiter, Gabriel Peyre, Charles Dossal, and Jalal Fadili. Robust Sparse Analysis Regularization. *IEEE Transactions on Information Theory*, 59(4):2001–2016, April 2013. Conference Name: IEEE Transactions on Information Theory.
- [VPF13] Samuel Vaiter, Gabriel Peyré, and Jalal Fadili. Robust Polyhedral Regularization. In *SAMPTA*, page 4, 2013.
- [VPF15] Samuel Vaiter, Gabriel Peyré, and Jalal Fadili. Low Complexity Regularization of Linear Inverse Problems. In Götz E. Pfander, editor, *Sampling Theory, a Renaissance*, pages 103–153. Springer International Publishing, Cham, 2015. Series Title: Applied and Numerical Harmonic Analysis.
- [VPF18] Samuel Vaiter, Gabriel Peyre, and Jalal Fadili. Model Consistency of Partly Smooth Regularizers. *IEEE Trans. Inform. Theory*, 64(3):1725–1737, March 2018.
- [WB09] Zhou Wang and Alan C. Bovik. Mean squared error: Love it or leave it? A new look at Signal Fidelity Measures. *IEEE Signal Processing Magazine*, 26(1):98–117, January 2009. Conference Name: IEEE Signal Processing Magazine.

- [Wen05] Holger Wendland. *Scattered data approximation*. Cambridge University Press, 2005.
- [Wer23] M. Wertheimer. Untersuchungen zur lehre der gestalt, ii. *Psychologische Forschung*, 4:301–350, 1923.
- [YXS16] Zai Yang, Lihua Xie, and Petre Stoica. Vandermonde decomposition of multilevel toeplitz matrices with application to multidimensional super-resolution. *IEEE Transactions on Information Theory*, 62(6):3685–3701, 2016.
- [Zuh48] S.I. Zuhovickii. Remarks on problems in approximation theory. *Mat. Zbirnik KDU*, pages 169–183, 1948. (Ukrainian).
- [Zuh62] S.I. Zuhovickii. On approximation of real functions in the sense of P.L. Čebyšev. *AMS Translations of Mathematical Monographs.*, 19(2):221–252, 1962.
- [ZZL⁺18] Cheng Zheng, Guangyuan Zhao, Wenjie Liu, Youhua Chen, Zhimin Zhang, Luhong Jin, Yingke Xu, Cuifang Kuang, and Xu Liu. Three-dimensional super-resolved live cell imaging through polarized multi-angle tifr. *Optics letters*, 43(7):1423–1426, 2018.

Résumé

Par leur flexibilité et les garanties de reconstructions qu'elles apportent, les méthodes variationnelles donnent des outils puissants pour la résolution des problèmes inverses, en particulier dans le traitement du signal et des images. Ce mémoire, consacré aux méthodes variationnelles convexes, met en évidence l'importance cruciale des notions de face et de point extrémal dans le comportement des modèles, et notamment leur influence sur la structure des solutions. Nous démontrons un théorème de représentation qui décrit les solutions en fonction des points extrémaux des ensembles de niveau de la fonctionnelle de régularisation. Ce principe permet de décrire les solutions de problèmes en dimension infinie, par exemple dans l'espace des mesures de Radon (BLASSO). Le cas de la variation totale du gradient est également étudié. Nous discutons de la stabilité de ces représentations en fonction du bruit et de la régularisation. Enfin, nous montrons que cette représentation peut être exploitée par des algorithmes efficaces, qui tirent parti de la nature continue des problèmes considérés, et qui suppriment les artefacts de discrétisation.

Mots Clés

Points extrémaux; méthodes variationnelles; variation totale; problèmes inverses; mesures de Radon

Abstract

Due to their flexibility and to the recovery guarantees they provide, variational methods are powerful tools for the resolution of inverse problems, especially in signal and image processing. The present habilitation thesis, devoted to convex variational methods, highlights the crucial importance of the notions of face and extreme point in determining the behavior of variational models, and notably the structure of solutions.

We prove a representer theorem which describes the solutions using the extreme points of the level sets of the regularizer. That principle allows to describe the solutions of infinite-dimensional problems, e.g. in the space of Radon measures (BLASSO). The case of the total gradient variation is studied too. We discuss the stability of those representations when the noise and the regularization parameter vary. Eventually, we show that such a representation may be exploited by efficient algorithms which take advantage of the continuous nature of the considered problems, and which do not suffer from the standard discretization artifacts.

Keywords

Extreme points; variational methods; total variation; inverse problems; Radon measures